Short-term dynamics of nano- and picoplankton in the southern Benguela upwelling system

Nicole Rebecca Dames

Thesis presented for the Degree of
Doctor of Philosophy
in the Department of Biological Sciences
Faculty of Science
University of Cape Town
August 2021

Supervisor: A/Prof. Coleen L. Moloney
Co-Supervisors: Dr. Emma Rocke, Prof. Edward Rybicki and Dr. Maya Pfaff

Declaration

I, ... **Nicole Rebecca Dames**..., hereby declare that the work on which this thesis is based is my original work (except where acknowledgements indicate otherwise) and that neither the whole work nor any part of it has been, is being, or is to be submitted for another degree in this or any other university.

I empower the university to reproduce for the purpose of research either the whole or any portion of the contents in any manner whatsoever.

Signature: ……

Date: …….

Dedication

This thesis is dedicated to my parents Stephney and Brian who have led by example and always supported me in my “long” academic journey.

A special dedication to my grandmother, Hatwig Prins, who is the person I hope I grow up to become.

Acknowledgements

I would firstly like to acknowledge my supervisors without whom this PhD would not have been possible. Prof. Coleen Moloney, who gave me a chance to do research I never thought I would have the opportunity to do and allowed me the freedom to do it. Thank you for your invaluable advice and guidance not only in academics but also life. Dr Emma Rocke, for being a great friend and colleague. Thank you for trusting me and guiding me at every step of this thesis. Dr Maya Pfaff for your friendly energy, perspective, and your willingness to lend a hand or equipment and Prof Edward Rybicki for allowing me to get my fix of "lab" life and welcoming me into your lab.

I would like to acknowledge all the people who helped me collect and analyse samples during my PhD, Raquel Flynn, Dr Zimkhita Gebe, Sina Walschuss, Jessica Burger, Nwabisa Malongweni, Katherine Wallis and Dr Andrew Ndlovu. I would like to acknowledge Dr Grant Pitcher and Dr Sarah Fawcett for their invaluable knowledge surrounding biogeochemistry, oceanography, and St. Helena Bay. Thank you to Pieter Truter, Andre du Randt and Lisa Mansfield for support at sea. An additional thank you to the NRF for funding me personally and this research.

A big thank you to the Moloney lab for your friendship and the creation of a supportive lab that made being at UCT a great experience. Dr Zimkhita Gebe who became a friend as soon as we shared a car ride to Elands Bay. I learnt a lot in those first two weeks and what I learnt shaped my entire PhD.

Steffi, Annica, Keren and Vee for keeping me inspired and entertained, you guys are the best. To my oldest friends Zoë and Ange for the continued support and being the people who I can look up to.

Chris you are the best big brother. Thank you for the support, the love and the random weekend visits to Cape Town which made me miss home less. Mom, for the long chats every night on the drive home from work, allowing me talk through my ideas and struggles. You are the best friend, the best mom, and the most motivating person I know, thank you. Dad, thank you for listening to me work out research problems on the phone even though you don't understand. Without you guys I wouldn't be who I am.

***A special thank you to Uncle Harry and Aunty Rène, from whom I learnt a lot about family, fellowship and success.**

Abstract

Wind driven coastal upwelling influences the overall physical and chemical properties of coastal regions, as well as the small phytoplankton and microbial communities responsible for the productivity and biogeochemistry governing many of these properties. These environmental changes can influence picoplankton (0.3–3 µm) and nano-picoplankton (0.3–10 µm) at different time scales; in this thesis daily changes were of interest because of the cyclic (3–7 days) nature of wind-driven upwelling. Daily variability of picoplankton was studied during an upwelling cycle at a single station in Elands Bay. Using amplicon sequencing of the 16S and 18S rRNA gene region, as well as additional supplementary environmental data, it was found that picoplankton diversity, community structure and primary metabolism varied between the active and relaxation periods of an upwelling cycle. The results highlighted the complexity of picoplankton dynamics in variable environmental settings. However, the question then became whether nano-picoplankton dynamics were as complex in a post-upwelling setting. This was assessed in autumn (post-upwelling period) in St. Helena Bay by measuring primary productivity and nitrogen cycling over five days from three depths at a single station. Using stable isotope tracer and flow cytometry analyses it was determined that primary productivity was supported by regenerated production and that nano-picoplankton were responsible for up to 90% of the net primary production, with nanoeukaryotes and heterotrophic bacteria dominating at the surface and at depth. Increased resolution of nano-picoplankton community composition, structure and potential metabolism was obtained using metagenomic analyses of samples taken at the same depths and days as the productivity study. A strong depth-differentiation in community structure and potential metabolism was found over the five-day period, with little variability observed from day to day. Metagenome abundances of transporter genes for processes like ammonium uptake and nitrite oxidation were found to be good indicators of measured process rates using isotope tracers. This research has highlighted the complex structure of picoplankton and nano-picoplankton communities in a coastal setting, and has shown how diversity, function and biotic interactions are strongly influenced by the properties of the surrounding water column.

Table of Contents

1. Chapter 1: General Introduction

1.1. Marine plankton

Microorganisms inhabit all parts of the marine environment, from the deep-sea to surface waters. Marine plankton, which include microorganisms, drift passively via water currents (Newell and Newell, 1966). These organisms are categorized into log sizes as micro-, nano- and pico- size fractions. Of interest in this study are the picoplankton (0.3–3 µm) and nanoplankton (3–20 µm) and a combination of the two size groups referred to in this thesis as nano-picoplankton (0.3–10 µm), which are all important contributors to the total biomass of lower trophic levels (Vaulot et al., 2008; Worden and Not, 2008; Jardillier et al., 2010; Massana, 2011). These small planktonic prokaryotes and eukaryotes employ autotrophy (obtaining carbon through photosynthesis), heterotrophy (obtaining carbon from organic sources) and mixotrophy (using various degrees of heterotrophy and autotrophy) to grow and proliferate in the water column (Willey et al., 2011; Mitra et al., 2014, 2016). The nano- and picoplankton make up a large portion of planktonic abundances and play an important role in primary production and nutrient cycling in different parts of the ocean, from the open ocean to coastal systems.

1.2. The small eukaryotic plankton

The nano- and picoeukaryotes are a small, ubiquitous, heterogeneous group of protists ranging in size from 3–10 µm and 0.3–3 µm, respectively. These organisms can be photosynthetic, heterotrophic (Massana et al., 2006; Jürgens and Massana, 2008), symbiotic (Cachon and Caram, 1979; Worden and Not, 2008), parasitic (Guillou et al., 2008) or mixotrophic in nature (Worden and Not, 2008). As vital members of the marine food web, particularly as drivers of carbon export (photosynthesis), it is important to understand the contribution these small eukaryotic organisms make through their diversity and ecology (Guidi et al., 2016).

The small eukaryotes consist of a variety of “super-groups” like Alveolates, Archeaplastida, Centrohelids, Cryptophytes, Excavata, Haptophytes, Stramenopiles and Rhizarians (Massana, 2011). The Alveolates include dinoflagellates, ciliates,

apicomplexans (Guillou et al., 2008). Marine alveolates (MALV), are among the most dominant marine eukaryotic groups surveyed. Additionally, MALV lineages are known parasites of dinoflagellates, radiolarians, ciliates, and fish eggs (Coats et al., 2002; Guillou et al., 2010). Stramenopiles account for a large portion of the sequences archived in genome databases. This group consists of heterotrophic and chloroplast-containing organisms. Diatoms, chrysophytes, pelagophytes, dictyochophytes and bolidophytes are well represented in the databases as well (Vaulot et al., 2008). Most of the stramenopile sequences form part of the MAST (marine Stramenopiles) clade (Massana et al., 2006; Not et al., 2009). The heterotrophic stramenopiles include parasites, osmotrophs and bacteriovores. Rhizaria are the amoeboid protists (cercozoa, radiolaria and formanifera), whereas the prasinophytes (Archeaplastida) include the most well-known picoeukaryotes, namely Bathycoccus, Micromonas and Ostreococcus. Ostreococcus is the smallest eukaryote known, with a diameter of 0.8 µm, a genome of 13Mb and 8000 genes (Worden et al., 2009). Eukaryotes contribute the most (of the picoplankton groups) to biomass and primary production, but bacteria and archaea play equally important roles in marine microbial ecology (Karl, 2007; Yilmaz et al., 2016).

1.3. Bacteria and Archaea

Bacteria that are capable of photosynthesis also play an important role in global primary production (Falkowski et al., 1998). Archaea and bacteria are also key catalysers of biochemically important reactions involving macronutrients and micronutrients required by other members of the plankton. Research in marine microbiology over past decades has focused largely on identifying marine archaea and bacteria. With the advent of new molecular techniques and technologies this research has moved towards a focus on their ecology (Heidelberg et al., 2010).

Archaea were originally thought to be purely extremophiles, but researchers have discovered some taxa that are ubiquitous in the water column (Delong, 1992; Fuhrman et al., 1992; Delong, 1998; DeLong, 2021). The classification of archaea is rapidly changing, with a recent article describing in detail the changes in Archaeal phylogeny (Parks et al., 2020; Rinke et al., 2021). Members of archaeal Marine Group I, for example, are closely linked to the nitrogen cycle because of the capacity these organisms have for ammonia oxidation (Walker et al., 2010; Pester et al., 2011).

The most abundant bacterial phyla sequenced from marine environments include Actinobacteria, Bacteroidetes, Chloroflexi, Deferribacteres, Planctomycetes, Proteobacteria (Alpha-, Beta-, Delta- and Gamma-) and Verrucomicrobia. The Actinobacteria can make up 10% of the bacterioplankton and are ubiquitous in the marine environment, whereas the Bacteroidetes are known to associate with organic aggregates and higher trophic organisms like phytoplankton and sponges (DeLong et al., 1993; Eilers et al., 2001; Giovannoni and Stingl, 2005; Grossart et al., 2005; Webster and Taylor, 2012; Yilmaz et al., 2012). Perhaps the most extensively studied marine bacteria phylum, the Proteobacteria, includes the ubiquitous SAR11 clade, Alphaproteobacteria like Rhodobacterales and SAR116, the OMG clade and the Deltaproteobacteria SAR324 (Marine Group B) clade (Mullins et al., 1995; Fuhrman et al., 2006; Biers et al., 2009; Yilmaz et al., 2016). The ubiquitous phototrophic prokaryotic phylum, Cyanobacteria, includes two important members of the picoplankton, *Synechococcus* and *Prochlorococcus*. *Prochlorococcus* is known to be present from the surface to depths of ~150 m in often oligotrophic waters whereas *Synechococcus* is not thought to extend to great depths but has a wide geographical distribution that covers oligotrophic, mesotrophic, and nutrient-rich waters (Partensky et al., 1999a). Like the other archaea, bacteria and eukaryotes, the populations of these picophytoplankton are not only shaped by the environment but also by grazing and virus-mediated mortality (Suttle, 1994; McManus et al., 2007; Gobler et al., 2008; Jürgens and Massana, 2008; Rocke et al., 2015). While recognizing the significant roles grazers and viruses play in top-down control of microbial populations and biogeochemistry, it was beyond the scope of this thesis to enumerate and identify these groups.

1.4. Biogeochemical cycling and the microbial loop

The marine food web is the culmination of all the above-mentioned groups including larger eukaryotic phytoplankton and grazers, from the heterotrophs to the autotrophs and the viruses, in a cycle that runs the so-called biological pump (Fenchel, 1988). The biological pump refers to sequestration of carbon from the atmosphere to the deep ocean. In the ocean, eukaryotic and bacterial phytoplankton fix carbon in the form of CO_2 through photosynthesis in the euphotic zone. After their death or consumption by grazers, these particles form particulate organic matter (POM) which

sinks in the form of aggregates to increase sinking rates and are then stored in the sediments. Dissolved organic matter (DOM) is released and used by bacteria, feeding back into the food web, while inorganic nutrients are predominantly released by the heterotrophic remineralization of phytoplankton. Phytoplankton and bacteria are grazed upon by zooplankton, which in turn affect the abundance and, to an extent, the composition of these planktonic assemblages (Azam et al., 1983; Hahn and Höfle, 2006). The energy released in these processes is looped back to the phytoplankton, hence the term the microbial loop. Viruses, which form the most abundant microbial group in the ocean, commonly infect and lyse the phytoplankton and the bacteria, releasing their cell contents in the form of DOM into the surface waters. This is utilized by bacteria, contributing more carbon to the microbial loop in the surface waters (Fuhrman and Suttle, 1993; Suttle, 1994, 2007). Viruses also release growth-limiting macronutrients needed by the phytoplankton (nitrogen in the form of amino acids as well as iron and phosphate) as well as carbon-rich material from their hosts' cells which is exported to the deep ocean. This in turn increases the efficiency of the biological pump. It is these complex interactions that occur on short time scales, which are of primary interest in this thesis.

Marine microbial organisms play key roles in the biological pump, in nutrient recycling and overall primary production. It is important to improve understanding of the diversity of these groups and their potential to influence a large range of biogeochemical and biological processes. Understanding how these organisms interact with each other under a variety of environmental conditions, on a timescale befitting their small sizes and life spans, will benefit overall understanding of the marine food web and the cycling of important macro- and micro-elements like carbon, iron, nitrogen, phosphorus, sulphur, and oxygen. Two cycles of specific focus are that of carbon and nitrogen.

1.5. Productivity in coastal systems

The carbon cycle is important in describing the fertility of a marine environment. It is dependent on carbon fixation through photosynthesis, which is termed primary production (Falkowski et al., 2003). Net primary production, a metric used to describe the biomass gain of the food web (Eppley and Peterson, 1979), is controlled by environmental factors such as light, micronutrients and macronutrients and

temperature (Boyd et al., 2014). Physical, chemical, and biological processes in turn influence nutrient availability and light in the euphotic zone (**Figure 1.1**).

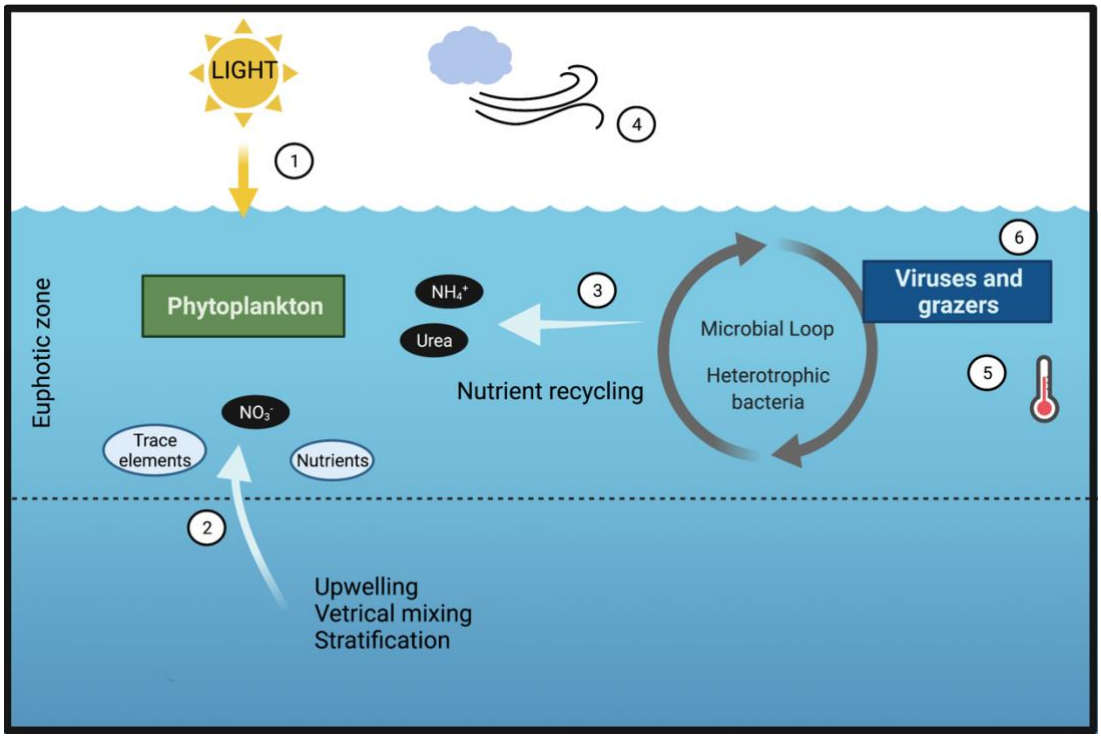

Figure 1.1. The environmental factors controlling primary production in the euphotic zone, adapted from Boyd et al. (2014). Primary production is controlled by (1) light availability; (2) introduction of new sources of nutrients, specifically nitrate from depth during periods of mixing and upwelling, and (3) regenerated sources of nutrients (ammonium and urea) from remineralisation of organic matter in the euphotic zone. These processes are dependent on physical, chemical, and biological processes, like (4) wind direction and speed and cloud cover. Temperature (5) is an important factor for the optimal growth of phytoplankton in the euphotic zone as well as the rate of heterotrophic bacterial remineralization. Viruses and grazers (6) are top-down controlling agents on the phytoplankton. Created with BioRender.com.

In the open ocean, nutrient rich deep waters are rarely mixed into the euphotic zone, resulting in lower chlorophyll concentrations and thus productivity in surface waters in comparison to net primary production rates found in coastal waters (Falkowski and Raven, 2013; Finkel, 2014). In coastal upwelling waters, which are the focus of this thesis, seasonal mixing of the relatively shallow water column and wind induced coastal upwelling introduce cold nutrient rich waters to the surface, supporting the growth of large concentrations of phytoplankton biomass. This high

rate of productivity is a key feature of a coastal upwelling ecosystem. The most important nutrient in supporting productivity is nitrogen, which is often a limiting factor for phytoplankton growth (Vitousek and Howarth, 1991). Nitrogen in the ocean comes in different forms, so growth can be supported by nitrate imported into surface waters from depth or by nitrogen sources that are cycled continuously in the euphotic zone, namely ammonium and urea. When a nitrogen source is introduced from depth and is supporting most of the net primary production in the euphotic zone, this production is termed new production (Dugdale and Goering, 1967). If productivity is supported by nitrogen sources such as ammonium or urea, which are recycled in the euphotic zone or introduced via nitrogen fixation, then it is referred to as regenerated production. It should be noted that there is also evidence for nitrification, specifically ammonia oxidation in the euphotic zone, which produces nitrate which can be contributing to regenerated production (Shiozaki et al., 2016).

The phytoplankton that are responsible for primary productivity include: cyanobacteria, diatoms, dinoflagellates and nanoflagellates (Falkowski et al., 2003). The most abundant of these phytoplankton depend on the region, season, and environmental conditions in the euphotic zone. Diatoms are most often the first to bloom after an injection of nutrients into the euphotic zone, succeeded by the dinoflagellates and nanoflagellates (Litchman, 2007). The carbon biomass produced by these phytoplankton is exported from the surface in the form of sinking aggregates or is remineralised into dissolved organic matter by heterotrophic organisms within the euphotic zone and throughout the rest of the water column. This dissolved organic matter as well as the faecal pellets from grazers, supports much of the microbial loop, which are predominantly responsible for the cycling of nitrogen.

Net primary production can be measured remotely or *in situ*. Satellite remote sensing uses ocean colour (chlorophyll) to estimate biomass changes over time as a proxy for primary production (Cullen, 2001). This method is often used to estimate global levels of net primary production, which is important to determine the global carbon budget. In addition, *in situ* measurements of productivity are more commonly used for accurate measures of primary production in a region at a specific time. Multiple techniques could be used to measure primary production like light-dependent changes in dissolved oxygen, light-dependent changes in dissolved inorganic carbon,

the ^{14}C method, the ^{13}C method and the ^{18}O method (Cullen, 2001). In this thesis the ^{13}C method was used to determine primary production rates.

1.6. Nitrogen Cycle: It all revolves around nitrogen

One of the most important biogeochemical cycles in the ocean is that of nitrogen (**Figure 1.2**). As a nutrient that is often limiting to primary production and microbial growth, understanding how it is cycled through out the water column is important in the study of overall microbial dynamics (Falkowski, 1997; Zehr and Kudela, 2011). There are major sources and sinks of nitrogen in the ocean, with biological nitrogen fixation and atmospheric deposition being the major sources and denitrification and anaerobic ammonium oxidation (anammox) being the sinks (Gruber and Galloway, 2008). There are many good review articles synthesising the current understanding of the marine nitrogen cycle (Zehr and Ward, 2002; Ward et al., 2007; Kuypers et al., 2018; Pajares and Ramos, 2019).

Briefly, nitrogen is fixed from the atmosphere (N_2 gas to ammonia (NH_3)) by diazotrophic organisms found in the surface waters (**Figure 1.2**). Diazotrophs, which include cyanobacteria (Villareal, 1992; Capone et al., 1997; Zehr et al., 2001, 2016; Thompson et al., 2012), heterotrophic and phototrophic bacteria, strict anaerobes, methanogenic Euryarcheota and Planctomycetes (Bombar et al., 2016; Delmont et al., 2018), contain the nitrogenase complex which is the catalyser for the nitrogen fixation process (Zehr et al., 2003). The biomarker used to study diazotrophs is often the *nif*H gene, which encodes for dinitrogenase reductase.

Nitrogen is also retained within the water column through processes like nitrification, which is a two-step aerobic process that oxidizes ammonia to nitrate. The two processes of nitrification are ammonia oxidation and nitrite oxidation. Ammonia oxidation, the oxidation of ammonia to nitrite, is carried out by ammonia-oxidising bacteria such as *Nitrosomonas*, *Nitrosospira* and *Nitrosococcus* (Purkhold et al., 2000) and more commonly ammonia-oxidising archaea in the Thaumarchaeota (Könneke et al., 2005) and Crenarchaeota phyla (Hallam et al., 2006; Wuchter et al., 2006). Ammonia oxidation is catalysed by the AMO enzyme encoded by the *amo*ABC operon and the biomarker most used in studying these organisms is *amo*A. Nitrite oxidoreductase (*nxr*ABC) catalyses the oxidation of nitrite into nitrate during nitrite oxidation. Nitrite oxidizing bacteria include the genera *Nitrospira* and *Nitrospina*

(Daims et al., 2016). Complete ammonia oxidation or comammox is the single step oxidation of ammonia nitrate in one organism (**Figure 1.2**) and has been shown to be a process present in members of lineage II within the *Nitrospira* (Daims et al., 2015). The activity of nitrifiers, as well as many of the other processes in the nitrogen cycle, are measured using not only genetic marker analyses but also stable isotope tracer analysis (Billen, 1976). Stable isotope analyses can produce a rate measurement, not unlike the use of transcriptomics and quantitative PCR (qPCR) analyses and are used to determine the active cycling of nitrogen through the nitrification process in an ocean system.

Another nitrogen retention process is dissimilatory nitrate reduction to ammonia (DNRA), which is an anaerobic process that reduces nitrate to nitrite and then to ammonia, or sometimes just nitrite to ammonia. Nitrate reduction produces nitrite, which is used in other nitrogen cycling processes, like nitrite oxidation and anammox and reduces nitrate in the same way as in denitrification. The intersection of DNRA with other nitrogen cycling processes underlines the importance of understanding the activity of each process when studying the nitrogen cycle, to get a holistic understanding of the system of interest. Nitrite reduction to ammonium is catalysed by cytochrome C nitrite reductase encoded by the *nrf*A gene, which is often the gene used to study DNRA in the environment (Welsh et al., 2014). Nitrogen loss processes also occur in anoxic and hypoxic (low oxygen) conditions, namely denitrification and anammox (**Figure 1.2**). After nitrate reduction, denitrification is then a stepwise reduction to nitric oxide then nitrous oxide and finally dinitrogen or nitrogen gas. Denitrifiers are found in both bacterial and archaeal populations. Anaerobic ammonia oxidation (Anammox) is the conversion of ammonium and nitrite to nitrogen gas. This process occurs in the absence of oxygen and is therefore common in the oxygen minimum zones (Pitcher et al., 2011; Dalsgaard et al., 2012, 2014) and sediments of the ocean (Dalsgaard et al., 2005; Bale et al., 2014). Anammox has been found in many *Candidatus* species in the Planctomyctetales order (van de Vossenberg et al., 2008; Kartal et al., 2012).

Particulate organic nitrogen (PON), in the form of aggregates, faecal pellets and dead cells, sinks and is remineralized to release various metabolites including ammonium, which is converted to NO_3^- through nitrification. There is also evidence of a possible cryptic-sulphur cycle linked to anammox processes and other nitrogen

cycling in oxygen-minimum zones (Canfield et al., 2010; Callbeck et al., 2018). Understanding the nitrogen cycle is therefore a vital part of studying the dynamics of smaller plankton as well the productivity of a marine system.

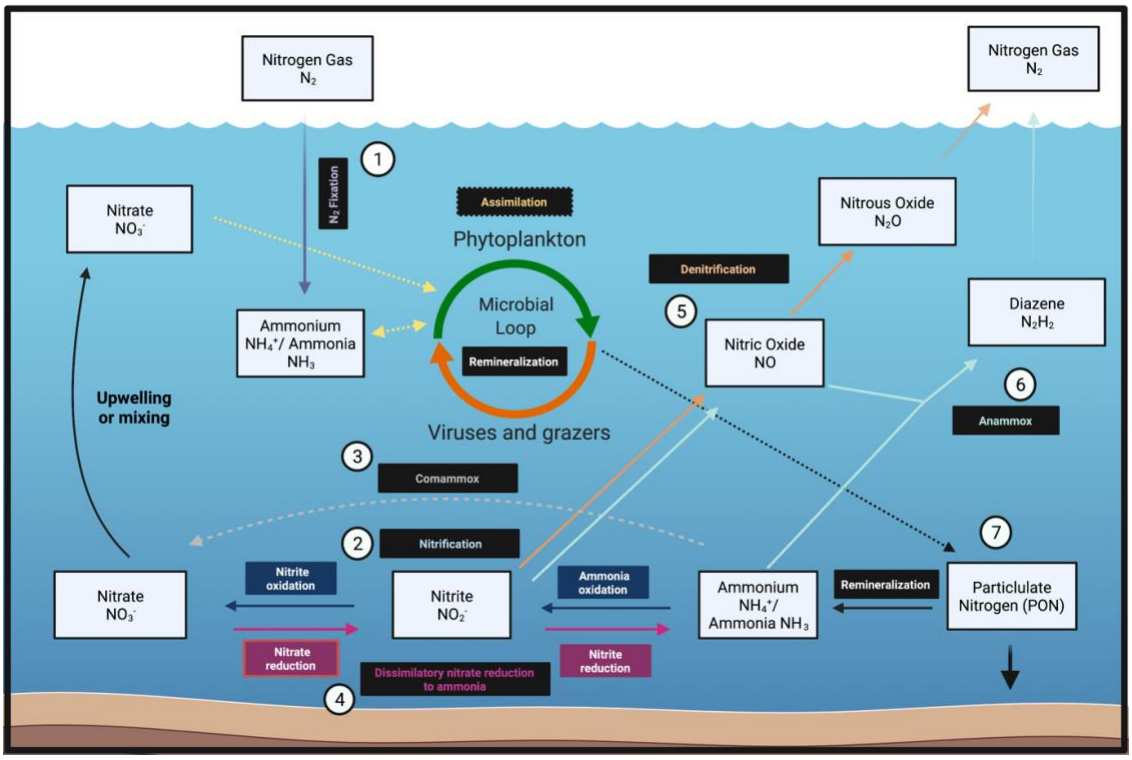

Figure 1.2. Processes involved in the marine nitrogen cycle adapted from the review article by Pajares and Ramos, 2019. Nitrogen is introduced into the marine environment via (1) nitrogen fixation and atmospheric deposition. It is regenerated or recycled within the water column aerobically via (2) nitrification and anaerobically via (3) comammox or (4) dissimilatory nitrate reduction to ammonia. Nitrogen is lost from the marine system through anaerobic processes like (5) denitrification and (6) anammox. Nitrate, ammonium, and other sources of nitrogen are assimilated by phytoplankton and bacteria in the microbial loop (in yellow). Phytoplankton (7) aggregate and sink and particulate organic nitrogen is introduced into the sediment this way.

1.7. Microbial dynamics

The study of these complex biogeochemical cycles in the ocean can happen at various scales, in time, physical space and size and is reflected in the variability in the structure and functioning of microbial communities. Studies of microbial dynamics have shown that there are patterns in the way that community compositions change, that can be predicted (Fuhrman et al., 2015). Time series of community composition and associated environmental variables provide insight in the factors that affect

microbial dynamics and help understand the complex interactions and feedback loops that characterize the functioning of microbial communities.

The increase in affordability and accessibility of sequencing technologies has allowed for more comprehensive sampling strategies, determining microbial dynamics through time series and across more space. Metabarcoding (16S and 18S rRNA) and "omics" (metagenomics, metatranscriptomics etc.) data help with the description of the communities as well as assist in predicting functionality but cannot be used alone to put microbes in the context of the environment. In order to understand the role of microbes in the marine environment, additional parameters need to be considered. Microbial dynamics refer to changes over time or space, and time series analyses of microbes and their surrounding environment are good ways to study these dynamics (Moncoiffé et al., 2000; Morris et al., 2005; Faust et al., 2015, 2018; Martin-Platero et al., 2018). Microbial dynamics can be influenced by physical, chemical, or biological factors, from light and water column mixing to injections of new nutrients and grazing by zooplankton. Depending on the question, all or a few of these factors would be important in understanding the dynamics of the community of interest. Different timescales are suitable for different questions. At an hourly rate, community changes will take place mostly in the fast-growing organisms (Fuhrman et al., 1985; Kuipers et al., 2000; Gilbert et al., 2010; Aylward et al., 2017; Hu et al., 2018) and at daily to weekly timescales the dynamics observed could be related to changes in the environment, such as upwelling or eddies (Needham and Fuhrman, 2016; Choi et al., 2018). Diel cycles or shifts are also present in many marine microbial communities like bacterioplankton (Kuipers et al., 2000), phytoplankton (Fuhrman et al., 1985), protists (Hu et al., 2018) and viruses (Aylward et al., 2017). Seasonal changes are observed over months and years as well as long-term variability introduced by climate change (Treusch et al., 2009; Collado-Fabbri et al., 2011; Gilbert et al., 2012; Suh et al., 2015; Bunse and Pinhassi, 2017; Ward et al., 2017; Auladell et al., 2019; Reji et al., 2020). There have been many studies focused on the long-term patterns in microbial dynamics, but few have looked at daily dynamics outside of studying environmental events. In coastal ecosystems where the physical environment and topography cause dynamic changes to the water column, studying daily microbial dynamics becomes a complex and interesting endeavour.

1.8. The Benguela: An Eastern Boundary Upwelling System

Eastern boundary upwelling systems (EBUS) are among the most productive marine ecosystems and, therefore, support a disproportionately large part of the world's fish catch. On the west coast of southern Africa is the Benguela upwelling system (BUS), one of the world's four major EBUSs. It extends from Angola to South Africa and is divided into the northern and southern Benguela by the Lüderitz upwelling cell off Namibia (27˚S) (Duncombe Rae, 2005). In summer, the southern Benguela upwelling system (SBUS) experiences consistent wind-driven upwelling cycles (typically lasting 3-7 days) during which there is active upwelling for a few days followed by a period of relaxation and then upwelling again (Hutchings et al., 2009). The high level of biomass produced in this highly productive region is retained close to the coast, because of the topography of the coastline and the continental shelf (Nelson and Hutchings, 1983; Shannon and Nelson, 1996). Inlets and bays facilitate water-mass retention and a concentration of particulate matter, including plankton. One such bay is St. Helena Bay, which is downstream of Cape Columbine, an upwelling cell within the SBUS (Hutchings et al., 2009).

1.9. St. Helena Bay

St. Helena Bay on the west coast of South Africa is a large embayment downstream, i.e. north, of Cape Columbine, a major upwelling centre within the greater southern Benguela upwelling region (Hutchings et al., 2009). The area is subject to intermittent, wind-driven upwelling during the austral spring and summer, when periods of active upwelling are interspersed by periods of wind relaxation (and occasional reversal), which usually recur on a 3–7 day cycle. The strong, short-term variability makes St. Helena Bay an ideal site to study picoplankton dynamics in relation to upwelling events. The bay is a retention zone for much of the productivity produced (Largier, 2020), making it a nursery ground for many commercially important fishes. In the post-upwelling seasons (autumn to winter) the water column becomes stratified, and the bottom waters of the bay are subject to hypoxic conditions due to the remineralization of much of the biomass that is produced during upwelling periods. These conditions are perfect to determine if nano- and picoplankton dynamics are variable on a daily timescale when the physical environment is not strongly influenced by weather conditions. Microbial composition during the upwelling season has been studied in the bay (Rocke et al., 2020); however, the nuances of the daily

dynamics of nano-and picoplankton in the bay is still unknown. The dynamic environment found in the bay, due to the topography and seasonal changes, makes it an ideal site to study the effect of the environment on small plankton and vice versa.

Therefore, the aim of this thesis is to characterize the short-term (daily) dynamics of nano-and picoplankton in the southern Benguela upwelling ecosystem, with a focus on St. Helena Bay.

1.10. Hypotheses

There have been few studies concerning short-term nano- and picoplankton dynamics in the southern Benguela, especially in recent years, and therefore there is a strong exploratory component to this thesis. Knowing the dynamic nature of the southern Benguela due to the short-term (daily) environmental changes caused by wind-driven upwelling, I hypothesize that there will be a corresponding short-term variability in picoplankton taxonomic diversity and metabolic functionality during an upwelling cycle, including enhanced levels of primary production, resulting in high levels of autotrophy among the picoplankton. I further hypothesise that, in the post-upwelling season, there will be less variability on a daily scale because episodic, large, nutrient inputs are curtailed. Productivity will be reduced, and picoplankton diversity will include autotrophic and heterotrophic elements. The taxonomic dynamics of nano-picoplankton will likely be driven by their individual metabolic potential in the context of the properties of the water column. Based on numerous studies from other ecosystems, I hypothesize that there will be discrete microbiomes associated with strong environmental gradients in this coastal ecosystem.

1.11. Thesis outline

To test these hypotheses, it is necessary to study the nano- and picoplankton in the context of their environment. This thesis identifies the nano- and picoplankton groups that are present in the ecosystem, investigates how their relative and absolute abundances change in relation to environmental variables, measures size-differentiated rates of primary production and nutrient uptake, and links these ecological measurements to inferred metabolisms and nutrient cycling in the water

column. The thesis is presented as five chapters, with the first chapter constituting the general introduction.

In **Chapter 2**, daily variability in picoplankton dynamics is investigated over 10 continuous days, which include a wind driven upwelling cycle in St. Helena Bay. The corresponding picoplankton (0.2-3 µm) dynamics is studied using 16S and 18S rRNA amplicon sequencing analysis and put into the context of supplementary biological and environmental data. Primary metabolism is inferred from the genetic data to place the taxa functionally in the context of the environment and to determine whether function also shows daily variability.

In **Chapter 3,** the daily variability in size-fractionated primary productivity and nitrogen uptake is investigated over five days in the post upwelling season (autumn) in St Helena Bay, using stable isotope analysis in the context of supplementary biological and environmental data. Specific phytoplankton groups in the nano- and pico- size range are identified to better define the roles of different phytoplankton groups in primary production and nitrogen uptake during this sampling period.

In **Chapter 4,** I take a closer inspection of taxonomic diversity and functional potential of the nano-picoplankton identified in Chapter 3 using shotgun metagenomic analysis. The daily dynamics of nano-picoplankton community structure and potential functionality is put into the context of the environment outlined in Chapter 3. The nitrogen cycle is the focus of the potential function analyses, to understand the cycling of nitrogen over this five-day period in autumn in St. Helena Bay

Chapter 5 is the concluding chapter, which synthesises the findings of my PhD and my experiences and insights, including the limitations of this research and potential future research directions.

2. Chapter 2: Variability in picoplankton dynamics during an upwelling cycle in the southern Benguela

2.1. Abstract

Pulsed, wind-driven coastal upwelling occurs in the southern Benguela ecosystem on a three to seven-day cycle during spring and summer. This study investigated how this short-term variability affected the dynamics of picoplankton (<3 µm) in coastal waters under active upwelling conditions. Picoplankton community sampling occurred once per day at a fixed station at two depths (surface and 10 m) during the upwelling season in November/December 2016, in a comprehensive 10-day expedition in St. Helena Bay. Spatial and temporal variability in community composition and structure was determined using Illumina sequencing of 16S and 18S rRNA amplicons. Bacterioplankton OTUs were more abundant in samples taken during the relaxation period after upwelling, changing from a *Rhodobacteraceae* and *Flavobacteriaceae*-dominated water column during mixing to an increase in *Nitrosopumilaceae* at depth after stratification. Picoeukaryotes showed no preference for a mixed or stratified water column but were more abundant in low oxygen samples. Compositional changes were not pronounced in the picoeukaryotes, which were dominated by the parasitic Syndiniales. Photoheterotrophic and autotrophic lifestyles dominated during active upwelling, when nutrients were abundant throughout the water column, and then shifted to a predominately heterotrophic lifestyle during stratification, when nutrients were exhausted at the surface. This study has revealed that picoplankton diversity, distribution and functionality can vary with the cycles of wind-driven coastal upwelling. The importance of the functional role of picoplankton on the interaction between taxa was highlighted in this dynamic system. These findings highlight the complexity of picoplankton dynamics and microbial interactions in St. Helena Bay and the implication of this complexity for biogeochemical cycling and carbon export.

2.2. Introduction

Microbial communities consisting of archaea, bacteria, and eukaryotes, and their associated viruses (Ducklow, 2000; Suttle, 2007; Falkowski et al., 2008), are the driving force behind biogeochemical cycling in the marine environment. Understanding how these communities change and interact over time and space is one of the fundamental aims of marine microbial ecology, as evidenced by the amount of research focused on this topic (Morris et al., 2005; Faust et al., 2015, 2018; Fuhrman et al., 2015; Choi et al., 2018; Hernando-Morales et al., 2018; Needham et al., 2018). The development of high throughput sequencing technologies has made it possible to investigate whole microbial communities at a fine resolution, improving understanding of microbial ecosystems across a range of scales, from large ocean gyres to localised coastal upwelling. Time series data in particular have allowed for the prediction and illumination of poorly understood processes in microbial community dynamics (Countway et al., 2010; Roux et al., 2017; Martin-Platero et al., 2018).

Analyses of time series of microbial communities typically have focused on discerning inter-annual and seasonal patterns by applying high resolution sampling at monthly and yearly intervals (Fuhrman et al., 2006; Gilbert et al., 2012; Teeling et al., 2012; Teeling et al., 2016; Hernando-Morales et al., 2018). These long time series provided evidence of clear temporal patterns in the response of bacterioplankton to environmental changes, but often did not identify short (e.g. daily), intense fluctuations in relative abundances of species or operational taxonomic units (OTUs) or the processes underlying this variability (Blaxter et al., 2005; Hatosy et al., 2013). In recent years, several high-resolution time series of microbial communities have shown rapid (daily to weekly) changes in bacterial, eukaryotic and viral communities due to biotic factors (Lindh et al., 2015; Needham and Fuhrman, 2016; Needham et al., 2018; Martin-Platero et al., 2018). These include the impacts of grazing, microbe-microbe interactions as well as viral lysis. High resolution time series are also needed to understand the influence of bottom-up, environmental processes on microbial picoplankton dynamics. Such factors might be expected to be important during active coastal upwelling conditions, which can exert both physical and chemical influences on microbial community structure and function (Pitcher et al., 1992). For instance, in a coastal zone of the Concepción upwelling system in Central Chile, researchers found that short-term biological productivity and plankton community structure were

variable depending on wind conditions, but these researchers did not identify the roles of specific taxa during these upwelling events (Daneri et al., 2012).

Coastal upwelling occurs in temperate coastal regions on the eastern boundaries of the ocean basins, when equatorward winds, together with the Coriolis force, advect surface waters offshore. These surface waters are replaced by cold, nutrient-rich water from depth. Coastal upwelling regions are very productive and often support large populations of commercially exploited fish (Hutchings et al., 2009). The Benguela ecosystem, on the west coast of southern Africa, is one of the four major eastern boundary upwelling systems in the world, the others being the California, Canary, and Humboldt systems (Nelson and Hutchings, 1983). In the southern Benguela, off the west coast of South Africa, seasonal upwelling occurs predominantly between Cape Agulhas and Lüderitz **(Figure 2.1**) (Hutchings et al., 2009). The microbial ecology of this coastal system has not been well studied, especially in recent years. During the 1980s and 1990s, several studies focused on bacterial, phytoplankton and microzooplankton community dynamics in the southern Benguela, both through field studies, microscosms and modelling efforts (Verheye-Dua and Lucas, 1988; Painting et al., 1989, 1992, 1993b; Brown et al., 1991; Pitcher et al., 1991). A comprehensive Eulerian "anchor station" study examined phytoplankton production and composition during upwelling, focusing specifically on the micro- and nanophytoplankton (Pitcher et al., 1991). This study found that phytoplankton followed a predictable succession in response to nutrient inputs from upwelling events, especially at higher taxonomic levels.

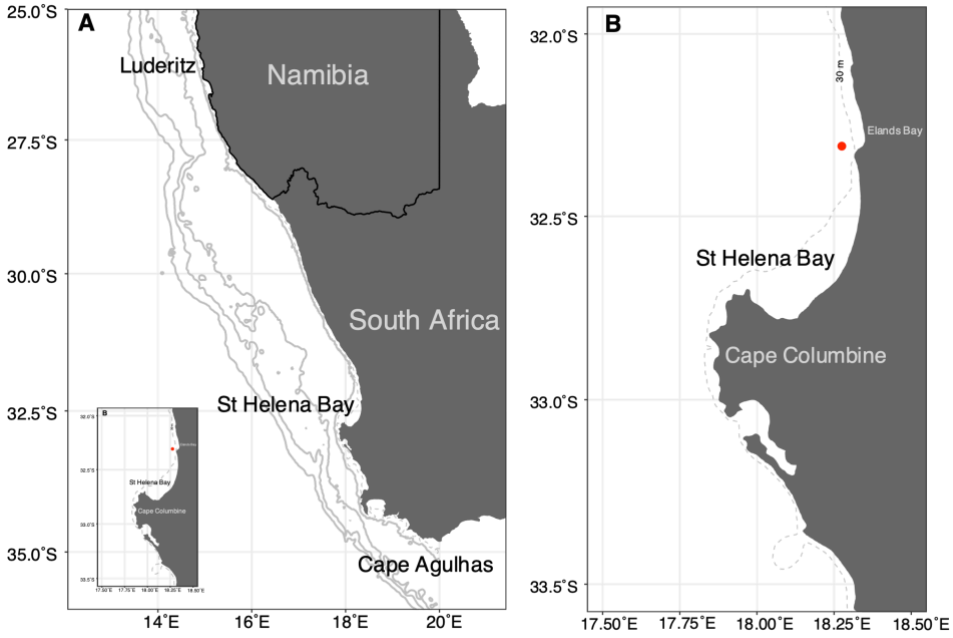

Figure 2.1. Maps showing the position of the sampling station in St. Helena Bay in relation to the whole southern Benguela. The (A) southern Benguela spans from Lüderitz to Cape Agulhas. The (B) red point (Lat: -32.306; Long: 18.275) indicates the fixed-point station where sampling was conducted for this study from 29 November to 8 December 2016.

Advances in molecular technologies and techniques now provide opportunities to study plankton communities at a greater resolution and accuracy than was possible in the past, in terms of both microbial size and taxonomic classification. This has made it possible to investigate previously overlooked groups, such as the relatively small picoplankton (0.2–3 µm). This group plays an important role in primary production and biogeochemical cycling and contributes to marine food webs as grazers and parasites (Azam et al., 1983). Picoplankton comprises mainly bacterial and archaeal groups (referred to as bacterioplankton in this study), including the ubiquitous and well-studied cyanobacterial genera *Prochlorococcus* and *Synechococcus* as well as several marine picoeukaryotic phylogenetic "super-groups" (Massana, 2011; Massana and Logares, 2013). The significance of these picoplankton during upwelling in the southern Benguela region has only recently been considered and so the role of picophytoplankton as well as other heterotrophic and chemo-autotrophic components of the microbial community are still poorly documented. A recent study of the seasonal variability in picoplankton community composition in the southern Benguela

upwelling region using amplicon sequencing analysis, found considerable variability in the structure of bacterioplankton and picoeukaryote communities in the St. Helena Bay area between the shelf and off shelf region as well as between seasons, and suggested that upwelling is a major driver of picoplankton dynamics (Rocke et al., 2020).

St. Helena Bay on the west coast of South Africa is a large embayment downstream, i.e. north, of Cape Columbine, a major upwelling centre within the greater southern Benguela upwelling region (Hutchings et al., 2009). The area is subject to intermittent, wind-driven upwelling during the austral spring and summer, when periods of active upwelling are interspersed by periods of wind relaxation (and occasional reversal), which usually recur on a 3–7 day cycle. This strong, short-term variability makes St. Helena Bay an ideal site to study picoplankton dynamics in relation to upwelling events. To determine the interactions between different taxa in relation to upwelling events, this study aims to assess microbial variability during a 10-day upwelling event in terms of both structure and functioning of the communities. This study is part of an interdisciplinary project that examines daily changes in a range of physical, chemical and biological variables at a coastal site in St. Helena Bay during early summer (Burger et al., 2020; Gebe et al., unpublished). Using an Eulerian approach, daily changes in the abundances of various picoplankton groups in response to active upwelling are observed over a 10-day period in the upwelling season. A Eulerian approach was used due to the limitations of the sampling equipment. Samples from two depths (surface waters and 10 m) are collected to provide genetic material, from which regions of the 16S and 18S ribosomal RNA (rRNA) genes are amplified and sequenced. Concurrent physical-chemical and biological measurements are used to determine whether environmental factors drive picoplankton community succession. This study provides new information on microbial diversity in St. Helena Bay and contributes to understanding the succession and associations of picoplankton groups during an active upwelling event in the southern Benguela.

2.3. Materials and Methods

Sample collection

Samples were collected at a single station with a water depth of ~30 m in St. Helena Bay, South Africa (32˚18’ 21.6” S, 18˚16’30” E) from November 29th to December 8th, 2016 (**Figure 2.1B**). Sampling was conducted from the MA-RE 1, a 7.3-m Gemini semi-rigid inflatable raft. All seawater samples were taken using a 5 L hand-held Niskin bottle at 0 m and 10 m. A RBRconcerto CTD was used to measure the temperature, salinity, and oxygen concentrations in the water column on day 1. This CTD malfunctioned and a Seabird 1900 plus CTD was used to record these variables from day 5 to day 10. Temperatures for the three missing days (day 2, 3 and 4) were inferred from the strong statistical regression (R = 0.8253) between temperature (˚C) and nitrate concentration (µmol. L^{-1}) (Burger et al., 2020).

Duplicate unfiltered 50 mL seawater samples were taken at five depths (surface, 5 m, 10 m, 15 m and 20 m) for nutrient measurements and stored at –20˚C until further analyses (Burger et al., 2020). Dissolved oxygen samples were collected from the same depths in 300 mL glass bottles (Burger et al., 2020). For chlorophyll *a* (Chl-*a*) measurements, water was collected in 2 L opaque HDPE bottles from the surface, 5 m, 10 m, 15 m and 20 m (Burger et al., 2020). Samples for DNA extraction were collected from the surface and 10 m in 1 L acid washed bottles and processed.

Sample processing

After the Chl-*a* samples in the 2 L opaque HDPE bottles were homogenised, 1 L of the sample was filtered through a 10 µm (47 mm diameter) polycarbonate filter, 500 mL through a 3 µm (47 mm diameter) polycarbonate filter and another 500 mL through a 0.2 µm polycarbonate filter. The filters were stored at –20˚C until further analyses.

Each DNA sample was first pre-filtered through a 200 µm mesh, then the resulting filtrate was sequentially filtered through 10 µm, 3 µm and 0.2 µm 47 mm diameter polycarbonate filters. All filters were immediately flash-frozen in liquid nitrogen and stored at -80°C until processing.

Hydrography and biogeochemistry

The potential density anomaly (σ_θ; $kg.m^{-3}$) was calculated using absolute salinity ($g.kg^{-1}$) and temperature. The daily mixed layer depth (MLD) of the water column was calculated using σ_θ and the surface (0 m) as the reference value, according to the criteria set out by de Boyer Montégut et al. (2004). Each depth was successively examined until one was found with a density that differed from the reference value by more than 0.03 $kg.m^{-3}$; this depth was assigned as the MLD for that day (**Table S2.1**).

The methods for the measurement of Chl-*a*, dissolved oxygen, inorganic nutrient (ammonium (NH_4^+), nitrate (NO_3^-), nitrite (NO_2^-), phosphate (PO_4^{3-}) and silicate (SiO_2^{4-})) concentrations and the calculation of the mixed layer depth are discussed in detail in Burger et al. (2020). In brief, concentrations of $NO_3^- + NO_2^-$ and SiO_2^{4-} were measured using the Lachat QuikChem® Flow Injection Analysis platform, while NO_2^- and PO_4^{3-} concentrations were measured colorometrically with a Thermo Scientific Genesys 30 visible spectrophotometer, respectively using the methods of Grasshoff et al. (1983) and Murphy and Riley (1962). Ammonium and Chl-*a* concentrations were measured fluorometrically on a Turner Designs Trilogy fluorometer, respectively using the methods of Holmes et al. (1999) and Welschmeyer (1994). Dissolved oxygen samples were analysed using the Winkler method (Golterman, 1983). Particulate organic carbon (POC) and nitrogen (PON) concentrations were measured using a Thermo Delta V Plus isotope mass ratio mass spectrometer interfaced with a Flash 2000 elemental analyser (EA-IRMS).

A biplot was produced using principal component analysis from the factoextra package (Kassambara and Mundt, 2020) to visualise groupings of the different sample depths and days based on the contributions of the measured metavariables. In this study samples were analysed according to the identified upwelling periods (active and relaxation), upwelling water column status (mixed, upper mixed layer (UML) and bottom layer (BL) and oxygen status (oxic and low oxygen (<2 $mL.L^{-1}$)). These classifications of the water column were determined from the hydrographic data in Burger et al. (2020).

DNA extraction, amplification, and sequencing

Biomass filtered onto the 0.2 µm polycarbonate filters was used to study the picoplankton (0.2–3 µm size fraction). Filters were sterilely cut, and DNA was

extracted using the QIAGEN® DNeasy® Blood and Tissue Kit (Qiagen, USA) according to the manufacturer's protocol. DNA quality and quantity were assessed by the ratio 260/280 nm and 260/230 nm using a Nano Drop ND- Spectrophotometer (NanoDrop Technologies Inc., Wilmington, DE) as well as through a 2% agarose gel stained with ethidium bromide in the lab and with a Qubit® 2.0 fluorometer at Novogene, where sequencing was done. Samples for day 2, 3 and 5 at 1 m and day 2 and 3 at 10 m did not have enough good quality DNA for sequencing after extraction. There was not enough good quality DNA from samples taken from 1m on day 6 and 7 and 10 m on day 4 for both 16S and 18S rRNA sequencing. After DNA quality and quantity determination, metabarcoding was done on 13 samples, carried out using the 16S ribosomal RNA (rRNA) V3-V4 primer set 341F (5'-CCTAYGGGRBGCASCAG-3') and 806R (5'-GGACTACNNGGGTATCTAAT-3') (Muyzer et al., 1993; Caporaso et al., 2011). The V4 region of the 18S ribosomal RNA gene was amplified from 15 samples using the barcodes TAREUK454FWD1 (5'-CCAGCASCYGCGGTAATTCC-3') and TAREUKREV3 (5'-ACTTTCGTTCTTGATYRA-3') to identify the picoeukaryote community in each sample (Stoeck et al., 2010). All PCR reactions were carried out with Phusion® High-Fidelity PCR Master Mix (New England Biolabs) and MID adaptor linked primers. Amplifications were verified on a 2% agarose gel stained with ethidium bromide. PCR products were mixed in equidensity ratios and then purified with Qiagen Gel Extraction Kit (Qiagen, USA). The libraries were generated with TruSeq® DNA PCR-Free Sample Preparation Kit and quantified via Qubit and qPCR and sequenced using the HiSeq Illumina platform.

Bioinformatics

Paired-end reads were assigned to samples based on their unique barcode and truncated by cutting off the barcode and primer sequence. Paired-end reads were merged using FLASH (V1.2.7). Quality filtering on the raw tags was performed under specific filtering conditions to obtain high-quality clean tags according to the Qiime (V1.7.0) quality-control process (Caporaso et al., 2010). Samples that successfully passed the quality control after 16S rRNA amplification were surface samples from days 1, 4, 6-10 and 10 m samples collected on days 1 and 5-10. For the 18S rRNA

amplification, samples that successfully passed the quality control were from the surface on days 1, 4, and 6-10 and from 10 m on days 1 and 4-10.

Subsequent sequence analysis was performed using MOTHUR version 10.14 following the MiSeq SOP (Schloss et al., 2009; Kozich et al., 2013). All the resulting sequences were further screened by removing low-quality reads, such as reads shorter than 300 nucleotides, incomplete or inaccurate primer sequences, chimeras, and reads with unidentified nucleotides present. A 97% cut-off was applied to all sequences for subsequent analysis using MOTHUR and the final numbers of sequences and operational taxonomic units (OTUs) for both 16S and 18S rRNA libraries can be found in **Table 2.1** and **Table 2.2**. To assign each OTU, the Silva version 138 reference database was used for bacterioplankton (16S rRNA) and the PR2 version 4.12 database for picoeukaryotes (Guillou et al., 2012; Quast et al., 2013; Yilmaz et al., 2014; Glöckner et al., 2017). Operational taxonomic units (OTUs) classified as chloroplasts, mitochondria and metazoa were excluded from further analysis. Family level taxonomic assignment was used for most analyses, as it is the highest taxonomic unit with the most physiological and ecological information available without losing broader ecological meaning. Computations were performed using facilities provided by the University of Cape Town's ICTS High Performance Computing team: hpc.uct.ac.za.

Table 2.1. 16S rRNA quality sequencing reads, observed OTUs, diversity, evenness and coverage for samples with corresponding identified upwelling condition

Sampling Day	Date	Upwelling condition	Water column status	Depth	Quality 16S rRNA Reads	Number of OTUs (97%)	Evenness	Shannon diversity index	Coverage
Day 1	29/11/2016	Upwelling	Mixed	Surface	36921	961	0.123	2.913	0.983
Day 4	2/12/2016	Upwelling	Mixed	Surface	39449	858	0.130	2.986	0.987
Day 8	6/12/2016	Relaxation	UML	Surface	54952	1145	0.133	3.816	0.991
Day 9	7/12/2016	Relaxation	UML	Surface	38069	574	0.142	3.274	0.994
Day 10	8/12/2016	Relaxation	UML	Surface	61318	895	0.133	3.331	0.993
Day 1	29/11/2016	Upwelling	Mixed	10 m	39475	613	0.136	2.999	0.991
Day 5	3/12/2016	Upwelling	Mixed	10 m	44481	454	0.158	4.271	0.997
Day 6	4/12/2016	Relaxation	BL	10 m	53928	1704	0.127	3.981	0.984
Day 7	5/12/2016	Relaxation	BL	10 m	63555	1473	0.132	4.344	0.990
Day 8	6/12/2016	Relaxation	UML	10 m	46067	1391	0.127	3.642	0.983
Day 9	7/12/2016	Relaxation	BL	10 m	41201	1153	0.134	3.904	0.986
Day 10	8/12/2016	Relaxation	BL	10 m	50978	862	0.140	3.797	0.991

(active upwelling vs. relaxation) and water column status (UML =upper mixed layer; BL = bottom layer) taken from the surface and 10 m on the 28 November 2016–8 December.2016.

Table 2.2. 18S rRNA quality sequencing reads, observed OTUs, diversity, evenness and coverage for samples with corresponding identified upwelling condition (active vs. relaxation) and water column status (UML = upper mixed layer; BL = bottom layer) taken from the surface and 10 m on the 28 November 2016—8 December 2016.

Sampling Day	Date (D/M/Y)	Upwelling condition	Water column status	Sampling Depth	Quality 18S rRNA reads	Number of OTUs (97%)	Evenness	Shannon diversity index	Coverage
Day 1	29/11/2016	Upwelling	Mixed	Surface	53147	493	0.090	1.972	0.997
Day 4	2/12/2016	Upwelling	Mixed	Surface	57668	409	0.130	2.478	0.997
Day 6	4/12/2016	Relaxation	UML	Surface	55811	624	0.109	2.053	0.995
Day 7	5/12/2016	Relaxation	UML	Surface	31010	209	0.120	2.134	0.997
Day 8	6/12/2016	Relaxation	UML	Surface	57097	290	0.091	1.667	0.998
Day 9	7/12/2016	Relaxation	UML	Surface	73116	560	0.115	2.510	0.997
Day 10	8/12/2016	Relaxation	UML	Surface	45209	308	0.040	0.880	0.997
Day 1	29/11/2016	Upwelling	Mixed	10 m	39983	607	0.047	1.157	0.993
Day 4	2/12/2016	Upwelling	Mixed	10 m	52118	570	0.137	2.680	0.995
Day 5	3/12/2016	Upwelling	Mixed	10 m	57068	839	0.139	3.896	0.993
Day 6	4/12/2016	Relaxation	BL	10 m	31130	950	0.096	2.612	0.985
Day 7	5/12/2016	Relaxation	BL	10 m	53640	672	0.114	2.863	0.995
Day 8	6/12/2016	Relaxation	UML	10 m	56807	838	0.106	2.710	0.994
Day 9	7/12/2016	Relaxation	BL	10 m	61410	599	0.100	2.291	0.996
Day 10	8/12/2016	Relaxation	BL	10 m	61802	562	0.073	1.657	0.996

Alpha diversity

The bacterioplankton (16S rRNA) and picoeukaryote (18S rRNA) community diversity (observed richness, Shannon index, evenness, and coverage) were estimated using the summary single command in Mothur. These indices were compared for both communities between the identified periods of an upwelling cycle, upwelling water column types and the two oxygen states. After checking for normality and homoscedasticity, either a two-sample t-test or a Wilcoxon rank sum test was used for the comparisons between periods of the upwelling cycle and between the two oxygen states, using a significance level of 0.05. To compare diversity measurements between upwelling water column types (mixed, UML, BL), an ANOVA was performed with a Tukey HSD post hoc test to identify significant differences.

Beta diversity

Bacterioplankton and picoeukaryote abundance data were normalised to the median sequencing depth. For each picoplankton group, weighted unifrac distances were calculated in Mothur following the MiSeq SOP guidelines (Kozich et al., 2013). PERMANOVAs were performed on the distance matrix to identify factors (day, depth, identified upwelling water types, oxygen state and upwelling period) and environmental variables that significantly influenced variability between samples. Non-metric multidimensional scaling (NMDS) analysis was used to visualise the variability between samples. Canonical correspondence analyses (CCA) were done on log-transformed bacterioplankton and picoeukaryote abundances, constrained with the selected upwelling-relevant environmental variables. The CCA was visualized using the ggord function in R (Beck, 2019).

Differential abundances and SIMPER analysis

The differential abundances between upwelling periods and between oxygen states were calculated for the families that represent at least 1% of reads in at least one sample of the bacterioplankton (30 families) and picoeukaryotes (46 families), using the MicrobiomeSeq package (Ssekagiri et al., 2017; Torondel et al., 2016). SIMPER (similarity percentage) analysis was performed to identify families that contribute significantly to the dissimilarity between samples from different upwelling periods,

water types and oxygen states. All analyses were run using vegan and phyloseq packages (R Core Team, 2013; Oksanen, 2016).

Flow cytometry

To enumerate the picoplankton, specifically *Synechococcus*, *Prochlorococcus* and picoeukaryotes, fresh samples were run through a BD Accuri C6 flow cytometer (Gebe et al., unpublished). In total, 60 samples (10 days of two depths in triplicate) were analysed. Picoplankton communities were enumerated following the method of Marie et al. (1997) and van Dongen-Vogels et al. (2011). FlowJo® version 9 was used to analyse the flow cytometric data, by analysis of the signals emitted on the orange (phycoerythrin PE: 585/42 band pass) versus red (phycocyanin PC: 661/16 band pass) and chlorophyll fluorescence signals. *Synechococcus* numbers were distinguished from picoeukaryotes through their higher PE signal. *Prochlorococcus* numbers were identified according to their Chl-*a* signal.

Functional group assignments

The bacterioplankton families that represent 1% of reads in at least one sample were assigned primary metabolisms according to known taxonomic information (**Table S2.2**). The top 46 picoeukaryote families were assigned functional groups based on the functional trait table of marine protists developed by Ramond et al. (2018, 2019) (**Table S2.3** and **S2.4**). In the marine protist FLAT (floating autotrophs) are defined as non-swimming abilities vs SWAT (swimming autotrophs) can swim. A PERMANOVA was performed using a Bray-Curtis dissimilarity distance matrix to determine whether there was a difference in functional group composition between upwelling periods, upwelling water types and oxygen states for bacterioplankton and picoeukaryotes. These differences were visualised using a NMDS plot. As with community taxon structure, CCA analysis was performed on function compositional data following the same method.

Network analysis

Spearman rank correlations were calculated using the Hmsic package for log-transformed abundance data of the same bacterioplankton and picoeukaryote families

for which function was assigned (**Table S2.3** and **S2.5**) (Harrell and Dupont, 2020). Data pairs that had Spearman rank correlations with values > 0.7 and < -0.7 and that were statistically significant ($p < 0.01$) were used to create the co-occurrence network. The network was created with igraph and visualized in Cytoscape version 3.180 (Csardi and Nepusz, 2006). The functional assignments of the OTUs included in the co-occurrence network were incorporated in the node labels. As there are not enough samples to add weight to any interactions, the co-occurrence network is used as a visualization tool to infer broad hypothetical relationships.

Data availability

Sequences are archived in the European Nucleotide Archive under the project accession number PRJEB29578 and sample accessions ERS2890520-ERS2890569.

2.4. Results

Environmental characterisation of the water column during upwelling periods

This study was performed during a period of wind-driven upwelling in St. Helena Bay (**Figure 2.2**, **Figure S2.1**). The physical and biogeochemical characteristics of the water column at the sampling site over the 10-day sampling period are discussed in detail by Burger et al. (2020). Briefly, the hydrography of the water column separated into two distinct periods of an upwelling cycle: (1) active upwelling with potential density (σ_θ) showing a well-mixed water column on the first five days followed by (2) a period of relaxation and stratification from day 6 to day 10 (**Figure 2.2A**). The surface mixed layer on days 6 and 7 increased in depth on day 8, after which the bottom of the mixed layer shoaled again on days 9 and 10, corresponding to an upward mixing event on day 9 (Burger et al., 2020). During the sampling period three different water types were identified from which the picoplankton communities were sampled: (1) active upwelling (mixed), followed by relaxation and stratification when the samples were taken from either (2a) the upper mixed layer (UML) or (2b) the bottom layer (BL) (**Table 2.1** and **2.2**, **Table S2.1**).

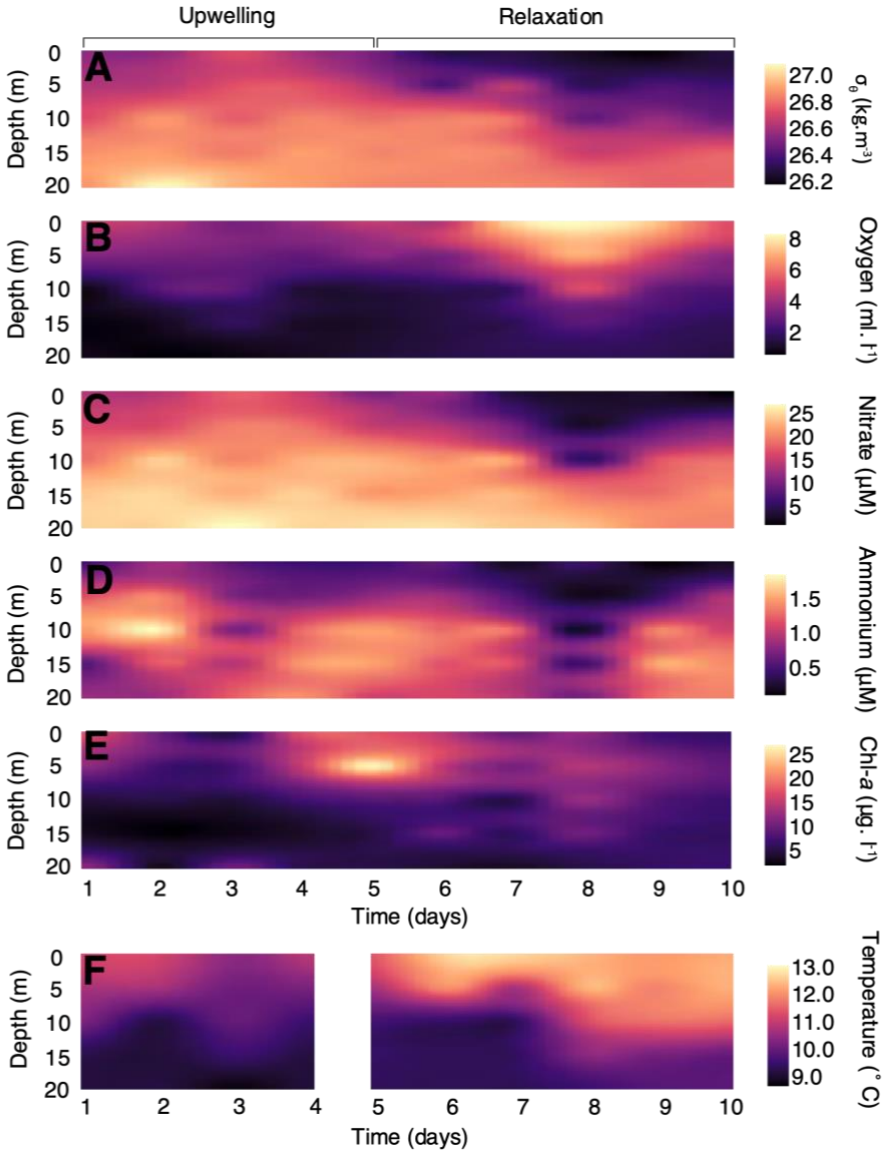

Figure 2.2. Water column distribution of physical and chemical variables (A) potential density anomaly σθ (kg.m^{-3}), (B) oxygen (ml.L^{-1}), (C) nitrate (µM), (D) ammonium (µM), (E) chlorophyll *a* (µg.L^{-1}) and (F) temperature (˚C) for the duration of the experiment. Note that nitrate is nitrate minus nitrite. Days 1-5 represent active upwelling conditions while days 6-10 are the relaxation period.

Samples from 10 m were defined as low-oxygen (< 2.0 mL.L^{-1}) on day 1 and days 4–6 (**Figure 2.2B**, **Table S2.2**). Nitrate concentrations were greater at 10 m (5.04 to 24.34 µM) than at the surface (0.96 to 17.60 µM) on each day of sampling (**Figure 2.2C**). Concentrations of particulate organic matter (POM) were consistently larger at the surface than at depth, with the largest concentrations at the surface on

day 8 (POC: 80.46 µM and PON: 10.66 µM) (**Table S2.2**). On average, mean (± SE) chlorophyll concentrations increased from day 4 (12.09 ± 0.76 $\mu g.L^{-1}$) onward, with a peak at 5 m on day 5 (**Figure 2.2E**). The deeper mixed layer of 15 m on day 8 corresponded with the highest concentration of chlorophyll at 10 m (12.55 $\mu g.L^{-1}$) (**Table S2.2**).

The biplot from the principal component analysis separates the samples at the surface from those at 10 m, with nutrient concentrations higher in samples at depth while biomass (POM, Picoeukaryote, *Synechococcus* and *Prochlorococcus* abundance), oxygen and temperature increase at the surface (**Figure 2.3**). Most of the variability is accounted for along the first principal component (Dim 1; 59.9%). The 10-m sample on day 8 is grouped with the surface samples, which is expected because the mixed layer extended to 15 m on that day (**Table S2.1**).

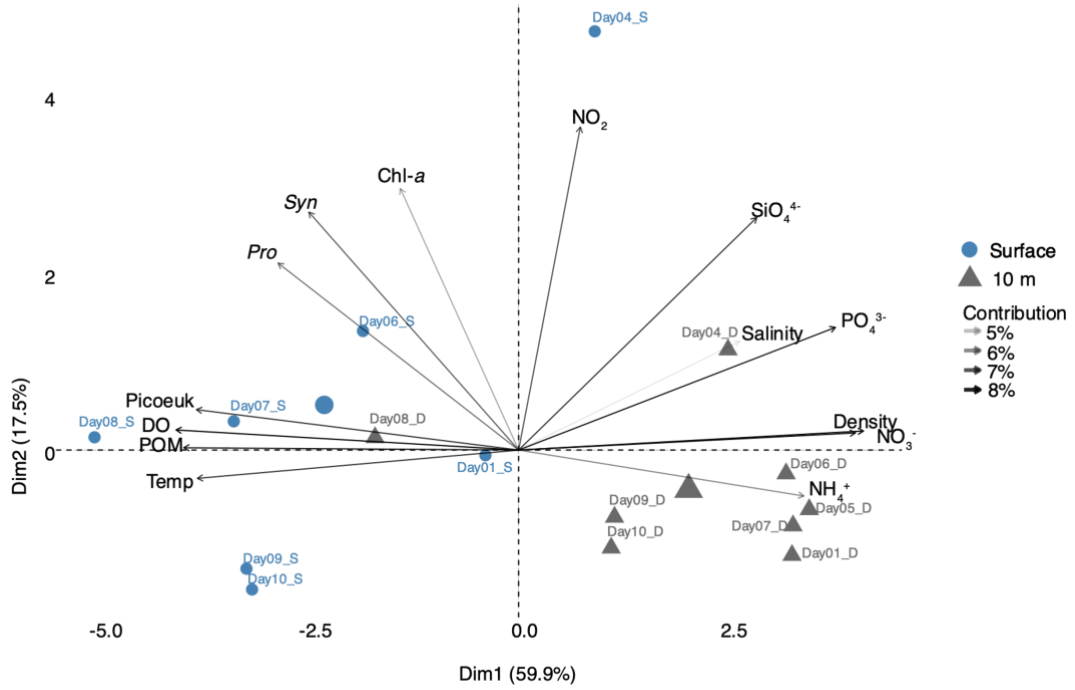

Figure 2.3. Principal component analysis (PCA) Biplot of the days and depths where samples were taken. The variability associated with each dimension or principal component are indicated on the x and y axis. The influence of metavariables on the principal components are shown here as eigenvectors. The more the metavariables influence a principal component the darker the shade of grey of the arrow. Surface ('S') samples are indicated as blue circles while 10 m ('D') samples are grey triangles. The larger blue circle and grey triangle indicate the mean of surface and depth samples, respectively. Chl-a=Chlorophyll a; DO=Dissolved Oxygen; POM=Particulate Organic Matter; Picoeuk=Picoeukaryotes; *Syn=Synnechococcus*; *Pro=Prochlorococcus*; Temp=Temperature.

Bacterioplankton diversity

The 16S ribosomal RNA (rRNA) sequence libraries resulted in a total of 570 394 reads from which a total of 12 083 OTUs were classified (after removal of chimeras, chloroplasts and mitochondria), of which 6 001 were taxonomically unique/distinct OTUs. Species diversity was greatest on day 5 (Shannon index: 4.271) and day 7 (Shannon index: 4.344) at 10 m (**Table 2.1**). Observed richness (number of OTUs) ranged from 454 (day 5 at 10 m) to 1 704 (day 6 at 10m) OTUs (**Figure 2.4C**, **Table 2.1**), with evenness indices between 0.123 (day 1 at the surface) and 0.158 (day 5 at 10 m). There were no significant differences respectively for diversity and evenness

between upwelling periods ($W_{diversity}$=7, n=12, p=0.15; $W_{evenness}$=16, n=12, p=1.00) and oxygen states ($t_{diversity}$=-1.54, df=10, p=0.16; $W_{evenness}$=13, n=12, p=0.68). However, the observed richness of bacterioplankton communities differed between active upwelling and relaxation periods (t=-2.10, df=10, p=0.06), with higher richness during the relaxation period (**Figure 2.4C**, **Table 2.1**). Richness did not vary between oxygenated and low oxygen samples. Diversity did not differ between the mixed water column, the upper mixed layer and the bottom layer.

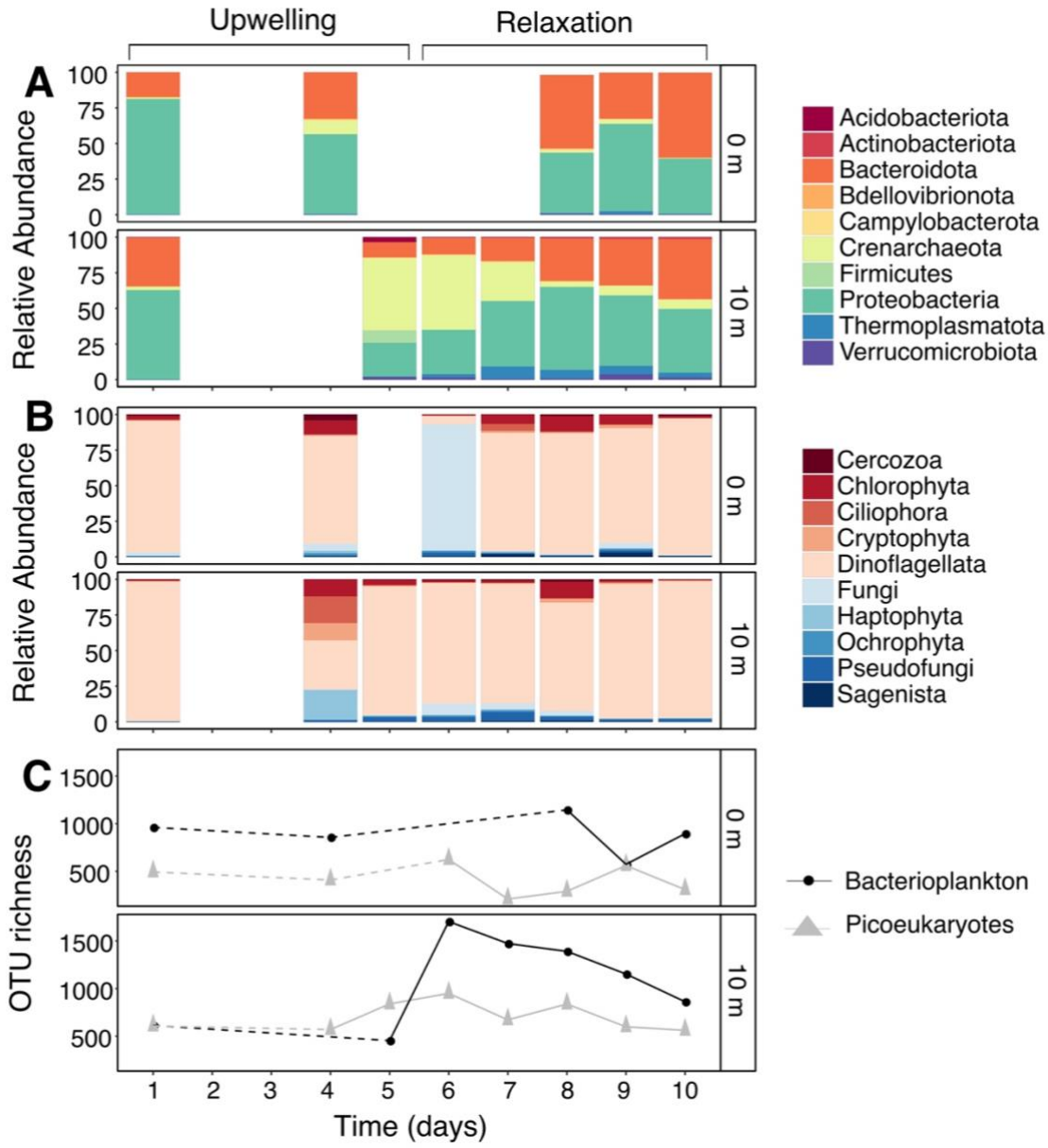

Figure 2.4. The top 10 phyla of (A) bacterioplankton and (B) picoeukaryotes throughout the experiment from the two sampling depths (0 m and 10 m). (C) The OTU richness of each sample for the bacterioplankton (black) and picoeukaryotes (grey) for the 10 day sampling period from the two depths. Dashed lines connect non-sequential (days) samples while solid lines connect continuous (days) samples.

Bacterioplankton community structure

Fifty-five bacterioplankton phyla were identified in the 12 samples. Most OTUs belonged to the phyla Proteobacteria (45%, including Rhodobacterales, Burkholderiale and Oceanospirillales) and Bacteroidota (22%, Flavobacteriaceae) (**Figure 2.4A**). The most abundant archaeal phylum was Crenarchaeota (3%,

specifically *Candidatus Nitrosopumilus* and *Candidatus Nitrosopelagicus*), with the highest abundances found at depth (**Figure 2.4A**). The bacterioplankton OTUs with greatest relative abundance belonged to the genera *Amylibacter* (16%), *Aurantivirga* (10%) and *Planktomarina* (8%).

Bacterioplankton samples grouped according to the physical or chemical characteristics of the water column, based on weighted unifrac distances (**Figure 2.5**). The bacterioplankton communities differed significantly in the water types associated with different stages of an upwelling event (**Figure 2.5B**; PERMANOVA: R^2=0.359, p=0.015), specifically between the mixed water column and the bottom layer (PERMANOVA $_{\text{Mixed vs. BL}}$: R^2=0.327, p=0.021); but not significantly different between upwelling periods (**Figure 2.5A**; PERMANOVA: R^2=0.186, p=0.055) or between oxygen states (**Figure 2.5C**; PERMANOVA: R^2=0.184, p=0.056).

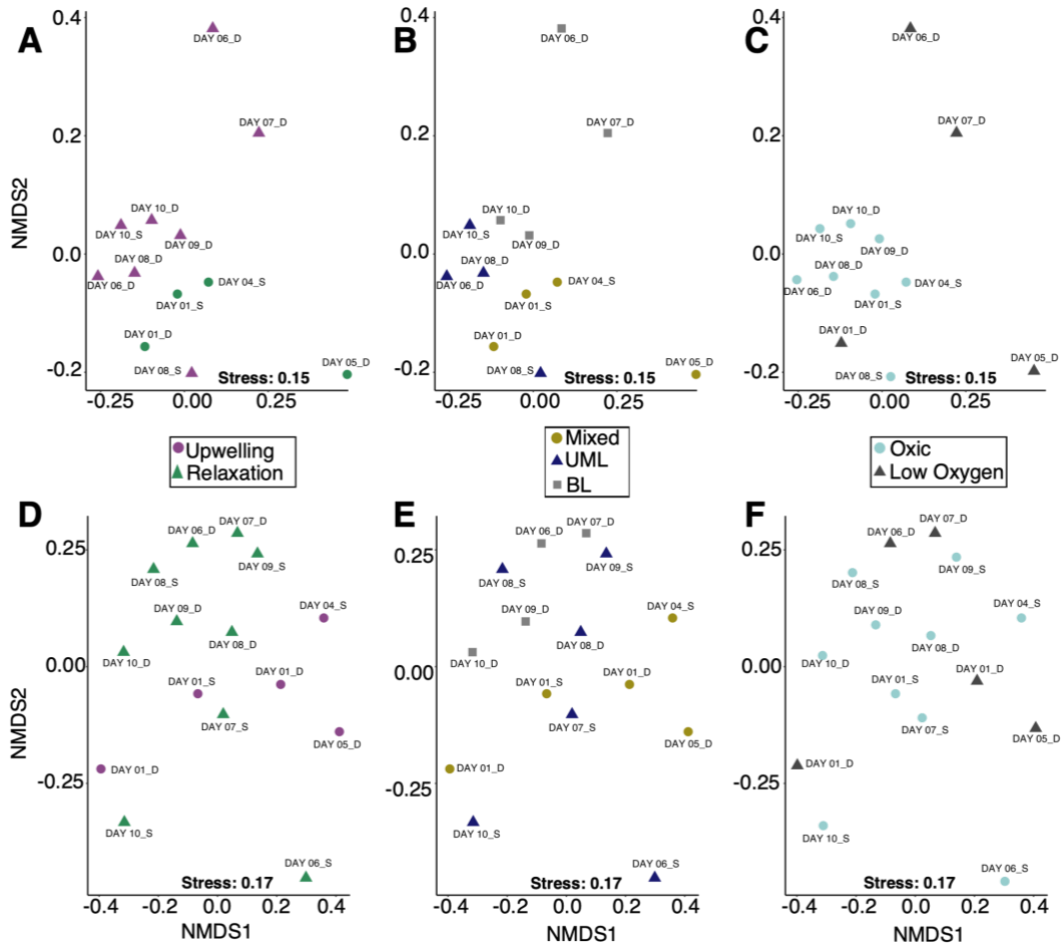

Figure 2.5. Non-metric multidimensional scaling (NMDS) analysis of the weighted unifrac distances between (A–C) bacterioplankton taxon-abundance and (D–F) picoeukaryote taxon-abundance samples, respectively. The stress for the NMDS analysis is shown at the bottom of the plot. The shape and colour of the points in (A and D) indicates upwelling condition, in (B and E) water column type and in (C and F) the oxygen status of the depth where the sample was taken. The 'S' in the sample name refers to samples taken from the surface and the 'D' refers to samples taken at depth.

The CCA model constrained with the environmental variables associated with upwelling conditions (nitrogen species (NO_3^- and NH_4^+), temperature, particulate organic matter (POM), dissolved oxygen concentrations and picoeukaryote cell counts) explained 45% of the variation between bacterioplankton samples (**Figure 2.6A-C**), whereas the CCA model (nitrogen species, temperature, POM and picoeukaryotes) used to show the separation between oxygen states explains 50.5% of the variability in community structure among samples (**Figure 2.6C**). Of the environmental factors measured, only ammonium concentrations (PERMANOVA: R^2=0.270, p=0.005) and temperature (PERMANOVA: R^2=0.287, p=0.007) significantly influenced the dissimilarity between bacterioplankton samples (**Table 2.3**). When constrained, bacterioplankton samples do not separate clearly by any of the factors, with overlap between all groupings (**Figure 2.6A-C**). Temperature, dissolved oxygen, POM and picoeukaryote concentrations were associated with variability in the bacterioplankton community structure in the upper mixed layer and therefore the relaxation period, while increased NO_3^- and NH_4^+ concentrations were associated with variability in samples in the bottom layer (**Figure 2.6A and B**). Increased nitrate and ammonium concentrations were associated with samples in low-oxygen waters while warm temperature and increased POM and picoeukaryote concentrations were associated with samples in oxygenated waters (**Figure 2.6E**).

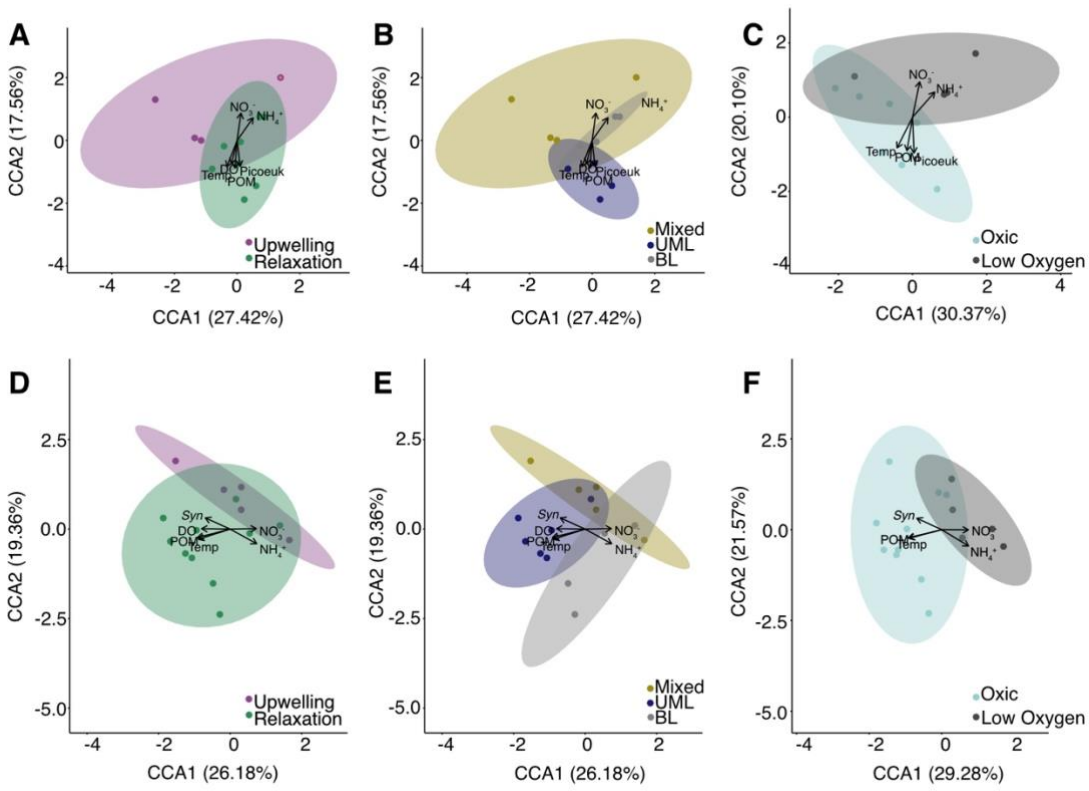

Figure 2.6. Canonical correspondence analysis (CCA) ordination plots showing the constrained 16S rRNA taxon-abundance data grouped by (A) the upwelling condition, (B) the identified water column type, (C) oxygen status of the water column and the constrained 18S rRNA taxon-abundance data grouped by (D) upwelling condition, (E) water column type and (F) oxygen state. The x and y axis shows the percent variability between samples explained by the constrained ordination models. The metavariables related to upwelling used to constrain the data are shown as eigenvectors. Ellipses are the 95% confidence around the mean of each centroid. Mixed=Mixed water column; UML=Upper mixed layer; BL=Bottom layer; DO=Dissolved oxygen; NH_4^+=Ammonium; NO_3^-=Nitrate; POM=Particulate Organic Matter; *Syn*= *Synechococcus*; Temp=Temperature.

Table 2.3. PERMANOVA results (R^2, F-statistic and p-value) testing significance of upwelling relevant vectors (**Figure 2.6**) on weighted-unifrac distances between bacterioplankton samples and picoeukaryote samples, respectively (95% cut-off). Asterisks indicate significant results.

	Bacterioplankton (A, C and E)			**Picoeukaryotes (B, D and F)**		
	R^2	**F**	**p**	**R^2**	**F**	**p**
Temperature (Temp)	0.29	4.03	0.004*	0.09	1.30	0.29
Dissolved Oxygen (DO)	0.13	1.52	0.23	0.04	0.57	0.71
Particulate Organic Matter (POM)	0.17	2.11	0.10	0.07	0.93	0.45
Nitrate (NO_3^-)	0.18	2.18	0.08	0.07	0.95	0.44
Ammonium (NH_4^+)	0.27	3.70	0.004*	0.08	1.11	0.318
Picoeukaryotes (Pioeuks)	0.14	1.59	0.22	-	-	-
Synnecococcus (*Syn*)	-	-	-	0.07	1.03	0.37

Thirty bacterioplankton families that represent 1% of reads in at least one sample were selected as the most abundant bacterioplankton families (**Figure 2.7**). Hierarchical clustering grouped these bacterioplankton by upwelling condition. The 30 families were used to determine differential abundance between upwelling water types and between oxygen states. The read abundances of these top bacterioplankton families represent 91% of all the 16S rRNA data. Of these 30 families, representatives of the *Marine Group II_fa* were differentially abundant during the relaxation period, while families like *Rhodobacteracea*e and *Flavobacteriaceae* were more abundant during the active upwelling period (**Figure 2.7**, **Figure S2.2**). *Rhodobacteracea*e (SIMPER: contribution: 28%) and *Flavobacteriaceae* (SIMPER: contribution: 17%) were thus the most influential families contributing to differences in community structure between the active upwelling and relaxation periods (**Table S2.6**, **Figure S2.2**). When considering the differences in community structure in samples taken from the different upwelling water types (mixed, upper mixed layer and bottom layer), *Rhodobacteracea*e (SIMPER: contribution: 27%), which was more abundant during active upwelling, and *Nitrosopumilaceae* (SIMPER: contribution: 18%), which was more abundant in the bottom layer, contributed most to differences in community structure between mixed and bottom layer samples (**Table S2.6**).

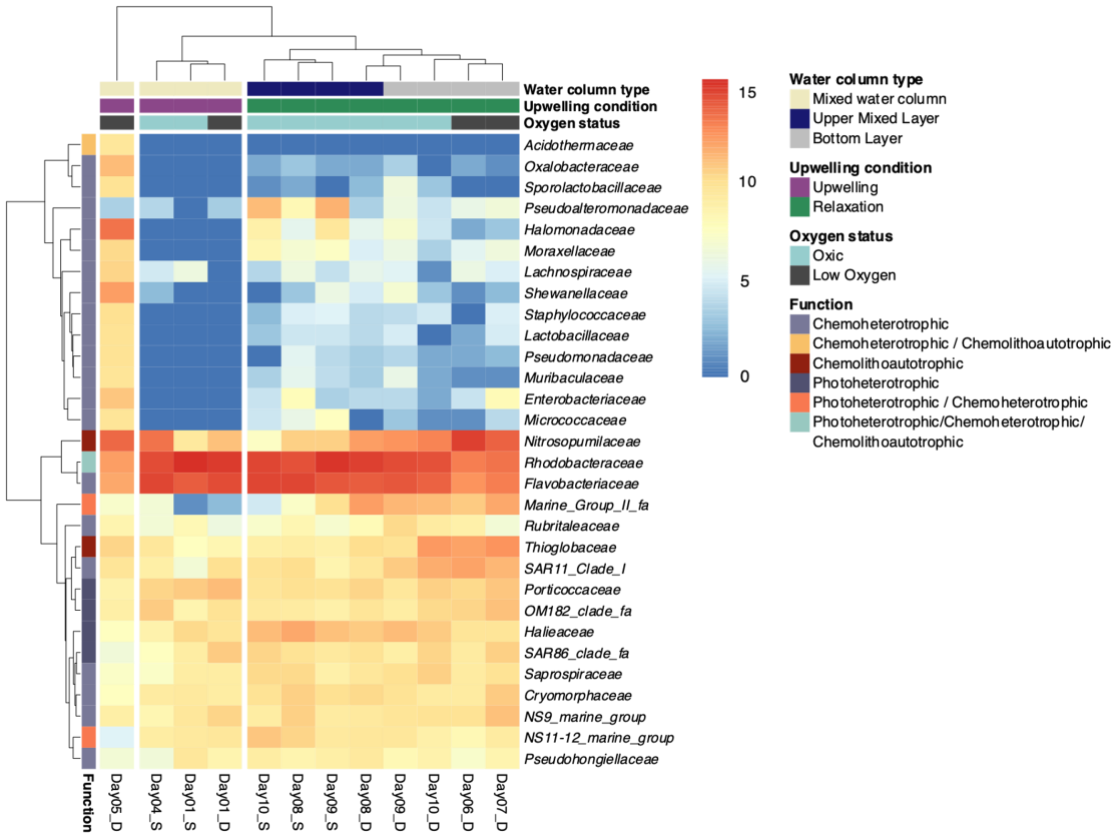

Figure 2.7. Comparisons between the log transformed abundances of the top 30 bacterioplankton families (class and phylum information in **Table S2**). in each sample from which the 16S rRNA gene was sequenced. Samples are clustered hieratically the heatmap was sectioned into 3 hierarchal clusters. Boxes on the top of the heatmap indicate the upwelling condition, water column type and oxygen status of each sample, while the box on the left of the heatmap indicate the functional group of each bacterioplankton family. The 'S' in the sample name refers to samples taken from the surface and the 'D' refers to samples taken at depth.

Picoeukaryotic diversity

The 18S rRNA sequence libraries resulted in a total of 787 016 reads, from which 8 530 OTUs were classified and 3 062 of these were unique. Although using the V4 region of the 18S rRNA gene for amplification is known to overestimate and underestimate certain picoeukaryotic taxa, this probe is conventionally used to get the best representation of the eukaryotic community (Stoeck et al., 2010). It should be noted that some of the organisms found in the picoeukaryote size fraction are known to be larger than the traditional picoeukaryote size range and are likely fragments from

larger size fractions, however they will still be discussed in this section. Diversity of the picoeukaryotes was highest at 10 m on day 5 (Shannon index: 3.896) (**Table 2.3**). The greatest richness was found at 10 m on day 6 (950 OTUs) and the smallest at the surface on day 7 (209 OTUs) (**Figure 2.4C**, **Table 2.3**). Evenness ranged from 0.073 on day 10 at 10 m to 0.139 on day 5 at 10 m. The observed richness of picoeukaryotic communities did not vary between upwelling periods ($t=0.19$, $df=13$, $p=0.85$) but was different between oxygen states ($t=-2.41$, $df=13$, $p=0.03$), with higher mean ± SE richness in low-oxygen (727.6 ± 72.2 OTUs) than oxygenated samples (489.2 ± 59.6 OTUs). There were no differences in evenness and thus diversity for picoeukaryotes between upwelling periods ($t=0.75$, $df=13$, $p=0.46$) or the two oxygen states ($t=-0.57$, $df=13$, $p=0.58$).

Picoeukaryotic community structure

Thirty picoeukaryote phyla were identified in 15 samples. Dinoflagellata (34%) and Cercozoa (14%) made up most of the picoeukaryotic OTUs throughout the sampling period (**Figure 2.4B**). Dino-Group-II (11%) and Dino-Group-I (8%) were the most representative orders of Dinoflagellata in the picoeukaryote dataset, while the Cercozoa were represented by Cryomonadida (3%) and Ventricleftida (1.5%). The picoeukaryote OTUs that were most abundant belonged to *Dino-Group-I-Clade-I_X_sp.* (51%) and the ascomycetous yeast *Candida parapsilosis* (4%). There was a high proportion of fungi found on day 6 at the surface, mainly representatives of the genera *Candida* and *Rhodotorula* (**Figure 2.4B**). The top 46 picoeukaryote families in all samples represented 93% of the 18S rRNA dataset (**Figure 2.8**).

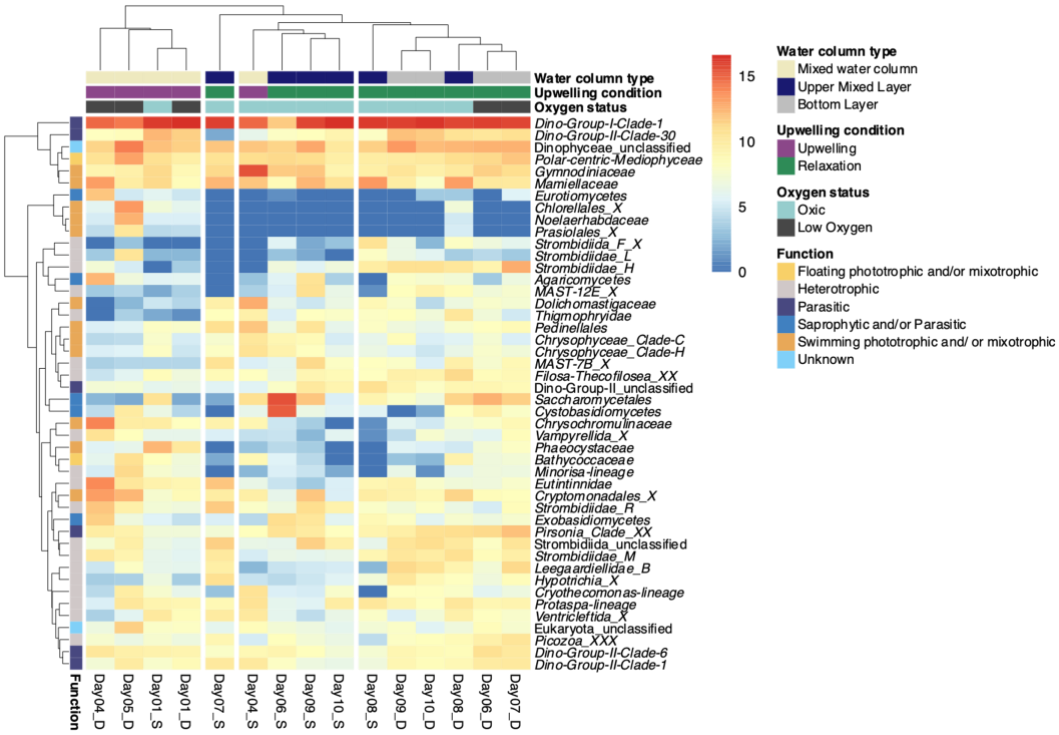

Figure 2.8. Comparisons between the log transformed abundances of the top 46 picoeukaryotic families in each sample from which the 18S rRNA gene was sequenced. Samples are clustered hieratically and the heatmap was sectioned into 4 hierarchal clusters. Boxes on the top of the heatmap indicate the upwelling condition, water column type and oxygen status of each sample, while the box on the left of the heatmap indicate the functional group of each picoeukaryote family. The 'S' in the sample name refers to samples taken from the surface and the 'D' refers to samples taken at depth.

Picoeukaryote community structure did not group by upwelling period (PERMANOVA: R^2=0.099, p=0.221), upwelling water type (PERMANOVA: R^2=0.192, p=0.193) or oxygen state (PERMANOVA: R^2=0.042, p=0.681), based on weighted unifrac distances (**Figure 2.5D–F**). The environmental variables selected for the constrained ordination of the log transformed picoeukaryote abundances were DO, NO_3^-, NH_4^+, POM, temperature and *Synechococcus* concentrations. The CCA model containing all these variables only explained about 46% of the variability between samples and, when comparing oxygen states (without DO constraining the ordination), the model explained about 51% of the variability in community structure (**Figure 2.6D–F**). Increased *Synechococcus* concentrations, DO, POM and temperature were associated with variability in community structure during the relaxation period (**Figure 2.6D**), more specifically in the upper mixed layer

(**Figure 2.6E**). Increased nitrate and ammonium concentrations were associated with the community structure of samples found in the bottom layer. As with bacterioplankton, increased NO_3^- and NH_4^+ concentrations were associated with low-oxygen samples (**Figure 2.6F**). None of the measured environmental variables significantly influenced dissimilarity between samples (**Table 2.3**).

Functionality of bacterioplankton groups

The top 30 representative families of bacterioplankton selected for functional analysis comprised the following primary metabolisms: chemoheterotrophy, chemolithoautotrophy, photoheterotrophy or a combination of those (**Figure 2.9A**, **Table S2.3**). The bacterioplankton were composed of mostly heterotrophic organisms, able to utilise organic molecules for energy, with the archaea having a lithotrophic lifestyle. Eight of the bacterioplankton families (*NS11-12*, *Rhodobacteraceae*, *Porticoccaceae*, *Halieaceae*, *SAR86*, *Marine Group II*) were identified as photoheterotrophic or having members that can be photoheterotrophic. The abundance of chemoheterotrophs increased at depth on day 5, after which there was an increase in relative abundance of photoheterotrophs and chemolithoautotrophs at depth (**Figure 2.9A**). Bacterioplankton functional composition grouped according to upwelling period (PERMANOVA: R^2=0.246, p=0.025), upwelling water type (PERMANOVA: R=0.44, p=0.011, PERMANOVA $_{\text{Active upwelling vs. UML}}$: R^2=0.299, p=0.129; PERMANOVA $_{\text{Active upwelling vs. BL}}$: R^2=0.360, p=0.054; PERMANOVA $_{\text{UML vs. BL}}$: R^2=0.524, p=0.066) and oxygen state (PERMANOVA: R^2=0.236, p=0.048) (**Figure 2.10A–C**).

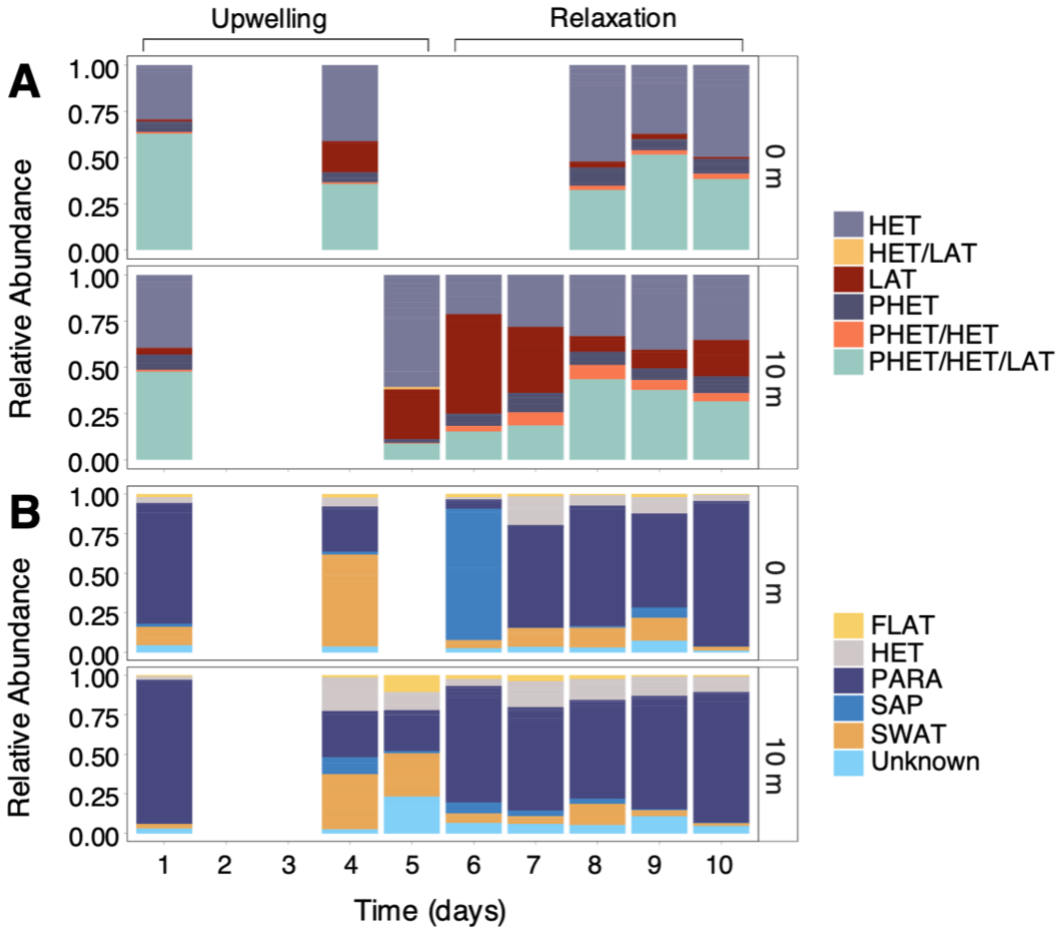

Figure 2.9. The functional composition of the (A) top 30 bacterioplankton and the (B) top 46 picoeukaryote families for each sample taken throughout the experiment. HET=Chemoheterotrophs; LAT=Chemolithoautotrophs; PHET=Photoheterotroph; FLAT=Floating Autotroph or Mixotroph; PARA=Parasite; SAP=Saprophyte or Parasite; SWAT=Swimming Autotroph or Mixotroph.

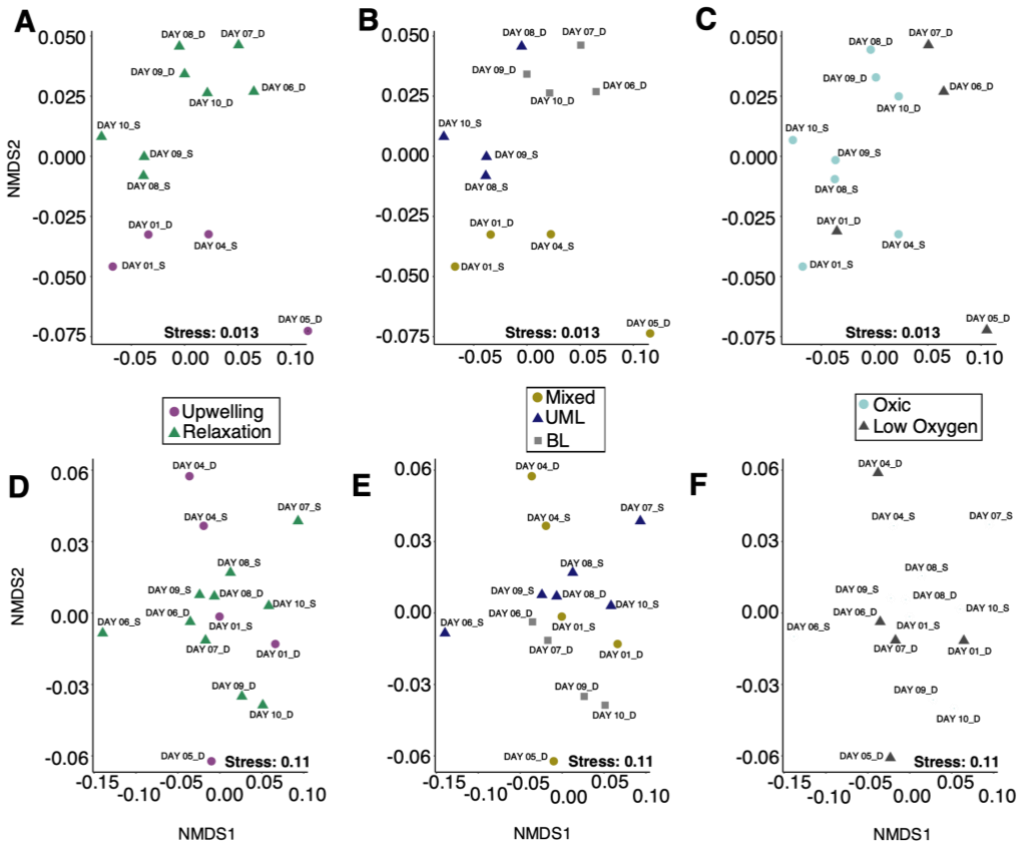

Figure 2.10. Non-metric multidimensional scaling (NMDS) analysis of the weighted unifrac distances between (A–C) bacterioplankton functional-abundance and (D–F) picoeukaryote functional-abundance samples, respectively. The stress for the NMDS analysis is shown at the bottom of the plot. The colour and shape of the points in (A and D) indicates upwelling condition, in (B and E) water column type and in (C and F) the oxygen status of the depth where the sample was taken. The 'S' in the sample name refers to samples taken from the surface and the 'D' refers to samples taken at depth.

The chemolithoautotrophs were most influential in separating the UML and BL groups (SIMPER: contribution: 35%), with increased abundance in the BL, while photoheterotrophs/chemoheterotrophs (SIMPER: contribution: 36%) and chemolithoautotrophs (SIMPER: contribution: 30%) separated the functional profile of the active upwelling period from the relaxation period (UML+BL) (**Table S2.7**). There was a larger proportion of taxa making use of these primary metabolisms during the relaxation phase. Chemolithoautotrophs (SIMPER: contribution: 35%) were also the most influential in separating oxygenated and low-oxygen groups as these taxa are on average more abundant in low oxygen waters. The constrained ordination of the functional composition explained approximately 98% of the variance between samples

(**Figure 2.11A–C**). None of the metavariables seemed to contribute to the functional profile of samples found during active upwelling (**Figure 2.11A–B**), while DO, POM, temperature and picoeukaryote abundance were associated with the functional profile of UML samples. (**Figure 2.11B**). Increased ammonium and NO_3^- concentrations were associated with samples from the bottom layer and, therefore, also low oxygen samples (**Figure 2.11B–C**).

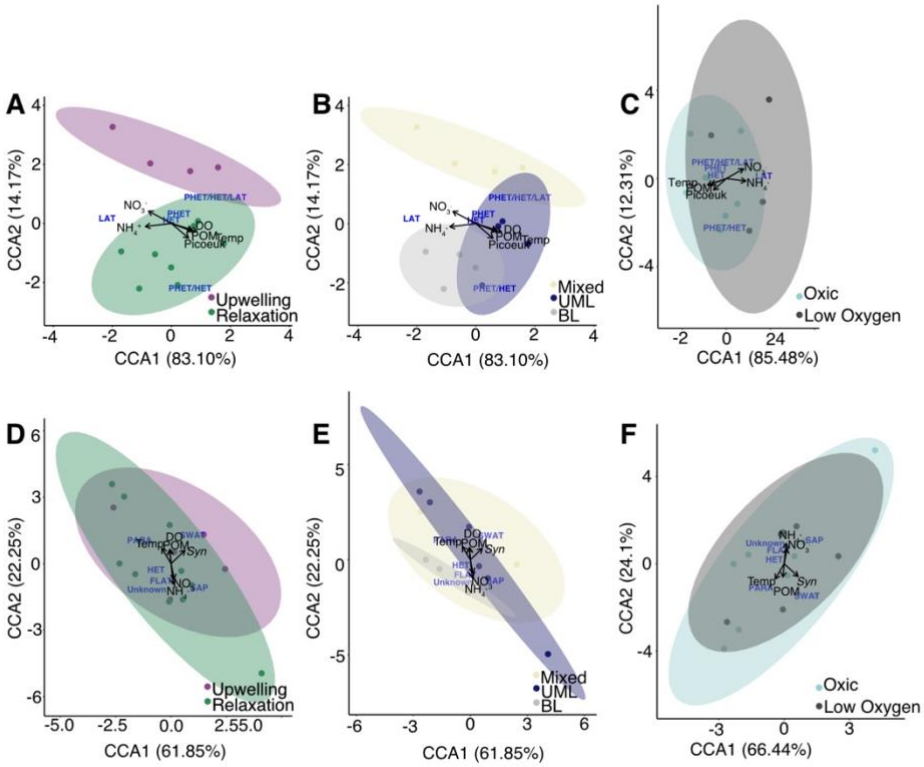

Figure 2.11. Canonical correspondence analysis (CCA) ordination plots showing the constrained top 30 bacterioplankton families functional abundance data grouped by (A) the upwelling condition, (B) the identified water column type, (C) oxygen status of the water column and the constrained top 46 picoeukaryotes families functional abundance data grouped by (D) upwelling condition, (E) water column type and (F) oxygen status. The x and y axis shows the percent variability between samples explained by the constrained ordination models. The positions of the various functional groups are superimposed onto the plot. The metavariables related to upwelling used to constrain the data are shown as eigenvectors. Ellipses are the 95% confidence around the mean of each centroid. Mixed=Mixed water column; UML=Upper mixed layer; BL=Bottom layer; DO=Dissolved oxygen; NH_4^+=Ammonium; NO_3^-=Nitrate; POM=Particulate Organic Matter; *Syn*=*Synechococcus*; Temp=Temperature; HET=Chemoheterotrophs; LAT=Chemolithoautotrophs; PHET=Photoheterotroph; FLAT=Floating Autotroph or Mixotroph; PARA=Parasite; SAP=Saprophyte or Parasite; SWAT=Swimming Autotroph or Mixotroph.

Derived functionality of picoeukaryotic groups

The top representative families for the picoeukaryotes (46 families) were selected for functional analysis (**Figure 2.8**). The picoeukaryotes had a mix of

functions, including swimming and floating autotrophy or mixotrophy, heterotrophy, parasitism and saprotrophy (**Figure 2.9B**). Of the top 46 most abundant picoeukaryotic families, 19 were heterotrophic, 11 were autotrophic or mixotrophic, six were parasitic and five were saprophytic or parasitic (**Figure 2.9B**). During active upwelling there was a high proportion of autotrophs/mixotrophs (swimming and floating autotrophs), which switched to a high proportion of heterotrophs during the relaxation phase (**Figure 2.9B**). Picoeukaryote functional composition did not group by upwelling period (PERMANOVA: R^2=0.485, p=0.732), water type (PERMANOVA: R^2=0.080, p=0.825) or oxygen state (PERMANOVA: R^2=0.009, p=0.926) (**Figure 2.10D–F**). There was much overlap between groups in the CCA analysis of functional grouping in the picoeukaryote community (**Figure 2.11D–F**). Increased values for dissolved oxygen, POM, temperature and picoeukaryote abundance were associated with the active upwelling, UML and oxygenated samples, while increased NH_4^+ was associated with the functional profile of picoeukaryotes in the bottom layer (**Figure 2.11E**).

Network Analysis

Three distinct co-occurrence networks were produced when correlating bacterioplankton and picoeukaryote families (**Figure 2.12**). One network (bottom left, **Figure 2.12B**) represents the relationships between the saprophytic fungi, the heterotrophic eukaryote family *Eutininnidae*, and the swimming autotrophs/mixotrophs *Gymnodiniaceae* and *Pedinellales*. All of the other eukaryotes are not naturally in the picoeukaryote size range. A second network (bottom right, **Figure 2.12C**) shows the possible interaction between the parasitic families *Dino Group II Clade 4*, *6* and *30* and the *Phaeocystaceae*. In the main network (**Figure 2.12A**) the biggest cluster contains the heterotrophic bacterioplankton, where *Muribaculaceae* had the most interactions (edges). Many of the heterotrophs in the main cluster have positive interactions with other heterotrophs, but negative interactions with the photoheterotroph *Porticoccaceae* and the heterotrophic picoeukaryotes from the *Cryothecomonas* lineage. A small cluster was found around the *Halieceae*, with only positive relationships with other heterotrophs, including the parasitic unclassified Dino Group II. Other notable interactions included a positive correlation between the two identified chemolithoautotrophs (*Nitrospumilaceae* and *Thioglobaceae*), this being the only significant positive interaction for

Nitrospumilaceae. These two taxa were both negatively correlated with the functionally heterogeneous *Rhodobacteraceae* family. All bacterioplankton (orange) were highly connected with each other, with each family connected to at least one other bacterioplankton family, but the same was not true for the picoeukaryotes (in blue).

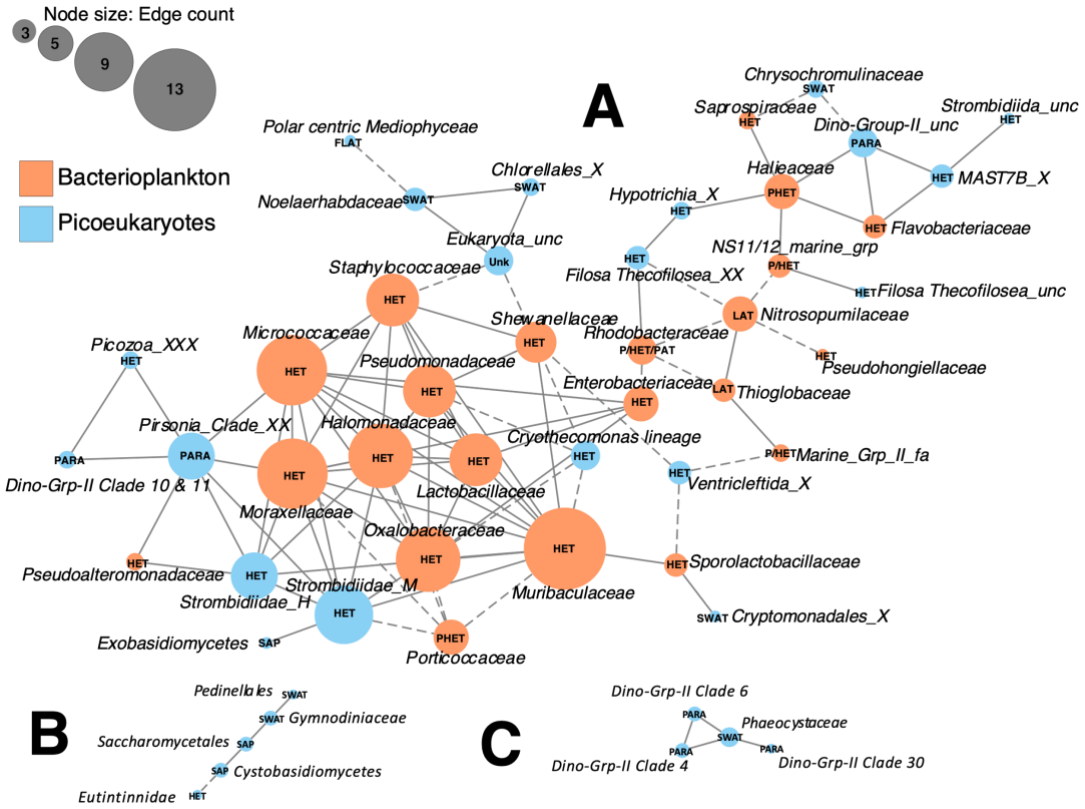

Figure 2.12. Co-occurrence network analysis of the top 30 bacterioplankton and top 46 picoeukaryote families present in this study. Spearman rank correlations that were strong ($r > 0.70$ and $r < -0.07$) and statistically significant ($p < 0.01$) are shown (grey lines). Edges with dashed line indicate negative correlations, and node size is relative to the number of interactions (edges) with each node. Nodes are labelled with the functional grouping associated with each family. HET=Chemoheterotrophs; LAT=Chemolithoautotrophs; PHET=Photoheterotroph; FLAT=Floating Autotroph or Mixotroph; PARA=Parasite; SAP=Saprophyte or Parasite; SWAT=Swimming Autotroph or Mixotroph; Unk=Unknown.

2.5. Discussion

This study is one of the first to investigate both prokaryotic and eukaryotic picoplankton community dynamics during an active upwelling event in South African waters, making use of sequencing technology. The fixed station sampled in this study, located in St. Helena Bay, is known to experience active wind-driven upwelling in the austral spring and summer months (Hutchings et al., 2009). The recent identification by Rocke et al. (2020) of unique picoplankton communities associated with different upwelling seasons and oxygen states in the same region has highlighted the importance in understanding the variability upwelling introduces to the dynamics of these microorganisms, especially over the short-term. This study highlighted that, in order to comprehend the ecosystem function of these small plankton, community structure, dynamics and function of both bacterioplankton and picoeukaryotes near the surface and also in deeper waters need to be considered. Active upwelling creates a dynamic environment, known to cause changes in larger size fractions of plankton over time, including succession from diatoms as the dominant phytoplankton directly after upwelling to dinoflagellates as nutrients are depleted (Pitcher et al., 1991; Walker and Pitcher, 1991). The results of our study, which focused on the daily variability of picoplankton over a 10-day upwelling cycle, have indicated successional changes occur amongst the picoplankton after upwelling, with responses confounded by the high diversity of energy acquisition mechanisms present in this size class.

An upwelling cycle in St. Helena Bay

During the 10-day monitoring study a period of active upwelling was identified (day 1–5), followed by a period of relaxation (day 6–10; Burger et al., 2020). Active upwelling over the first five days was characterised by high NO_3^- concentrations, cool sea surface temperatures (SSTs), high potential density and undersaturated oxygen concentrations throughout the water column (**Figure 2.2)**. The mixed layer during active upwelling was found to be deeper than the euphotic zone, causing light limitation for any phytoplankton growth during this period. In the relaxation period there was an increase in stratification due to warm SSTs, with a decrease in NO_3^- concentrations at the surface over the following three days due to the shallow euphotic zone in which there was an increase in phytoplankton production.

As a retention zone in the southern Benguela, St. Helena Bay supports much of the primary production of the southern Benguela upwelling system (Brown et al., 1991; Flynn et al., 2018). One impact of this high primary production is that the subsequent termination of this biomass and its remineralization at depth results in the formation of low oxygen conditions (Pitcher et al., 2014). Low oxygen water samples, which were defined as samples with oxygen concentrations < 2 mL L^{-1}, were found at 10 m on day 1, at the beginning of the mixing period when there was under-saturated subsurface water (Burger et al., 2020), and at 10 m from days 4-6 as the water column began to stratify and microbial respiration increased (Robinson, 2019). The size fraction of interest in our study, the picoplankton, were shown to have a negligible contribution to primary production and nutrient (ammonium and nitrate) uptake, as the larger nanophytoplankton and diatoms rapidly consumed the available nutrients (Burger et al., 2020). This is typical of the southern Benguela upwelling system (Pitcher et al., 1991; Probyn, 1992) and other upwelling systems (Chavez, 1991; Fawcett and Ward, 2011). However, the roles of picoplankton extend to other biogeochemical and ecological processes. These roles have been identified during this upwelling event through a close look at the composition and function of the range of organisms that comprise this size fraction.

Bacterioplankton diversity and composition

Bacterioplankton diversity was on average higher during the relaxation period (**Table 2.1**) than the active upwelling period, when the water column was mixed. Water column mixing is known to influence bacterioplankton community structure and diversity, either positively or negatively depending on the conditions (Weithoff et al., 2000). Deep convection in the open ocean resulted in homogenization of prokaryote communities, with a predominance of bacterioplankton that are typically found at the surface (Severin et al., 2016). Increased turbulence has been shown to decrease the abundance of bacterioplankton, but nutrient input into the euphotic zone can lead to an increase in bacterial abundance when the water column stratifies again (Cushing, 1989), which is what has been observed in this study (**Figure 2.4C**).

Samples taken from low oxygen waters did not differ in biodiversity from those found in oxygenated waters. The availability of nutrients like NO_3^- and NH_4^+ promotes growth in most bacterial species, despite low oxygen conditions. This trend is similar

to what was recently found in offshore hypoxic waters in St. Helena Bay (Rocke et al., 2020). As the current study was focused on event scale variability, it is unclear whether the seasonally recurrent hypoxia in bottom waters of St. Helena Bay causes diversification in the bacterioplankton community compared to surface waters (Pitcher et al., 2014). In permanent oxygen minimum zones, diverse and distinct bacterial communities have been found compared to those in surface waters (Stevens and Ulloa, 2008; Beman and Carolan, 2013).

Despite the missing samples, the picture that emerged from the 10-day monitoring effort shows how bacterioplankton community diversity is variable during an upwelling event (**Figure 2.4**). The dominance of *Rhodobacteraceae* and *Flavobacteriaceae* (**Figure 2.7**) in the bacterioplankton throughout this study is unsurprising, as these two families are ubiquitous in marine ecosystems (Dang et al., 2008), including in upwelling areas (Gregoracci et al., 2015); they also have been identified recently in St. Helena Bay on and off the continental shelf (Rocke et al., 2020). *Rhodobacteraceae* are well known primary colonizers in aquatic environments, where these organisms gain advantages like protection from predation and conditions which are adverse for other organisms as well as increased nutrient availability on surfaces, like on detritus (Hall-Stoodley et al., 2004; Dang et al., 2008). In turn, these organisms, as well as the heterotrophic *Flavobacteriaceae*, play a vital role in the remineralization of particulate organic matter (Kirchman, 2002), which is found throughout the water column. As key primary consumers, *Flavobacteriaceae* and *Rhodobacteraceae* can accumulate nutrients quickly, possibly outcompeting other microorganisms, which would be considered advantages during mixing events when light availability is low throughout the water column. As fast growing, small organisms, taxa such as *Flavobacteriaceae* may be subject to grazing pressure from larger protists and in this way contributing to the larger food web (Kirchman, 2002). It is interesting that SAR11 was not the most abundant bacterioplankton found in the study, as it usually dominates in specifically surface waters (Morris et al., 2002; Rappé et al., 2002; Haro-Moreno et al., 2020). This is likely due to the primer selection in the current study, which has been found to underestimate SAR11.

At the onset of the stratification, specifically on day 5, the bacterioplankton diversity and abundances changed completely (**Figure 2.7**). Additionally, phytoplankton community composition, as determined through microscopy, changed

from day 5 onwards, with increased numbers of taxa (Burger et al., 2020). The peak in total phytoplankton standing stock was found on day 8 in the Burger et al. (2020) study, mainly comprising large centric diatoms like *Thalassiosira* spp. as well as large dinoflagellates (Burger et al., 2020). The bacterioplankton in this study responded to the increased availability of substrates released by these large phytoplankton, recapturing it back into the microbial loop (Azam, 1998), with an increase in abundance of Gammaproteobacteria family OTUs (*Halomonadaceae*, *Shewanellaceae*, and *Oxalobacteraceae*) (**Figure 2.7**). The *Shewanellacea,* of the order Altermonadales, for example, are known to colonize diatoms and accelerate their dissolution (Bidle and Azam, 2001). *Pseudoaltermonadaceae,* another known colonizer of diatoms (Eloe-Fadrosh et al., 2016), did not respond immediately to the increase in abundance in diatoms but rather increased on day 9 and 10, when large centric diatoms decreased in relative abundance (Burger et al., 2020). SAR11, a ubiquitous bacterial clade found in the surface ocean (Morris et al., 2002), was found on all days and at both depths (**Figure 2.7**), but abundance was likely underestimated due to the use of the 806R primer used (Apprill et al., 2015). This was also true for the identified photoheterotrophic taxa (SAR86 clade, OM182 clade, *Porticoccaceae* and *Halieaceae* families) (Dupont et al., 2012). The dual metabolic nature of these organisms perhaps explains their presence in both carbon-rich surface waters and in light-limited deeper waters. The low abundance of Cyanobacteria is unexpected in this eutrophic system and may be an indication of the selectivity of the primers chosen.

The results for Archaea need to be interpreted with some caution because the V3-V4 primer is known to underestimate species diversity, especially of Archaea (Eloe-Fadrosh et al., 2016). *Candidatus Nitrosopumilus* and *Candidatus Nitrosopelagicus,* which were the most abundant archaea taxa identified, are important ammonia oxidisers (Könneke et al., 2005; Pester et al., 2012; Santoro et al., 2015). The *Nitrosopumilaceae* were the third most abundant taxonomic family identified in this study. This family occurred in greater abundances at 10 m, being found mostly in the bottom layer during the relaxation period. Bioavailable NH_4^+ at depth would support the growth of these chemolithoautotrophic *Nitrosopumilaceae* (Qin et al., 2016). It could be for this reason that *Nitrosopumilaceae* differentiated the bacterioplankton community in the bottom layer from that found in the mixed water column during active upwelling conditions.

The variability between bacterioplankton samples explained by the concentrations of NO_3^-, NH_4^+, dissolved oxygen, POM and picoeukaryotes was between 45 and 51% (**Figure 2.6A-C**). Increased light availability, oxygen, temperature and the resulting phytoplankton biomass at the surface were all associated with unique surface bacterioplankton composition. A similar positive relationship between these metavariables and bacteria was found in a study of daily variations in prokaryotes after a spring bloom in the East China Sea (Choi et al., 2018). Bacteria are known to process a significant proportion of the biomass produced by phytoplankton derived organic matter in upwelling areas (Troncoso et al., 2003; Cuevas et al., 2004). The increased abundance in the surface waters of nanophytoplankton, which are preferentially consumed by protozoan grazers, could also have reduced the predation pressure on bacterioplankton communities (Jochem, 2003; McManus et al., 2007, Gebe et al., unpublished data). Nitrate was introduced to surface waters during active upwelling, as were bacterioplankton from depth, possibly explaining why NO_3^- is positively related to the community composition of the mixed water column. Bioavailable NH_4^+ occurred at greatest concentrations at depth, which could influence the bacterioplankton composition, favouring chemolithoautotrophic microorganisms such as *Nitrosopumilaceae.*

Up to 55% of the variance in community structure is unexplained in this study, pointing to other environmental and biotic factors (not measured), which may have more control on bacterioplankton abundance and community structure during active upwelling (**Figure 2.6**). These factors may include predation and viral mortality, which were not measured in this study. However, the influence of these controls on specific picoplankton groups, such as *Synechococcus*, *Prochlorococcus* and picoeukaryotes, have been explored in more detail in a separate study (Gebe et al., unpublished data). Understanding the effects of predators and viruses on picoplankton dynamics during an upwelling event is important to fully understand ecosystem functioning in St. Helena Bay.

Picoeukaryote composition and diversity

This study is the first to look at short term (daily) variability in picoeukaryote community diversity under upwelling conditions. Little is known about the rate at which these small organisms react to changes in their environment and whether a daily

sampling interval is appropriate for studying their dynamics. The general variability caused by upwelling events seems to be echoed in the lack of distinct picoeukaryote communities under different environmental conditions. It should be noted that the lack of statistical diversity in the picoeukaryotic community structure may be confounded by the small sample size for the upwelling period.

Nevertheless, picoeukaryote diversity was, on average, similar during active upwelling and into the relaxation period (**Table 2.2**). There was a notable decrease in richness at the surface on day 7, which coincided with a decrease in available macronutrients because of the growth of nanophytoplankton (Burger et al., 2020). Picoeukaryote richness increased in low oxygen waters in this study, but diversity was similar to that found in oxygenated water. Low oxygen conditions have been shown to shift community diversity in picoeukaryotes in hypoxic zones in the Gulf of Mexico (Rocke et al., 2013) and Rocke et al. (2016) found that picoeukaryotes decreased in both diversity and richness in response to a hypoxic event in a sub-tropical harbour. Perhaps the difference in these results lies in the response of picoeukaryotes to anthropogenic hypoxic events compared with natural, episodic low oxygen events in a coastal system. Alternatively, the richness is representative of a fresh injection of picoeukaryotes at depth from the surrounding waters.

Picoeukaryotes consisted primarily of dinoflagellates and cercozoa, with the most abundant picoeukaryote order belonging to the ubiquitous dinoflagellates Syndiniales (**Figure 2.8**). This is likely the signal of a high proportion of parasitic spores, as was found in the smaller size fractions of samples taken from the Southern Ocean (Sassenhagen et al., 2020). The Syndiniales are obligate parasites, with a large range of hosts (Guillou et al., 2008, 2010; Anderson and Harvey, 2020). As parasites of other dinoflagellates and possibly diatoms (Anderson and Harvey, 2020) their large relative abundance could be in response to the abundance of hosts in the nanophytoplankton, such as large and small diatoms, which were abundant throughout the 10-day study (Burger et al., 2020). The Syndiniales were represented mostly by Dino-Group-I and Dino-Group-II, with Dino-Group-I, specifically *Dino-Group-I Clade 1,* having the highest abundance of any identified picoeukaryotic family (**Figure 2.8**). This result was different to that from a separate study in St. Helena Bay, which found Dino-Group-II represented 26 % of the whole dataset while Dino-Group-I represented only 12% (Rocke et al., 2020). The high proportion of *Dino-Group-I*

Clade 1 towards the end of this study (day 7-10) could indicate that these parasites are an important source of mortality for phytoplankton, especially of large diatoms, which decreased in abundance from day 7 (Burger et al., 2020). The high abundance of parasites at depth may be another explanation for this phenomenon; further studies linking these parasites with their hosts in the St. Helena Bay area are underway (Rocke et al. unpublished data).

Unicellular fungi were found in high relative abundance at the surface on day 6 (**Figure 2.8**). The reasoning for this large dominance of fungi may be an indication of a new water mass entering the sampling site (increased fungal abundance matched with changes in salinity at the sampling site on this day), however the exact event has not been elucidated. The role of marine yeasts in coastal waters is still unclear but it is likely that they were associated with other phytoplankton or had responded to an environmental cue not measured in this study (Amend et al., 2019). Marine yeasts are ubiquitous in the marine system, from the open ocean (Fell, 1976) to the deep ocean, where they are often found associated with benthic organisms (Nagahama et al., 2003a, 2003b; Nagahama, 2006). The high proportion of fungi at the surface, specifically the *Saccharomycetales* family, caused the overall difference in picoeukaryote communities between the upper mixed layer and the bottom layer. This result, however, is likely an artefact of the unusually high numbers at the surface on day 6. Further elucidation of the role of these yeasts in the coastal area of the southern Benguela ecosystem is necessary.

Picoeukaryote families like the *Phaeocystaceae*, *Bathycoccaceae* and *Gymnodiniaceae* all increased in abundance during active upwelling. Their increased abundance was likely caused by mixing to the top layer and, as autotrophs, they would contribute to the increased oxygenation of the water column by photosynthesis. *Gymnodiniaceae* is a family with species that are athecate (without a protective sheath), so their abundance in turbulent waters is surprising (Kubiszyn and Wiktor, 2016); perhaps their size is more important than their physiology during mixing. The mixotrophic nature of *Chrysophyceae* and the heterotrophic metabolism of the *Filoso-Thecofilosea* and *Thigmophyridae* could have allowed these organisms to thrive in low-oxygen conditions. Alternatively, physiological features like their theca (Dumack et al., 2018) or cysts (Lundholm et al., 2011; McMinn and Martin, 2013) might allow

these organisms to occur in large abundances during the unfavourable conditions of a low-oxygen environment.

Picoeukaryote community structure is known to differ spatially between the offshore and shelf, as well as seasonally in St. Helena Bay (Rocke et al., 2020). That variability was not seen in this study between upwelling periods, spatially in the different parts of the water column or between oxygen states. Most likely this is caused by the low replication during the upwelling period undermining the statistical significance. There does seem to be some separation in community structure between upwelling and relaxation conditions and transition into a stratified water column with distinct mixed and bottom layer communities. The picoeukaryotic community structure on day 8 is interesting in this case, as it represents a mix of both the upper mixed and bottom layer, explaining why it may be grouped with the bottom layer samples. This lack of diversity between upwelling periods could also be caused by overshadowing of dinoflagellate DNA after amplification, because of the different copy number of SSU rRNA, masking the true diversity of the picoeukaryotes (Hackett et al., 2004; Medinger et al., 2010). However, the use of weighted-unifrac distances corrected for this overabundance as much as possible. As with the 16S primer set used in this study, the 18S primer set used also underestimates certain taxa, specifically in this case many of the haptophytes (Balzano et al., 2015). The chosen primers also contribute to picoeukaryote diversity or lack thereof. Alternatively, it is possible that the community structure of picoeukaryotes under variable conditions caused by upwelling and over the short time period measured did not have time to diversify, compared to bacterioplankton that adapt more quickly. Perhaps picoeukaryote community structure in the short-term, even under upwelling conditions, is driven by something other than the environmental factors associated with active upwelling. Similar to the prokaryotes, this study did not quantify grazing or viral lysis, and it is unclear how these factors might shape picoeukaryote communities under upwelling conditions.

Increased light availability, warm temperatures and increased dissolved oxygen concentrations at the surface were not only positively associated with large phytoplankton but some of these factors could have also shaped the community structure of the picoeukaryotes (**Figure 2.6**). Light limitation in the bottom layer was a contributing factor describing the picoeukaryote community, probably benefiting a

heterotrophic or parasitic lifestyle. As with the bacterioplankton, mixing not only introduced NO_3^- to the surface, but also changed the picoplankton community, diluting surface-abundant organisms and introducing picoeukaryotes found at depth to the surface waters. Picoeukaryotes have been shown to have faster maximum uptake rates of NO_3^- at low irradiance depths compared to the surface (Painter et al., 2014), and this could shape their composition at depth. Further insight into picoeukaryote nitrogen metabolism is required to better understand these dynamics.

Functional diversity in picoplankton

Functional diversity gives an indication of the variability in ecosystem functioning, which is impossible to interpret solely from 16S and 18S rRNA sequencing data alone (Krause et al., 2014; Ramond et al., 2018). With the use of information obtained about each of the most abundant picoplankton families (**Table S2.3 and S2.4**), a picture has been constructed of the possible ecological contributions of picoplankton during an upwelling event. Heterotrophy was the main primary metabolism of the most abundant organisms found throughout this study; picoplankton capable of utilising organic matter as an energy source were abundant in both the bacterioplankton and picoeukaryote communities.

The study site in Elands Bay is in a highly productive system (Hutchings et al., 2009), therefore a large proportion of picoplankton leading a heterotrophic lifestyle is expected. During mixing the dominant taxa within bacterioplankton was the multi-functional family *Rhodobactereace*. This family hosts species that use a variety of trophic strategies (Pujalte et al., 2014), and so the exact functional dominance during active upwelling could not be identified. It is also possible that this family is making use of a variety of metabolic strategies to avoid interspecies competition. As the water column stratified, heterotrophic bacteria became more important, in response to increased POM. In the NW Iberian upwelling coastal region, researchers found that the picoplankton community was responsible for heterotrophy in the system and hypothesised that the pelagic food web was multivorous, with the picoplankton in the microbial loop always present and larger plankton added to the system in response to upwelling (Barber and Hiscock, 2006; Teixeira et al., 2011; Espinoza-González et al., 2012). This may also apply to this study, with an increase of carbon sources increasing the abundance of the standing stock of heterotrophs.

Another trophic strategy present among the abundant bacterioplankton was photoheterotrophy. The ability to use light as a source of energy allowed photoheterotrophic organisms to maintain consistent abundance throughout this study (**Figure 2.9**). More research is required on the benefits of a photoheterotrophic lifestyle in comparison to heterotrophy, as well as the role of photoheterotrophs in relation to primary and secondary production. During the relaxation period there was an increase in chemolithoautotrophy at depth (**Figure 2.9**). This was likely in response to bioavailable NH_4^+ and low light attenuation at depth, as stratification began. In bottom waters, which were not sampled in this study, oxygen concentrations are low, which could support the use of alternative electron acceptors other than oxygen for respiration, such as nitrate, sulphur and methane (Pajares and Ramos, 2019). Studies on anaerobic biogeochemical processes like annamox, denitrification, and dissimilatory nitrate reduction in St. Helena Bay, during and after active upwelling, are few (Tyrrell and Lucas, 2002), which opens the door to further research questions surrounding the role of chemolithoautotrophy in the picoplankton of the southern Benguela and St. Helena Bay specifically.

Parasitism was a major functional trait of the most abundant picoeukaryotes identified in this study. In the Humboldt current system fungal parasites of the *Thalassiosira* and *Skelotonema* diatoms were identified, and the researchers proposed that these fungi contribute to controlling the phytoplankton population as well as the release of organic matter which directly influences the carbon export (Gutiérrez et al., 2016). It is thus possible that picoplankton parasites contribute significantly to the cycling of carbon in the St. Helena Bay area. Picoeukaryotes were also identified as autotrophs or mixotrophs in this study, defined as either their ability to swim or not (Ramond et al., 2018). The FLAT and SWAT picoeukaryotes seemed to be most abundant as the mixing period ended and when stratification began on day 4 and 5. Mobility benefited organisms closest to the fluorescence maxima, mostly at the beginning of stratification when there was less turbulence, in their efforts to move vertically into the euphotic zone to photosynthesize.

Bacterioplankton primary metabolism constrained by the environmental factors closely associated with upwelling, differed between upwelling periods, water column types, and oxygen states, whereas taxonomic diversity differed only between water column types associated with the different stages of an upwelling event, namely the

mixed water column and the bottom layer. Within the bacterioplankton, the functional response to environmental change introduced during upwelling was more distinct than the taxonomic changes. The relationship between diversity and ecosystem function can often take on multiple mechanisms, such as complementary selection effects and facilitation effects (Krause et al., 2014). Selection occurs when taxa that benefit from environmental conditions outcompete others, whereas facilitation occurs when the presence of one organism assists the growth of another. The intricate way diversity and function interact under variable environmental conditions like upwelling is complex. Variability between the functional composition of each was almost completely explained by NO_3^-, NH_4^+, DO, POM, picoeukaryote concentrations and temperature (97.3-97.8%), which are all variables dependent on the physical environment, such as mixing and light availability, as well as other microorganisms (Nitrate production depth nitrifiers or POM). This supports the notion of multiple mechanisms at work controlling the functional composition of the bacterioplankton.

Understanding function could be more enlightening than taxonomic identification during these variable environmental conditions. For functional differences in communities in low oxygen and oxygenated waters, a large proportion of bacterioplankton species would be expected to be able to adapt their respiration processes to low oxygen environments (Han et al., 2011). However, for picoeukaryotes in this study, neither taxonomic diversity nor function corresponded uniquely with the stages of upwelling or environmental conditions. This may be an indication that function in this size fraction of eukaryotes does not play a role in shaping the environment, or that despite the small size of these organisms they do not respond taxonomically or functionally to changes in the environment as quickly as the bacterioplankton. The best explanation may be the “paradox of plankton” where the environmental variability found in the water column creates several niches that always support a variety of functional and taxonomic picoeukaryotic groups (Hutchinson, 1961). It is suggested that more replication is required to confirm the lack of pattern in picoeukaryote community structure. Primary metabolism can be used to indicate why a microorganism can thrive in a specific environment, but it may not be enough to fully understand the functional role and interactions of all picoplankton during upwelling cycles, which determine their relative abundances.

Network analysis

The co-occurrence network analysis revealed possible interactions between picoplankton families, including between bacterioplankton and picoeukaryotes, and allowed a visual summary of this correlation information (Chaffron et al., 2010). The addition of the trophic strategies of these families provided a clearer picture of their functional roles within the picoplankton (**Figure 2.12**). Positive interactions from co-occurrence networks can be used to infer ecologically meaningful parasitic or mutualistic associations between OTUs or it could be inferred that these OTUs occupy the same ecological niche. Negative correlations are an indication of competition between two OTUs or perhaps predation among these groups of taxa. The presence of three networks may be an indication of three distinct ecological processes occurring during this period. These are broadly the role of yeasts in this marine environment, parasitism by a ubiquitous dinoflagellate and the interactions of bacterioplankton with each other and with picoeukaryotes.

There was a negative association between the saprophytic yeast family *Cystobasidiomycetes* and the ciliate protists of the *Eutininnidae*, which could indicate that these yeasts are a food source for this ciliate family. Bacteria and yeasts are known to be eaten by ciliates (Fenchel, 1968). Other associations between marine yeasts and protists are not well understood. Syndinales parasites infect a wide range of hosts, including dinoflagellates, ciliates, radiolarians and diatoms (Anderson and Harvey, 2020). The positive association between *Dino-Group_II Clade* 4, 6, and 30 and the Prymnesiophyte family *Phaeocystaceae* was unlike what was found in the Protist Interaction Database (PIDA), where authors did not note a parasite host interaction between these two families (Bjorbækmo et al., 2020). It is possible that parasite dynamics of the Dino-Group-II vary globally, since their dynamics haven't been studied in detail in coastal waters. Alternatively, it may just be that the symbionts (*Phaeocystaceae*) and parasites (Syndinales) thrive under the same conditions and co-exist within the environment. These interactions require further study.

In the main co-occurrence network, heterotrophic organisms had the most associations (edges) and these were predominantly positive among all the heterotrophic families. This could indicate these organisms occupy the same environmental niche (Faust and Raes, 2012) or facilitate each other's growth. Interestingly, many of the heterotrophic families (like *Oxalobacteraece* and

Moraxellacea) were strongly negatively correlated with the photoheterotroph *Porticoccaceae*. This association could be the result of a competitive advantage offered by a photoheterotrophic lifestyle compared with heterotrophy in this environment (Tittel et al., 2003; Cottrell and Kirchman, 2009; Ward, 2019), where photoheterotrophs are more adaptable to changing nutrient availability than heterotrophs (Nygaard and Tobiesen, 1993). The Archaeal family *Nitrosopumilaceae* could possibly be preyed on by some of the heterotrophic picoplankton, resulting in the observed negative associations. These negative associations could also indicate a competitive relationship with the other chemolithoautotrophic bacterioplankton family, *Thioglobaceae*. The parasitic unclassified Dino-Group-II was positively associated with the heterotrophic MAST-7B clade, suggesting a host-parasite relationship might exist between these two picoeukaryotes, which was a relationship also suggested in Anderson and Harvey (2020). The identification of these associations highlights the need for studies focused on microbial interactions and trophic relationships in coastal ecosystems, specifically in upwelling settings. Overall, picoplankton associations in this study tended to be linked to function, with heterotrophic organisms competing for food, photoheterotrophic bacterioplankton possibly having a functional advantage over heterotrophs when the water column stratifies, parasitic picoeukaryotes following similar dynamics as their potential host organisms, and bacteria and yeasts succumbing to the heterotrophic lifestyle of the surrounding picoplankton (**Figure 2.13**).

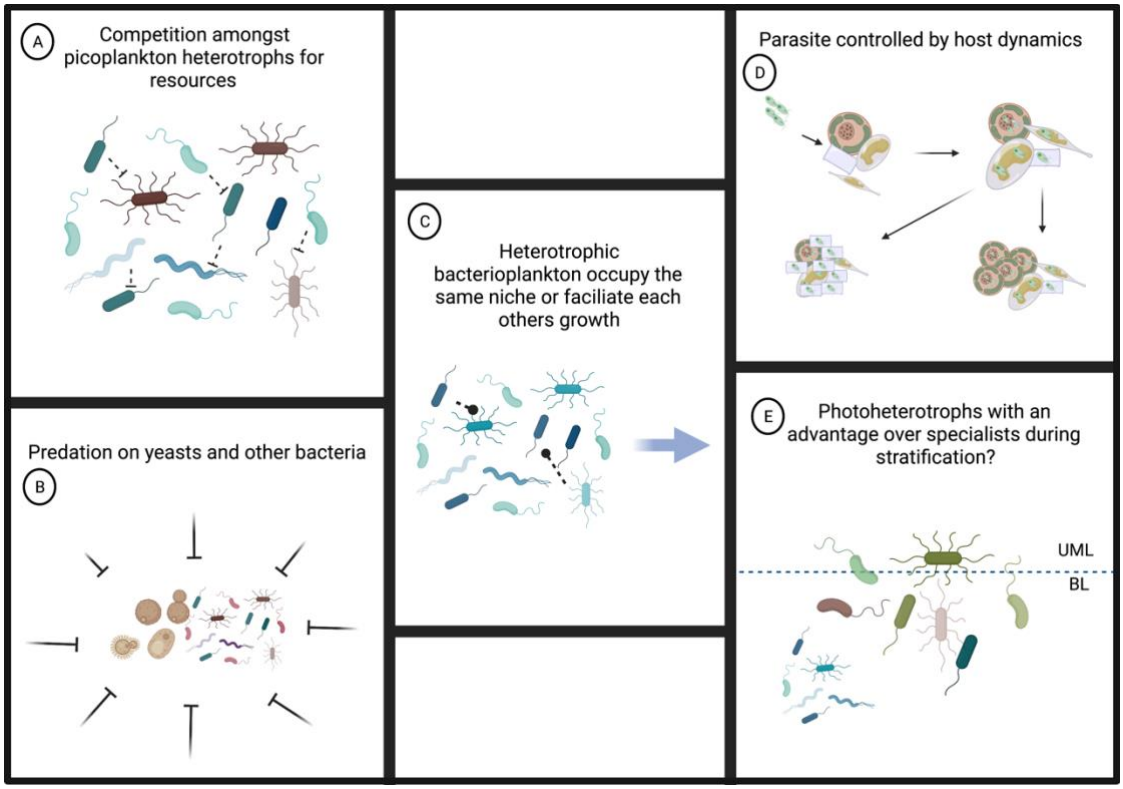

Figure 2.13. An illustration summarising the dynamic functional relationships between picoplankton during an active upwelling cycle in St. Helena Bay. These hypothesised interactions stemmed from findings in the network analysis in **Figure 2.12**. A) This hypothesis stems from the positive correlations between most heterotrophic bacterioplankton and picoeukaryotes. B) This hypothesis stems from the negative correlation between *Cystobasidiomycete* yeasts and the heterotrophic *Eutintinnidae*. C) Many positive correlations between heterotrophic bacterioplankton. D) Dinoflagellate parasites possibly increase or decrease in abundance depending on their potential host (*Phaeocystaceae*) and E) The photoheterotrophs are more abundant in stratified waters which points to a competitive advantage. Created with BioRender.com.

2.6. Conclusion

This study examined the succession of picoplankton through an upwelling event in a key area of the southern Benguela upwelling ecosystem. Physical variability introduced by upwelling was echoed in the variability found in the bacterioplankton, but less so in the picoeukaryotes. Changes in picoplankton dynamics during upwelling were evident in both the changes in overall abundances and the succession of dominant bacterioplankton and picoeukaryote groups on daily time scales. Bacterioplankton community structure responded rapidly to changes in the environment, showing short-term variability both temporally and spatially. The presence and role of bacteria has been documented previously in the St. Helena Bay area (Painting et al., 1992, 1993a and b; Rocke et al., 2020) but the identification of groups of heterotrophic bacteria during an upwelling event has extended our knowledge of their potential role in productive systems. Rhodobacterales and *Flavobacteriaceae* were some of the primary metabolisers identified, which is consistent with previous studies in St. Helena Bay (Rocke et al., 2020) and elsewhere (Hall-Stoodley et al., 2004; Dang et al., 2008). The role of Archaea in a rapidly changing environment requires further investigation, especially their potential activity at fairly shallow depths. Picoeukaryotes did not vary much in community structure or function, as was originally expected based on their small size and high diversity. It is most likely that they were outcompeted by large nanophytoplankton during this upwelling event (Burger et al., 2020). The dominance of parasitic Syndiniales in the samples echoed what was found recently in the St. Helena Bay area (Rocke et al. 2020). However, exactly how parasitism contributes to carbon cycling in this upwelling area is still unknown. Highlighted correlations between members of Syndiniales and other protist groups will add to ongoing studies aiming to identify host-parasite relationships. How marine yeasts contribute to these upwelling communities is another question that has emerged from this study; this is one of the first studies to record yeasts in such high numbers in the water column of St. Helena Bay, and the first to highlight their possible connections with other picoeukaryotes.

This single 10-day sampling programme has identified a wealth of potential ecological processes and interactions within the picoplankton during an upwelling event (**Figure 2.14**). More short time series observations are needed to confirm these findings, to extend understanding and to quantify the biogeochemical and ecological

processes occurring in St. Helena Bay. Furthermore, the addition of virus diversity, virus dynamics and virus-host interactions will expand what is known about the community structure of picoplankton. As one of very few studies on picoplankton diversity and dynamics during active upwelling conditions, this work has elucidated the rapid response of picoplankton communities to environmental change and how much the physical and chemical properties of the water column might affect picoeukaryote and bacterioplankton community composition and function.

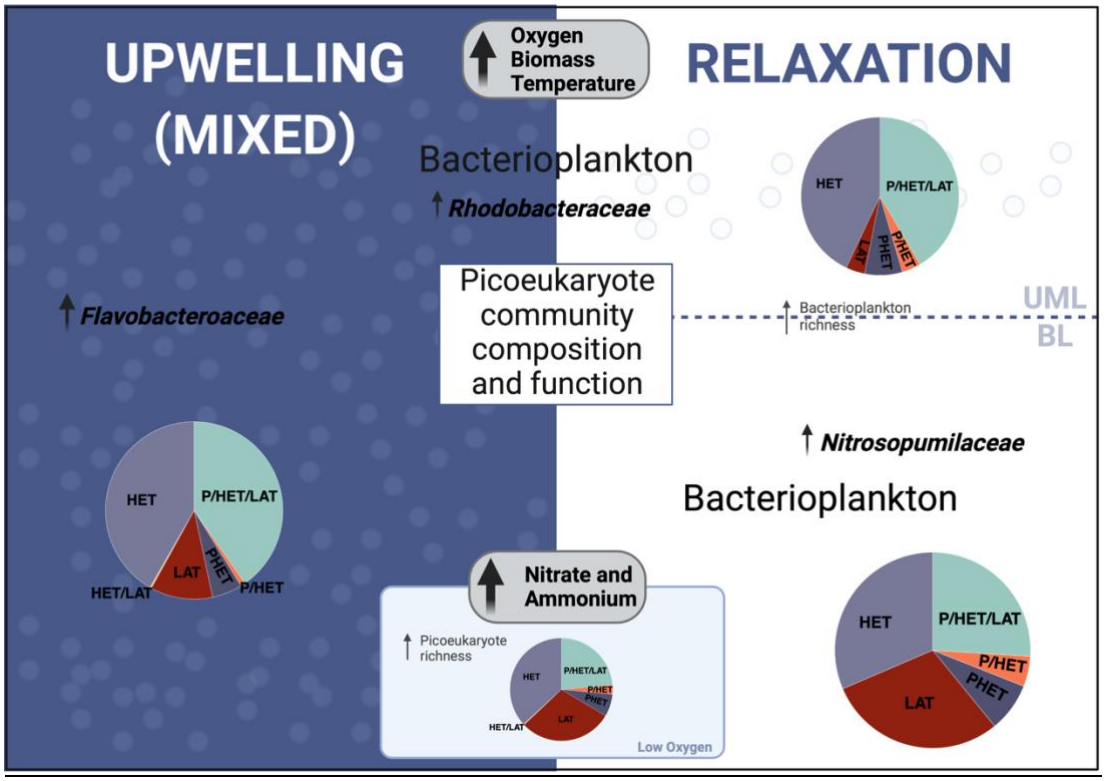

Figure 2.14. Conceptual model of the picoplankton community composition and function between the different stages of upwelling (Upwelling and Relaxation), water column types (Mixed, UML and BL) as well as oxygen states (Low oxygen environment shown in light blue box) including the environmental factors associated with physical environments shown in grey boxes. When boxes and text overlap two physical environments, this represents a shared community structure (taxonomic or functional) or environmental condition. HET=Chemoheterotrophs; LAT=Chemolithoautotrophs; PHET=Photoheterotrophs; P/HET= Photoheterotrophs/Chemoheterotrophs. Created with BioRender.com.

3. Chapter 3: Short-term dynamics of nano-picoplankton production during autumn in an embayment in the southern Benguela upwelling region

3.1. Abstract

St. Helena Bay, in the southern Benguela upwelling system, is a retention zone for plankton biomass produced during wind-driven coastal upwelling in summer. In winter, the resulting organic matter is remineralized, creating ideal environmental conditions for microbial growth and productivity throughout the water column. To study these wintertime changes on a short time scale, net primary production, uptake rates of nitrate, ammonium, and urea, as well as nano-picoplankton community composition and biomass were measured over five consecutive days. Samples were collected in March 2018 from three depths (1 m, 25 m, and 50 m) at a single sampling station in St. Helena Bay and the abundances of the nanoeukaryotes, picophytoplankton and heterotrophic bacteria populations were determined using flow cytometry. Depth-differentiation was found in net primary production and nitrogen uptake, with the highest rates found at the surface. Primary production was very low at 25 m and 50 m, likely due to the lack of light. Ammonium and urea uptake rates were 2-6-fold higher than those of nitrate suggesting that most of the biomass was produced through regenerated production. Nano-picoplankton (0.3-10 µm) contributed to the majority of carbon (67%) biomass and were responsible for 90% of net primary production as well as 79-85% of the nitrogen uptake compared to the micro-nanoplankton (>10 µm). Cell size conferred advantages to nanoeukaryotes in the nutrient-deplete euphotic zone and also to picoeukaryotes in low oxygen conditions at depth. Heterotrophic bacteria, as part of the picoplankton, had high carbon contributions at all depths, suggesting a major remineralization happening throughout the water column during these five days. This study has emphasised the importance of nanoplankton and picoplankton as major contributors to autumnal primary production and nitrogen uptake in St. Helena Bay, which is strongly influenced by the physical and chemical variability throughout the water column. This has implications on our understanding of carbon export and nitrogen cycling in St. Helena Bay and possibly the southern Benguela ecosystem.

3.2. Introduction

St. Helena Bay is the largest embayment on the west coast of South Africa and is a well-known retention zone for much of the biomass produced in the southern Benguela (Weeks et al., 2006). In summer and spring, St. Helena Bay experiences the effects of cyclic upwelling events, with autotrophic and heterotrophic communities responding quickly (daily) to variable environmental conditions caused by physical mixing and then stratification of the water column (Burger et al., 2020). As water moves offshore, the upwelled water ages and its properties change (Nelson and Hutchings, 1983). Surface waters become depleted of nutrients, and phytoplankton that bloomed in the euphotic zone are grazed upon or sink and are remineralized. Sinking material is degraded by heterotrophs as it sinks through the water column, remineralising nutrients at depth through aerobic respiration and lowering the oxygen concentrations to hypoxic and sometimes anoxic levels. Within the southern Benguela, St. Helena Bay most commonly experiences seasonal anoxia or hypoxia, especially in bottom waters (Pitcher and Probyn, 2011, 2017).

Net primary production (NPP) is an indication of the fertility of a marine ecosystem (Falkowski et al., 2003; Falkowski and Raven, 2013) and is an important metric to understand the richness of the food web in the area (Eppley and Peterson, 1979). One limiting factor for net primary production is nitrogen. Nitrogen sources like ammonium, nitrate and urea are growth-limiting macronutrients for phytoplankton in the ocean (Vitousek and Howarth, 1991). Ammonium and urea are produced through heterotrophic metabolism and are thus considered to be a regenerated source of nitrogen for phytoplankton. Nitrate is produced below the euphotic zone by organisms that oxidise remineralized ammonium into nitrite and nitrate in a process known as nitrification (Ward, 2008). Vertical mixing and upwelling transport NO_3^- from depth to the surface, where it is used for phytoplankton growth as a source of new nitrogen. NPP fuelled by new or regenerated nitrogen respectively is termed “new production” or “regenerated production” (Dugdale and Goering, 1967). The theoretical framework proposes that, over appropriate measures of time and space, the rate of NO_3^- fuelled production (new production) should be balanced by a downward flow of organic matter and, therefore, new production can be used as a proxy for carbon export. The f-ratio or flux ratio determines the proportion of measured new

production relative to total production (NPP) to estimate the amount of carbon exported from the surface (Eppley and Peterson, 1979).

Nanoeukaryotes and picoplankton are significant contributors to primary production and cycling of carbon and nitrogen in the ocean (Stockner, 1988; Fogg, 1995; Leblanc et al., 2018), and their importance has been highlighted in St. Helena Bay (Burger et al., 2020). These small organisms can thrive under low nutrient and low oxygen conditions, because of their large surface to volume ratios (Finkel et al., 2010). Phytoplankton fix carbon in the form of CO_2 through photosynthesis, and incorporate it into carbon biomass, which can be exported from the surface by sinking aggregates or excreted as dissolved organic matter (DOM), a by-product of autotrophic and heterotrophic metabolism (Volk and Hoffert, 1985). DOM is used predominantly by bacterioplankton (archaea and bacteria) as a source of energy and this DOM is further integrated into the food web through bacteriovory by heterotrophic or mixotrophic nano- and picoeukaryotes (Massana et al., 2004). Organic matter is converted and assimilated as dissolved organic carbon, a process that is a key part of the microbial loop (Azam et al.,1983; Fenchel, 2008).

Autotrophic picoplankton are represented predominately by two genera, namely *Prochlorococcus* and *Synechococcus*. *Prochlorococcus* is the smallest and most abundant photosynthetic organism in the world (Partensky et al., 1999b). These cyanobacteria display niche partitioning, with multiple ecotypes making them adaptable to different environmental conditions, although they are most often found in the open ocean in oligotrophic waters (Moore et al., 1998). *Synechococcus* is ubiquitous in the marine environment because of their genetic diversity and ability to utilise most nitrogen sources. They are often abundant in the nutrient-rich areas in the euphotic zone of the ocean (Partensky et al., 1999a; Moore et al., 2002). Picoeukaryotes, another portion of the picoplankton, are represented by multiple taxa of varying functional diversity and are found throughout the ocean (Worden and Not, 2008). These taxa include groups belonging to the Chlorophyta and Haptophyta, and parasitic dinoflagellates like the Syndiniales (Guillou et al., 2008; Vaulot et al., 2008). The larger nanoplankton include naked flagellates, diatoms and dinoflagellates that employ mixotrophic lifestyles, making them part of the trophic level that consumes picoplankton (Campbell and Carpenter, 1986; Estep et al., 1986). Some of the picoplankton consumed are the heterotrophic bacteria, which are responsible for

recycling much of primary production produced (Kirchman, 2000), the rest of which is sequestered into the marine food web through grazing or sinks to the seafloor as aggregates for long term storage (Arístegui et al., 2009). In this study, the term nano-picoplankton refers to plankton in the 0.3–10 µm size fraction.

In summertime primary production in the SBUS is dominated by new production, because of wind-driven upwelling of remineralised nutrients (Burger et al., 2020). In autumn and winter upwelling favourable winds subside, shifting from southerly to northerly winds (Shannon and Nelson, 1996), and evidence strongly suggests that phytoplankton growth in the SBUS is supported by ammonium during winter specifically (Flynn et al., 2018). High concentrations of ammonium were found to limit nitrate uptake and therefore carbon drawdown (Dortch, 1990; Flynn et al., 2018). It is hypothesized that, at ammonium concentrations >1 µM, nitrate uptake becomes inhibited due to the preferential uptake of ammonium (Dortch, 1990). There are few high-resolution studies on autumnal or wintertime productivity and nutrient uptake rates in St. Helena Bay to test this hypothesis (Pitcher and Probyn, 2017; Flynn et al., 2018, 2020).

This study adds to the building body of work on NPP and nitrogen uptake in the southern Benguela, and specifically in St. Helena Bay (Brown, 1984; Brown and Field, 1986; Brown et al., 1991; Barlow et al., 2009; Lamont et al., 2014; Flynn et al., 2018; Burger et al., 2020). Most of those studies observe spring and summer rates, with fewer data available outside of the upwelling season in the southern Benguela. In this study the aim was to determine the variability in net primary production and nitrogen uptake rates in autumn over a five-day period at a single station in St. Helena Bay. Additionally, the bulk phytoplankton and distinct size groups responsible for NPP and nitrogen uptake are further elucidated. With the use of daily flow cytometry and productivity assessments, short-term drivers of plankton community composition, production, and nutrient (nitrate, ammonium, and urea) uptake and recycling were characterized throughout the water column at the end of the upwelling season.

3.3. Materials and Methods

Sampling location

To study the short-term dynamics of phytoplankton productivity in St. Helena Bay, a Eulerian sampling approach was used. Samples were collected at a single station (32°35’ 75.0” S, 18°02’60.0” E) in St. Helena Bay, on the west coast of South Africa (**Figure 3.1**), from 11 to 15 March 2018, referred to in this manuscript as day 1 to day 5. Sampling was conducted from an inflatable craft (Department of Forestry, Fisheries and the Environment) and all samples were collected using a 5 L hand-held Niskin bottle. The bottom depth at this sampling site is ~50 m and samples were collected at 1 m, 25 m and 50 m on day 1 to 4 and only from 50 m on day 5 (because of sea conditions that made sampling dangerous). Depths were pre-selected, without access to real-time CTD data, with the objective of analysing as much of the water column as possible.

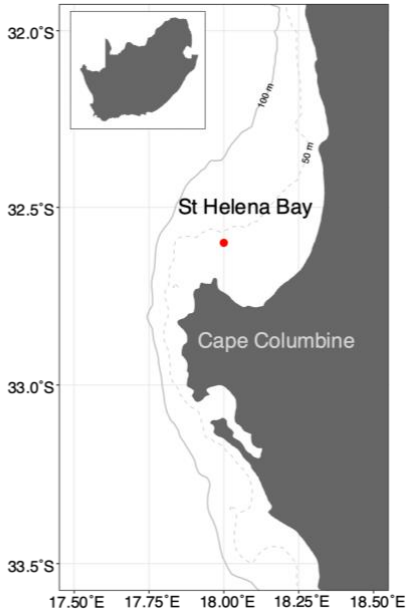

Figure 3.1. Map of St. Helena Bay on the west coast of South Africa, showing the sample site for this study (red dot).

Hydrography

A hand-held CTD (SBE-19 CTD) was deployed once at the start of each sampling session on day 1 to 5. The CTD casts were used to measure the conductivity and temperature of the water column, with additional sensors (WETLabs fluorometer

(WETStar) sensor and the SBE 43 oxygen sensor) providing measurements of fluorescence and oxygen concentrations. Euphotic zone depth (Z_{eu}) was calculated as the depth at which the fluorescence is 10% of the maximum fluoresce RFU value. Fluorescence measurements were converted to chlorophyll and were corrected for depth using the formula:

1. CTD-derived Chlorophyll concentration ($\mu g.L^{-1}$) =
   2,1485 - 0,8075*LOG10(depth (m))

which was calculated by plotting the multipliers of the relationships between the fluorescence readings and measured chlorophyll readings at multiple depths. The potential density anomaly of seawater ($\sigma\theta$ $kg.m^{-3}$) was calculated from absolute salinity ($g.kg^{-1}$) and conservative temperature (˚C) using a reference pressure of 0 dbar according to IOC et al. (2010). All calculations for $\sigma\theta$ were calculated in R using the package oce (Kelley, 2013).

Extracted chlorophyll a from samples

Size fractionated chlorophyll *a* (Chl-*a*) was measured at each sampling time and depth. Five litres of seawater were collected from 1 m, 25 m, and 50 m on day 1–5 in duplicate and pre-filtered directly from the Niskin bottle through a 200 µm mesh into dark 5 L HDPE bottles. From these 5 L bottles, 500 mL (day 1 and 5) and 250 mL (day 2–4; volume decreased based on observed biomass) was filtered sequentially through a 10 µm (nylon) and 0.3 µm (GF/F) membrane filter. The filter membranes were flash frozen and stored at -20˚C while in the field and then at -80˚C in the Department of Biological Sciences at the University of Cape Town until further analysis.

The chlorophyll *a* concentration of the 0.3–10 µm and 10–200 µm size fractions were measured using a fluorometric method. Each filter was transferred to a glass vial, covered with 8 mL of 90 % acetone and incubated at -20˚C for 20–30 hours. Measurements were done on a fluorometer with a Chl-NA module using 90 % acetone as a blank. Relative fluorescence unit (RFU) measurements were converted to chlorophyll concentrations using the equation:

2. Chlorophyll concentration ($\mu g.L^{-1}$) = (RFU_{sample} – $RFU_{acetone\ blank}$) x 0.163 $\mu g.L^{-1}$ x ($Vol\ (L)_{acetone}$ / $Vol\ (L)_{seawater}$)

Nutrient analysis

Triplicate unfiltered 50 mL samples were taken at each sampling time for ammonium (NH_4^+), nitrate (NO_3^-), nitrite (NO_2), silicate (SiO_4^{4-}), phosphate (PO_4^{3-}) and urea measurements. These samples were stored at –20˚C until further analyses. Ammonium concentrations were measured fluorometrically according to the methods of Holmes et al. (1999). Nitrate + nitrite and silicate were measured using a Lachat QuickChem Flow Injection Analysis platform. All measurements were corrected for instrument drift through measurement of standards every 10 minutes. Nitrite was measured colorimetrically according to the method described by Grasshoff et al. (1983) using a Thermo Scientific Genesys 30 visible spectrophotometer. Nitrate concentrations for each sample were calculated by subtraction where nitrate=(nitrate+nitrite) - nitrite. Phosphate was measured colorometrically according to the method of Murphy and Riley (1962) using a Thermo Scientific Genesys 30 visible spectrophotometer.

Nitrification: Nitrite oxidation rates

Nitrite oxidation rates were measured to determine the proportion of nitrate that feeds directly into primary production estimates. Ammonia oxidation rates, although important to quantify to understand the redox balances in the nitrification pathway, were not measured. For this analysis it is assumed that ammonia oxidation rates are similar to nitrite oxidation rates.

Seawater was collected from three sampling depths (1 m, 25 m and 50 m), and for each sample 1 L was prefiltered (200 µm filter) into a dark bottle. For samples taken at each depth two dark bottles were rinsed three times with the water from the appropriate depths and 250 mL of prefiltered seawater was added to each bottle. For each depth a final concentration 0.4 µM (100 µL) of $^{15}N\text{-}NO_2$ and was added to the bottles. Immediately, the bottles were homogenised and a 30 mL $T_{initial}$ sample was taken from each bottle and frozen at -20˚C until further analysis. The remaining sample in the bottles was incubated for 24 hours at *in situ* temperature, after which a 30 mL T_{final} sample was collected and frozen at -20˚C. The nitrite remaining in both $T_{initial}$ and T_{final} was removed by adding 0.3 mL of 5% sulfamic acid (Granger and Sigman, 2009). After the pH was adjusted to approximately 7-8 using 2M NaOH, the denitrifier method (Sigman et al., 2001) was used to identify the N isotopic composition:

3. $\partial^{15}N$, in per mil (‰) vs. N_2 in air, = $\{(^{15}N/^{14}N)_{sample}/(^{15}N/^{14}N)_{ref} - 1\} \times 1.000$) of the sample NO_3^-. A Delta V Plus IRMS with custom-built purge-and-trap front end was used for this analysis (McIlvin and Casciotti, 2011). The $^{15}NO_3^-$ enrichment resulting from NO_2^- oxidation was determined from the difference between $T_{initial}$ and T_{final} $\partial^{15}N\text{-}NO_3^-$. Nitrate oxidation rates (nmol L^{-1} d^{-1}) were calculated by determining the change in $^{15}NO_3^-$ concentration during the experiment. The formula used for nitrite oxidation (Peng et al., 2015) was:

4. Nitrite oxidation (nmol L^{-1} d^{-1}) = $\frac{\Delta[^{15}NO_3^-]}{f_{NO2}^{15} \times T}$

where $\Delta[^{15}NO_3^-]$ is the change in $^{15}NO_3^-$ concentration between $T_{initial}$ and T_{final}; f_{NO2}^{15}– is the fraction of the NO_2^- pool labelled with ^{15}N at the beginning of the experiment, and *T* is the length of incubation (days).

Net primary production and nitrate, ammonium, and urea uptake rates

Seawater was collected at three sampling depths (1 m, 25 m and 50 m) for incubation experiments to measure net primary production (NPP) and uptake of NO_3^-, NH_4^+ and urea. For each sampling depth one litre of seawater was taken in duplicate per analysis (9 L total). The samples were pre-screened (200 µm) to remove large grazers and were transferred into nine 1 L polycarbonate bottles. The isotope tracers $NaH^{13}CO_3$ and $^{15}NH_4Cl$ were added to three 1 L bottles with final tracer concentrations of 100 µmol.L^{-1} and 0.05 µmol.L^{-1} respectively. Potassium nitrate ($K^{15}NO_3$) was added to three bottles at a final tracer concentration of 0.5 µmol.L^{-1} and Urea-N_2 ($H_2{}^{15}NCO_2{}^{15}NH_2$) was added to the final three bottles at a final tracer concentration of 0.5 µmol.L^{-1}. Bottles were transported in the dark back to land (approximately 1 hour). The nine bottles per depth (27 bottles) were incubated for 3-5 hours in a custom-built incubator cooler with running seawater and natural density filters to simulate the 55%, 10% and 1% light levels. Surface samples were incubated at 55% light density, and 25m samples at 10% and 50 m samples at 1%. Samples from 25 m and 50 m were introduced to light to assess the potential for productivity. These experiments were terminated by filtrations, where for each 1 L bottle, 300 mL of treated seawater was filtered through a 25 mm 10 µm nylon filter and 300 mL through a 25 mm 2.7 µm combusted (450˚C for 5 hours) glass fibre (GF/D) filter. The particulate organic matter (POM) collected on the 10 µm nylon filter was resuspended in ~30 mL of 0.2 µm

filtered seawater and then re-filtered onto a 25 mm 0.7 µm combusted GF filter. All filters were stored in combusted foil envelopes and frozen at -80˚C until further analysis.

Filters were oven dried for 24 hours at 45˚C and then acidified for a further 24 hours in the presence of 37.5 % HCl to remove inorganic carbon. The acidified filters were oven dried for 30 minutes at 45˚C, cored with a 20 mm punch and folded into tin cups. The tin cups were stored in clean 96-well trays placed in a desiccator until analysis using a Thermo Delta V Plus isotope mass ratio spectrometer (IRMS) coupled with a Flash 2000 elemental analyser. Sample blanks were run every 10-20 samples and laboratory standards (Merck) were run after every five samples. Standard curves were used to determine particulate organic carbon (POC) and particulate organic nitrogen (PON) content of each sample, which was then normalized for the volume of seawater filtered to determine concentrations.

The transport rates (µmol.L^{-1}.$hour^{-1}$) of NPP and uptake of NO_3^-, NH_4^+ and urea (ρNO_3^-, ρNH_4^+ and ρUrea) were calculated according to Dugdale and Goering (1967) and Dugdale and Wilkerson (1986). Briefly, transport was calculated by multiplying the specific carbon uptake rate (V_C) by [POC] and the nitrogen uptake rates (V_{NO3}, V_{NH4} and V_{Urea}) by [PON]. Euphotic zone integrated productivity rates (mmol.m^{-2}.h^{-1}) were computed by summing distance integrated surface NPP, ρNO_3^-, ρNH_4^+ and ρUrea samples between 0 m and the bottom of the euphotic zone. The f-ratio, which is the proportion of NPP that is fuelled by nitrate, was calculated as $V_{NO3}/(V_{NO3} + V_{NH4} + V_{Urea})$ according to Eppley and Peterson (1979). Biomass and uptake rates were calculated for three different size classes of plankton: the total plankton (> 0.3 µm), the nano-microplankton (> 10 µm) and the nano-picoplankton (0.3–10 µm), which was calculated by subtracting the micro-and nanoplankton from the total plankton values.

Nano-microplankton (> 10 µm) samples on day 1 for NPP and ρNH_4^+ at 25 m and 50 m, ρNO_3^- at 25 m and ρUrea at 1 m and 25 m did not pass quality control and were thus omitted from the study.

Flow cytometry

Samples for flow cytometry analysis (200 µm filtered seawater) were collected in triplicate in 2 mL cryovials at each sampling time. Glutaraldehyde was added to

each sample at a concentration of 0.25 %, after which the samples were incubated at room temperature for 15–20 minutes, flash frozen in liquid nitrogen and stored at -20˚C while in the field and then at -80˚C in the Department of Biological Sciences at the University of Cape Town until further analysis.

To enumerate cells in the pico-nano size fraction, samples were stained with SYBR 1 Green (Sigma), incubated in the dark for 10 minutes and run on the BD LSR flow cytometer at the Institute of Infectious Disease and Molecular Medicine (IDM), Medical School, University of Cape Town. In total, 39 samples were analysed, including replicates. *Synechococcus, Prochlorococcus*, picoeukaryotes (0.2-3 µm) and nanoeukaryotes (2-20 µm) were enumerated following the method of van Dongen-Vogels et al. (2011) and Marie et al. (1997). FlowJo® was used to enumerate picoeukaryotes through their signal emitted on the orange (PE: 585/42 band pass) versus red (PC: 661/16 band pass) and chlorophyll fluorescence signals. Nanoeukaryotes were differentiated from picoeukaryotes by their higher forward scatter signal. *Synechococcus* numbers were distinguished from the picoeukaryotes through their higher PE signal. *Prochlorococcus* numbers were discriminated from other bacteria by their chlorophyll signal. Heterotrophic bacteria were enumerated by plotting side scatter versus FITC. To correct for the suspected under estimation of heterotrophic bacteria, bacteria were counted using FISH (Fluorescence *in situ* hybridization) and microscopy. The same samples were briefly preserved in Formaldehyde (1%) and filtered onto a 47mm polycarbonate filter were stained with DAPI (300nM final concentration) for 5 minutes, then rinsed 3 times with PBS. Filter slices were mounted onto slides with 90% glycerol, then heterotrophic bacteria cells were enumerated under 63X magnification on a Zeiss Axio observer inverted microscope under UV light. A 1100X correction was applied to the HBac flow cytometry abundances.

Nano- and picoplankton cell abundances (cells.mL^{-1}) were converted into carbon (µgC.L^{-1}) and nitrogen (µgN.L^{-1}) biomass using cell to carbon/nitrogen conversions from the literature (**Table 3.1**). Carbon and nitrogen biomass respectively were expressed as µmolC.L^{-1} and µmolN.L^{-1}, calculated by dividing biomass concentrations by the molar mass of carbon (12) or nitrogen (14).

Table 3.1. Carbon and nitrogen biomass conversion ($fgC.cell^{-1}$) factors obtained from (Hernández-Hernández et al., 2020) for the taxa of interest: nanoeukaryotes, picoeukaryotes, *Synechococcus*, *Prochlorococcus* and heterotrophic bacteria.

Species	Carbon biomass conversion ($fgC.cell^{-1}$)	Nitrogen biomass conversion ($fgN.cell^{-1}$)
Nanoeukaryotes	3100	673.9
Picoeukaryotes	500	98
Synechococcus	120-	22
Prochlorococcus	43	13
Heterotrophic bacteria	18	4.9

Data Analysis

All data visualisation and analyses were conducted using the R software (R Core Team, 2013). For reproducibility, seed was set at 201 in R. An analysis of variance (ANOVA) was performed to determine whether nutrients, POC, PON, NPP and nitrogen uptake rates, cell abundances and cell biomasses were different between depths and days using the 'lm' function in base R and 'Anova' function in the car package (Fox and Weisberg, 2019). When the ANOVA results were significant a Tukey HSD post hoc test was performed using the 'tuckey_hsd' function.

A principal component analysis (PCA, n= 13, where n is the number of samples) was performed to determine the associations among the environmental factors (Chl-*a*, temperature, salinity, fluorescence, oxygen, NO_3^-, NH_4^+, NO_2, PO_4^{3-}, Urea, SiO_4^{4-}, POC and PON) at the different depths and on the different days. Redundancy was reduced by using correlation analysis to drop highly correlated (R >0.9) variables. The PCA was performed and visualized using the FactoMineR and factoextra packages (Lê et al., 2008; Kassambara and Mundt, 2020).

An nMDS (non-metric multidimensional scaling) using the Bray-Curtis similarity index was performed on carbon biomass values for each group to visualise differences between samples using the vegan package (Oksanen, 2016). Environmental factors were fitted to the nMDS using the 'envfit' function with 999 permutations from the vegan package. A permutational multivariate analysis of variance (PERMANOVA) was performed to verify the differences between depths (1 m, 25 m, and 50 m) and days 1-5 using the 'adonis' function from the vegan package.

3.4. Results

Environmental conditions over the five-day sampling period

The wind during the sampling period blew from a north easterly direction on the first day of sampling followed by four days from a southerly direction (**Figure S3.1A**). Wind speeds were relatively low on the first four days (2.9 to 3.8 $m.s^{-1}$), increasing on day 5 to 8.8 $m.s^{-1}$, which caused logistical issues for sampling at 1 m and 25 m on day 5 (**Figure S3.1B**).

The potential density anomaly (σ_θ) data, which are used to denote the mixed layer depth (MLD), showed a stratified water column throughout the five sampling days, with the MLD between 13.9 and 20.7 m (**Figure 3.2A**, **Table 3.2**). The euphotic zone depth was shallow throughout, ranging from 3.2 m to approximately 6 m (**Figure 3.2B**, **Table 3.2**). Seawater temperatures ranged between 9.62 to 15.12˚C, with warmer temperatures observed from the surface to approximately 20 m depth, whereafter temperatures decreased rapidly to less than 10˚C (**Figure 3.2C**).

The water column was most oxygenated above 20 m throughout the study (**Figure 3.2D**), with the highest oxygen concentrations ($[O_2]$) found at the surface on day 2, and reaching lows of 25.01 $\mu mol.L^{-1}$at 50 m. Low oxygen water is defined in this study as having a $[O_2] < 89.32$ $\mu mol.L^{-1}$. Surface waters were consistently oxygenated on all 5 sampling days. All samples taken from 50 m were low oxygen samples, with oxygen concentrations below 89.32 $\mu mol.L^{-1}$. The only other low oxygen sample was at 25 m on day 4. There seemed to be an intrusion of oxygen to almost 40 m on day 3, which was not reflected on any other sampling day. Salinity varied between 34.67 PSU on day 2 at the surface to 34.84 PSU the next day, also at the surface (**Figure 3.2E**).

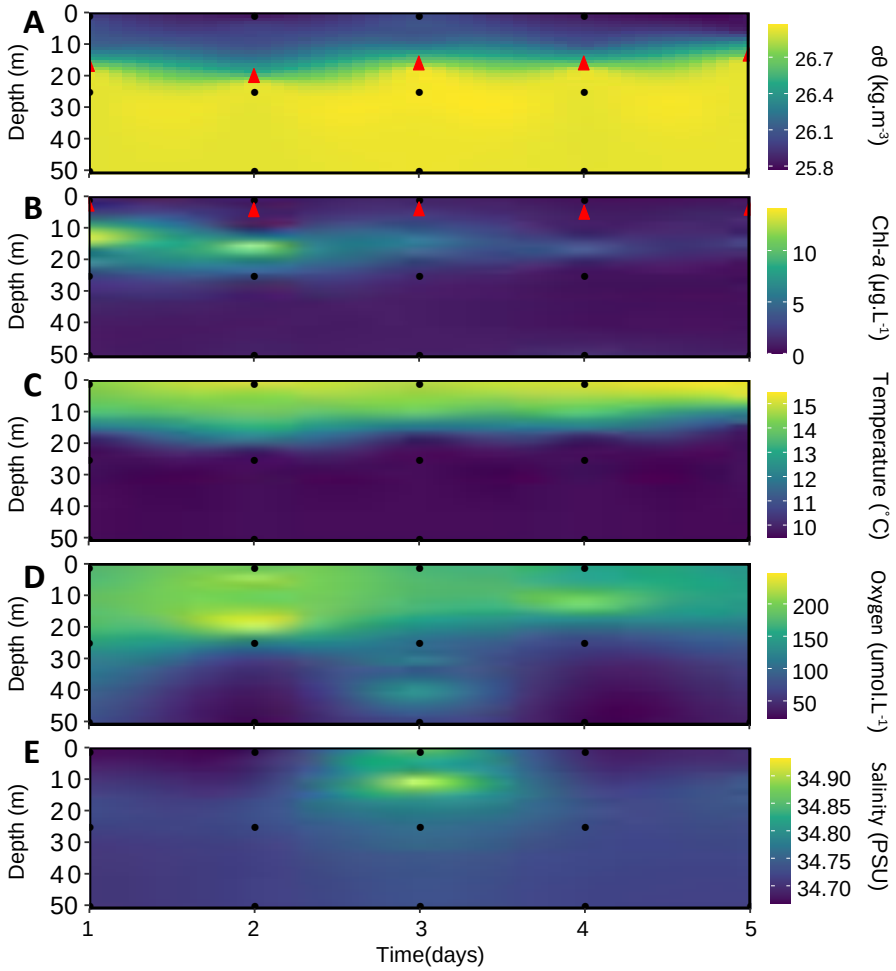

Figure 3.2. Profiles of the water column in St. Helena Bay in March 2018 showing potential density anomaly σθ (A; (kg.m^{-3})), chlorophyll-*a* concentrations (B; µg.L^{-1}), temperature (C; ˚C), oxygen concentrations (D; µmol.L^{-1}) and salinity (E, PSU). Black dots indicate the depths at which discrete samples were taken. Red triangles in (A) show the mixed layer depth (MLD) and in (B) the euphotic zone depth (Z_{eu}) on each day of the experiment.

Table 3.2. The depths of the mixed layer, euphotic zone and deep chlorophyll maximum, depth-integrated net primary production (NPP; $mmol.m^{-2}.d^{-1}$), uptake rates of ammonium (ρNH_4^+; $mmol.m^{-2}.d^{-1}$), nitrate (ρNO_3^-; $mmol.m^{-2}.d^{-1}$), and urea (ρUrea; $mmol.m^{-2}.d^{-1}$) and the depth-weighted average f-ratio for each of the five sampling days at the sampling station in St. Helena Bay in March 2018. As only one depth was sampled on day 5, no integrated NPP, ρNH_4^+, ρNO_3^- , ρUrea or f-ratio were calculated for this day.

Time (day)	Mixed layer depth (m)	Euphotic zone depth (m)	Deep chlorophyll maxima (m)	NPP	ρNO_3^-	ρNH_4^+	ρUrea	f-ratio
1	17.2	3.2	13.6	4.32	1.19	3.80	0.58	0.30
2	20.7	5.0	15.8	2.52	1.11	12.13	3.36	0.20
3	16.7	4.7	17.5	5.53	0.08	0.40	0.33	0.18
4	16.7	5.8	17.6	4.03	0.02	0.55	0.61	0.14
5	13.9	4.5	15.2	-	-	-	-	-

A subsurface chlorophyll maximum was found at approximately 15 m, seemingly dissipating as the sampling period progressed (**Figure 3.2B**). It should be noted that the chlorophyll maxima were not sampled in this study. The highest daily chlorophyll concentrations, as estimated by CTD-derived fluorescence, were found on day 1 and 2 (**Figure 3.2B**). Measurements of extracted size-fractionated (>10 µm and 0.3–10 µm) chlorophyll *a* taken from sampling depths of 1 m, 25 m and 50 m showed that larger organisms (>10 µm) were found to contribute most chlorophyll *a* during this study in comparison to the smaller (0.3–10 µm), nano-picoplankton fraction (**Figure 3.3**). The highest measured chlorophyll *a* concentrations were found on day 1 across all depths. Nano-picoplankton had larger mean ± standard deviation (SD) chlorophyll *a* concentrations at the surface (0.61–0.28 $\mu g.L^{-1}$) in comparison to those at depth (**Figure 3.3A**), and contributed a greater portion to the total Chl-*a* than at depth.

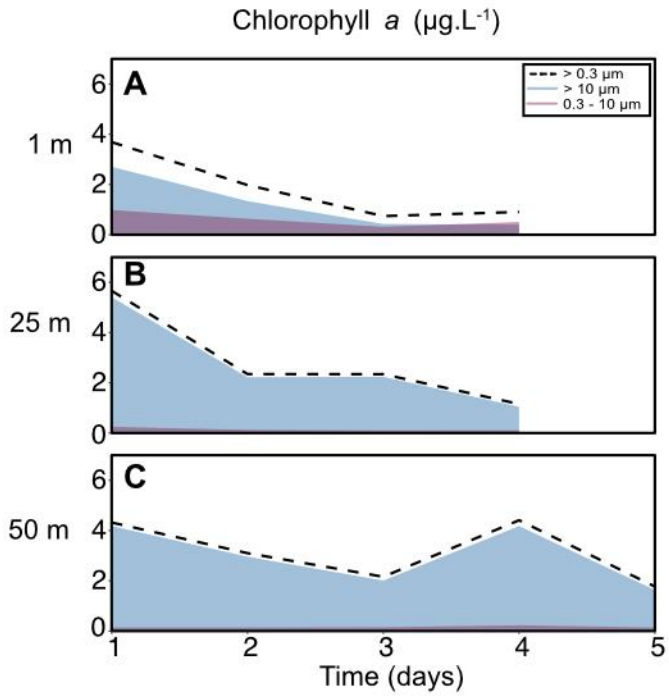

Figure 3.3. Size-fractionated daily chlorophyll-*a* concentrations (µg.L^{-1}) from a station in St. Helena Bay in March 2018 at 1 m (A), 25 m (B) and 50 m (C). The dotted line indicates the measured total Chl-*a* concentrations (>0.3 µm) and the shaded areas indicate the proportions contributed by different size fractions. Blue shading = >10 µm, pink shading = 0.3–10 µm, calculated by subtracting the >10 µm size fraction from the total Chl-*a* concentrations.

Throughout the study surface waters were nutrient-depleted, with an increase in NO_3^-, NO_2, SiO_4^{4-} and PO_4^{3-} at depth (**Figure 3.4**, **Table S3.2**). The nutrient profile of NO_3^- throughout the sampling period was typical of a stratified water column, with low concentrations at the surface and higher concentrations at depth. On day 2 at 25 m there is a decrease in NO_3^-, which corresponds to an increase in NO_2 concentrations (**Figure 3.4**). Despite trends of low ammonium concentrations at the surface in comparison to depth this variability is not significant over time or depth, with ammonium concentrations ranging from below detection limit to 1.33 µM (**Figure 3.4D–F**, **Table S3.2** and **S3.3**). Concentrations were, on average, lower at the surface, with the highest average concentration found at 25 m. Urea concentrations did not differ between depths, but at 25 m and 50 m concentrations differed between sampling days, increasing from day 1 to day 3 at 25 m and with lower concentrations of urea on day 1 in comparison to day 2, 3 and 4 at 50 m (**Table S3.2** and **S3.3**). Like NO_3^- concentrations, SiO_4^{4-} concentrations are higher at depth than at the surface,

reaching a maximum at 50 m on day 3 (**Figure 3.4M–O**, **Table S3.2** and **S3.3**). The high [SiO_4^{4-}] at and below 25m are located below the highest levels of biomass as inferred by chlorophyll concentrations (**Figure 3.2A**).

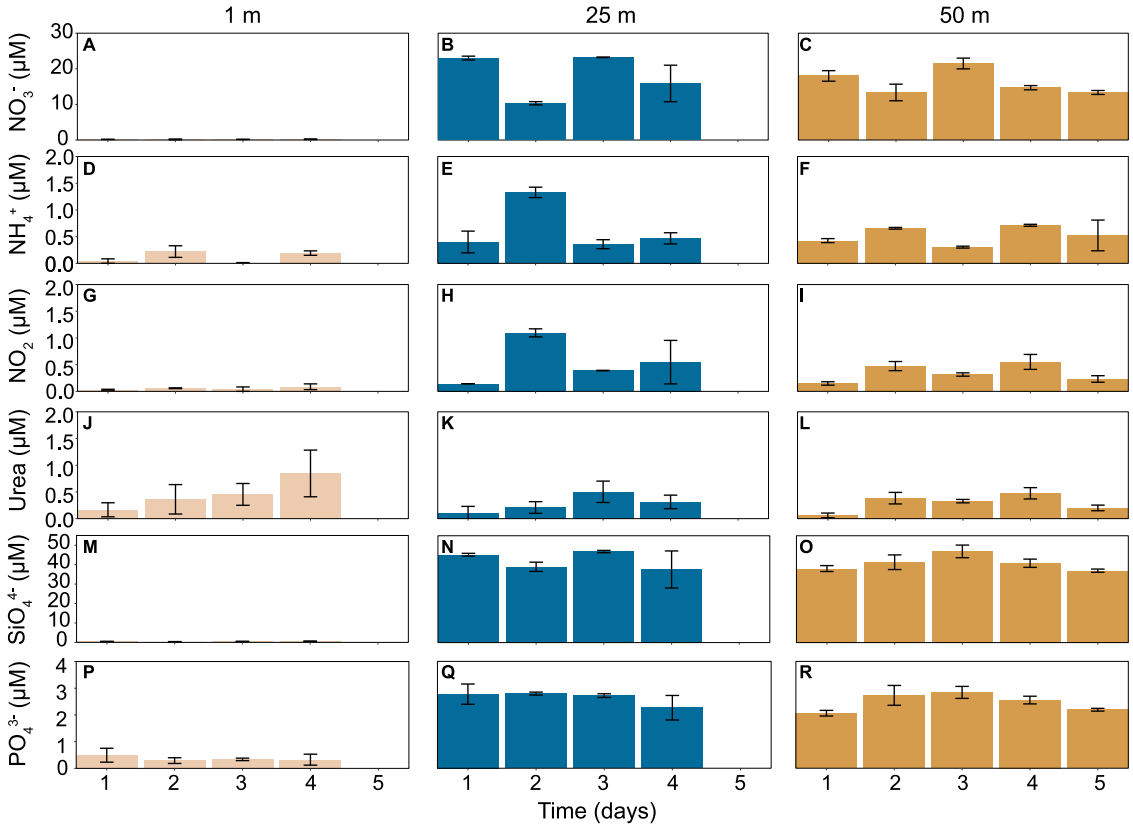

Figure 3.4. Nutrient concentrations at three depths from a station in St. Helena Bay in March 2018. The measured nutrients include (A–C) nitrate (NO_3^- (µM)), (D–F) ammonium (NH_4^+ (µM)), (G–I) nitrite (NO_2 (µM)), (J–L) urea (µM), (M–O) silicate (SiO_4^{4-} (µM)), and (P–R) phosphate (PO_4^{3-}). Error bars indicate the standard deviation (n=3). On day 5 there were no nutrients measured at 1 m and 25 m.

Total particulate organic carbon ($[POC]_{total}$) and nitrogen ($[PON]_{total}$) concentrations were greatest at 1 m throughout the study and lowest at 25 m (**Figure 3.5**). Spatially, POC_{total} concentrations were elevated at the surface in comparison to 25 m and $[PON]_{total}$ was higher at the surface in comparison to the deeper depths (**Figure 3.5**, **Table S3.2** and **S3.5**). Unlike for chlorophyll *a* concentrations, nano-picoplankton (0.3–10 µm) contributed 67 ± 9 % of the total POC and 78 ± 8 % of the total PON over the five days, exceeding the contributions by microplankton and larger nanoplankton (>10 µm). Particulate organic carbon

concentrations did not differ daily at the surface, but at 25 m, smaller concentrations of total POC were measured on day 4 in comparison to the other sampling days and, at 50 m, concentrations on day 1 are larger than those measured on the last three days of sampling (**Figure 3.5A–C**, **Table S3.3** and **S3.6**). This same pattern is seen in the nano-picoplankton size fraction as the biggest contributor to total POC. The concentration of POC contributed by the >10 µm size fraction is no different between depths or days. There is a general decline in POC concentrations over the 5-day sampling period at all 3 depths (**Figure 3.5A–C**). Total PON, however, only differs temporally at 25 m, where all days differ in PON concentrations except for day 2 and 3 (**Figure 3.5D–F**, **Table S3.3** and **S3.6**).

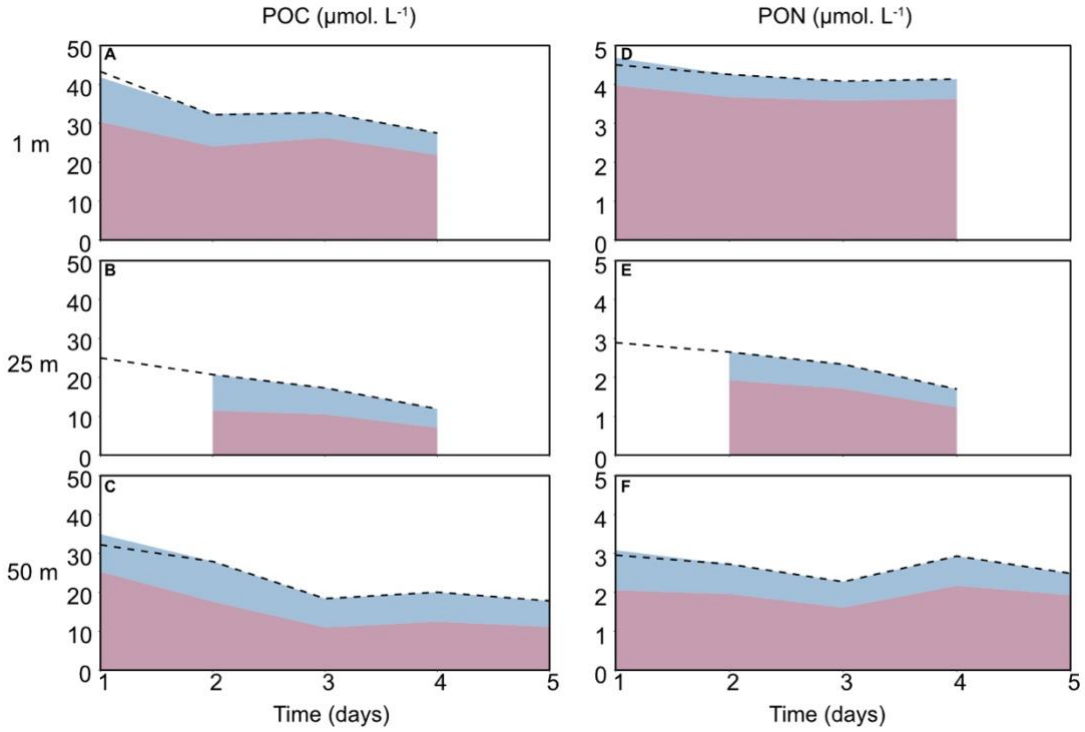

Figure 3.5. Size fractionated concentrations of particulate organic matter (µmol.L^{-1}) on five days in March 2018 from a station in St. Helena Bay. (A) POC at 1 m, (B) POC at 25 m, (C) POC at 50 m, (D) PON at 1 m, (E) PON at 25 m, (F) PON at 50 m. The dotted line indicates the measured total concentrations (>0.3 µm) and the shaded areas indicate the proportions contributed by different size fractions. Blue shading = >10 µm, pink shading = 0.3-10 µm, calculated by subtracting the >10 µm size fraction from the total concentrations. The data on each day is the average of two concurrent and independent measurements.

Total POC:PON in the samples is always >6.63:1, the expected Redfield ratio of marine biomass (**Figure 3.6A**). Of all sampling days, POC:PON was closest to Redfield on day 4, with an average ± SD (n=4) across all depths of 6.8 ± 0.2. The day with the highest measured POC:PON was day 1 (9.7 ± 1.2, n=3) and the depth with the highest POC:PON was 50 m (8.6 ± 1.8, n=5). POC:PON is closest to Redfield at 1 m (6.4 ± 1.2). The average POC:PON of the >10 µm size fraction (12 ± 2) is much is higher than the 0.3-10 µm size fraction, (7.1 ± 1.9) (**Figure 3.6B–C**).

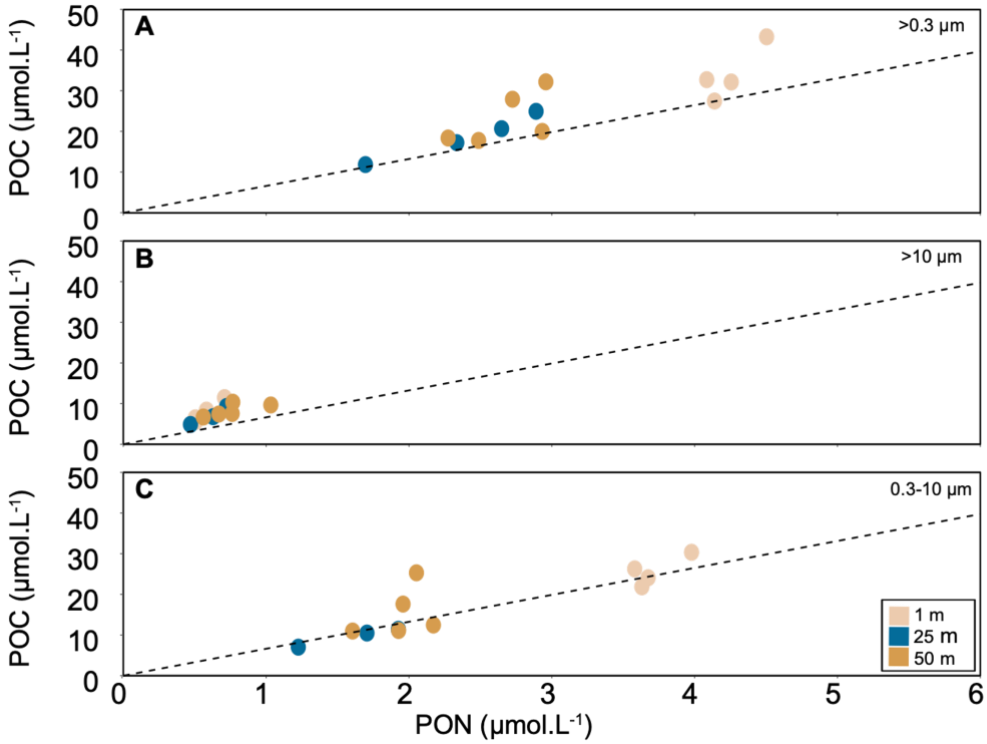

Figure 3.6. The relationship between the particulate organic carbon (POC µmol.L-1) and particulate organic nitrogen (PON µmol.L-1) concentrations of the A) total (>0.3 µm), B) >10 µm and C) 0.3-10 µm size fractions. The dashed black 6.63:1 line is the Redfield ratio. Samples taken from 1 m are in beige, 25 m in blue and 50 m in gold.

Samples clustered by depth, based on their environmental variables, and were separated by distinct environmental and physical factors in the PCA analysis (**Figure 3.7**). The first three dimensions of the PCA explain 78.8% of the variability between samples based on the environmental factors (light, inorganic nutrients, salinity, oxygen, and particulate organic matter) (**Table 3.3**). The first dimension (Dim1) is negatively correlated with oxygen, POC and PON, and positively correlated

with fluorescence and nutrient concentrations, which are all factors separating oxygenated, nutrient-deplete and sunlit surface waters from the deeper samples. The second dimension (Dim2) was positively correlated with chlorophyll *a* and negatively with urea and salinity. The third dimension was not correlated with any environmental variables. High nutrient concentrations, except for urea, and fluorescence were associated with deep samples at 25 m and 50 m. The surface samples are influenced by warm temperatures, high oxygen, and high particulate organic matter concentrations.

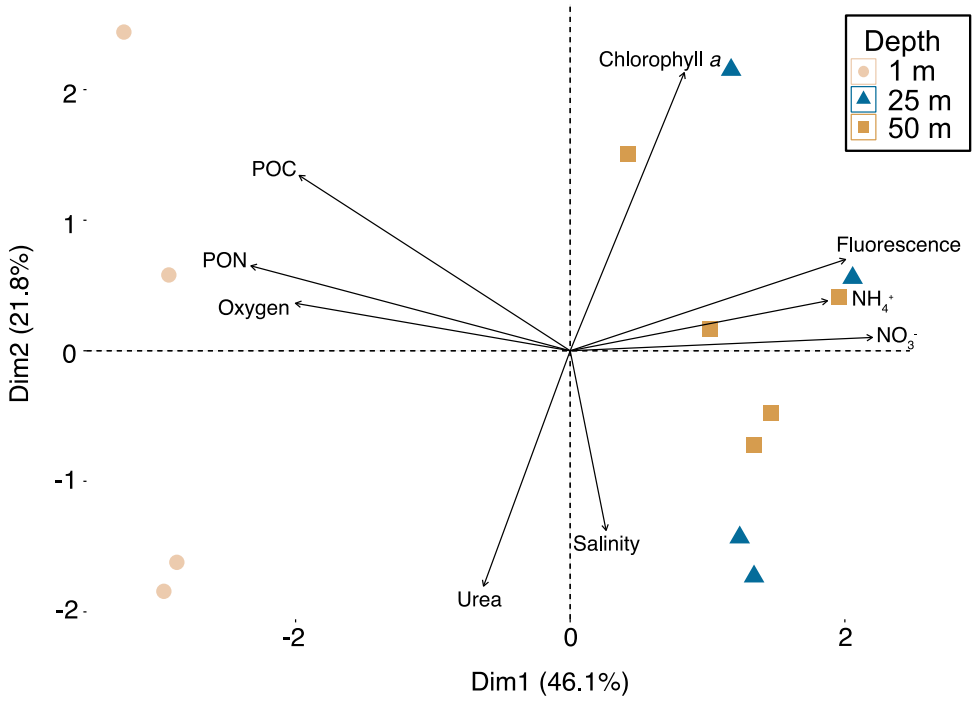

Figure 3.7. Principal component analysis (PCA) showing the spread of the environmental variables associated with this study. Plot of the Dim1 and Dim2 showing the distribution of environmental variables (chlorophyll *a*, salinity, oxygen, fluorescence, POC, PON, nitrate, ammonium, and urea). Beige circles represent samples from 1 m, blue triangles represent 25 m samples and gold squares represent samples taken at 50 m.

Table 3.3. Results of principal component analysis (PCA) showing the contributions of the environmental variables to the first three axes (Dim1, Dim2, Dim3) as well as the percentage variance explained by each dimension.

Variables	Dim1	Dim2	Dim3
Chlorophyll-*a*	2.57	35.77	2.41
Fluorescence	14.98	3.85	0.64
Salinity	0.25	14.92	45.50
Oxygen	14.92	1.04	2.11
Ammonium	13.08	1.16	22.10
Nitrate	18.04	0.08	10.16
Urea	1.48	25.62	15.01
Particulate organic carbon (POC)	14.52	14.22	0.83
Particulate organic nitrogen (PON)	20.15	3.33	1.25
% explained	46.1	21.8	10.9

Nitrification

Nitrite oxidation rates at the surface were negligible in comparison to 25 m and 50 m (**Figure 3.8**). The highest measured nitrite oxidation rate, measured on day 1 at 25 m was 199 ± 4.8 nmol.L^{-1}.day^{-1}. The measurements rates are not significantly different between 25 m and 50 m (ANOVA-Tuckey: df=2, p=0.52). At 25 m, nitrite oxidation rates were significantly faster on day 1 in comparison to day 4 (ANOVA-Tukey: df=3, p=0.04), but nitrite oxidation was no different daily at 50 m.

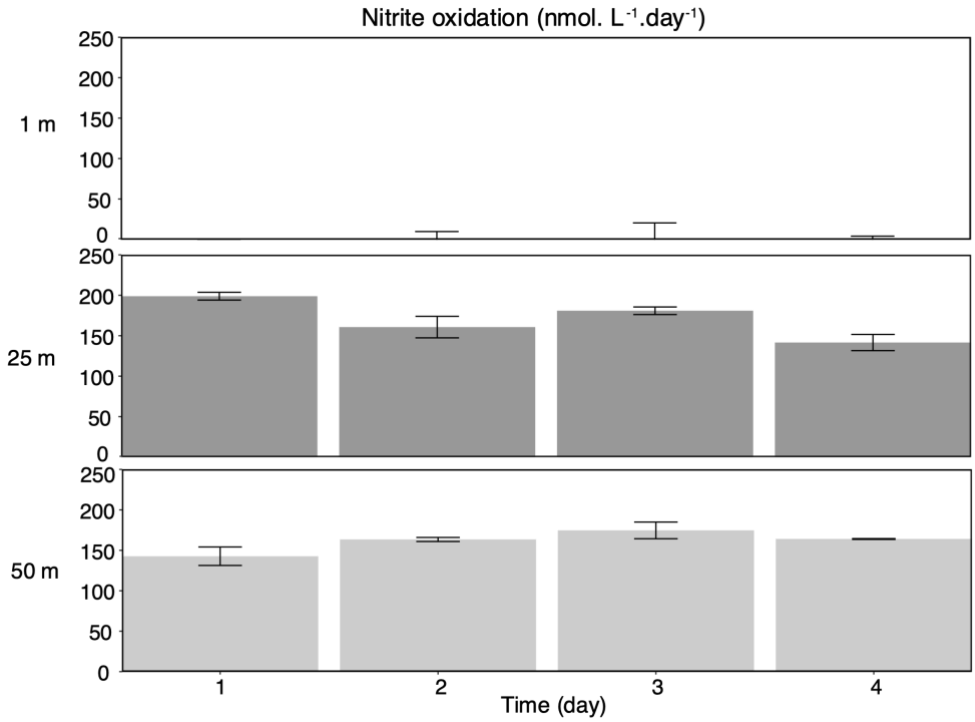

Figure 3.8. Nitrite oxidation rates (nmol.L^{-1}.day^{-1}) measured on day 1 to 4 at 1 m, 25 m, and 50 m. Standard error (n=2) bars are shown.

NPP and nitrogen uptake rates

Uptake experiments were done in duplicate (n=2); therefore, the mean is reported with the standard deviation. When no standard deviation is reported, the sample number was 1 (n=1). On average, nano-picoplankton contributed the most to NPP (90 ± 1.7%) and nitrogen uptake (ρNO_3^-: 79 ± 10%; ρNH_4^+: 79 ± 7%; ρUrea: 85 ± 18%) in comparison to the >10 µm size fraction (**Figure 3.9**). All productivity and uptake rates are faster at the surface than at 25 m and 50 m (**Table S3.2** and **S3.5**)

Total net primary production rates were on average faster at 1 m (3.36 ± 1.82 µmol.L^{-1}.day^{-1}) than at 25 m (1.01 ± 0.93 µmol.L^{-1}.day^{-1}) and 50 m (0.21 ± 0.03 µmol.L^{-1}.day^{-1}) (**Figure 3.9A–C**). At 1 m, there was a general increase in NPP_{total} from 1.35 µmol.L^{-1}.day^{-1} on day 1 to 5.53 µmol.L^{-1}.day^{-1} on day 3 (**Table S3.3** and **S3.6**). This general trend of a peak on day 3 was also seen at 25 m. At 50 m, NPP_{total} remained relatively similar from one day to the next (**Figure 3.9C**). As the greatest contributor to total NPP, the trends in the nano-picoplankton size fraction match those found in total NPP. The >10 µm size fraction is a small proportion of the total NPP and was found to decrease where NPP_{total} increased and vice versa.

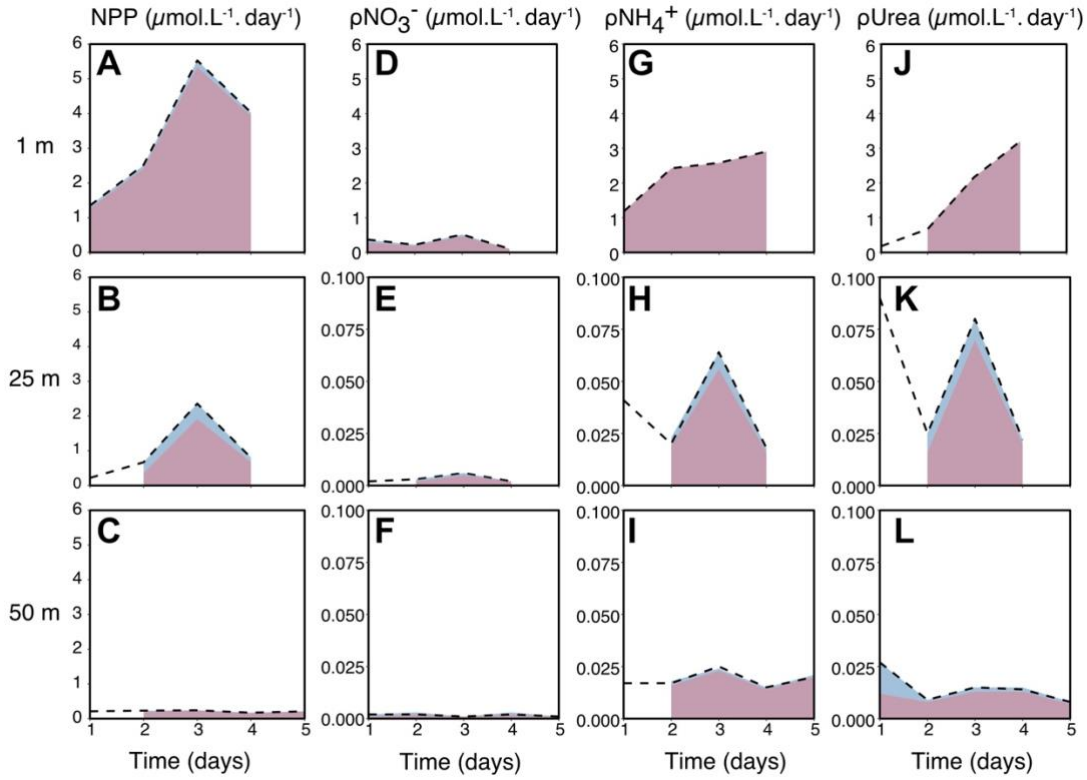

Figure 3.9. Size fractionated rates of net primary production (A–C; NPP (μmol.L^{-1}.day^{-1})), nitrate uptake (D–F; ρNO_3^- (μmol.L^{-1}.day^{-1})), ammonium uptake (G–I; ρNH_4^+ (μmol.L^{-1}.day^{-1})) and urea uptake (J–L; ρUrea (μmol.L^{-1}.day^{-1})) measured at 1 m, 25 m and 50 m. The dotted line indicates the measured total rates (>0.3 μm), and the shaded areas indicate the proportions contributed by different size fractions. Blue shading = >10 μm, pink shading = 0.3–10 μm, calculated by subtracting the >10 μm size fraction from the total rate. The data on each day is the average of two concurrent and independent measurements. It should be noted that y-axis of the nitrogen uptake rates at 25 m and 50 m are different from those of NPP at the same depths.

As with NPP, average ± SD $\rho NO_{3\text{total}}^-$ was higher at the surface (0.30 ± 0.18 μmol.L^{-1}.day^{-1}) than at 25 m and 50 m (**Table S3.2** and **S3.5**). The trend in $\rho NO_{3\text{total}}^-$ at 1 m showed a peak on day 3, which was significantly faster than the rates found on day 4 (**Figure 3.9D**, **Table S3.3** and **S3.6**). At 25 m there was a peak in total ρNO_3^- on day 3 as well. No temporal difference in total ρNO_3^- was found at 50 m. Nitrogen uptake rates at 25 m and 50 m are negligible in comparison to those at 1 m (**Figure 3.9D–F**).

Ammonium uptake rates (ρNH_4^+) were faster than ρNO_3^- in this study. The contribution of the > 10 µm size fraction to ρNH_4^+ is negligible in comparison to the nano-picoplankton at 1 m (0.2 ± 0.1%) and 50 m (6 ± 2.5%) but the > 10 µm size fraction contribute more, on average, at 25 m (16 ± 5.3%). There was no statistical difference in ammonium uptake rates from day to day at any sampling depth (**Figure 3.9G–I**, **Table S3.3**). General trends in urea uptake rates at 25 m and 50 m are like ρNH_4^+; however, at the surface, ρUrea on day 4, was significantly faster than day 1 and 2 (**Table S3.3** and **S3.5**). Urea uptake rates were also relatively faster in comparison to ρNO_3^- (**Figure 3.9J–L**).

Depth integrated NPP and ρNO_3^- were greatest on day 3 and, ρNH_4^+ and ρUrea on day 4 (**Table 3.2**). The smallest integrated NPP, ρNH_4^+ and ρUrea was on day 1, whereas the integrated ρNO_3^- was lowest on day 4. In general, integrated NPP and ρNO_3^- increased until day 3 and then decreased on day 4, whereas ρNH_4^+ and ρUrea increased from day 1 to day 4. In general, integrated ρNO_3^- was lower (3–27 times) than ρNH_4^+ on all days of the experiment. On all days the f-ratio was below 0.5, ranging from 0.14–0.30 (**Table 3.2**).

Nanoeukaryotic and picoplankton abundance

The specific taxa and groups which make-up the nano-picoplankton bulk measurements was determined. *Synechococcus* was the least abundant organism in this study across all depths. The highest average ± SD abundances were found at 25 m (log(3.37) ± log(0.31) cells.mL^{-1}) which were significantly different to those at 1 m and 50 m (**Figure 3.10A–C**, **Table S3.2** and **S3.5**). *Synechococcus* cell numbers differed temporally at each depth (**Table S3.2** and **S3.5**).

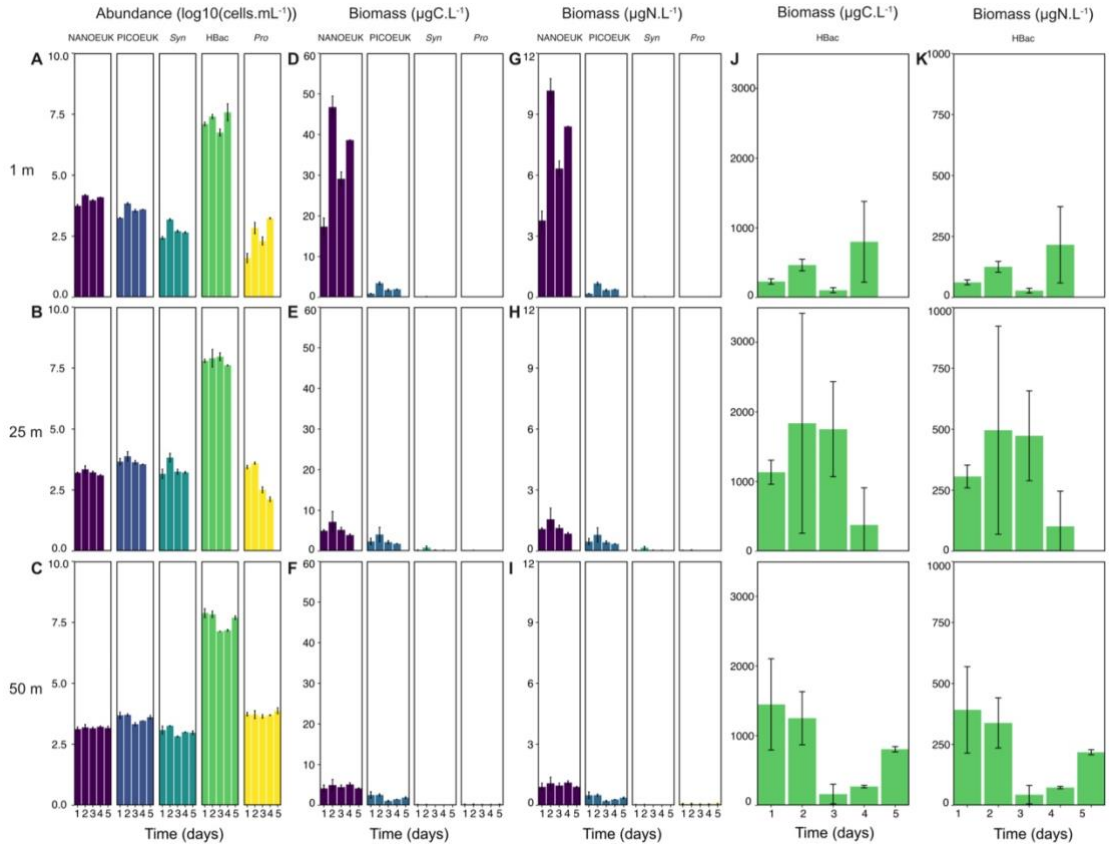

Figure 3.10. The distribution of the cell abundance (A–C; log10(cells.mL^{-1})) of nanoeukaryotes (NANOEUK), picoeukaryotes (PICOEUK), *Synechococcus (SYN*), heterotrophic bacteria (HBAC), and *Prochlorococcus* (*PRO*), carbon biomass (D–F; µgC.L^{-1}), nitrogen biomass (G–I; µgN.L^{-1}) of nanoeukaryotes (NANOEUK), picoeukaryotes (PICOEUK), *Synechococcus (SYN*), and *Prochlorococcus* (*PRO*) and carbon (J) and nitrogen (K) biomass of heterotrophic bacteria (HBAC) at the three depths, 1 m, 25 m and 50 m, on each sampling day.

Log transformed abundances of *Prochlorococcus* showed depth differentiation, with larger abundances at 50 m than 1 m and 25 m (**Figure 3.10A–C**, **Table S3.2** and **S3.5**). Temporally, there were differences in abundances at 1 m and 25 m (**Table S3.4** and **S3.7**). At 1 m *Prochlorococcus* concentrations were only similar on day 2 and 4 and at 25 m, day 1 and 2 were the only similar days (**Figure 3.10**, **Table S3.4** and **S3.7**).

Picoeukaryotes were relatively more abundant (21% contribution) than either cyanobacterium genus, *Synechococcus* (17%) or *Prochlorococcus* (18%), throughout this study. At 1 m picoeukaryotes ranged in abundance from log (3.24) ± log (0.02) cells.mL^{-1} on day 1, with a peak of log (3.84) ± log (0.04) cells.mL^{-1} on day 2 followed

by two days of relatively equal abundance (**Figure 3.10A**, **Table S3.4** and **S3.7**). Although no changes were found at 25 m, at 50 m there were fewer picoeukaryotes on day 3 and 4. Picoeukaryotes did not differ in abundance by depth (**Table S3.2**).

Nanoeukaryotes were most abundant at the surface, ranging from log (3.17) to log (4.00) cells.mL^{-1} (**Figure 3.10A**, **Table S3.2**). On day 3, at 1 m, nanoeukaryotes were more abundant than the heterotrophic bacteria, unlike the other days of the study (**Figure 3.10A**). At the surface, nanoeukaryotes peak on day 2 and 4 (**Table S3.4** and **S3.7**).

Heterotrophic bacteria were the most abundant organisms identified during this study, with significantly higher concentrations at 25 m (log(7.82) ± log(0.15) cells.mL^{-1}) and 50 m (log(7.55) ± log(0.36) cells.mL^{-1}) in comparison to 1 m (**Figure 3.10A–B**). Unlike the other nano-picoplankton groups, heterotrophic bacteria concentrations were significantly more abundant than all the other groups (ANOVA; df=4, $p < 0.0001$).

Nanoeukaryotes and picoplankton carbon and nitrogen biomass

Heterotrophic bacteria contributed the most carbon and nitrogen biomass throughout this study, averaging 98% respectively (**Figure 3.10J–K**). This is followed by nanoeukaryotes contributing an average of 1.7% carbon and 1.4% nitrogen biomass respectively (**Figure 3.10D–I**). Picoeukaryotes contributed 0.3 ± 0.02 % to carbon biomass (**Figure 3.10D–F**) and 0.2 ± 0.01% to nitrogen biomass (**Figure 3.10G–I**), followed by *Synechococcus* and *Prochlorococcus* whose contributions are negligibl in comparison.

At all depths heterotrophic bacteria dominated carbon and nitrogen biomass (**Figure 3.10K–J)**. Heterotrophic bacteria contributed more carbon and nitrogen biomass at 25 m and 50 m than at 1 m (**Figure 3.10E–I**). Nanoeukaryotes have the highest biomass at the surface, in comparison to depth (**Figure 3.10D and G**). Nanoeukaryote carbon biomass decreased with depth, with surface samples significantly different from 25 m and 50 m samples (**Figure 3.10D-F**, **Table S3.2**). This same pattern was seen with nitrogen biomass (**Figure 3.10G–I**). At 25 m and 50 m, picoeukaryotes contributed half the proportion of carbon (0.2%) and nitrogen (0.1% and 0.2%) biomass (**Figure 3.10E–I**) in comparison to nanoeukaryotes. These depths (25 m and 50 m) coincide with higher concentrations of nutrients and lower

oxygen concentrations (**Figure S3.2**). The contribution of *Synechococcus* and *Prochlorococcus* to biomass at each depth was negligible in comparison to nanoeukaryotes, picoeukaryotes and heterotrophic bacteria.

Influence of environmental factors on nanoeukaryote and picoplankton biomass

The plankton community distribution is explained more by depth (43%) than by day (16%), according to the PERMANOVA test for depth R^2=0.43, p=0.015 and between days R^2=0.16, p=0.93.

Nanoeukaryote and picoplankton groups were not distributed according to specific days (**Figure 3.11**). *Synechococcus* were mainly associated with 25 m samples, where there were high nitrate and chlorophyll *a* concentrations. *Prochlorococcus* were associated with mostly 50 m samples, but not with any environmental factors. Picoeukaryote carbon biomass did not seem to be associated with any depth, day, or environmental factor. Heterotrophic bacterial biomass was associated with 25 m samples, where there were high concentrations of nutrients like nitrate, silicate, and phosphate. Nanoeukaryotes were mainly associated with 1 m samples, where there were warm temperatures, high oxygen, increased primary production and nitrate uptake, and increased concentrations of urea and particulate organic matter.

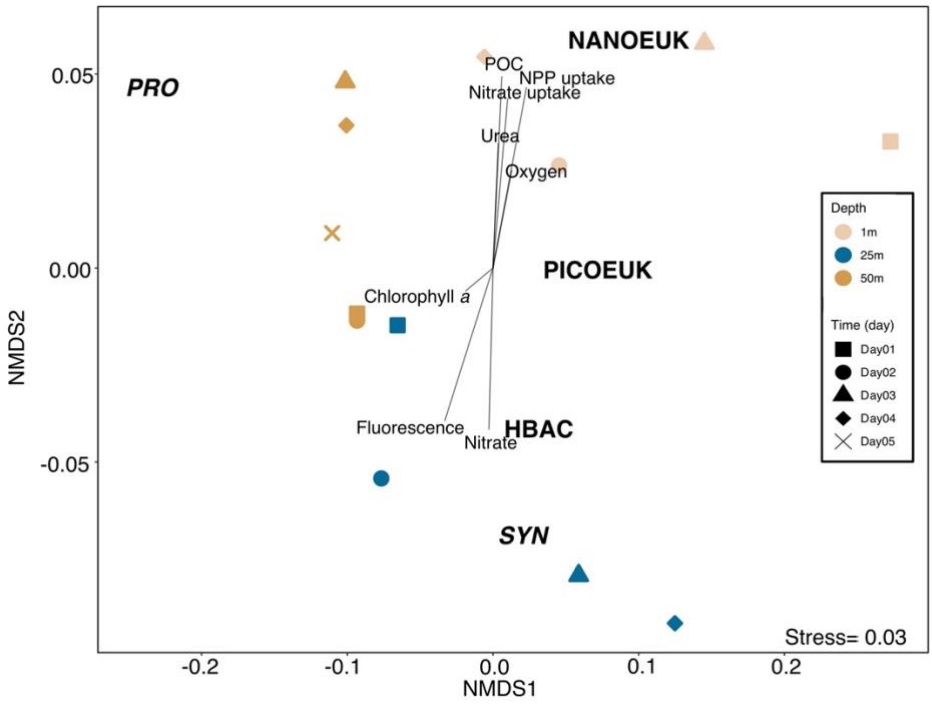

Figure 3.11. Non-metric multidimensional scaling (nMDS) ordination (stress = 0.03) showing the clustering of samples based on the carbon biomasses of the five major nanoeukaryote and picoplankton groups. NANOEUKS=Nanoeukaryotes, PICOEUK=Picoeukaryotes, HBAC=Heterotrophic bacteria, *SYN*=*Synechococcus* and *PRO*=*Prochlorococcus*. Colours represent the depths at which samples were taken at 1 m in beige, 25 m in blue and 50 m in gold. Square samples were taken on day 1, circles on day 2, triangles on day 3, diamond on day 4 and crosses represent samples taken on day 5.

3.5. Discussion

With this chapter an attempt was made to investigate the water column over 5 days starting on a larger system overview moving towards more a detailed look at cell taxonomic identifications and contributions within the water column. It is recognized that the opposite approach could be used as well, where the cells present are first described and then their function is elucidated.

Primary production in St. Helena Bay in autumn is depth differentiated and supported by the regenerated sources of nitrogen (ammonium, and urea) (**Figure 3.12**). Daily variability was not distinct in primary production and nitrogen uptake rates. The bulk plankton group responsible for most of the productivity at the surface is the nano-picoplankton (0.3–10 µm), specifically the nanoeukaryotes which were identified from flow cytometry results. With depth, as light availability diminishes and

oxygen concentrations decrease, picoeukaryotes contributed much of the measured carbon biomass in this study.

The hydrographic data over the five-day sampling period showed that cold nutrient rich Subantarctic Mode Water (SAMW) was overlaid with modified upwelled water (MUW) at the sampling station (Duncombe Rae, 2005; Lamont et al., 2015). These findings match a previous study done during winter in the southern Benguela (Flynn et al., 2018). Modified upwelled water (MUW) is derived from cold nutrient rich SAMW, with changed water properties as the upwelled water at the surface moves away from the coastline (Duncombe Rae, 2005). Increased temperature and light availability as well as the introduced nutrients allow for the proliferation of phytoplankton in surface waters after upwelling. As the water moves offshore, nutrients are used up by these phytoplankton and surface waters become nutrient-depleted. During this study, the sampling station experienced no wind-driven upwelling, and sea surface temperatures were warmer than expected for newly upwelled water (Lamont et al., 2015). Wind data showed moderate southerly winds four days prior to sampling (**Figure S3.1**), indicating some upwelling before the wind shifted to the northeast on the first day of sampling. Thus, the sampling station was typical of a stratified water column in which surface nutrients have been depleted and phytoplankton biomass might be expected to be at reduced levels. The larger concentrations of nitrate at depth in comparison to the surface is most likely produced by microorganisms during nitrification and this nitrate accumulates at depth until it is reintroduced to surface waters with mixing or upwelling (Ward, 2008; Lamont et al., 2014; Flynn et al., 2020). Remineralized nutrients were found to be trapped on the shelf of the southern Benguela in summer until winter (Flynn et al., 2020). Silicate in the water column may be associated with the degradation of diatoms (Tang et al., 2014), which are present in the chlorophyll maxima in the >10µm size fraction or are introduced into the water column from the ground water supplies (Frings et al., 2016). The larger organisms contain more chlorophyll-*a* per cell and thus contribute more to measured chlorophyll in comparison to the highly productive 3 - 10 µm size fraction. The higher chlorophyll values below the MLD are most likely sinking, undegraded cells from the high biomass found at the surface on day 1 (Wassmann et al., 1990).

The wind direction changed on the second day of sampling, from a northerly to a southerly direction, but with reduced wind speed (**Figure S3.1**). This may have

caused a deepening of the mixed layer on day 2 and subsequent shoaling of the pycnocline (**Figure 3.2A**), which in turn introduced more nitrate to the surface from depth, where concentrations became higher. The signal of this event on day 2 of sampling was echoed in the primary production and nitrogen uptake rates on day 3 (**Figure 3.9**). However, despite this event, the water column remained stratified throughout the sampling period, with a clear UML and bottom layer. Increased remineralization of particulate organic matter through aerobic respiration as well as a lack of ventilation, is responsible for the oxygen deficient waters found at depth during winter in St. Helena Bay (Pitcher and Probyn, 2017).

Nitrification

Nitrification is an important nitrogen retention process in the nitrogen cycle (Pajares and Ramos, 2019). During summer and autumn, remineralised nutrients have been shown to be trapped on the shelf of the southern Benguela, becoming a pool of enhanced nutrients capable of supporting the productivity of the region (Flynn et al., 2020). As a process that contributes nitrate to this enhanced pool of nutrients, understanding nitrification is vital to understanding ecosystem function. Nitrite oxidative bacteria are more sensitive to light than ammonia oxidizers (Olson, 1981) which would explain the lack of nitrite oxidation occurring at the surface in this study. Additionally, nitrifying bacteria may be outcompeted for bioavailable ammonium and nitrite at the surface, where photoautotrophic phytoplankton are more metabolically efficient users of dissolved inorganic nitrogen (Zakem et al., 2018).

At 25 m the high nitrite oxidation rates were faster on day 1 in comparison to day 4, which could be attributed to this sample being close to the chlorophyll maximum on day 1. There was likely an increased release of nitrite from phytoplankton at 25 m (French et al., 1983), which was immediately consumed by nitrifiers in the low light conditions. Nitrifiers were originally thought to only thrive in aerobic conditions; however, there are specialist nitrifiers that have adapted to low oxygen conditions and are able to oxidise ammonia and nitrite under microaerophilic conditions (Füssel et al., 2012; Bristow et al., 2016, 2017; Sun et al., 2017). In the first four days of this study, nitrite oxidation rates at 50 m ranged from 142.8-174.6 $nmol.L^{-1}.d^{-1}$ and oxygen concentrations ranged from 25.0–80.8 $\mu mol.L^{-1}$. These rates are similar to those found at 25 m, where oxygen concentrations ranged

from 67.0-151.8 µmol.L^{-1}. These oxygen concentrations are relatively high compared to other studies focused on nitrification in oxygen minimum zones (Füssel et al., 2012; Bristow et al., 2016, 2017; Sun et al., 2017), where oxygen measurements ranged from below detection to 11 µmol.L^{-1}. This could indicate that there is enough oxygen at the study site for nitrification to occur at these rates at 50 m.

NPP and nitrogen uptake rates

The stratified water column coincided with depth-stratified carbon biomass, primary production, and nitrogen uptake, based on the availability of light and nutrients, as well as differences in temperature and oxygen concentrations. Light and nutrient limitations as well as cell physiology interact to control the growth and accumulation of phytoplankton in the ocean (Sverdrup, 1953; Malone, 1980; Geider et al., 1997). Grazing pressure by larger zooplankton (> 200 µm) was not determined in this study; therefore, their effect on biomass concentrations or species composition is not known. It should be mentioned that, because of the 200 µm pre-screen filtration, the POM concentration, NPP and nitrogen uptake rates were determined in the absence of large grazers.

Rates of NPP were fastest at the surface throughout the sampling period, decreasing with depth as light availability decreased. However, there was a peak of NPP on day 3 at the surface and 25 m, probably in response to the deepening of the upper mixed layer on day 2. The deepening of the upper mixed layer on day 2 introduced nitrate from depth to the surface, stimulating growth (Lamont et al., 2014). There was no measured increase in the nitrate concentration on day 3 at the surface, but a significant decrease in concentration was measured at 25 m (**Figure 3.4A**), indicating rapid uptake. The subsequent growth was apparent in the POC data, with a slight increase in biomass on day 3 at the surface, influencing the rates of NPP. As the sampling days progressed, POC and PON concentrations gradually decreased, only increasing slightly in relation to the increase seen on day 3 in NPP. The decrease in POM over time may be attributed to the lack of nutrients at the surface, which would have inhibited new phytoplankton growth, with degradation and sinking of POM outcompeting regenerated production at the surface.

Euphotic zone integrated NPP rates measured during winter in SHB were 289.51 mmol.m^{-2}.d^{-1} at a nearby station in May 2016 (Station 4 of the Departmental

Affairs Integrated Ecosystem Programme: Southern Benguela), which was much faster than the highest integrated NPP rates measured on any day at our station in this study (Flynn et al., 2018). The measurements in the current study are closer to the open ocean stations in the Department of Forestry, Fisheries and the Environment's Integrated Ecosystem Programme: Southern Benguela (Flynn et al., 2018). There is a possibility that the single surface measurement integrated across the entire euphotic zone is not a good estimation of primary production in the euphotic zone in this study, but more likely that there were more nutrients available at the surface than at Station 4 to support the higher rates of primary production these researchers measured (Flynn et al., 2018). This study shows that, from day-to-day, NPP rates can change rapidly with small physical changes in the water column, and single measurements cannot be applied to understand the range of NPP happening in SHB during winter.

On-shelf, winter NPP rates ranged between 0.7 and 3.8 $gC.m^{-2}.d^{-1}$ in other studies done in SHB (Brown, 1984; Barlow et al., 2009; Lamont et al., 2014), which is similar to the findings in this study. These results also fall within the range of NPP rates measured in coastal and shelf stations during winter in central Chile (0.15-1.93 $gC.m^{-2}.d^{-1}$, (Montecino et al., 2004). In summer during wind driven upwelling, at a station within SHB, NPP rates ranged from 10.02–74.4 $mmol.m^{-2}.d^{-1}$ during active mixing caused by upwelling, and 153.1–277.9 $mmol.m^{-2}.d^{-1}$ during the relaxation phase (stratified water column) which followed (Burger et al., 2020). Generally, in the southern Benguela NPP rates are greater in summer than in winter (Lamont et al., 2014; Flynn et al., 2018, 2020; Burger et al., 2020).

Nitrogen uptake rates were greatest at the surface and decreased to almost negligible rates with depth. Nitrate uptake requires a lot of energy from phytoplankton and so, at depth, this process becomes energetically unfavourable as light becomes limiting (Losada and Guerrero, 1979). Despite being an energetically "cheap" process, due to the lower oxidation state of ammonium, ρNH_4^+ rates were also slower at depth because ammonium uptake requires some light (Raven, 1984). Ammonium and urea uptake rates were found to be 2 to 6-fold higher per day than ρNO_3^-. Ammonium uptake rates from this study are comparable to those observed on-shelf in summer (0.02 - 0.08 $\mu mol.L^{1}.h^{1}$) (Probyn, 1985), at a coastal upwelling station during active upwelling (Burger et al., 2020), and in winter in the euphotic zone of the southern Benguela (Flynn et al., 2018). The similarity between summer and winter ammonium

uptake rates has been previously noted and attributed to the transience of available ammonium in the water column (Flynn et al., 2018; Burger et al., 2020). Ammonium has a short residence time and efflux from sediments (Sheng and Lick, 1979; Dugdale et al., 2006), and heterotrophic remineralization (Dugdale et al., 1977; Seitzinger, 1988; McCarthy et al., 2015) can contribute to enhanced concentrations within the water column.

As with ρNH_4^+, ρUrea is dependent on ambient concentrations of urea in the water column. Urea is produced in the euphotic zone from remineralization of carbon biomass (Cho et al., 1996; L'Helguen et al., 2005) and is a natural nitrogenous waste product excreted by micro and macro-organisms (Lomstein et al., 1989; Therkildsen et al., 1997; Miller and Glibert, 1998). In the southern Benguela, urea uptake rates for the total phytoplankton community (<212 µm) at inshore stations, similar to our station, were < 0.007 $\mu mol.L^{-1}.h^{-1}$ during summer (Probyn, 1985). These rates are smaller than those measured in our study; however, as with ammonium concentrations, the variability of available urea in the water column may account for this difference.

Nitrate uptake rates in St. Helena Bay have been found to be significantly higher in summer than in winter (Probyn, 1985, 1992; Burger et al., 2020; Flynn et al., 2020). In summer there are consistently high concentrations of nitrate available at the surface because of wind-driven upwelling supporting large phytoplankton (like diatoms) that can rapidly take up nitrate (Walker and Peterson, 1991; Pitcher et al., 1992; Burger et al., 2020). The ρNO_3^- rates measured in this study are similar to those found at 5 m (approximately 0.57 $\mu mol.L^{-1}.d^{-1}$) in St. Helena Bay during winter at the same Station 4 mentioned above (Flynn et al., 2018). In that same study it was found that ρNO_3^- was not coupled to bioavailable nitrate but rather controlled by the availability of ammonium (Flynn et al., 2018). Flynn et al. (2018) observed ρNO_3^- inhibition at ammonium concentrations above 1 $\mu mol.L^{-1}$, while in this study it is unlikely that ρNO_3^- inhibition was seen at the surface (**Figure S3.5**). Nitrate concentrations were not high enough at 1 m to support the hypothesis that the concentration of bioavailable ammonium inhibits the uptake of nitrate. It is possible that, had more of the euphotic zone been sampled, inhibition may have been found. Unlike in winter, in summertime, ρNO_3^- has been shown to have a strong relationship to V_{NO3} and is not inhibited by ammonium in St. Helena Bay (Dugdale et al., 2006; Burger et al., 2020).

Throughout the water column the most likely control to consider is light availability. In the present study, the MLD was greater than the Z_{eu} on all sampling days, so phytoplankton were mixed to depths where light exposure was limited (van Oostende et al., 2015; Flynn et al., 2018). This mixing may explain the decrease in biomass and production on day 2 at the surface, as phytoplankton growth is dependent on light availability (Geider, 1987; Finkel et al., 2001). At depth, light dependent processes such as nitrate, ammonium and urea uptake become slower, despite the availability of nutrients. All processes at the surface are thus nutrient limited, while processes at depth (25 m and 50 m) are light limited. Another possibility is that a preference for ammonium and urea as a nitrogen source throughout the water column stems from the cell sizes associated with the nano-picoplankton, like the heterotrophic bacteria (Marañón, 2009; Marañón et al., 2013).

Cell size in relation to primary production and nitrogen uptake

Particulate organic matter concentrations, NPP and nitrate uptake rates at the surface, 25 m, and 50 m, were dominated by nano-picoplankton in this study. In mature upwelled water the phytoplankton community succession goes from being predominantly large cells, such as large diatoms, to small cells like nanoflagellates, small diatoms and picoplankton (Chavez, 1991; Brink et al., 1995; Fawcett and Ward, 2011). Surface samples were dominated by heterotrophic bacteria and nanoeukaryotes in this study. Nanoeukaryotes have been one of the most important contributors to primary production and therefore carbon biomass in St. Helena Bay (Probyn, 1992; Burger et al., 2020). These intermediate-sized plankton have a few advantages to acclimate to this highly variable environment (Bronk et al., 1998; Allen et al., 2002; Bradley et al., 2010). Nanoeukaryotes are sufficiently small to avoid predation from larger zooplankton and to remain in the euphotic zone, avoiding sedimentation. These organisms also have a faster growth rate in comparison to microphytoplankton (>10 µm) and are capable of efficiently consuming available nutrients, which is beneficial in a nutrient deplete environment, like in the surface waters of this study (Litchman, 2007; Marañón et al., 2013; Sommer et al., 2017).

The picoplankton include heterotrophic bacteria, which are responsible for recycling organic matter in the euphotic zone (Azam et al., 1983; Stockner, 1988). Heterotrophic bacteria were shown to be an important component of the overall plankton biomass in this study (**Figure 3.10**). The large biomass of these organisms

during this stratified period, points to higher rates of remineralization in comparison to productivity, although remineralization was not measured here. Additionally, picoplankton are less susceptible than larger cells to light limitation, with some picoeukaryotes capable of moving vertically through the water column to find light (Raven, 1998). It could be for this reason that there were increased abundances of picoeukaryotes at 25 m. Large surface to volume ratios also benefit small cells, like picoplankton, allowing them to tolerate harsh environmental conditions, such as the low oxygen waters found at 50 m and sometimes even at 25 m (Fenchel et al., 1990; Fenchel and Finlay, 2008; Rocke et al., 2013). Although these conditions would not necessarily be considered harsh for the bacteria. The specific carbon fixation rate (V_C) and ammonium and urea assimilation rates for nano-picoplankton were higher than those of the microplankton (**Figure S3.4**), except for NO_3^- assimilation rate, which was higher in the microplankton. Small phytoplankton (nano-and picoplankton) have shown a preference for NH_4^+ and urea as sources of nitrogen like bacteria, followed by nitrate, while large plankton mainly use nitrate (Probyn, 1992).

Linking carbon fixation with nitrogen uptake

The POC:PON ratio in the plankton in this study was always >6.63:1. A high carbon to nitrogen ratio has been seen in cases where there is nitrogen limitation, where more carbon is fixed in comparison to nitrogen consumed (Probyn, 1990). There is either a decoupling of NPP and nitrogen uptake or there is an accumulation of detritus rich in carbon in surface waters (Lee and Fuhrman, 1987).

If NPP and nitrogen uptake are tightly coupled, the relationship between the specific uptake of carbon (V_C) and nitrogen (V_N (V_N=V_{NO3} + V_{NH4} + V_{UREA})) would be 1:1, as the organisms that use these nitrogen sources are actively growing. The ratios for the >10 µm size fraction fall closer to the 1:1 line, but the nano-picoplankton fall below this line at the surface (**Figure S3.2**). Since the nano-picoplankton are responsible for the highest proportion of NPP, this part of the phytoplankton community assimilated more nitrogen than the amount of carbon fixed. This analysis does not consider the contribution of nitrogen fixation to total nitrogen uptake. A portion of the excess nitrogen uptake is most likely because of heterotrophic bacteria assimilating nitrogen in the euphotic layer (Kirchman, 1994). This is further supported by the preferential uptake of ammonium at the surface as well as the high specific rates of ammonium assimilation in the nano-picoplankton community (**Figure 3.9G** and

Figure S3.4). Significant rates of heterotrophic assimilation of inorganic nitrogen have previously been observed during phytoplankton blooms in other parts of the world (Kirchman, 1994) and in the southern Benguela (Flynn et al., 2018). The accumulation of carbon-rich detritus happens when the rate of heterotrophic degradation by bacteria with a low C:N requirement (Flynn et al., 2018) is equal to or more than regenerated production, which would drive the C:N ratio above the Redfield ratio (Kirchman, 2000). This is what was hypothesised, in a previous study, to be an important driver of the high C:N ratio during winter in St. Helena Bay (Flynn et al., 2018) and could be the same reason for the high C:N ratio in this study.

The f-ratio is a proxy used to determine carbon export, under the assumption that carbon and nitrogen cycling is coupled and in a steady sate (Eppley and Peterson, 1979). The proportion of new production to total nitrogen consumption, which is the f-ratio, can indicate whether NPP is supported by new or regenerated production. An f-ratio >0.5 means the NPP in the euphotic zone mainly is supported by new production while an f-ratio <0.5 is indicative of regenerated production (Dugdale and Goering, 1967; Eppley and Peterson, 1979). Even though the nitrogen and carbon cycling are most likely not strongly coupled in this study, it is useful to compare the calculated f-ratios with those from other studies in St. Helena Bay, especially during winter. The f-ratio in this study was <0.5 on every sampling day, indicating that NPP was supported by regenerated production in this study (**Table 3.2**). It is likely that the low f--ratio resulted from preferential ammonium and urea uptake, given the observed high values for ρNH_4^+, ρUrea, V_{NH4} and V_{UREA}, rather than ammonium inhibition of nitrate uptake, as was found in another winter study in the southern Benguela (Flynn et al., 2018). In summer, however, it seems that NPP is supported by new production, with an f-ratio of 0.71 estimated for the southern Benguela upwelling region (Probyn, 1985).

Composition of nano-picoplankton bulk measurements

Having shown the importance of the small nano-picoplankton size class in autumnal productivity of St. Helena Bay, elucidating the community composition of this size class will improve understanding of the processes mediated by these organisms. The composition of the nano-picoplankton was more strongly influenced by spatial (vertical) factors such as nutrient concentrations, light, temperature and

oxygen, and did not respond as rapidly as NPP and nitrogen uptake processes to daily changes, at least at the population scale (Ladau and Eloe-Fadrosh, 2019)

Nanoeukaryotes were on average 6-7-fold more abundant at the surface than at 25 m and 50 m. In nutrient-deplete surface waters, the low half saturation constants (K_s) of these cells for nutrient uptake allow them to perform better than larger phytoplankton (Probyn, 1990). The carbon content of nanoeukaryotes contribute, in addition to heterotrophs and detritus, to the high POC concentrations found at the surface in the nano-picoplankton size fraction and contributed to the high rates of NPP, ammonium and urea uptake, as they prefer these nitrogen sources over nitrate (Walker and Pitcher, 1991; Pitcher et al., 1992). Despite not knowing the exact species composition, the presence of nanoeukaryotes in surface waters is expected as they most likely succeeded larger diatoms that bloomed in newly upwelled water (Pitcher et al., 1991).

Another significant contributing group to the processes and production found in this study are the picoplankton, including autotrophic picoeukaryotes, *Synechococcus* and *Prochlorococcus,* and heterotrophic bacteria. Picoeukaryotes were equally abundant at all depths throughout this study. After heterotrophic bacteria and nanoeukaryotes, picoeukaryotes contributed the most to POC. The cold, nutrient-rich, oxygenated waters at 25 m were conducive to picoeukaryotic growth, similar to what was found when studying contribution of nano-picoplankton to carbon biomass in the south Brazilian Bight (Bergo et al., 2017). It is possible that the picoeukaryotes found at the surface and those found at depth are different communities, one adapted to high light conditions and the other not. The small cell size of these organisms makes them more adaptable to the low oxygen conditions at 50 m, with some picoeukaryotes thriving at lower oxygen concentrations where bacteria are abundant for predation in the case of mixotrophic picoeukaryotes (Fenchel et al., 1990; Fenchel and Finlay, 2008).

Synechococcus were the least abundant group of organisms identified in this study. The nutrient-deplete surface water, especially in terms of nitrate and phosphate concentrations, may be why these organisms did not proliferate in the high-light surface waters (Zubkov et al., 1998; van Dongen-Vogels et al., 2011), as *Synechococcus* prefer mesotrophic waters (Bergo et al., 2017). The slight increase in *Synechococcus* on day two, when the upper mixed layer depth increased, could be

further evidence that reduced nutrients are suppressing their proliferation at the surface, despite their small size. During wind-driven upwelling, when nutrients are supplied to the surface, *Synechococcus* are often highly abundant (Bergo et al., 2017); however, this does not seem to be the case in the St. Helena Bay coastal region, during (Gebe et al., unpublished) or after upwelling.

Prochlorococcus has higher abundances at depth than at the surface, but at the surface abundances of both cyanobacterial populations were relatively low in comparison to the other picoplankton (**Figure 3.10**, **Table S3.1**). *Prochlorococcus* have previously been found to be abundant at depths of up to 100 m and are known to be less abundant in surface waters (Moore et al., 1998; Johnson, 2006). These organisms have various ecotypes adapted to different depths, and this suggests the presence of a low light adapted population in this study (Partensky et al., 1999b). Unicellular cyanobacteria are more typically associated with oligotrophic oceanic waters than eutrophic coastal waters; their abundance at the nutrient-replete 50 m station contrasts with conventional understanding of their habitats (Kirchman et al., 1994; Bronk et al., 1998; Allen et al., 2002; Bradley et al., 2010).

Heterotrophic bacteria are often linked to high concentrations of dissolved and particulate organic matter (Pitcher and Probyn, 2016) and that is the case in this study with the high abundances found. At depth, heterotrophic bacteria concentrations increased, resulting in higher rates of remineralization which corresponds well with the increase in ammonium at depth. The aerobic breakdown of organic matter with depth is also the cause of the low oxygen water found at 50 m, which is a known to exhibit low oxygen concentrations, especially in the month of March (Pitcher and Probyn, 2016). The high abundance of heterotrophic bacteria at the surface and depth are expected and could be further evidence for nitrogen uptake in the absence of carbon fixation, as well as degraders outcompeting primary producers (cyanobacteria, nanoeukaryotes and picoeukaryotes) as a cause for the higher-than-Redfield C:N ratio. Nonetheless, heterotrophic bacteria are present in abundances that are probably supporting the regenerated production by the cyanobacteria, picoeukaryotes and nanoeukaryotes in the euphotic zone.

3.6. Conclusions

Making use of a daily Eulerian sampling strategy, this study showed how phytoplankton metabolic processes (primary production and nitrogen uptake), more than community structure, respond rapidly to changes in the environment, where process rates can peak on a single day and decrease again the next day. However, variability was more pronounced spatially within the water column, where factors such as nutrient concentration, light availability, and cell size-controlled phytoplankton distribution from the surface to depth (**Figure 3.12**). As expected, the observed St. Helena Bay NPP in winter was fuelled predominately by regenerated production (f-ratio < 0.5), as was seen in previous studies in this area. This regenerated production was dominated by nano-picoplankton, which preferentially assimilated ammonium rather than nitrate. It was thus unsurprising that the nano-picoplankton were the biggest contributors to NPP, carbon biomass as well as nitrogen uptake at the surface and depth. Surface waters were dominated by heterotrophic and nanoeukaryotes biomass while samples at depth had higher concentrations of picoeukaryote and nanoeukaryotes carbon biomass. *Synechococcus* and *Prochlorococcus* abundances and contributions to carbon biomass were negligible in comparison. This study further highlights the importance of the nano-picoplankton as the main contributors to primary production and carbon biomass during winter in St. Helena Bay.

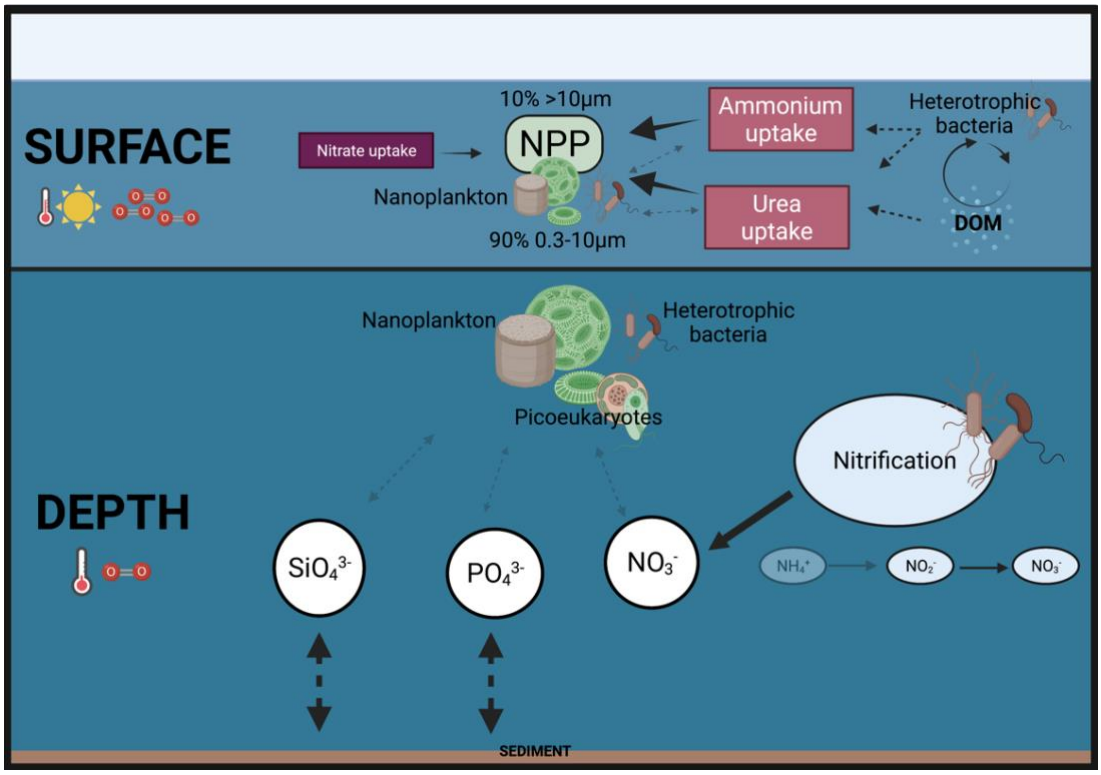

Figure 3.12. Conceptual model illustrating the main findings of this chapter. High light, oxygen and temperature conditions at the surface are conducive for greater rates of primary production (NPP) in the nano-picoplankton size fraction, specifically the nanoeukaryotes. Primary production is supported by regenerated forms of nitrogen, specifically ammonium and urea. At depth picoeukaryotes become more abundant. Nitrification rates, as measured by nitrite oxidation, was highest at 25 and 50 m where the greatest concentrations of nitrate were found. Concentrations of phosphate and silicate were also highest at depth. Created with BioRender.com.

4. Chapter 4: Depth-differentiated nano-picoplankton dynamics during five days in autumn in an embayment of the southern Benguela upwelling region

4.1. Abstract

Shotgun metagenomic analyses were used to study nano-picoplankton community composition, structure, and functional potential at the end of a coastal upwelling season. Samples were collected over five consecutive days in March 2018 from three depths at a single sampling station in St. Helena Bay, South Africa. There was clear depth-differentiation in both taxonomic diversity and function throughout the sampling period, with little daily variability. Changes in community composition, specifically eukaryote diversity, were more pronounced at 1 m and 25 m than at 50 m. with increased abundances of eukaryotes like Syndinales and Bacillariophyta closest to the chlorophyll maxima. Surface waters were dominated by photosynthetic and photoheterotrophic organisms, while samples at depth were linked to nitrogen cycling processes, like nitrification, denitrification and anaerobic oxidation to ammonia (anammox). Particulate biomass played an important role as a source of carbon and in the creation of microenvironments for microbial processes. Metagenome associated transporter and gene abundances of certain processes like ammonium uptake and nitrogen oxidation were found to be good indicators of measured process rates. This study showed that nano-picoplankton community dynamics were driven by the abiotic and biotic conditions associated with each sampling depth. These factors included light availability, nutrient concentrations, carbon biomass and oxygenation. These plankton were important for overall productivity over the five days and played key roles in biogeochemical cycling. The nano-picoplankton group helps sustain ecosystem functioning in St. Helena Bay, emphasizing the need to monitor this size fraction of the plankton.

4.2. Introduction

The seasonal productivity and dynamics of phytoplankton and bacterioplankton in coastal upwelling systems is well studied globally (Kerkhof et al., 1999; Cuevas et al., 2004; Fawcett and Ward, 2011; Bergen et al., 2015; Cuadrat et al., 2015; van Oostende et al., 2015; Reji et al., 2020). This includes studies on the west coast of South Africa, in the southern Benguela region (Painting et al., 1992; Pitcher et al., 1992; Rocke et al., 2020). Phytoplankton are the main source of particulate (POM) and dissolved organic matter (DOM) in these systems. POM and DOM are utilized by bacterioplankton (Archaea and Bacteria) and heterotrophic or mixotrophic nano-picoeukaryotes for energy and carbon and are responsible for the cycling of much carbon and other vital nutrients within the water column. These processes, which can change on daily timescales, are of particular interest in coastal upwelling regions, where the environment is dynamic and can influence community composition and function of nano-picoplankton (Chapter 2). Daily dynamics of marine microorganisms are often studied in relation to environmental changes that occur such as during phytoplankton blooms (Teeling et al., 2012; Klindworth et al., 2014) and during active upwelling events (Chapter 2). Even with long-term high-frequency studies, deviations on short timescales in surface microbial communities from underlying seasonal patterns were due to events like upwelling or downwelling (Chafee et al., 2018).

Eastern boundary upwelling systems support much (>20%) of the world's fish catch, due to the eutrophic nature of these coastal regions (Croll et al., 2005). The southern Benguela upwelling system experiences consistent (3–7-day cycles) wind-driven upwelling during spring and summer (Hutchings et al., 2009), followed by a period of wind relaxation in autumn and winter (Shannon and Nelson, 1996). During the upwelling season, cold nutrient-rich water is supplied to the sunlit surface from depth, and in the sunlit ocean these nutrient-rich waters promote high levels of phytoplankton growth. The high biomass and high primary productivity are sustained close to the coast, due to the topography of the coastline. Inlets and bays drive water-mass retention, which in turn traps this high biomass (Largier, 2020). One such bay is St. Helena Bay, which is downstream from Cape Columbine, an upwelling cell within the southern Benguela upwelling system.

In spring and summer, St. Helena Bay experiences the effects of the 3–10-day upwelling cycles. Picoplankton communities have been shown to respond to the variable environmental conditions caused by pulsed upwelling and subsequent stratification of the water column (Chapter 2). In the post upwelling season, in autumn, the water column is stratified for longer periods than during summer (Lamont et al., 2015), the surface waters are consistently nutrient-depleted and primary production is reduced, with a greater contribution of regenerated than new production (Flynn et al., 2018, 2020, Chapter 3). Due to the high productivity of St. Helena Bay and the retention and bacterial decay of biomass, the inshore region is subject to seasonal and episodic hypoxic events (Pitcher et al., 2014; Jarre et al., 2015), which are known to have a negative effect on fishes and benthic invertebrate communities (Monteiro et al., 2006; van der Lingen et al., 2006). There are, however, microorganisms capable of proliferating in low oxygen conditions, remineralizing biomass and cycling important macronutrients such as carbon, nitrogen and sulphur (Canfield et al., 2010; Lam and Kuypers, 2011; Füssel et al., 2012; Ulloa et al., 2012; Wright et al., 2012; Letscher et al., 2015).

There have been few studies of bacterioplankton and picoeukaryote dynamics in St. Helena Bay. One of the earliest studies (Painting et al., 1993a) found that bacteria played an important role in planktonic food web structure in the bay, and that bacterioplankton dynamics were closely coupled with the upwelling cycle. More recently, a study of microbial community dynamics during the upwelling season in the southern Benguela found that bacterioplankton and picoeukaryotes differed in community composition according to sampling site (on or off the shelf), upwelling status, and season (Rocke et al., 2020). A closer look at the effect of upwelling status on picoplankton community composition found that community structure was influenced by physical mixing of the water column and oxygen availability in St. Helena Bay during an active upwelling cycle (Chapter 2), confirming that upwelling is a vital part of the dynamics of the bay. However, several key questions remain unanswered. Are the environmental changes during upwelling the main factors influencing nano-picoplankton, or are other, biotic factors equally or more important? Simulations of short-term phytoplankton dynamics have shown that controls on these small plankton communities in a post upwelling environment could be attributed to grazing pressure in the southern Benguela (Painting et al., 1993a). However, more

recent experimentation of nano- and picophytoplankton daily dynamics has shown that this is not necessarily the case (Gebe et al. unpublished). When there is no wind driven upwelling, does the nano-picoplankton community structure and function still change on a daily basis? How do environmental variables shape the community's diversity and functional potential on a daily time scale?

The nano-picoplankton size fractions are in the size range of 0.3–10 µm, and include small, unicellular autotrophic and heterotrophic protists, archaea, and bacteria. The group consists of organisms that are important for primary production and nutrient cycling in the bay during autumn (Chapter 3). One such cycle is the nitrogen cycle, which has a strong link to productivity and carbon export (Falkowski, 1997). Ammonium oxidizing archaea, such as *Nitrosopumilus*, and nitrifying bacteria, such as Nitrospinae, have been identified in the waters of St. Helena Bay (Rocke et al., 2020), indicating the importance of these processes in the bay. However, these and other metabolically important pathways have not been expanded upon beyond the presence or absence of nano-picoplankton communities in the area.

This study describes genetic diversity and functionality of nano-picoplankton during autumn in St. Helena Bay, using metagenomic approaches, flow cytometry, and productivity assessments with a daily sampling frequency. The aim was to characterize the variability in nano-picoplankton assemblages at three depths in the water column (1 m, 25 m, and 50 m) during a five-day sampling period. Specifically, the study aims to describe nano-picoplankton community composition and functional potential, and to elucidate any variability in community structure and potential metabolism between sampling days. It was hypothesised that nano-picoplankton community dynamics would be more variable at the surface than at 50 m, and that daily variability would only be found when there were chemical and physical changes to the water column.

4.3. Materials and Methods

Sample collection

A Eulerian sampling approach was used. Samples were collected daily at a single station (32°35’ 75.0” S, 18°02’60.0” E) in St. Helena Bay, on the west coast of South Africa, from March 11th to March 15th, 2018, referred to in this manuscript as day 1 to day 5 (**Figure 4.1**). Sampling was conducted from an inflatable craft operated by the Department of Forestry, Fisheries and the Environment, and all samples were collected using a 5 L hand-held Niskin bottle. The bottom depth at this sampling site is ~50 m and samples were collected at 1 m, 25 m and 50 m on March 11th to March 14th and only from 50 m on March 15th. A hand-held CTD (SBE-19 CTD) was deployed once at the start of each sampling session from day 1 to day 5 of the study.

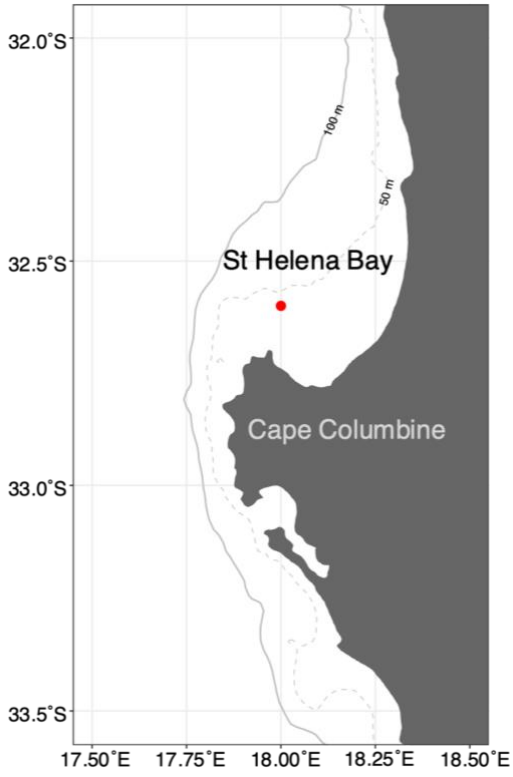

Figure 4.1. Map of St. Helena Bay on the west coast of South Africa, where the experimental site for this study is indicated by a red dot.

Seawater was collected at each sampling time for total gDNA extraction and metagenomic analysis. For DNA extractions, 5 L of pre-filtered (200 µm mesh) seawater were collected, in triplicate, in dark acid-washed bottles, at each sampling

time and depth. The seawater was sequentially filtered through a 10 µm nylon or cellulose filter membrane followed by a 0.2 µm cellulose acetate filter membrane, using either a vacuum or peristaltic pump. Filters were placed in 2 mL cryovials (45 mm diameter filters) and 50 mL falcon tubes (142 mm diameter filters), flash frozen in liquid nitrogen and stored at -20˚C while in the field and at -80˚C in the Department of Biological Sciences at the University of Cape Town until further analysis. The collection and processing of supplementary environmental variables are provided in Chapter 3.

DNA extraction, sequencing and assembly

Filters of each replicate per sampling depth and day were combined, resulting in one sample per sampling depth and day (13 total). Total gDNA was extracted according to a modified Sucrose Lysis Method (Hu., 2007; Wilcox and Worden., 2009). Filters were cut into smaller pieces (approximately 50 mm by 50 mm) using a sterile blade. The filter pieces were covered with Sucrose Lysis Buffer with lysozyme (50 mM Tris-HCL, pH 8; 40 mM EDTA, pH 8; 0.75 M Sucrose; 1mg.mL^{-1} lysozyme) and incubated at 37˚C for 1 hour, gently shaking every 10 minutes. After 30 minutes the filter pieces were flipped over in the buffer. 5X Proteinase K/SDS solution (0.5 mg.mL^{-1} Proteinase K, 1% SDS in Sucrose Lysis Buffer + lysozyme) was added to the petri dish at the end of the incubation and mixed with the buffer already present. The petri dish was then incubated at 55˚C for 2 hours, repeating the mixing and flipping as before. The lysate was gently pipetted into a 15 mL tube. The filters were covered with more lysate and incubated at 55˚C for 2 hours with periodic mixing. A standard phenol: chloroform: isoamyl alcohol extraction was then done. The DNA was precipitated in glycogen and isopropanol alcohol overnight at 4˚C and washed with ethanol. The DNA was then resuspended in TE Buffer and stored at -80˚C until sequencing.

Library preparation and sequencing was done at Novogene, Hong Kong. After sample quality control, library preparation was done using the TruSeq DNA PCR-Free Library Preparation Kit. The metagenomes were sequenced using an Illumina HiSeq 2000 to produce 6 GB of data per metagenome. In total, 13 metagenome libraries were sequenced.

Taxonomic diversity

Taxonomic diversity was inferred from metagenomes using the MGnify 5.0 pipeline (Mitchell et al., 2019) on the raw metagenomic reads before assembly. This was to obtain better taxonomic classification, due to the high abundance of short reads in the metagenomes. Briefly, raw reads were merged using SeqPrep and filtered, removing reads less than 100bp in length. Ambiguous bases (>10%) were filtered out using a Biophython filtering step. Small subunit ribonucleic acid (SSU rRNA) was identified using RFAM and taxonomic classification was done with MAPSeq using the SILVA database. Further analysis of the classified taxa was performed using the phyloseq package (McMurdie and Holmes, 2013) in R (R Core Team, 2013). The abundance and taxonomic tables were combined into a phyloseq object with tables that contained physiochemical and biological data, as analysed in Chapter 3. Sequences classified as metazoan and mitochondria were filtered out. Total read counts for the 13 metagenomes imputed into the phyloseq object ranged from 3956 to 8573. Metagenome assembly data found in Table S4.1.

Statistical analysis of raw reads (no assembly) taxonomic abundances

Alpha diversity was computed using the alpha() function in the microbiome package (Lahti and Shetty, 2019) and visualised using ggplot2 (Wickham, 2016). Diversity data were log-transformed and differences in diversity between the three depths and between the 5 days were tested using a two factor ANOVA. Interactions were not tested because of the lack of sample duplication.

Read data were transformed to the median sequencing depth (seed set at 201). The phyloseq object on which analysis was performed contained 878 taxa observed from 13 samples. Ordinations were performed using the cca() function from vegan (Oksanen, 2016). Canonical correspondence analysis was used to constrain community structure to determine which environmental variables (non-redundant) contribute to the spread of samples, which was based on identified taxa from raw read metagenomes. Redundancy among the environmental variables was reduced by dropping variables where two variables were found to be highly correlated ($R > 0.9$; Chapter 3). Analysis of similarity (ANOSIM) and PERMANOVA analyses were used to determine the similarity between community structures across depths and between days. Homogeneity of dispersion among samples from each depth was determined

using the betadisper() function in vegan. In order to determine the environmental factors that correlate best with the Bray-Curtis dissimilarity associated with all samples and at each depth, the bioenv() function in vegan was implemented. To determine whether specific phyla and orders differ across the three sampling depths or the five sampling days, single factor ANOVAs were performed using the lm() function with the seed set at 201. Tukey HSD post hoc tests were performed in cases where a significant difference was found.

Metagenomic analysis

Bioinformatic analysis of metagenome assemblies was done through the European Bioinformatics Institute's Mgnify portal using pipeline version 5.0 (Mitchell et al., 2019). Quality control was done based on sequence lengths, where contigs with a sequence length less than 500 nucleotides were removed before further analysis. Infernal was run using rRNA hidden Markov models from RFAM to identify large subunit (LSU) and small subunit (SSU) rRNA genes using families found in the CL00111 (SSU) and CL00112 (LSU) clans. In this study only SSU taxonomy was reported. Taxonomic classification of these genes, using the unit OTU, was done using the SILVA database (Quast et al., 2013; Yilmaz et al., 2014) in conjunction with MAPseq (Matias Rodrigues et al., 2017), to assign corresponding confidence scores for assignment at each taxonomic level. Protein coding sequences (pCDS) were predicted using a combined gene caller that uses both Prodigal and FragGeneScan (Rho et al., 2010).

Protein function was assigned in multiple forms, including InterProScan annotations and KEGG ortholog predictions using HMMER v3.2.1 and a modified KOfam 2019-04-06 (based on KEGG 90.0). KEGG orthology (KO) annotations were used to identify genes associated with pathways of interest. In cases where no KO annotations were found for a pathway (biological nitrogen fixation and rhodopsins), InterPro annotations were used (**Table 4.1**). Gene-normalized KO/InterPro abundances (abundances in a pathway normalized to the total metagenomes gene abundances per sample) were used to compare abundances of genes associated with pathways for photosynthesis, metabolism of nitrogen, methane, and sulphur, as well as transport pathways.

Table 4.1. KO/InterPro terms and gene names used to determine the abundances of pathways of interest across all metagenomes.

Pathway	Gene name	KO/Interpro terms
Photosystem I	*psa*ABCDEF	K02689-K02694
Photosystem II	*psb*ABCDEF	K02703-K02708
Anoxygenic photosynthesis (APP)	*puf*LM	K08928-K08929
Rhodopsin	*bop*, Archaeal/bacterial/fungal rhodopsins, Heliorhodopsins	K04641; IPR001425; IPR041113
Methanogenesis (CO_2-methane)	KEGG pathway module M00567	K00125; K00200-K00205; K00319-K00320;K00399;K00401-K00402; K00519; K00577-K00578; K00580-K00584; K00672; K01499;K03388-K03390; K08264-K08265;K11260-K11261; K13942; K14126-K14128; K22480-K22482; K22516
Methane oxidation	*pmo*ABC, *mdh*12, *mxa*FI, *mmoBCD*XYZ, *xox*F	K01944-K01946; K14028-K14029; K16157-K16162; K23995
Nitrogen fixation (BNF)	*nif*HDK	K02588/IPR000392; K02586; K02591
Ammonia oxidation	*amo*ABC, *hao*	K10944- K10946; K10535
Nitrite oxidation/nitrate reduction	*nar*GH, *nxr*AB	K00370-K00371
Nitrate reduction	*nar*GHIV, *nxr*AB, *nap*AB	K00370-K00371; K00374; K02567; K02568
Dissimilatory nitrate reduction (DNRA)	*nar*GHI, *nxr*AB, *nap*AB, *nir*BD, *nrf*AH	K00362-K00363; K00370-K00371; K00374; K02567- K02568; K03385; K15876
Assimilatory nitrate reduction (ANRA)	*nas*AB, *nir*A, *nar*B	K00360; K00366-K00367; K00372
Remineralization	*glt*B	K00265
Denitrification	*nir*KS, *nar*GHIV, *nar*ZY, *nxr*AB, *nos*Z, *nor*BC, *nap*AB,	K00368; K00370-K00371; K00374; K00376; K02305; K02567- K02568; K04561; K15864
Anammox	*nir*KS, Hydrazine synthase, *hdh*	K00368; K15864; K20934-K20935
Comammox	*nar*GH, *nxr*AB, *hao*, *amo*ABC	K00370-K00371; K10535;K10944-K10946
N-damo	*amo*A, *nir*S	K10944; K15864
Thiosulphate oxidation	*sox*ABCXYZ	K17222-K17227

Table 4.1. Continued.

Pathway	Gene name	KO/Interpro terms
Dissimilatory sulphate reduction (DSRA)	*apr*AB, *sat*, *dsr*AB	K00394-K00395; K00958; K11180-K11181
Assimilatory sulphate reduction (ASRA)	*cys*CDJIHN, *sir*, *cys*NC, *sat, PAPSS*	K00380-K00381; K00390; K00392; K00860; K00955-K00958; K13811
Sulphur ABC transporter	*cys*APUW, *sbp*	K02045-K02048; K23163
Nitrate/nitrite ABC transporter	*nrt*ABCD, *nas*DEF, *cyn*ABD	K15576-K15579
Nitrate/nitrite MFS transporter	*NRT*, *nar*K, *nrt*P, *nas*A	K02575
Nitrite transporter	*nir*C	K02598
Phosphate transporter	*pst*ABCS	K02036-K02038; K02040
Phosphonate transporter	*phn*CDE	K02041-K02042; K02044
Urea transporter	*urt*ABCDE	K11959-K11963
Ammonium transporter	*amt*B	K03320

Statistical analysis of metabolic pathways and transporter gene abundances

In order to determine the environmental factors that correlated the best with the Bray-Curtis dissimilarity measure of gene pathway abundances in all samples and at each depth, the bioenv() function in vegan was implemented. To determine whether specific pathways differed across the three sampling depths or the five sampling days, single factor ANOVAs were performed using the lm() function with the seed set at 201. Tukey HSD post hoc tests were performed in cases where a significant difference was found.

Data Availability

Raw-read metagenomes were deposited in the European Nucleotide Archive (ENA) under the accession numbers ERS3350409–ERS3350421, and the metagenome assemblies were deposited in the ENA under the accession numbers ERS3350409-ERS3350421; this study can be found under Study ID MGYS00003669 on the Mgnify portal.

4.4. Results

Community structure differs by depth but not day

An environmental overview was given in detail in Chapter 3. Briefly, over the five-day period, the water column remained stratified, with warm nutrient-depleted surface water, nutrient-rich intermediate water, and nutrient-rich but low-oxygen bottom water (**Figure S4.1** and **S4.2**). There was a single day (day 2) when the mixed layer deepened (**Figure S4.2**), possibly entraining regenerated nutrients from deeper water (**Figure S4.1E**) and resulting in an increase in productivity at the surface. The surface and 25 m samples were subject to more environmental variability than the 50 m bottom samples, which experienced little change over the five-day sampling period (Chapter 3).

The greatest diversity, richness, and evenness measures were found on day 1 at 1 m and 25 m (**Figure 4.2**). Log transformed Simpson diversity was not significantly different between sampling days but did differ between depths (ANOVA: df=2, F-value=5.62, p=0.04). However, after the Tukey post-hoc test did not indicate which depths differed (Tukey: 1 m-25 m: p=0.07; 1 m-50 m: p=0.06; 25 m-50 m: p=1.00).

There were differences in community structure among samples, primarily associated with depth and not sampling day (**Figure 4.3**). The canonical correspondence analysis (CCA) explained 71.2% of the variability in community structure; the first axis (CCA1; 38.27%) indicates the depth gradient and the second axis (CCA2;32.93%) the spread between sampling days. At the surface, community structure was associated with increased primary production, with high biomass and high oxygen concentrations. At 25 m, chlorophyll-*a* was associated with the community structure of a specific day (day 1, 25 m) and nutrient concentrations were important variables at both 25 m and 50 m (**Figure 4.3**). Urea concentrations are associated with CCA2.

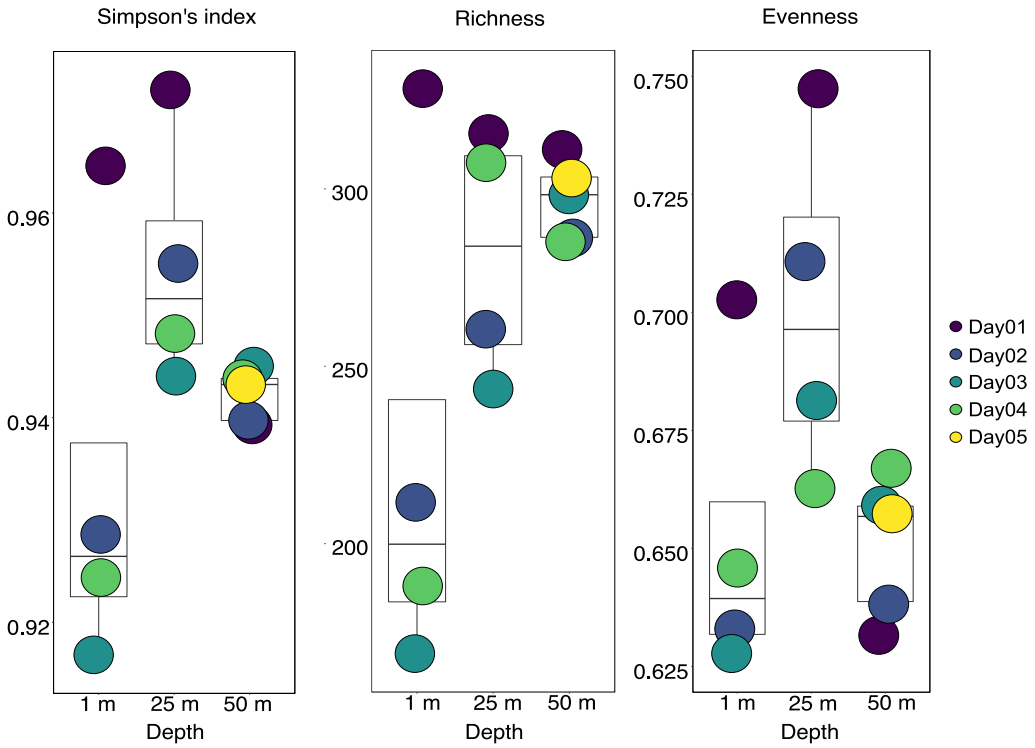

Figure 4.2. Alpha diversity (Simpson's index, richness and evenness) for OTUs in metagenomes from each sampling depth (1 m, 25 m and 50 m) and day in this five-day study. Each colour indicates a sampling day. Box and whiskers indicate the first quartile, median and third quartile.

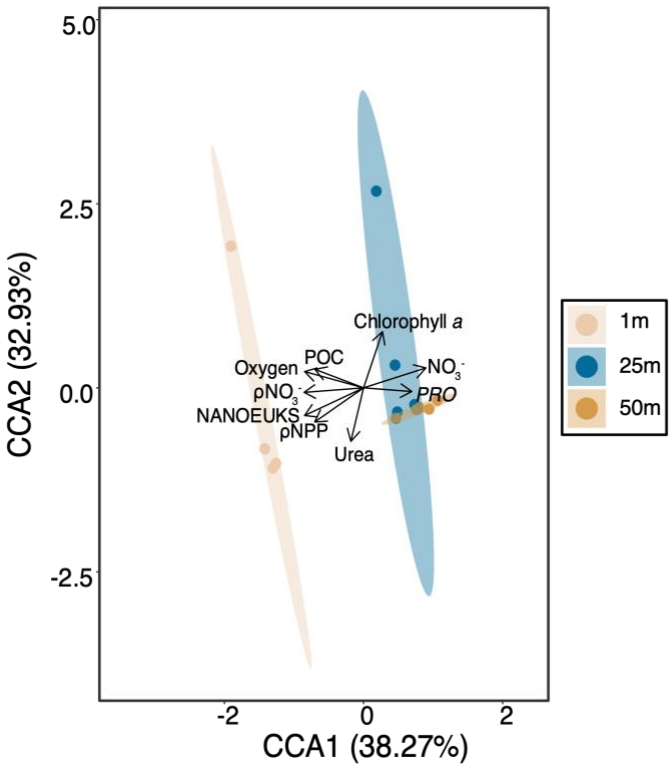

Figure 4.3. Canonical correspondence analysis (CCA) ordination plot grouping the taxonomic composition of raw read metagenome OTUs by sampling depth. Samples taken from 1 m are denoted in beige, 25 m in blue and 50 m in gold. The x and y axes denote the variability explained by the constrained ordination model and the ellipses indicate the 95% confidence around the mean of each depth group. Variables that significantly influence the beta diversity of the nano-and picoplankton community were used to constrain the model. PRO=*Prochlorococcus* carbon biomass; NANOEUKS=Nanoeukaryote carbon biomass; ρNO_3=Nitrate uptake rate; ρNPP=Net primary production.

Significant differences in community structure among sampling depths were confirmed by ANOSIM (R=0.59, p=0.001) as well as the PERMANOVA analysis (**Table 4.2**). Neither of these analyses was influenced by dispersion effects, as the dispersion within each group (community at each depth) was similar (**Table 4.2**). To understand community dissimilarity for each depth, variables were identified that were associated with this dissimilarity using a BIOENV rank-correlation analysis: chlorophyll *a*, oxygen and nutrient concentrations were important variables associated with the different community structures at the three depths (**Table 4.2**). At 1 m, increased urea and biomass concentrations were important determining variables (R^2=0.94), which was similar to the situation at 25 m, where increased chlorophyll *a*,

variable oxygen concentrations and lower urea concentrations were important. In contrast, at 50 m decreased biomass (total, *Synechococcus* and nanoeukaryotes) concentrations, low light and therefore low productivity were important (R^2=0.94).

Table 4.2. Results of the beta dispersion, ANOSIM, PERMANOVA and BIOENV statistical tests comparing variability in community structure across all depths and BIOENV test identifying the supplementary variables in the best model that explains community structure across all depths and at each depth.

Group	Homogeneity of group dispersion (betadisper)		ANOSIM		PERMANOVA (adonis)		BIOENV	
	F statistic	p-value	R	p-value	R^2	p-value	Variables in best model	Spearman's correlation
All depths (df=2)	0.80	0.48	0.60	0.002*	0.57	0.001*	Chl-*a*, Oxygen, NO_3^-	0.76
1m	-	-	-	-		-	Urea, POC^-	0.94
25m	-	-	-	-	-	-	Chl-*a*, Oxygen, Urea	1.00
50m		-	-	-	-	-	Fluorescence, POC, NPP, *Synechococcus* C biomass, Nanoeukaryotes C biomass	0.94

Nano-picoplankton taxonomic composition

The majority (46%) of the total classified sequences in this study belonged to the Proteobacteria (**Figure 4.4**). At the phylum level, Proteobacteria showed no preference for a specific depth and the relative abundance of this phylum did not change significantly on any day (**Table 4.3**). This was the same for the Bacteroidetes, Planctomycetes, Verrucomicrobia, unidentified Bacteria as well as the most abundant Eukaryota phyla. The rest of the taxa were depth differentiated, with abundances at the surface differing from those found at 25 m and 50 m (**Table 4.3**); the Archaea, Actinobacteria, Candidatus Marinimicorbia and Nitrospinae had greater abundances at depth and Cyanobacteria were more abundant at the surface.

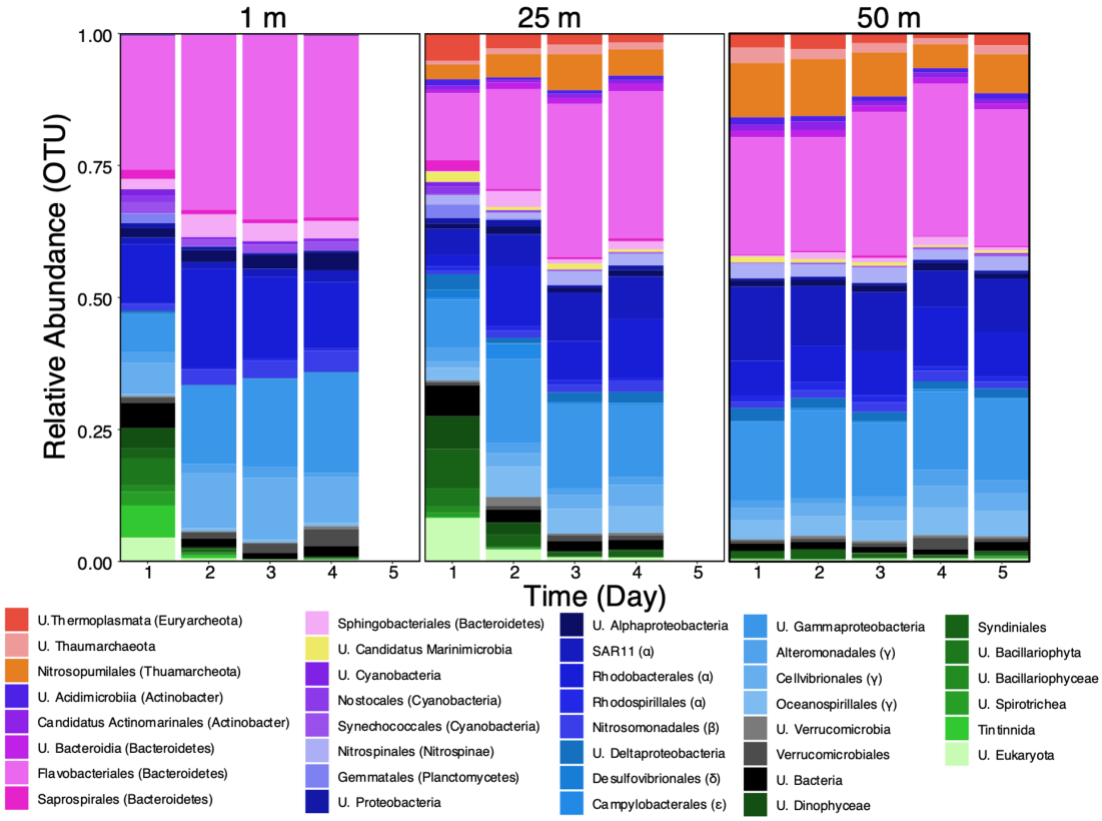

Figure 4.4. Order level relative abundances of archaeal, bacterial, and eukaryotic OTUs on each sampling day at 1 m, 25 m and 50 m as determined from raw metagenome reads. Only orders with a relative abundance of >1% in one sample are presented here. The phylum identification of the order group and class identity of the Proteobacteria are provided in brackets. Blank columns represent missing samples. The "U." refers to taxa which were unclassified at the order level.

Table 4.3. Results of single factor ANOVAs comparing mean values of variables across three depths for 1) the phyla which have at least 1 % abundance in one sample and 2) the orders which have at least 1 % abundance in one sample. Mean relative abundances found in Table S4.3. The degrees of freedom (DF) and sums of squares (SS) are shown for the influence of depth and the residuals, and the F statistics and resulting probabilities (p). Significant values ($p<0.05$) are shaded.

Variable	DF_{Depth}	$DF_{Residuals}$	SS_{Depth}	$SS_{Residuals}$	F	p
1) Phylum						
Euryarchaeota	2	10	62349	33492	9.31	0.005
Thaumarchaeota	2	10	781536	192513	20.30	0.0003
Actinobacteria	2	10	36801	4290	42.89	0.0001
Bacteroidetes	2	10	1063948	1238922	4.29	0.05
Candidatus Marinimicrobia	2	10	6510	4080	7.98	0.008
Cyanobacteria	2	10	48014	25323	9.48	0.005
Nitrospinae	2	10	47359	5772	41.03	0.0001
Planctomycetes	2	10	4855.7	24222	1.00	0.40
Proteobacteria	2	10	229438	2488309	0.46	0.64
Verrucomicrobia	2	10	2047	31894	0.32	0.73
U. Bacteria	2	10	19402	47953	2.02	0.18
Bacillariophyta	2	10	31409	229735	0.68	0.53
Ciliophora	2	10	44972	180385	1.25	0.33
U. Eukaryota	2	10	338212	1261852	1.34	0.31
2) Order						
U. Thermoplasmata	2	10	54802	25425	10.78	0.003
U. Thaumarchaeota	2	10	25287.5	8146.8	15.52	0.0009
Nitrosopumilales	2	10	482362	115031	20.97	0.0003
U. Acidimicrobiia	2	10	6202.5	1298.6	23.88	0.0002
Candidatus Actinomarinales	2	10	8191.6	1555.2	26.34	0.0001
U. Bacteroidia	2	10	11227.7	1313.9	42.73	0.0001
Flavobacteriales	2	10	945964	1145855	4.13	0.05
Saprospirales	2	10	4825.3	6863.5	3.52	0.07
Sphingobacteriales	2	10	48623	30900	7.87	0.009
U. Candidatus Marinimicrobia	2	10	6510.3	4080.8	7.98	0.009
U. Cyanobacteria	2	10	2508.8	2255.6	5.56	0.02
Nostocales	2	10	1336.4	7414.6	0.90	0.44
Synechococcales	2	10	20510	883.2	116.11	0.0001
Nitrospinales	2	10	46882	5928	39.54	0.0001
Gemmatales	2	10	13395	9630.7	2.78	0.10
U. Proteobacteria	2	10	1027.9	1331.8	3.86	0.06
U. Alphaproteobacteria	2	10	18886	6912.3	13.66	0.001
Pelagibacterales	2	10	599402	137067	21.87	0.0002
Rhodobacterales	2	10	443997	382313	5.81	0.02
Rhodospirillales	2	10	4019.5	1339.6	15.00	0.001
Nitrosomonadales	2	10	21806	21053	5.18	0.03
U. Deltaproteobacteria	2	10	25943.6	6654.7	19.49	0.0004
Desulfovibrionales	2	10	1091.1	4472	1.22	0.34
Campylobacterales	2	10	5737.4	16155.8	1.78	0.22
U. Gammaproteobacteria	2	10	28162	467829	0.30	0.75
Alteromonadales	2	10	499.3	16005.8	0.16	0.86
Cellvibrionales	2	10	431869	104434	20.68	0.0003
Oceanospirillales	2	10	129567	30371	21.33	0.0003
U. Verrucomicrobia	2	10	995.4	4087	1.22	0.34
Verrucomicrobiales	2	10	9500.1	17976.7	2.64	0.12
U. Bacteria	2	10	19483	48953	1.99	0.19

Table 4.3. Continued.

Variable	DF_{Depth}	$DF_{Residuals}$	SS_{Depth}	$SS_{Residuals}$	F	p
U. Dinophyceae	2	10	64322	57037	2.26	0.15
Syndiniales	2	10	35308	85239	2.07	0.18
U. Bacillariophyta	2	10	11072	76620	0.72	0.51
U. Bacillariophyceae	2	10	704.9	6412.3	0.55	0.59
U. Spirotrichea	2	10	2879.8	14416.6	1.00	0.40
Tintinnida	2	10	23396	81393	1.44	0.28
U. Eukaryota	2	10	40112	138343	1.45	0.28

Bacteroidetes were primarily represented by Flavobacteriales (89%), Sphingobacteriales (6%) and Saprospirales (3%) (**Figure 4.4**). Flavobacteriales were the most abundant order in the study, representing 27% of the total top reads. Cyanobacteria, although present in abundance in at least one sample, contributed only 1% of total sequences. The Synnechococcales constituted most of the identified Cyanobacteria, specifically species belonging to the *Synechococcus* genus. Of the most abundant sequences classified as Proteobacteria, most are Gammaproteobacteria (51%) and Alphaproteobacteria (40%). Most of the Gammaproteobacteria were unclassified to the order level and showed no spatial or temporal differences in abundance (**Figure 4.4**, **Table 4.3**). Cellvibrionales had a depth preference, with highest abundances found at the surface (**Table 4.3** and **4.4**) whereas Oceanospirillales were more abundant at depth (**Table 4.3** and **4.4**). The SAR11 clade (Pelagibacterales), most of which are unclassified, increased in abundance with depth, resulting in a significant difference between surface and the 25 m and 50 m samples (**Table 4.3** and **4.4**). The Gammaproteobacteria are represented in this study by Rhodobacterales, which, unlike SAR11 of the Alphaproteobacteria, are more abundant at the surface than at 25 m (Tukey-HSD; p=0.03) and 50 m (Tukey-HSD; p=0.04) (**Table 4.4**, **Figure 4.4**). The Rhodobacterales were also the most abundant classified order of Proteobacteria identified, constituting 10% of the most abundant orders.

Table 4.4. Results of Tukey multiple comparison posthoc tests showing probability values for pairwise comparisons between different depths for mean values of variables showing the phyla which have at least 1 % abundance in one sample and 2) the orders which have at least 1 % abundance in one sample. Significant values ($p<0.05$) are shaded.

Variable	1 m vs 25 m	1 m vs 50 m	25 m vs 50 m
1) Phylum			
Euryarchaeota	0.005	0.02	0.48
Thaumarchaeota	0.02	0.0002	0.05
Actinobacteria	0.0007	0.0001	0.02
Candidatus_Marinimicrobia	0.007	0.05	0.37
Cyanobacteria	0.02	0.005	0.70
Nitrospinae	0.0003	0.0001	0.11
2) Order			
Unclassified.Thermoplasmata	0.003	0.01	0.50
Unclassified.Thaumarchaeota	0.02	0.0007	0.16
Nitrosopumilales	0.02	0.0002	0.04
Unclassified.Acidimicrobiia	0.003	0.0001	0.13
Candidatus.Actinomarinales	0.005	0.0001	0.04
Unclassified.Bacteroidia	0.0001	0.0001	0.62
Sphingobacteriales	0.04	0.009	0.78
U. Candidatus Marinimicrobia	0.007	0.05	0.37
Unclassified.Cyanobacteria	0.10	0.02	0.71
Synechococcales	0.0001	0.0001	0.84
Nitrospinales	0.0003	0.0001	0.10
Unclassified.Alphaproteobacteria	0.002	0.003	0.91
Pelagibacterales	0.01	0.0002	0.05
Rhodobacterales	0.03	0.04	0.98
Rhodospirillales	0.06	0.0007	0.05
Nitrosomonadales	0.04	0.05	0.92
Unclassified.Deltaproteobacteria	0.0008	0.0007	0.98
Cellvibrionales	0.0006	0.0006	0.94
Oceanospirillales	0.0005	0.0005	0.98

The Archaea represented 8% of the total sequences identified in this study (**Figure 4.4**). Of the most abundant Archaea identified, 77% were Thaumarchaeota and 23% Euryarchaeota. Both Archaeal groups had higher abundances in metagenomes taken from 25 m and 50 m than 1 m (**Figure 4.4**, **Table 4.3** and **4.4**). The identified ammonia oxidizing Thaumarchaeota were represented by *Candidatus Nitrosopelagicus*, *Nitrosopumilus*, unclassified *Nitrosopumilaceae* and unclassified *Nitrososphaeria*. The Nitrosopumilales (*Nitrosopumilus* and unclassified *Nitrosopumilaceae*) were most abundant at 50 m, with significantly different abundances than those at the other two depths (**Table 4.3** and **4.4**). The Euryarchaeota were primarily unclassified Thermoplasmata.

Like Archaea, Eukaryotes also represented 7% of the overall dataset (**Figure 4.4**). None of the Eukaryotic orders identified in this study showed a preference for any depth (**Table 4.3** and **4.4**). Almost half (43%) of the most abundant

Eukaryotes were Dinophyceace, with the order Syndiniales (parasitic dinoflagellates) contributing a large portion of the taxa. There was a large abundance of Eukaryotes on day 1 at 1 m and 25 m and day 2 at 25 m, which were the times at which the sampling depths were closest to the chlorophyll maxima (**Figure S4.2**).

Taxonomic composition and functional potential from assembled metagenomes

The most abundant phyla found in the assembled metagenomes were similar to those found in the raw reads metagenomic analysis (**Figure S4.3**). To understand the functional potential of the nano-picoplankton community and whether there is variability over depth or time, selected metabolically-important pathways were investigated in each assembled metagenome.

Photosynthesis genes were prevalent in metagenomes at the surface (**Figure 4.5**), with the photosystem I pathway more abundant at the surface than at 50 m (**Table 4.5** and **4.6**). Photosystem II pathways, photoheterotrophy genes, rhodopsin and heliorhodopsins and bacteriochlorophyll gene abundances, associated with aerobic anoxygenic photosynthetic bacteria, were also more abundant in metagenomes found at the surface than at 25 m and 50 m (**Table 4.5** and **4.6**). There was no daily variability in the abundances of genes associated with light-dependent pathways.

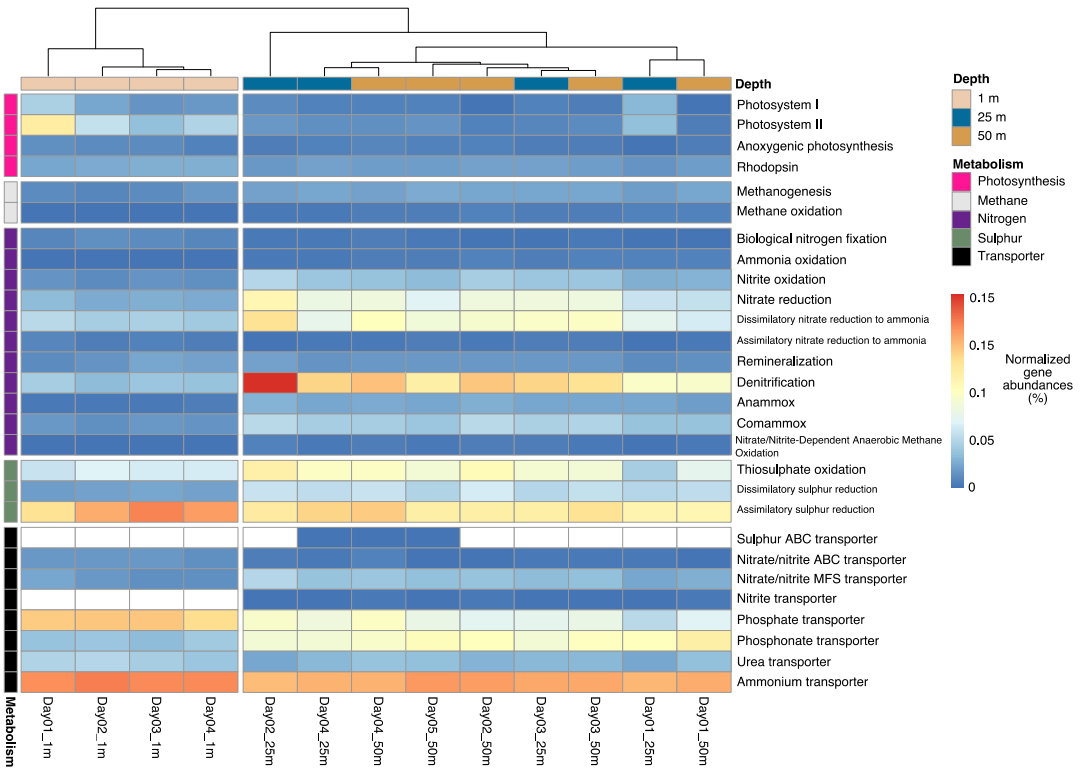

Figure 4.5. Normalized abundances of metabolic pathways or genes of interest in the 13 metagenomes. The colour of the cells relates to the normalized abundance (%) of the pathway/gene in the sample, ranging from least abundant (blue) to most abundant (red). The heatmap is clustered on the y-axis according to the metabolisms the pathway belongs to namely, photosynthesis, the methane cycle, the nitrogen cycle, the sulphur cycle, and cellular transporters. The clustering on the x- axis is by depth, with 1 m in beige, 25 m in blue and 50 m in gold. KO/InterPro terms used for estimating relative abundances of each pathway/gene are shown in **Table 4.1**.

Table 4.5. Results of single factor ANOVAs comparing mean values of variables across three depths for 1) gene pathways from assembled metagenomes. The degrees of freedom (DF) and sums of squares (SS) are shown for the influence of depth and the residuals, and the F statistics and resulting probabilities (p). Significant values ($p<0.05$) are shaded.

Variable	DF_{Depth}	$DF_{Residuals}$	SS_{Depth}	$SS_{Residuals}$	F	p
1) Pathway						
Photosytsem I	2	10	0.001	0.001	5.17	0.03
Photosytsem II	2	10	0.007	0.005	7.43	0.01
APP	2	10	7.5×10^{-5}	4.6×10^{-5}	8.16	0.008
Rhodopsin	2	10	0.001	0.00004	15.23	0.0009
Methanogenesis	2	10	0.0003	0.00004	34.61	0.0001
Methane oxidation	2	10	5.5×10^{-5}	1.6×10^{-5}	17.83	0.0005
BNF	2	10	0.0002	0.00002	39.83	0.0001
Ammonia oxidation	2	10	6.1×10^{-5}	1.7×10^{-5}	18.33	0.0005
Nitrite oxidation	2	10	0.002	0.0003	21.96	0.0002
Nitrate reduction	2	10	0.007	0.002	17.30	0.0007
DNRA	2	10	0.006	0.003	9.56	0.005
ANRA	2	10	3.1×10^{-5}	2.4×10^{-5}	6.53	0.02
Remineralization	2	10	1.1×10^{-5}	1.7×10^{-4}	0.30	0.75
Denitrification	2	10	0.03	0.008	16.93	0.0006
Anammox	2	10	0.001	0.00007	91.55	0.0001
Comammox	2	10	0.002	0.0003	42.44	0.0001
N_damo	2	10	3.8×10^{-5}	3.1×10^{-5}	6.11	0.02
Thiosulphate oxidation	2	10	0.002	0.004	2.42	0.14
DSRA	2	10	0.003	0.0002	69.72	0.0001
ASRA	2	10	0.003	0.003	6.93	0.01
Sulphur ABC transporter	2	10	-	-	-	-
Nitrate/nitrite ABC transporter	2	10	0.0005	0.00004	56.92	0.0001
Nitrate/nitrite MFS transporter	2	10	0.001	0.0005	10.37	0.004
Nitrite transporter	2	10	3.5×10^{-6}	4.8×10^{-6}	5.12	0.06
Phosphate transporter	2	10	0.01	0.002	35.53	0.0001
Phosphonate transporter	2	10	0.01	0.0005	98.55	0.0001
Urea transporter	2	10	0.0006	0.0002	20.04	0.0003
Ammonium transporter	2	10	0.0007	0.0002	20.56	0.0003

Table 4.6. Results of Tukey multiple comparison posthoc tests showing probability values for pairwise comparisons between different depths for mean values of variables showing 1) gene pathways from assembled metagenomes. Significant values ($p<0.05$) are shaded.

Variable	1 m vs 25 m	1 m vs 50 m	25 m vs 50 m
1) Pathway			
Photosystem I	0.29	0.02	0.33
Photosystem II	0.04	0.01	0.82
APP	0.007	0.05	0.38
Rhodopsin	0.001	0.003	0.74
Methanogenesis	0.0002	0.00004	0.50
Methane oxidation	0.003	0.0005	0.65
BNF	0.00004	0.00004	0.97
Ammonia oxidation	0.002	0.0005	0.71
Nitrite oxidation	0.0004	0.0005	0.89
Nitrate reduction	0.0008	0.002	0.69
DNRA	0.007	0.01	0.86
ANRA	0.02	0.05	0.64
Denitrification	0.0008	0.002	0.64
Anammox	0.0001	0.0001	0.82
Comammox	0.0001	0.0001	0.98
N_damo	0.03	0.03	1.00
DSRA	0.0001	0.0001	0.55
ASRA	0.02	0.02	1.00
Nitrate/nitrite ABC transporter	0.0001	0.0001	0.55
Nitrate/nitrite MFS transporter	0.008	0.006	1.00
Phosphate transporter	0.0001	0.0001	0.94
Phosphonate transporter	0.0001	0.0001	0.06
Urea transporter	0.0002	0.004	0.10
Ammonium transporter	0.0003	0.003	0.15

The biological nitrogen fixation (BNF) gene, *nif*H, was identified in all 13 metagenomes. More organisms (average ± standard deviation) capable of nitrogen fixation were found in surface (0.011 ± 0.002 % relative abundance) than deep (25 m: 0.003 ± 0.002 and 50 m: 0.003 ± 0.001 % relative abundance) samples (**Table 4.5** and **4.6**). In contrast, genes associated with the nitrification pathway were found in greater abundance at 25 m (**Table S4.2**, **Table 4.6**; NO_2^- oxidation: p=0.002, NH_3 oxidation: p=0.006) and 50 m (**Table 4.6**; NO_2^- oxidation: p=0.002, NH_3 oxidation: p=0.002) than at the surface. There was a greater proportion of nitrite oxidation genes (*nxr*AB) than ammonia oxidizing genes (*amo*ABC and *Hao*) (**Table S4.2**). Genes associated with dissimilatory nitrate reduction (DNRA), denitrification, N-damo (Nitrate/Nitrite-dependent anaerobic methane oxidation), annamox and commamox (complete ammonia oxidation) pathways were more abundant in metagenomes from deep than surface samples (**Table 4.5** and **4.6**, **Table S4.2**). Assimilatory sulphur cycling pathways were generally more abundant at the surface than depth, while

dissimilatory sulphur reduction was dominant in metagenomes found at depth (**Table 4.5** and **4.6**, **Table S4.2**).

The most dominant transporters across all depths were the ammonium transporters (*amt*B, without specific separation between photoautotrophs and ammonia oxidizing archaea), which were more abundant in metagenomes at the surface than at 25 m and 50 m (**Table 4.5** and **4.6**, **Table S4.2**). Phosphate, urea, and nitrate/nitrite ABC transporters were also abundant in metagenomes found at the surface (**Table 4.5** and **4.6**, **Table S4.2**). In contrast, phosphonate, and nitrate/nitrite MFS reporters were relatively more abundant at depth (**Table S4.2**).

Functional gene composition across all depths was associated with chlorophyll-*a* concentrations, oxygen concentrations, nutrient (ammonium and nitrate) concentrations and particulate organic matter and nanoeukaryote biomass (**Table 4.7**). In surface waters, high chlorophyll-*a* content, increased oxygen, and urea concentrations and Picoeukaryote biomass were strongly associated with the functional gene abundances (**Table 4.7**). Similarly, at 25 m, high chlorophyll-*a* and variable oxygen concentrations were associated with functional gene composition, in addition to high nitrate concentrations as well as the decreased concentrations of POC. Particulate organic matter was an important factor associated with the potential functionality of the taxa at 50 m.

Table 4.7. The results of the BIOENV statistical tests comparing depth changes in functional potential of taxa across all samples and a BIOENV test identifying the variables in the best model that explains functional potential at each depth.

Group	BIOENV	
	Variables in best model	Spearman's correlation
All depths	Chl-*a*, Oxygen, NH_4^+, NO_3^-, POC. Nanoeukaryote C biomass	0.84
1m	Chl-*a*, Oxygen, Urea, Picoeukaryote C biomass	1.00
25m	Chl-*a*, Oxygen, NO_3^-, POC	0.94
50m	POC	0.82

Linking functional potential in metagenomes to measured process rates

Abundances of genes associated with nitrite oxidation had a positive relationship with nitrification rates (R=0.68, Z=2.24, n=12, p=0.03). The only other positive relationship was found between log-transformed abundances of ammonium transporters and log-transformed ammonium uptake rates (R=0.84, t=5.04, df=11, p=0.0004). No relationship was found between urea and nitrate transporters and their related uptake rates. Nutrient uptake rates were significantly faster at the surface than at 25 m and 50 m (Chapter 3), which was the same pattern found in the related transporter abundances (**Figure 4.6**). Nitrite oxidation rates and the relative abundance of the genes associated with the nitrite oxidation pathway were greater at depth (**Figure 4.6**). Although there were some matching depth differentiations in the relative abundances of genes and their corresponding process rate, there was no similarity in trends over the sampling days.

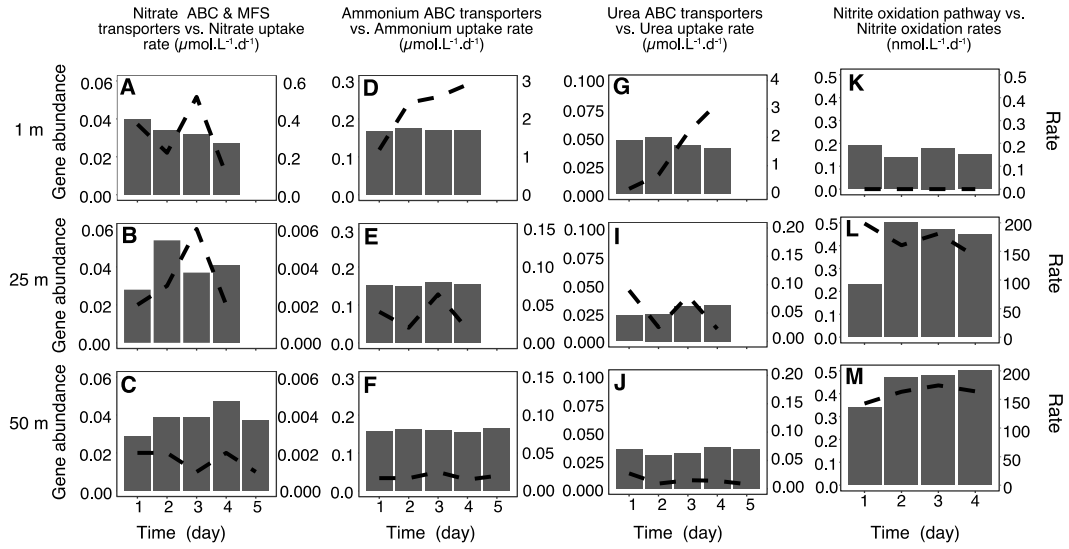

Figure 4.6. A comparison at each of the three depths between % gene abundances per metagenomes (bar) and rate measurements (dashed line) for (A–C) nitrate ABC and MFS transporters and nitrate uptake rates (μmol.L^{-1}.day^{-1}), (D–F) ammonium transporter and uptake rates (μmol.L^{-1}.day^{-1}), (G–I) urea transporters and uptake rates (μmol.L^{-1}.day^{-1}), and (J–L) nitrite oxidation gene abundance and rates (nmol.L^{-1}.day^{-1}).

4.5. Discussion

This chapter focuses on the nano-picoplankton group, diving into the depth stratification and potential functionality of these vital organisms. The role of nano-picoplankton in primary production and nitrogen cycling as well as their abundances and contributions to carbon and nitrogen of the general plankton size groups were elucidated in detail in Chapter 3. In this study the identities and functional potential of these nano-picoplankton were expanded upon. As with the primary production and nitrogen uptake rates, there was a clear depth-differentiation in nano-picoplankton abundance and functional potential under stratified conditions over this five-day period in St. Helena Bay (Chapter 3). Daily variability in either abundance of taxa or potential function were not as distinctive.

In spring and summer, the area in which this sampling station is located experiences the effects of episodic wind driven upwelling, which starts in September and tapers out when the southerly winds become less frequent, around the time this study took place in March (Hutchings et al., 2009). With no active upwelling occurring during this study, the water column remained stratified throughout the five-day sampling period (Chapter 3). With the exception of a deepening of the mixed layer on day 2, the physical properties of the water column remained similar from day to day, with most of the variability found in the physical and chemical properties of the water at the three different sampling depths.

Diversity of the total nano-picoplankton community

Throughout the sampling period, nano-picoplankton abundances showed a differential depth distribution, which was linked to physical and chemical factors that varied with depth, like light, oxygen, and biomass concentrations (Chapter 3). As is common in a stratified water column in the ocean (Walsh et al., 2016), taxonomic diversity of microorganisms increased with depth in this study, although the results were skewed by day 1 1m samples (**Figure 4.2**). There was a larger spread between diversity measurements of sampling days at the surface and at 25 m in comparison to 50 m (**Figure 4.2**). This is due to the high diversity found in metagenomes sampled close to the chlorophyll maxima on day 1 at the surface and 25 m (**Figure 4.4**). The high diversity could be attributed to an increase in the abundance and diversity of nano- and picoeukaryotes close to the chlorophyll maxima, and the release of dissolved

organic matter like polysaccharides, proteins, and lipids, which would have stimulated the growth of a diverse range of heterotrophic bacteria (Vallina et al., 2014).

The largest proportion of eukaryotes was found in metagenomes on day 1 at 1 m and 25 m, specifically diatoms, ciliates, and dinoflagellates (**Figure 4.4**). The main phytoplankton species at these depths, contributing much of the chlorophyll, was the diatom *Thalassiosira anguste-lineata* (Ndlovu et al., 2020, unpublished data), which would account for the large proportion of Bacillariophyta found in these samples. The break-down of the silica frustrules of these diatoms could have contributed to the high silicate concentrations found at 25 m and below, as these organisms sink and are remineralized (Yool and Tyrrell, 2003). The high proportion of dinoflagellates is most likely an indication of large genomes and copy number associated with the parasitic Syndiniales (Gong and Marchetti, 2019). Heterotrophic bacterial diversity was not significantly different in these two samples on day 1, and probably was not a large contributing factor to overall diversity. At the surface and 25 m, the water column is variable, being affected by mixing (Chapter 3), atmospheric deposition (Guieu et al., 2014) and nutrient fluctuations. This physical and chemical variability could contribute to increased variability in taxonomic diversity between days at these two depths.

Throughout this study, the mixed layer depth was never deeper than approximately 20m (Chapter 3). Therefore, the 50 m sampling depth was not subjected to physical mixing, creating consistent environmental conditions at this depth over the five-day sampling period (Chapter 3). At 50 m, the water was defined as having low oxygen (< 2 mL/L) on all days of sampling, creating conditions for a specific diversity of microorganisms to thrive, like picoplankton (Ganesh et al., 2014, 2015; Parris et al., 2014). This lack of physical variability contributed to the similarity in taxonomic diversity at 50 m over the sampling period (**Figure 4.2**).

Depth differentiation in community structure and potential function

In the well-lit surface waters, taxa like Bacteroidetes, Cyanobacteria, Cellvibrionales and Rhodobacterales were abundant. The Bacteroidetes were represented predominantly by the heterotrophic *Flavobacteriales,* primary consumers responsible for much of the uptake of dissolved organic matter (DOM), which starts off the microbial loop by breaking down high molecular weight organic matter into a

more bioavailable form (Kirchman, 2006). The presence of these organisms in surface samples can be explained by the large proportion of organic material at the surface (Chapter 3), as these bacteria are often particle-associated rather than free-living in oligotrophic surface waters.

Cellvibrionales is a diverse group of Gammaproteobacteria and includes genera that thrive and prefer oligotrophic conditions as well as those that are copiotrophic (Spring et al., 2015). Most Cellvibrionales are photoheterotrophic and this quality, as well as the ability of some species to thrive in nutrient-poor waters, like the surface samples in this study, could explain the increased abundances in metagenomes found at the surface.

The highly abundant Rhodobacterales are copiotrophic, anoxygenic phototrophs and, like the *Flavobacteriales*, are primary consumers, capable of the rapid uptake of DOM (Dang et al., 2008). Under resource deprivation, energy acquisition from light, making use of bacteriochlorophyll, would confer a fitness advantage to these taxa, which could be what is occurring at the surface in this study (Kolber et al., 2000; Koblížek, 2015). Rhodobacterales have been found to be a dominant taxon in shallow coastal waters in Monterey Bay (Reji et al., 2020), on and off the shelf in St. Helena Bay (Rocke et al., 2020) and close to the coastline during active upwelling (Chapter 2). Despite depth-preferences of anoxygenic phototrophs like the Rhodobacterales for surface waters, abundances of the *puf*LM genes were spread evenly throughout the water column across all days (**Figure 4.5**, **Table 4.5**). These AAP bacteria are photoheterotrophic, with a requirement for carbon substrates, and can therefore proliferate in dark oxygenated depths of the water column (Koblížek, 2015).

The most abundant light-harvesting proteins are microbial rhodopsins (Beja et al., 2000), which are present in this study as archaeal, bacterial and eukaryote rhodopsins, as well as heliorhodopsins, a recently discovered family of rhodopsins (Kovalev et al., 2020). Taxa such as SAR11 (Giovannoni et al., 2005) and certain Gammaproteobacteria would be hosts for rhodopsins, as well as a variety of other archaea and eukaryotes in this study. Primary production is supported by the photochemical reaction centers in photosystems I and II, while rhodopsins are primarily responsible for additional energy acquisition by photoheterotrophic organisms (Finkel et al., 2013).

Light availability, the resulting chlorophyll-*a* concentrations, as well as phosphate and silicate concentrations were identified as important factors associated with the community structure of microbiomes in surface waters (**Table 4.2**). Most taxa that were abundant in surface waters were photosynthetic or could utilize light for energy, such as the Cellvibrionales, Cyanobacteria or are primary consumers like Bacteroidetes. The availability of light also would be linked to increased concentrations of chlorophyll-a at the surface (Chapter 3), much of which belonged to the 10-200 µm size fraction. The increased chlorophyll concentrations contributed to the large concentrations of biomass found at the surface. This particulate organic matter would create microenvironments providing carbon sources for primary consumers (Biddanda and Pomeroy, 1988).

Phosphate and silicate are important macronutrients for phytoplankton growth and development, especially diatoms that use silicate to form their frustules (Yool and Tyrrell, 2003). The low concentrations of these nutrients at the surface could be attributed to the increased abundances of Bacillariophyta and other phytoplankton (**Figure 4.4**). Alternatively, during the succession of the bloom that may have occurred prior to this sampling, these nutrients were stripped by those organisms. Another important macromolecule for the growth of plankton is nitrogen. Nitrogen cycling is an important role of microorganisms in marine ecosystems, and understanding this cycling is especially important in a dynamic embayment like St. Helena Bay. The uptake of nitrogen species by the nano-picoplankton was discussed in Chapter 3, and here the potential nitrogen cycling occurring in the water column is expanded upon, beginning with the introduction of nitrogen into the water column through nitrogen fixation. The presence of genes associated with nitrogen fixation in these samples' points to the presence of diazotrophic organisms in the nano-picoplankton group, perhaps in the Cyanobacteria, Gammaproteobacteria and Planctomycetes, as well as protistan hosts of diazotrophic bacteria (Kneip et al., 2007). However, the functionality and the rate of nitrogen fixation during these 5 days is not known. In the Benguela, when upwelling was weak, nitrogen fixation, measured as nitrogenase activity, was more active in the northern Benguela in comparison to the below detection limits measured off the west coast of South Africa (Staal et al., 2007). Further research on nitrogen fixation rates, the plankton responsible for fixing nitrogen and the seasonal

effect of this activity in St. Helena Bay would be important to expand understanding of nitrogen cycling in the area.

Although much of the uptake of nitrogen occurred at the surface (Chapter 3), the cycling and transformation of nitrogen predominantly occurred at 25 m and 50 m during this study. These two depths were also very similar in taxonomic community structure and functional potential. Nitrogen cycling can be separated into three general groups of processes: nitrogen gain, nitrogen retention and nitrogen loss (Pajares and Ramos, 2019). With depth (25 m and 50 m), nano-picoplankton involved in nitrogen retention processes (nitrification, dissimilatory nitrate reduction to ammonia (DNRA), assimilatory nitrate reduction) and loss (denitrification and annamox) became more prevalent (**Figure 4.5**). It has been shown that, during summer and early winter, remineralised nutrients are trapped on the shelf of the southern Benguela Upwelling System, creating an enhanced nutrient pool that can support this highly productive area (Flynn et al., 2020). This enhancement of the nutrient pool was apparent in this study at depth. At 25 m and 50 m, nitrification and DNRA genes became abundant in metagenomes, as did the relative abundances of nitrifying archaea and bacterial taxa like *Nitrosopumilus*, Nitrospinales and Nitrosomondales. The ammonium oxidizing archaea, *Nitrospumilus*, previously have been identified in the waters of St. Helena Bay in summer, both on and off the shelf (Rocke et al., 2020) as well as in surface and 10 m samples throughout an active upwelling cycle (Chapter 2). This genus is known to host strains with diverse physiological capabilities, which ranges from those that are inhibited by light (Francis et al., 2005) to others that are both chemolithotrophic and able to assimilate organic carbon compounds (Qin et al., 2014), explaining their ubiquity in the water column and sediments.

Nitrite oxidation rates were largest at 25 m (**Figure 4.6**), which could be attributed to the nitrite oxidizing bacteria (NOB) phyla, Nitrospinales and Nitrosomondales. Nitrospinales are ubiquitous nitrite oxidising bacteria in the global ocean, playing a major role in carbon fixation, especially in the dark parts of the ocean (Pachiadaki et al., 2017). The abundance of these nitrifiers also has a strong ($R^2 = 0.93$) positive relationship with nitrite oxidation rates (**Figure S4.4**), confirming the importance of this group in nitrification and thus the continued fertility of the region (Flynn et al., 2020). A similar relationship between abundances of *Nitrospina* and nitrite oxidation rates was found in the upper water column and oxygen minimum zone

of the eastern tropical North Pacific, suggesting *Nitrospina* play a quantitatively important role in nitrogen cycling throughout the water column (Beman et al., 2013) Nitrifiers were originally thought to only thrive in aerobic conditions; however, there are specialist nitrifiers that have adapted to low oxygen conditions and are able to oxidise ammonia and nitrite under microaerophilic conditions (Füssel et al., 2012; Bristow et al., 2016, 2017; Sun et al., 2017). In the first four days of this study, nitrite oxidation rates at 50 m ranged from 142.8 - 174.6 nmol.L^{-1}.d^{-1} (**Figure S4.2**) with oxygen concentrations ranging from 25.0 - 80.8 µmol.L^{-1}. These rates are similar to those found at 25 m, where oxygen concentrations ranged from 67.0 – 151.8 µmol.L^{-1}. These oxygen concentrations are relatively high compared to other studies (Füssel et al., 2012; Bristow et al., 2016, 2017; Sun et al., 2017), where oxygen measurements ranged from below detection to 11 µmol.L^{-1}. This could indicate that there is enough oxygen at the study site for nitrifiers to function at 50 m.

Another nitrogen retention process is dissimilatory nitrate reduction (DNRA), the anaerobic step-wise reduction of nitrate, to nitrite and then ammonium (Pajares and Ramos, 2019). Due to the use of the same gene complex (*nar*GHI) in the nitrate reduction step, DNRA and denitrification compete for nitrate in the same environment. As DNRA is both a supplier of nitrite (nitrate reduced to nitrite by *nar*GHI) and a competitor for nitrite (nitrite reduced to ammonium by *nrf*A), its role in nitrogen cycling in St. Helena Bay should be considered closely. This process is not well studied *in situ* in coastal systems, although it is connected to many of the nitrogen cycling processes. Taxa capable of DNRA are diverse, including the Proteobacteria, Verrucomicrobia, Planctomycetes, Diatoms and Fungi (Tiedje, 1988; Takaya, 2002; Kamp et al., 2011; Welsh et al., 2014), all of which were present in this study (**Figure 4.4**).

Denitrification has been found to be a significant nitrogen loss process in other eastern boundary upwelling regions (Codispoti and Christensen, 1985), especially in the northern Benguela (Elodie et al., 2013); it was a significant contributor to nitrogen loss in this study as well. There was a large proportion of taxa capable of denitrification in comparison to the other nitrogen loss processes, like anammox, commamox and N-damo (**Figure 4.5**). It should be mentioned that the lowest oxygen concentrations in this study were higher than those that support transcription of denitrifying genes (Dalsgaard et al., 2014). It is likely that anaerobic microenvironments found in sinking

detritus support heterotrophic or autotrophic denitrifiers throughout the water column (Bristow, 2018).

If nitrate were limiting in the low oxygen waters at 25 m and 50 m, processes like manganese oxide reduction, iron oxide reduction and sulphate reduction would become more important for the anaerobic remineralisation of organic matter in this system, and there were indications of taxa with the potential for these functions. Measuring transcription or process rates of nitrogen cycling pathways would give a better indication of which processes dominate in St. Helena Bay in autumn, how they interact with each other, and the effects of these processes on the nitrogen budget of the region.

Metagenomic transporter and gene data and the relation to process measurements

Biogeochemical processes in the marine environment are often studied using multiple methods, like isotope reactions and genetic data. Here we determine if there is a relationship between the functional potential found in the metagenomes and the process rates of nutrient uptake as well as nitrite oxidation measured using stable isotope chemistry to determine whether cross disciplinary methods could be used to positively determine function from metagenomes (**Figure 4.6**). The importance of the nutrient profiles and uptake rates across the water column has been discussed in Chapter 3. However, the uptake and cycling of nutrients also has a genetic component and, in this chapter, it was shown that there are clear relationships between some transporter abundances and process rates. General patterns (highs and lows) were found linking normalized gene and transporter abundances and uptake rates at the different depths in this study (**Figure 4.6**), although these relationships were not always present.

ABC-type nitrate/nitrite transporters are driven by ATP hydrolysis and are important for assimilatory nitrogen processes (Moir and Wood, 2001). There were high proportions of these genes in surface metagenomes where most of the assimilation of nitrogen was happening, relating well to the increased proportion of nitrate uptake and possible nitrite fixation occurring at the surface in comparison to depth. In contrast, MFS-type transporters, which are associated with dissimilatory nitrogen processes like denitrification (Alvarez et al., 2019), increased in relative abundance at 25 m and 50 m, where oxygen concentrations were low, and

denitrification would occur. The relative abundance of the ammonium transporter (*amt*B) was the highest among all transporters and pathways identified in this study (**Figure 4.5**). Unlike the relationship between the other transporters and the process rates, there was a significant positive relationship between *amt*B abundances and ammonium uptake rates. The higher gene abundances at the surface match with increased ammonium uptake rates at the surface, despite the gene abundance not being an indication of activity, and this is further paired to low ammonium concentrations found at the surface.

Phosphate transport pathways were closely related to the concentrations of phosphate found in the water column (**Figure 4.5** and **Figure S4.1**). Phosphate transporters (*pst*ABCS) decreased in abundance with depth, where phosphate was readily available. In contrast to phosphate transporters, phosphonate transporters (*phn*CDE) increased in abundance with depth. Phosphonates constitute a large component of organic phosphorus in the ocean and are a possible alternative source of phosphate for bacterioplankton (Villarreal-Chiu et al., 2012). This increase at depth is possibly related to an increase in the abundances of taxa, like SAR11 (Sowell et al., 2009) and Planctomycetes (Martinez et al., 2010), that contain this pathway.

Across the entire water column, there was a significant positive relationship between log-log transformed nitrite oxidation rates and nitrite oxidation gene abundances, showing that gene abundances could be used to predict nitrite oxidation rates. However, at 25 m and 50 m, these relationships were not as distinctive, possibly because of the small sample sizes at each depth (**Figure 4.6**). A study done in the California Current did not find a correlation between nitrification rates and bacterial or archaeal *amo*A abundance, which is different to what was found in this study (Santoro et al., 2010). This may be because of the use of biomarker analysis or because they were analysing ammonia oxidation rates, which was not done here. Depending on the process, gene abundances from metagenomes could be good indicators of function when compared to bulk process rate data and are good indicators of depth-differentiation of biogeochemical processes; however, this hypothesis requires more robust research to confirm. In fact, previous studies have found that genetic data could be used to support isotope-based findings, such as in the case of nitrous oxide emission from manure treated soil (Snider et al., 2015). In the future, making use of

DNA stable isotope probing may a be a more direct method to link gene abundance and diversity with metabolic function (Chen and Murrell, 2010). In the DNA-SIP method, genomic DNA is extracted directly from the samples incubated with the isotope tracers. Although this would be a better method to link functionality with specific taxa, it is unclear whether logistically it would work with the low biomasses obtained throughout this study.

4.6. Conclusion

This study provided a daily view of nano-picoplankton communities in the water column during autumn in St. Helena Bay. Over the five-day period, under stratified conditions, nano-picoplankton community composition and potential functionality differed between the surface and subsurface (25 and 50 m), with community dynamics shaped by light conditions, carbon biomass and nutrient availability (**Figure 4.7**). Temporal variation on a daily time scale was not observed in archaeal, bacterial, or eukaryotic community structure, adding credence to the primary influence of the physical environment on microbial community structure. Adding more stations and days with variable upwelling conditions to a study such as this would give clearer indications of whether these findings are applicable to the entire bay in autumn.

The illumination of all the different light dependent pathways in the nano-picoplankton in St. Helena Bay highlighted the need for pathway specific research in the area, to have an in-depth understanding of the ecosystem functioning of the bay. Results indicated a large proportion of dissimilatory nitrogen processes, like DNRA and denitrification, occurred at depth, highlighting the possible importance of these functions in St. Helena Bay and the need for further research to elucidate their process and transcription rates. This study is one of the first to determine daily potential functionality and community composition of nano-picoplankton in the region in autumn, making use of metagenomic tools. The results emphasise the need to do targeted studies on the roles of nano-picoplankton in the biogeochemical cycling within the southern Benguela ecosystem.

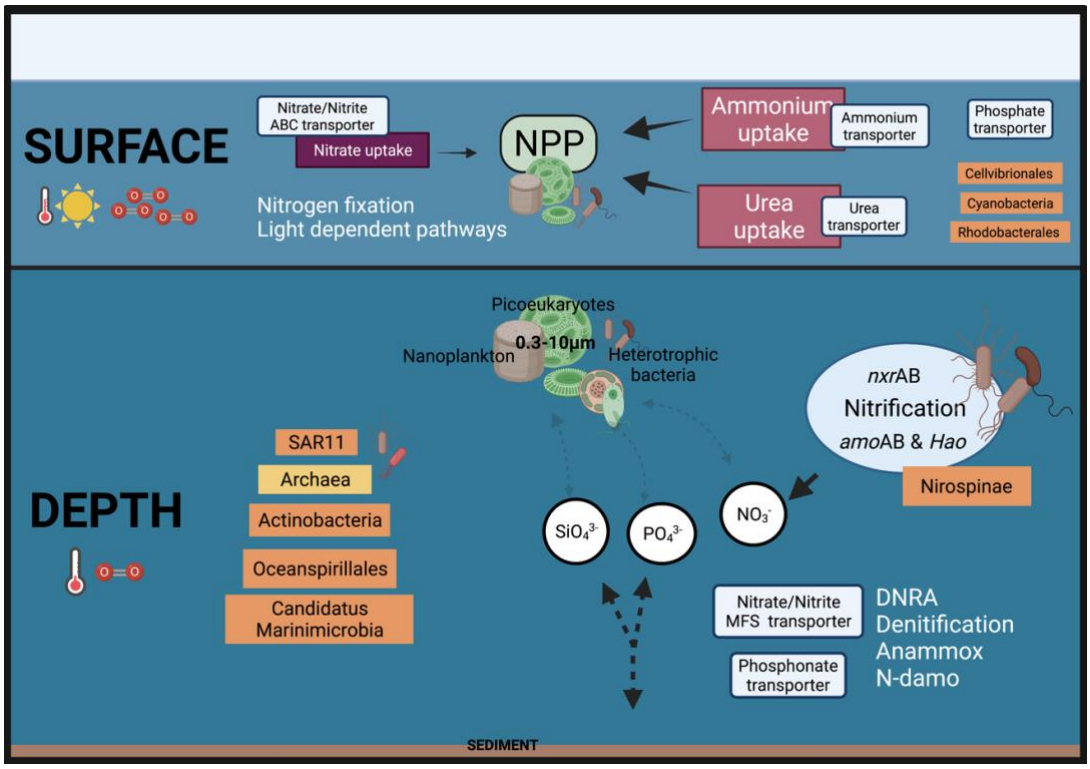

Figure 4.7. Conceptual model illustrating how Chapter 4 builds on the findings on Chapter 3. After identifying the nano-picoplankton as the main contributors to productivity in Chapter 3, the identity and potential functionality of these organisms were highlighted in Chapter 4. Photosynthetic organisms and copiotroph organisms are found at the surface and the genes for ammonia, urea and nitrate transporters were more abundant at the surface. At depth, Nitrospinae were strongly correlated with nitrite oxidation rates and there were high abundances of anaerobic nitrogen cycle processes. Organisms that were more abundant at depth are highlighted. Created with BioRender.com.

5. Chapter 5: Synthesis

5.1. Summary of main findings

The Benguela ecosystem is one of the four eastern boundary upwelling systems (Andrews and Hutchings, 1980; Carr and Kearns, 2003; Chavez and Messié, 2009; Blamey et al., 2015). A main feature of the southern Benguela is the wind driven coastal upwelling that occurs cyclically in austral spring and summer. This upwelling not only supports the major productivity associated with the area, but also creates dynamic environmental conditions that have an overarching effect on all trophic levels, including the smallest phytoplankton and microorganisms. It is these small planktonic organisms that became the focus of my research. Due to the topology of the coastline and shelf, as well as local currents and jets, embayments along the coast of South Africa retain much of this productivity, making them ideal sites to study the role of picoplankton and nano-picoplankton in the dynamics of the ecosystem and vice versa.

To understand the microbial ecology and not only the microbiology of *in situ* communities, I made an effort to not only identify diversity, functionality, and community structure but also to put all these variables in the context of the environment by generating timeseries of multiple variables that were collected in parallel. To study the dynamics of picoplankton and nano-picoplankton, an Eularian approach was used, so that variability between sites would be minimized as much as it could be under survey conditions. The spatial dimension included in the research was depth, and it was introduced to the sampling design to get a holistic view of the water column at one site over daily timescales. In line with the holistic approach, as much as was feasible within the logistic and funding limitations of this thesis the microbiome of the water column was analysed, which included bacteria, archaea, and eukaryotes.

Studying a wind driven upwelling cycle was an opportunity to dive into an environmentally important event, which is known to create dynamic water column conditions that would likely influence microbial and picoeukaryote community structure and function. In Chapter 2, I found that bacterioplankton (archaea and bacteria) communities were distinct between active upwelling and relaxation periods,

influenced heavily by the separation of the water column by mixed layer depth. Thus, physical separations in the water column created distinct bacterioplankton communities; however, the same could not be said about picoeukaryotes. There was no difference in picoeukaryote community structure between the upper mixed layer and the bottom layer during the highly stratified relaxation period, pointing to picoeukaryotic communities being either more homogenous throughout the water column or had not yet responded to environmental changes in the time period sampled. Relatively abrupt changes in functional and taxonomic diversity and process rates from one day to the next added credence to the notion that picoplankton, more specifically the bacterioplankton, rapidly change community structure over a short timescale when the water column is affected by physical factors like wind and thermal stratification. The research done in Chapter 2 was a great start to determining the nuances of picoplankton communities from a taxonomic diversity perspective and their functional roles and potential interactions with each other.

In Chapter 3, the research then moved to the post-upwelling period (autumn) when wind direction and speed were not causing cyclic upwelling and water column conditions were relatively constant and stratified. The overarching question became whether there would be daily changes in nano-picoplankton (0.3–10 µm) dynamics in a more stratified water column. A comprehensive 5-day, single station study was designed to answer this question.

A distinct characteristic of St. Helena Bay in autumn is the formation of seasonal hypoxic bottom waters, due to aerobic remineralization of large biomass blooms supported by the upwelling season as well as the retention of water within the bay due to the topology. A Eulerian study was designed to research the daily dynamics of nano-picoplankton throughout the water column at a single site, previously identified as having the lowest oxygen concentrations at depth in autumn (Pitcher and Probyn, 2017). I firstly took an overview look at bulk productivity and nitrogen uptake processes of size fractionated plankton groups, teasing apart the nano-picoplankton into more distinct taxa and size groups, and described the environment in which the plankton operate. The productivity rates, nitrogen uptake rates and nano-picoplankton cell abundances were depth-differentiated over the five-day period, with daily variability not being as distinct. This chapter was a good proof of concept that, in autumn in St. Helena Bay, nano-picoplankton are important in not only the cycling of

nutrients, but also primary production, which is vital for proper ecosystem functioning in the bay.

Microbes were often overlooked when discussing total ecosystem functioning in South African oceanographic research. In Chapter 4, I completed an in-depth description of the taxa that make up the nano-picoplankton fraction, making use of shotgun metagenomic sequencing. Like with productivity rates and cell abundances, nano-picoplankton community structure and potential metabolisms were depth differentiated, with the surface metagenomes different to those found at 25 m and 50 m. There were no significant daily differences in community structure or individual taxa over the five days. Interestingly, in some cases the abundances of transporters found in metagenomes had a good relationship with the associated process rates as measured using stable isotope tracer analyses, pointing to the potential for mixing techniques from different fields to determine ecological roles of the smallest organisms in plankton communities. From the findings of Chapter 3 and 4 it became clear that daily variability in the microbial plankton is much reduced in the absence of strong physical environmental changes.

It was hypothesised that short-term succession of diversity and function of picoplankton and nano-picoplankton will change with the variability that is introduced through the environment, physically, chemically, or biologically. It was found in this thesis that on a daily time scale there is a strong physical-biological coupling in the small plankton, in both upwelling and post-upwelling season. Furthermore, I confirmed that the position of taxa in the water column is connected to their metabolic potential in the context of the surrounding environment.

Based on the data obtained during this thesis, it is concluded that the short-term dynamics of picoplankton and nano-picoplankton under the environmental conditions described are primarily controlled by physical variability in the water column. These are some of the first studies to analyse daily changes in picoplankton and nano-picoplankton in the southern Benguela, contributing to the recent increase in marine microbial ecology research occurring in the coastal waters around South Africa.

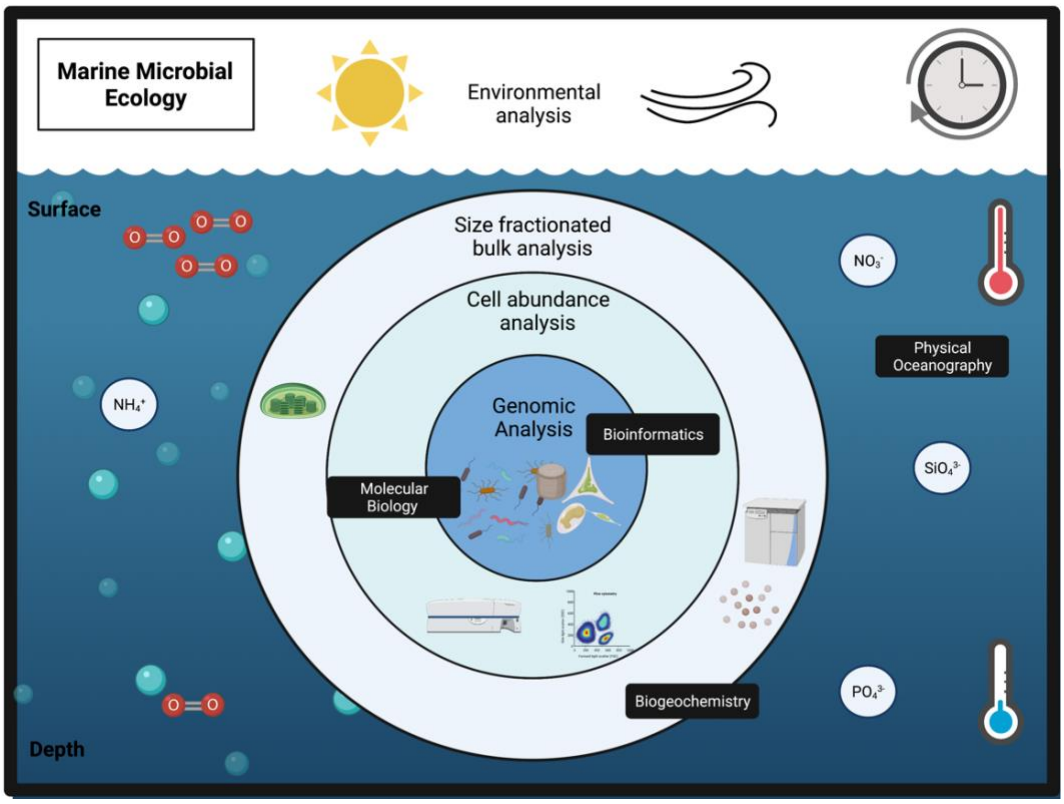

Figure 5.1. A summary figure of the approach taken in this thesis to study marine microbial ecology in St. Helena Bay. To understand the small plankton (nano- and picoplankton including the microorganisms), I first started with understanding the environment. The next layer made use of bulk measurements obtained from size fractionated analyses of chlorophyll *a* concentrations, POM, and uptake rates. The following layer required cell abundance analysis by flow cytometry, to enumerate specific phytoplankton groups identified as important in the bulk measurements. Finally, genetic analysis was used to identify taxa and potential functionality associated with the nano- and picoplankton found in different environments like active upwelling (represented by the bubbles) and a stratified water column. The different disciplines applied in this thesis are shown in black boxes. The daily times series (clock) and vertical water column sampling (depth) approach allowed for a dynamic inspection of the microbial ecology in St. Helena Bay. Created with BioRender.com.

5.2. Limitations and considerations of this research

I encountered several limitations and roadblocks in this thesis, as well as potential for improvement. In Chapter 2, the addition of replicated gene libraries on each day and depth would have allowed for stronger statistical power when determining daily changes and changes between upwelling periods or even oxygen

states. The first roadblock was the small amount of biomass collected on some days and depths because of the logistics (time and equipment) of sampling. This biomass was then size fractionated to isolate the picoplankton, creating even less biomass from which to extract DNA. The extraction kit protocols for seawater samples did not extract enough good quality DNA to ensure both 16S and 18S rRNA amplicon sequence analysis for all sampling times and depths. It was after this study that it became clear that planning and understanding the requirements of each step of your research before sampling is vital to truly understand how to sample in order to accurately answer the questions you may have.

The second roadblock was the amount of time and money spent on sequencing. At the time of this research, the cheapest option for sequencing was to outsource the job to a sequencing company overseas. This process was costly and time consuming, taking months for results to be produced. Despite these roadblocks, this study illuminated that picoplankton are present at a high diversity and with multiple metabolisms in an upwelling setting. In fact, highlighting the functional diversity of picoplankton has shown that there is still a lot that is not understood about the role of microorganisms in this ecosystem. Picoplankton were shown to have a negligible contribution to primary production and nitrogen uptake during an upwelling cycle (Burger et al., 2020, Chapter 2), but their presence, with such a diversity of functionalities and all the possible interactions among the picoplankton taxa, speaks to a complex microbial loop that is not well understood. At the time of writing this thesis, the results of a microbial grazing experiment, also done during this 10-day sampling period, had not yet been published, so the influence of grazing or even viruses on shaping the picoplankton community were not considered in this thesis. Furthermore, the results of the grazing experiment were not easily relatable to the findings in this thesis and without extensive additional analysis could not be used to interpret the results.

Results from Chapter 3 and 4 came from the same overarching project, describing short-term nano-picoplankton dynamics through different lenses. The limitation of this project was primarily logistical. The sampling strategy was designed based on the equipment available and the time it takes to filter seawater. This limited the design of the project, but ultimately the best outcome was obtained working within the scope of available resources. The design of this project stemmed from the notion

that there is more than one way to study microbial ecology in the marine environment, meaning that a truly interdisciplinary approach was required. The roadblock in this approach was the time it took to grasp the required information from each discipline to design a project that would sufficiently describe the broader role of nano-picoplankton in the productivity of the system as well as allow for a focused description of specific taxa or groups of taxa and their potential functionality.

In Chapter 4 the roadblocks lay in the laboratory. As in Chapter 2, extraction of the gDNA was a bottleneck step that required much troubleshooting to get enough good quality DNA for Illumina shotgun metagenomic analysis. In some metagenomics studies to date, separate 16S rRNA amplicon sequencing is done to determine relative taxonomic abundances (Reji et al., 2020). This is to make up for the loss of reads during the assembly and quality control steps of metagenomic analysis. In this study I was unable to include amplicon sequencing for each sample and, because of the quality control step in the Mgnify v.5 pipeline, which has a contig length cut off of 500 base pairs, discarded more than 90% of the assembled contigs (Mitchell et al., 2019). Therefore, I needed an alternative method to get a more accurate representation of the diversity present in the metagenomes. To this end, I adopted a modified approach of using metagenomic 16S rDNA Illumina tags as an alternative to amplicon sequencing, where 16S and 18S rRNA sequences are extracted from the raw metagenomic reads and classified (Logares et al., 2014). The MGnify portal was used to analyse the short Illumina raw reads before assembly through the same pipeline (v.5.0) as the assembled metagenomes. The length of raw reads cut off during quality control were all those with fewer than 100 base pairs, allowing for better taxonomic classifications from the metagenomes. The disadvantage of short read sequencing for metagenomes is that the assembly becomes difficult, depending on the program that is used and quality of the data, and reads are lost when they cannot be assembled into contigs. The caveat to Chapter 4, is that it is perhaps not a true reflection of nano-picoplankton diversity and function because of the variability and read loss introduced in the chosen DNA extraction protocols, sequencing methodology, metagenome assembly method and quality control steps. However, it is a good approximation of the microbial dynamics of this coastal region over this five-day period in autumn. Perhaps not a limitation but a consideration is that a more hands on metagenomic bioinformatic analysis would have produced additional data that could have added another layer of understanding of

the role of specific taxa in the stratified water column. However, the free assembly and analysis service offered by Mgnify allows for standardisation, which opened the possibility of comparing the metagenomes from this study to those from other studies.

The main limitation of this project was the exclusion of data pertaining to predation by larger zooplankton and the effect of viruses on nano-picoplankton community dynamics. Marine viruses are the most abundant biological entities in the ocean and their role in the maintenance of planktonic community diversity should be considered, especially in terms of carbon and nutrient cycling in the microbes (Bergh et al., 1989; Fuhrman and Suttle, 1993; Bratbak et al., 1994, 1996).

The overall limitations of the studies in this thesis were that they were only snap shots from single stations during an upwelling cycle in Elands Bay and a stratified water column in St. Helena Bay. The Eulerian approach is limited in that samples from different water masses may be sampled on the consecutive days. Ideally a Langerian approach would be used by sampling the same water mass over time, although this process may be more feasible during Autumn and Winter when the water column is stratified and not continuously mixing. This approach, however, is logistically not feasible. Capturing more data across both bays at the time of sampling would have given a larger overview of the entire ecosystem. However, since this thesis was focused on the dynamics of nano-picoplankton rather than bay ecosystem functioning, the findings are valuable and should inform future studies describing microbial communities in the southern Benguela; there are still many unanswered questions about the full range of ecological and biogeochemical processes and the roles of different microbial taxa or functional groups in this productive ecosystem.

5.3. Future research and questions that should be answered

From this thesis a host of future research possibilities and questions arose, including suggestions on how to improve each study. The thesis explores a very specific scale in time and space, meaning that in future studies there is an opportunity to expand and condense this scale. Daily changes in microbial communities probably depend on more than just the physical environment at different spatial and time scales. The variability in plankton community structure and function might not be at the daily scale, but rather in the diel cycle (Gilbert et al., 2010; Aylward et al., 2017; Hu et al., 2018) or at a daily scale but under different conditions like a blooming event

(Needham and Fuhrman, 2016; Choi et al., 2018). Alternatively, patterns of community variability could show up more clearly on a weekly timescale. Comparing different timescales could explain more about the ecosystem functioning of the picoplankton and nano-picoplankton in the southern Benguela. Apart from different time scales, additional environmentally-relevant sampling depths should be added to studies, such as the chlorophyll maximum, the fluorescence maximum and the oxycline, where differences in microbial dynamics compared to other depths would be expected.

Future studies could benefit from the addition of more biotic variables, namely the enumeration and identification of grazers from larger size-fractions and viruses. Grazing has been shown to influence the community structure of communities of small plankton (McManus et al., 2007; Jürgens and Massana, 2008; Rocke et al., 2015). Viruses can play a huge role in shaping community structure (Gobler et al., 2008; Cram et al., 2016; Våge et al., 2016; Middelboe and Brussaard, 2017), yet very little is known about the virus populations in coastal waters of South Africa, specifically in the southern Benguela. Changes in the virus community composition and structure on a daily timescale in coastal waters would be an important future step in this research. Yeasts were found in enhanced abundances on some sampling days (Chapter 2) and were found to be highly correlated with other picoeukaryotes. The role of marine yeasts in the marine coastal environment is still not understood, and future research could focus on the diversity and role of yeasts in coastal waters, especially during the upwelling season.

One aspect of microbial ecology that was partially explored in this thesis was whether the functional composition of a picoplankton or nano-picoplankton community changed more rapidly than the taxonomic diversity. It would be useful to expand this topic to help understand the ecosystem functions of these small plankton. Nitrogen cycling is a continued focus of much of the coastal research currently happening in the southern Benguela. The addition of molecular (genomic or transcriptomic) data regarding processes like dissimilatory nitrate reduction, denitrification and anammox/comommox, the genes for which were found at depth in Chapter 4 in varying abundances, would enhance the research currently happening regarding the cycling of nitrogen in embayments.

Finally, the expansion of low oxygen zones is a continuous worry in productive regions, including in the southern Benguela. Studying alternative electron acceptors (sulphur, methane, nitrate) for respiration in the low oxygen waters of the southern Benguela, which often occur at the sediment-water column interface, would be an interesting research topic to pursue. The presence of organisms capable of these metabolisms in metagenomes sampled from depth in Chapter 4 supports this research direction.

Future marine microbial studies would be enhanced using alternative equipment, methods, and technologies, a few of which will be discussed below. Beginning at the sampling stage, the addition of an *in-situ* sampler would minimize the logistical problems associated with filtering large volumes of water. This piece of equipment would minimize contamination, increase sample size and volume, and would possibly allow for transcriptomic and metatranscriptomics analyses. Having access to an *in-situ* sampler could change the type and design of future projects. Secondly, a standardised marine gDNA and RNA extraction protocol would allow for better comparisons among studies across the world and minimize expenses associated with extensive trouble shooting. With a limited budget, it is important to start analyses with good source data. Finally, obtaining in-house sequencing equipment, be it long read (®Oxford nanopore; Ion Torrent) or short read (®Illumina), would not only minimize costs over the long run, but also ensure more control over the sequencing portion of the project and the number of samples that can be sequenced. Easy access to this technology would change the way in which marine microbial ecology research could be done in the southern Benguela, allowing for more in depth and focused research on a group of organisms that are vital for the proper functioning of this eastern boundary upwelling region.

This thesis represents some of the first microbial ecology work done in embayments along the southern Benguela. The project focused on interpreting microbial assemblages in the context of their environment and ecological roles, making use of interdisciplinary techniques such as stable isotope tracer analysis, flow cytometry and genomics, both amplicon biomarker sequencing and shotgun metagenomics. Despite the complexity of plankton community dynamics, it is my hope that the importance of the small plankton organisms, and especially the microorganisms, is recognized through this work. I believe the work I have done

throughout this PhD has contributed to building marine microbial ecology as the next exciting and vital research area in South Africa.

6. Supplementary Materials

Table S2.1. Mixed layer depth (m) on each sampling day as calculated according to the criteria set out by de Boyer Montégut et al. (2004).

Sampling Day	Mixed layer depth (m)
Day 1	-
Day 2	-
Day 3	-
Day 4	-
Day 5	-
Day 6	5
Day 7	2.5
Day 8	15
Day 9	10
Day 10	10

Table S2.2. Environmental variables and cell concentrations of *Synechococcus*, *Prochlorococcus* and picoeukaryotes measured for the entire 10-day sampling period at the St. Helena Bay station in November/December 2016.

Sampling depth	Time (Day)	Temperature (°C)	Salinity (PSU)	Chlorophyll *a* ($\mu g.l^{-1}$)	Oxygen ($ml.l^{-1}$)	Nitrite (µM)	Nitrate (µM)	Phosphate (µM)	Ammonium (µM)	Silicate (µM)	POC (µM)	PON (µM)	*Synechococcus* ($cells.ml^{-1}$)	*Prochlorococcus* ($cells.ml^{-1}$)	Picoeukaryotes ($cells.ml^{-1}$)
Surface	Day 1	11.05	34.71	17.34	4.67	0.36	13.69	1.46	0.47	14.33	22.78	4.41	166	9196	2719
	Day 2	11.06	34.71	9.99	4.42	0.40	13.65	1.34	0.88	14.00	42.66	6.27	299	16517	3003
	Day 3	10.31	34.76	4.72	3.21	1.09	17.60	2.12	0.58	38.41	31.11	4.65	197	10096	3525
	Day 4	10.77	34.70	46.89	3.84	4.48	15.21	2.69	0.44	51.30	32.07	5.42	281	12251	3768
	Day 5	11.52	34.51	17.37	4.65	2.69	9.88	3.87	0.44	43.79	54.56	8.26	162	17561	11260
	Day 6	11.00	34.69	14.75	4.38	0.46	12.01	1.49	0.60	32.54	54.44	8.21	212	17985	12713
	Day 7	11.40	34.70	9.34	7.73	0.08	3.52	1.28	0.17	26.23	70.59	8.93	207	17984	14665
	Day 8	11.83	33.38	11.90	8.24	0.04	2.51	0.81	0.42	17.87	80.46	10.66	311	16177	17491
	Day 9	11.74	34.27	6.95	7.34	0.06	2.85	0.72	0.10	20.64	66.56	9.72	145	11851	9512
	Day 10	10.64	32.93	6.29	5.21	0.23	0.96	1.36	0.21	17.41	65.67	9.38	215	8078	9683
10 m	Day 1	10.09	34.72	4.42	0.76	0.43	18.77	2.40	4.47	29.01	10.39	1.78	97	7943	619
	Day 2	9.04	34.71	4.98	2.65	0.47	24.34	5.05	1.83	34.54	12.92	3.02	885	12902	3279
	Day 3	9.86	34.71	4.07	2.85	0.59	20.00	1.42	0.72	41.04	19.64	7.84	165	13604	3294
	Day 4	9.37	34.73	6.97	1.27	0.46	22.59	2.66	1.28	39.40	25.95	4.24	251	14219	5274
	Day 5	9.49	34.71	8.22	1.44	0.40	22.65	2.08	1.50	37.28	8.65	3.57	96	5158	1290
	Day 6	9.49	34.71	8.24	1.72	0.40	20.48	2.22	1.26	37.57	10.53	2.24	134	6288	1383
	Day 7	9.61	34.70	4.77	2.02	0.35	21.34	2.33	1.27	34.68	11.88	2.37	110	6585	1705
	Day 8	11.09	34.67	12.55	5.21	0.13	5.04	1.43	0.18	23.30	28.57	4.88	189	12519	13421
	Day 9	10.18	34.69	8.22	2.79	0.21	16.84	2.02	1.38	28.75	29.98	5.58	124	9260	4052
	Day 10	9.79	34.46	6.85	2.45	0.30	18.47	2.19	1.06	27.42	37.60	6.29	161	3709	1853

Table S2.3. Taxonomic (phylum, class and family) and functional information of the top 1% (30) representative families in the 16S rRNA dataset. References for function assignments are included.

Phylum	Class	Top 1% representative families	Primary metabolism	Reference
Actinobacteriota	Actinobacteria	*Micrococcaceae*	Chemoheterotrophic	(Dastager et al., 2014)
		Acidothermaceae	Chemoheterotrophic/chemolithoautotrophic	(Berry et al., 2014)
Bacteroidota	Bacteroidia	*Flavobacteriaceae*	Chemoheterotrophic	(Bernardet and Nakagawa, 2006)
		Saprospiraceae	Chemoheterotrophic	(McIlroy et al., 2014)
		Cryomorphaceae	Chemoheterotrophic	(Bowman, 2014)
		NS11-12_marine_group	Photoheterotrophic/Chemoheterotrophic	(Kämpfer, 2015)
		NS9_marine_group	Chemoheterotrophic	(Bernardet and Nakagawa, 2006)
		Muribaculaceae	Chemoheterotrophic	(Lagkouvardos et al., 2019)
Crenarchaeota	Nitrososphaeria	*Nitrosopumilaceae*	Chemolithoautotrophic	(Könneke et al., 2005)
Firmicutes	Bacilli	*Staphylococcaceae*	Chemoheterotrophic	(Lory, 2014)
		Lactobacillaceae	Chemoheterotrophic	(Dicks and Endo, 2014)
		Sporolactobacillaceae	Chemoheterotrophic	(Chang and Stackebrandt, 2014)
Firmicutes	Clostridia	*Lachnospiraceae*	Chemoheterotrophic	(Stackebrandt, 2014)
Proteobacteria	Alphaproteobacteria	*Rhodobacteraceae*	Photoheterotrophic/Chemoheterotrophic/Photoautotrophic	(Pujalte et al., 2014)
		SAR11_clade _1	Chemoheterotrophic	(Sun et al., 2011)
Proteobacteria	Gammaproteobacteria	*Thioglobaceae*	Chemolithoautotrophic	(Glaubitz et al., 2013)

Table S2.3. Continued.

Phylum	Class	Top 1% representative families	Primary metabolism	Reference
Proteobacteria	Gammaproteobacteria	*Porticoccaceae*	Photoheterotrophic	(Spring et al., 2015)
		Halieaceae	Photoheterotrophic	(Spring et al., 2015)
		OM182_clade	Photoheterotrophic	(Spring et al., 2015)
		Oxalobacteraceae	Chemoheterotrophic	(Baldani et al., 2014)
		SAR86_clade_fa	Photoheterotrophic	(Dupont et al., 2012)
		Pseudoalteromonadaceae	Chemoheterotrophic	(Ivanova et al., 2014)
		Halomonadaceae	Chemoheterotrophic	(de la Haba et al., 2014))
		Shewanellaceae	Chemoheterotrophic	(Satomi, 2014)
		Pseudohongiellaceae	Chemoheterotrophic	(Xu et al., 2016)
		Moraxellaceae	Chemoheterotrophic	(Teixeira and Merquior, 2014)
		Enterobacteriaceae	Chemoheterotrophic	(Octavia and Lan, 2014))
		Pseudomonadeaceae	Chemoheterotrophic	(Palleroni, 1981)
Thermoplasmatota	Thermoplasmata	*Marine_Group_II_fa*	Photoheterotrophic/Chemoheterotrophic	(Iverson et al., 2012)
Verrucomicrobiota	Verrucomicrobiae	*Rubritaleaceae*	Chemoheterotrophic	(Yoon et al., 2008)

Table S2.4. The relevant traits used to assign function to the top 46 Picoeukaryote families as adapted from the functional traits of marine protist resource (Ramond et al. 2018).

Function	Relevant Traits						
	Ingestion	**Symbioses**	**Motility**	**Cell Cover**	**Chloroplast**	**Trophy**	**Colonality**
Parasites	Parasite	Myzocytotic	Attached	Naked			
Strict-Heterotrophs	Phagotrophic or Myzocytotic				No		
Saprobes	Saprotrophic and osmotrophic						
Swimmer-phototrophs			Swimmer	Organic/Naked	Yes	Phototrophy (has chloroplasts) and mixotrophic	
Floater-phototrophs			Floater	Siliceous	Yes	Phototrophy (has chloroplasts) and mixotrophic	
Colonial-phototrophs			Floater		Yes	Strict phototrophy	Form colonies

Table S2.5. The functional grouping assignments of the top 46 picoeukaryote families based on the trait assignments in Table S2.2.

Picoeukaryote family	**Function**
Polar-centric-Mediophyceae	Floating phototrophic and/or mixotrophic
Bathycoccaceae	Floating phototrophic and/or mixotrophic
Eutintinnidae	Heterotrophic
Strombidiidae_H	Heterotrophic
Strombidiida_unclassified	Heterotrophic
Strombidiidae_R	Heterotrophic
Leegaardiellidae_B	Heterotrophic
Protaspa-lineage	Heterotrophic
Strombidiidae_M	Heterotrophic
MAST-7B_X	Heterotrophic
Filosa-Thecofilosea_XX	Heterotrophic
MAST-12E_X	Heterotrophic
Hypotrichia_X	Heterotrophic
Thigmophryidae	Heterotrophic
Picozoa_XXX	Heterotrophic
Vampyrellida_X	Heterotrophic
Minorisa-lineage	Heterotrophic
Strombidiida_F_X	Heterotrophic
Ventricleftida_X	Heterotrophic
Strombidiidae_L	Heterotrophic
Cryothecomonas-lineage	Heterotrophic
Dino-Group-I-Clade-1	Parasitic
Dino-Group-II-Clade-30	Parasitic

Table S2.5. Continued.

Picoeukaryote family	Function
Pirsonia_Clade_XX	Parasitic
Dino-Group-II-Clade-6	Parasitic
Dino-Group-II_unclassified	Parasitic
Dino-Group-II-Clade-1	Parasitic
Saccharomycetales	Saprophytic and/or Parasitic
Cystobasidiomycetes	Saprophytic and/or Parasitic
Exobasidiomycetes	Saprophytic and/or Parasitic
Agaricomycetes	Saprophytic and/or Parasitic
Eurotiomycetes	Saprophytic and/or Parasitic
Gymnodiniaceae	Swimming phototrophic and/ or mixotrophic
Mamiellaceae	Swimming phototrophic and/ or mixotrophic
Chrysochromulinaceae	Swimming phototrophic and/ or mixotrophic
Cryptomonadales_X	Swimming phototrophic and/ or mixotrophic
Chlorellales_X	Swimming phototrophic and/ or mixotrophic
Phaeocystaceae	Swimming phototrophic and/ or mixotrophic
Pedinellales	Swimming phototrophic and/ or mixotrophic
Noelaerhabdaceae	Swimming phototrophic and/ or mixotrophic
Dolichomastigaceae	Swimming phototrophic and/ or mixotrophic
Chrysophyceae_Clade-C	Swimming phototrophic and/ or mixotrophic
Prasiolales_X	Swimming phototrophic and/ or mixotrophic
Chrysophyceae_Clade-H	Swimming phototrophic and/ or mixotrophic
Dinophyceae_unclassified	Unknown
Eukaryota_unclassified	Unknown

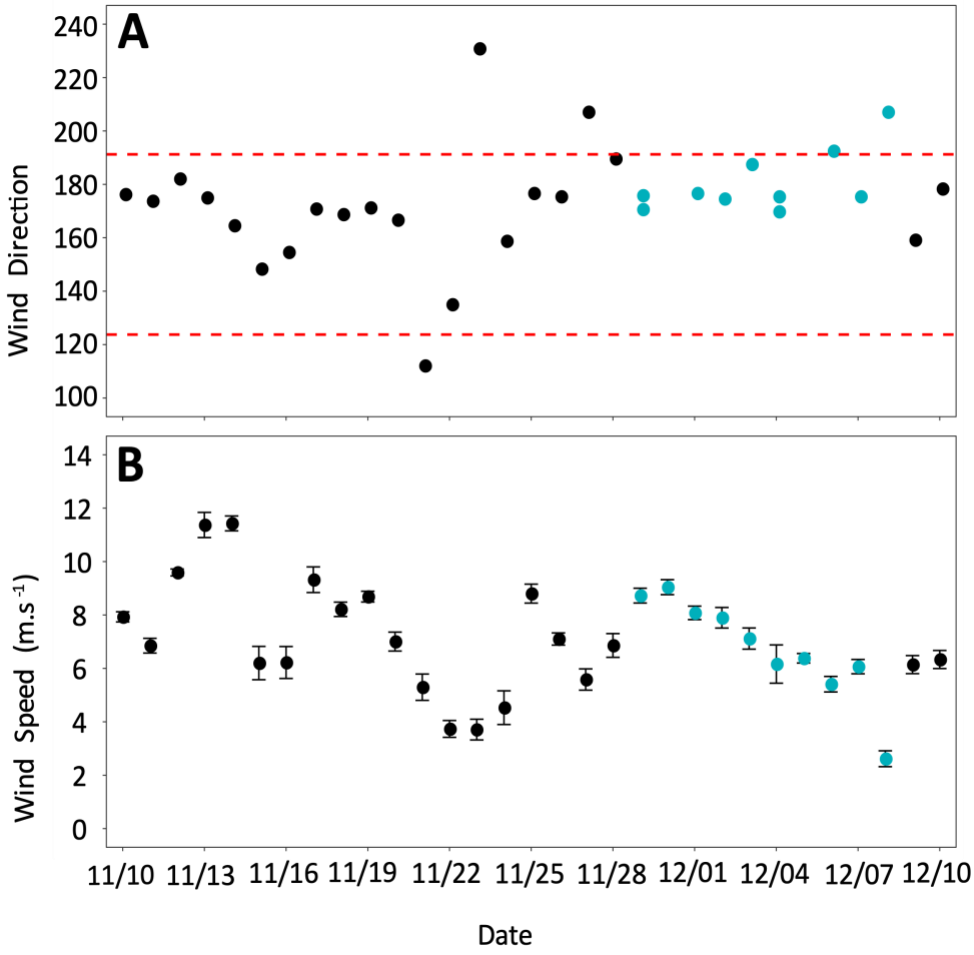

Figure S6.1. Wind data for St. Helena Bay from 10 November–10 December 2016. The data points that fall within the sampling period for this study are shown in turquoise. (A) Daily average (n=24 hours) wind direction in degrees clockwise from true north. South easterly (123.75˚) and southerly (191.4˚) wind directions, as defined by the South African Weather Service, are indicated by the red dashed lines; wind directions that fall between these lines are from the south or south east. (B) Mean (±SE) daily (n=24 hours) wind speeds ($m.s^{-1}$).

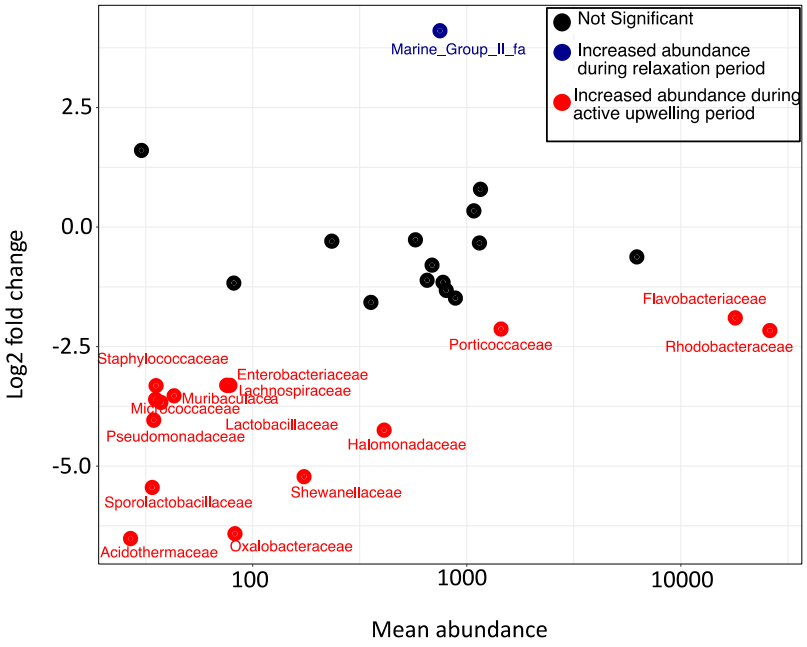

Figure S6.2. Dfferential abundance of the top 30 bacterioplankton families was determined using DESeq2 between the active upwelling and relaxation period. The significantly differentially abundant bacterioplankton families between the active upwelling and relaxation period are shown. Blue labeled families are upregulated (increased abunance) during the relaxation period while red labels indicate familes that are down regulated during relaxation and therfore increase in abundance during active upwelling.

Table S2.6. Similarity percentage (SIMPER) contribution and cumulative contribution (%) of bacterioplankton families between upwelling period, water types and oxygen states.

	Contribution (%)	**Cumulative contribution (%)**
Upwelling vs. Relaxation		
Rhodobacteraceae	28	28
Flavobacteriaceae	17	45
Nitrosopumilaceae	44	61
Cryomorphaceae	23	67
Marine_Group_II_fa	47	71
Oxic vs Low oxygen		
Rhodobacteraceae	27	27
Nitrosopumilaceae	20	47
Flavobacteriaceae	20	67
Halomonadaceae	5	72
Mixed vs UML		
Rhodobacteraceae	27	27
Nitrosopumilaceae	18	45
Flavobacteriaceae	17	62
Thioglobaceae	6	68
Halomonadaceae	5	73
Mixed vs BL		
Rhodobacteraceae	28	28
Flavobacteriaceae	18	46
Nitrosopumilaceae	13	60
Halomonadaceae	7	66
Halieaceae	4	70
UML vs BL		
Nitrosopumilaceae	26	26
Rhodobacteraceae	23	49
Flavobacteriaceae	20	69
Thioglobaceae	7	75

Table S2.7. Similarity percentage (SIMPER) contribution and cumulative contribution (%) of bacterioplankton family functions between upwelling period, water types and oxygen states.

	Contribution (%)	**Cumulative contribution (%)**
Upwelling vs. Relaxation		
Photoheterotrophic/Chemoheterotrophic	36	36
Chemolithoautrophic	30	66
Photoheterotrophic/Chemoheterotrophic/Photoautotrophic	16	82
Oxic vs Low oxygen		
Chemolithoautrophic	35	35
Photoheterotrophic/Chemoheterotrophic	25	60
Photoheterotrophic/Chemoheterotrophic/Photoautotrophic	21	81
Mixed vs UML		
Photoheterotrophic/Chemoheterotrophic	36	36
Chemolithoautrophic	29	65
Photoheterotrophic/Chemoheterotrophic/Photoautotrophic	17	82
Mixed vs BL		
Photoheterotrophic/Chemoheterotrophic	36	36
Chemolithoautrophic	31	67
Photoheterotrophic/Chemoheterotrophic/Photoautotrophic	15	82
UML vs BL		
Chemolithoautrophic	54	54
Photoheterotrophic/Chemoheterotrophic/Photoautotrophic	15	69
Photoheterotrophic/Chemoheterotrophic	15	84

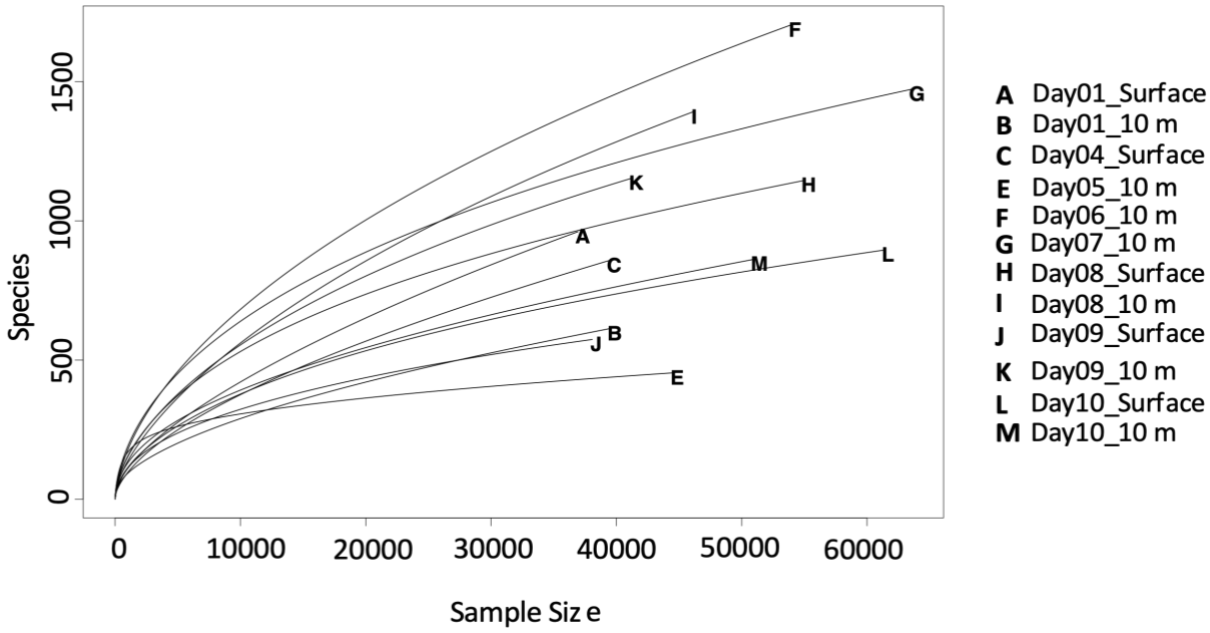

Figure S6.3. Rarefaction curves of the 12 samples from which 16S rRNA sequencing samples were taken. Each letter denotes the day and depth of sampling.

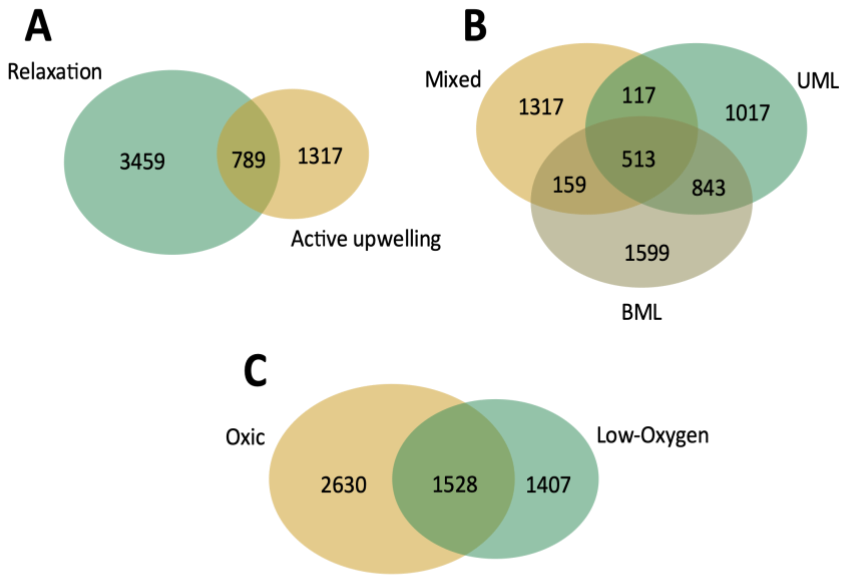

Figure S6.4. Venn diagrams showing the bacterioplankton OTU abundance shared between (A) the active upwelling and relaxation periods, (B) the water column types and the (C) oxygen states.

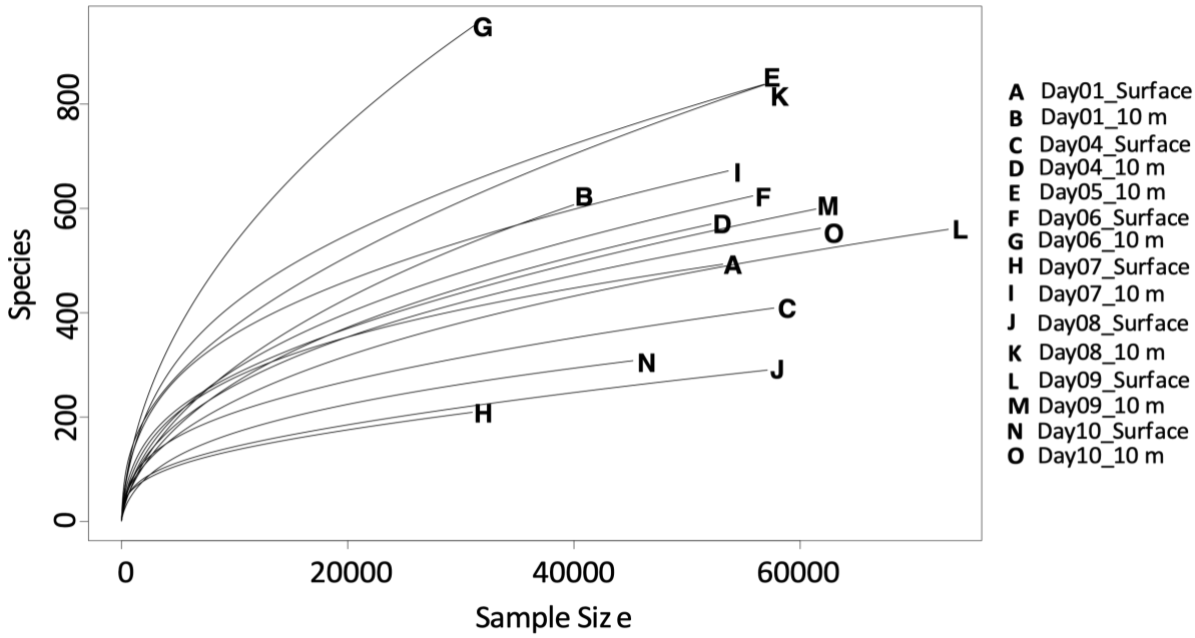

Figure S6.6. Rarefaction curves of the 15 samples from which 18S rRNA sequencing samples were taken. Each letter denotes the day and depth of sampling.

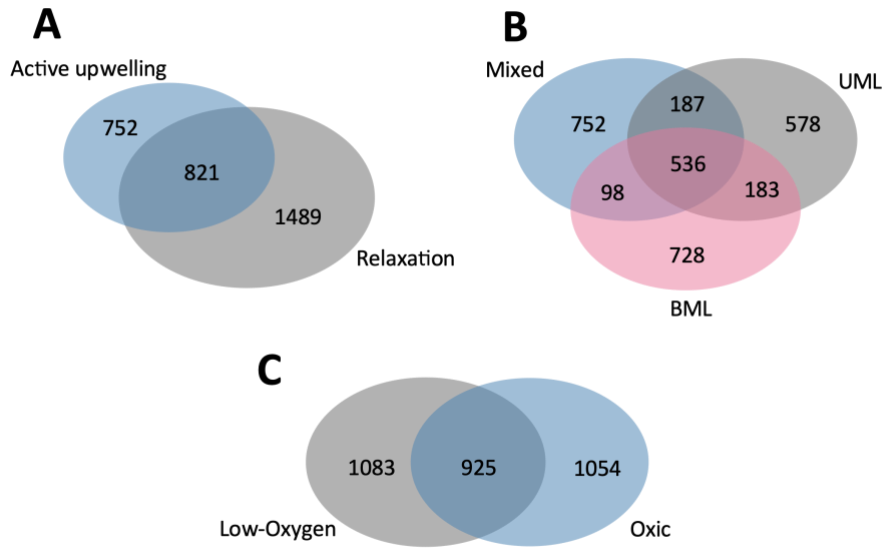

Figure S.6.5. Venn diagrams showing the picoeukaryotes OTU abundance shared between (A) the active upwelling and relaxation periods, (B) the water column types and the (C) oxygen states.

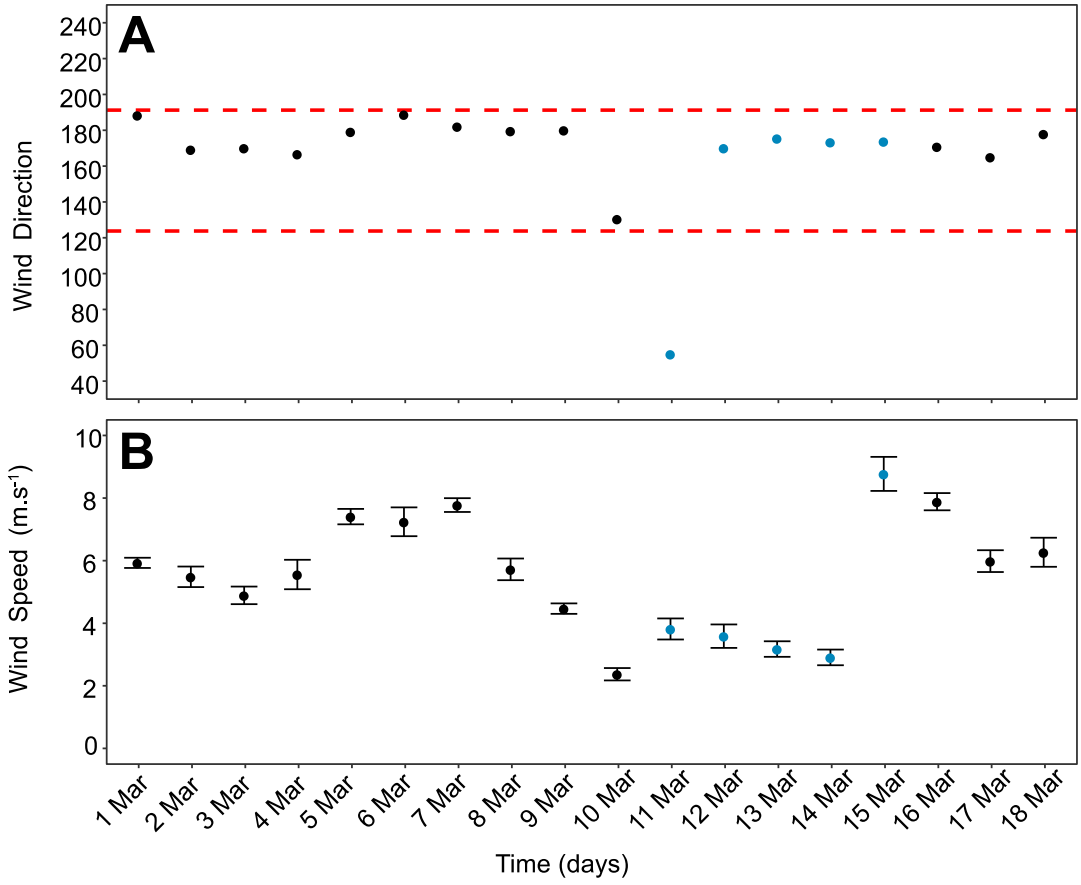

Figure S3.1. Wind data for St. Helena Bay from 1 March–18 March 2018. The data points that fall within the sampling period for this study are shown in turquoise. (A) Daily average (n=24 hours) wind direction in degrees clockwise from true north. South easterly (123.75˚) and southerly (191.4˚) wind directions, as defined by the South African Weather Service, are indicated by the red dashed lines; wind directions that fall between these lines are from the south or southeast. (B) Mean (±SE) daily (n=24 hours) wind speeds ($m.s^{-1}$).

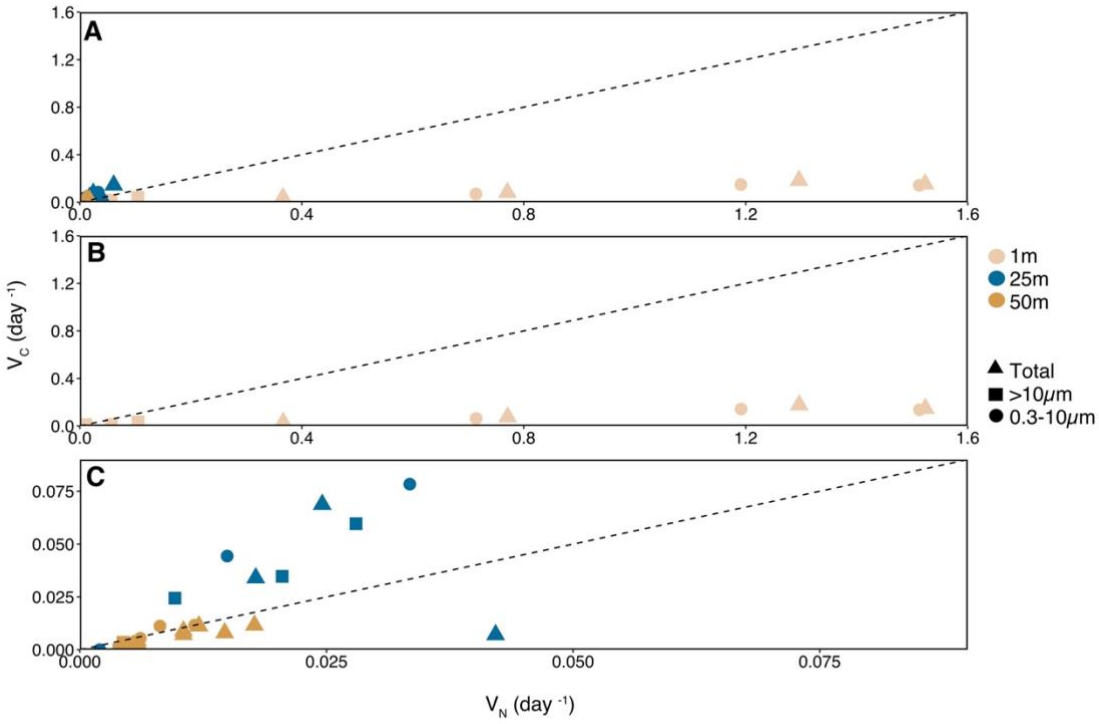

Figure S3.2. Comparison between the specific rate of carbon fixation (V_C; day^{-1}) and the total specific nitrogen uptake rate ($V_N=V_{NO3} + V_{NH4} + V_{UREA}$; day^{-1}) for the total (triangles), >10 µm (squares) and 0.3–10 µm (circles) size fractions at (A) each sampling depth (B) 1 m, (C) 25 m and 50 m. Beige symbols show 1 m samples, blue represents 25 m samples and 50 m samples are in gold.

Table S3.1. Mean, standard deviation (Stdev), minimum and maximum values of nano- and picoplankton abundances (cells.mL^{-1}) and carbon biomass (µgC.L^{-1}) for all 13 samples taken.

Plankton group	Abundance (cells.mL^{-1})		Range, n=13		Biomass (µgC.L^{-1})		Range, n=13	
	Mean	Stdev	Min	Max	Mean	Stdev	Min	Max
SYN	1.58×10^3	1.75×10^3	2.72×10^2	7.13×10^3	0.15	0.16	0.03	0.67
PRO	2.83×10^3	2.40×10^3	4.34×10^1	6.44×10^3	0.10	0.08	0.00	0.23
PICOEUK	4.31×10^3	1.77×10^3	1.78×10^3	8.15×10^3	2.89	1.19	1.19	5.46
NANOEUK	4.37×10^3	4.81×10^3	1.27×10^3	1.51×10^4	5.03	5.54	1.46	17.37
HBAC	4.13×10^4	3.09×10^4	5.31×10^3	9.27×10^4	1.45	1.08	0.19	3.25

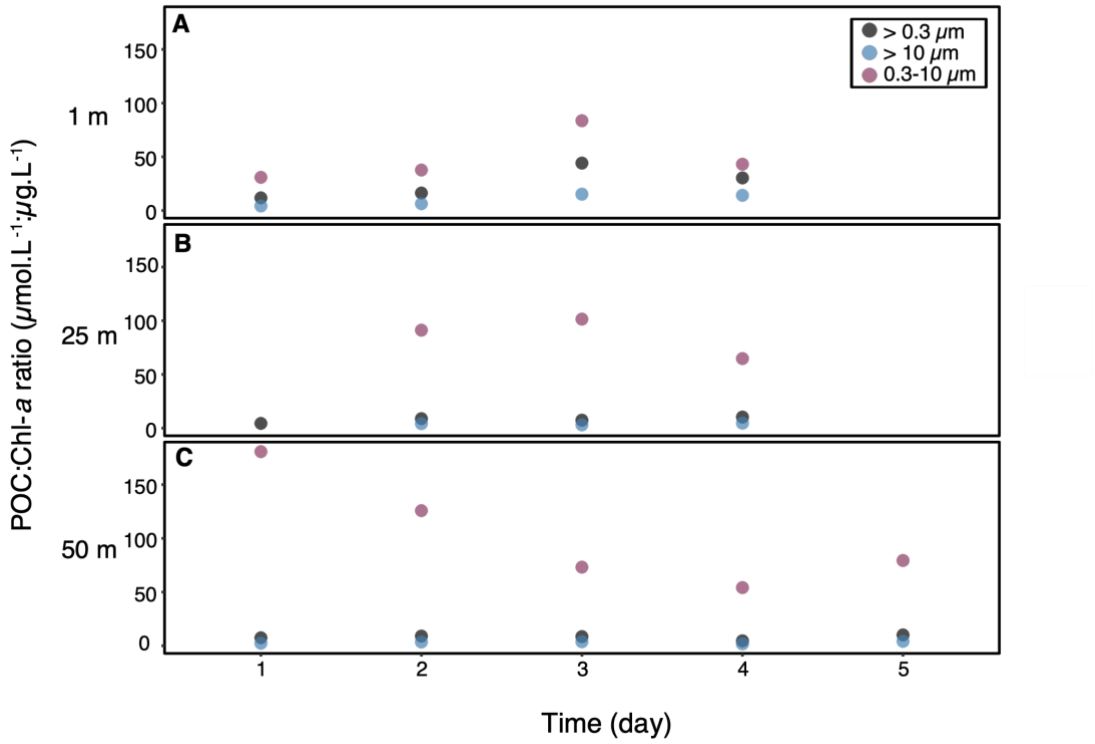

Figure S3.3. Particulate organic carbon (POC) to chlorophyll *a* ratio on each sampling day, for all size categories at A) 1 m, B) 25 m and C) 50 m. Black dots denote total POC (> 0.3 µm), blue dots the > 10 µm size fraction and pink dots the 0.3–10 µm size fraction.

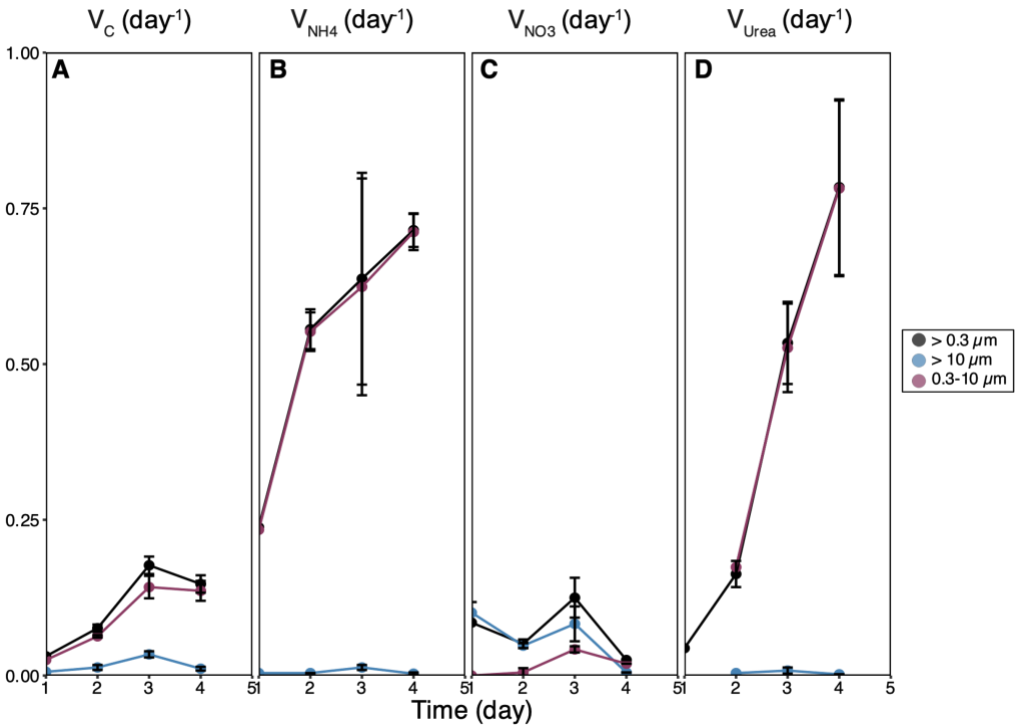

Figure S3.4. The specific uptake rates of A) carbon (V_C), B) ammonium (V_{NH4}), C) nitrate (V_{NO3}) and D) V_{UREA} measured at 1 m for the total plankton (black), >10 µm size fraction (blue) and nano-picoplankton (pink, 0.3–10 µm) over the sampling time. The average rate per day (n=3) and standard deviation are plotted.

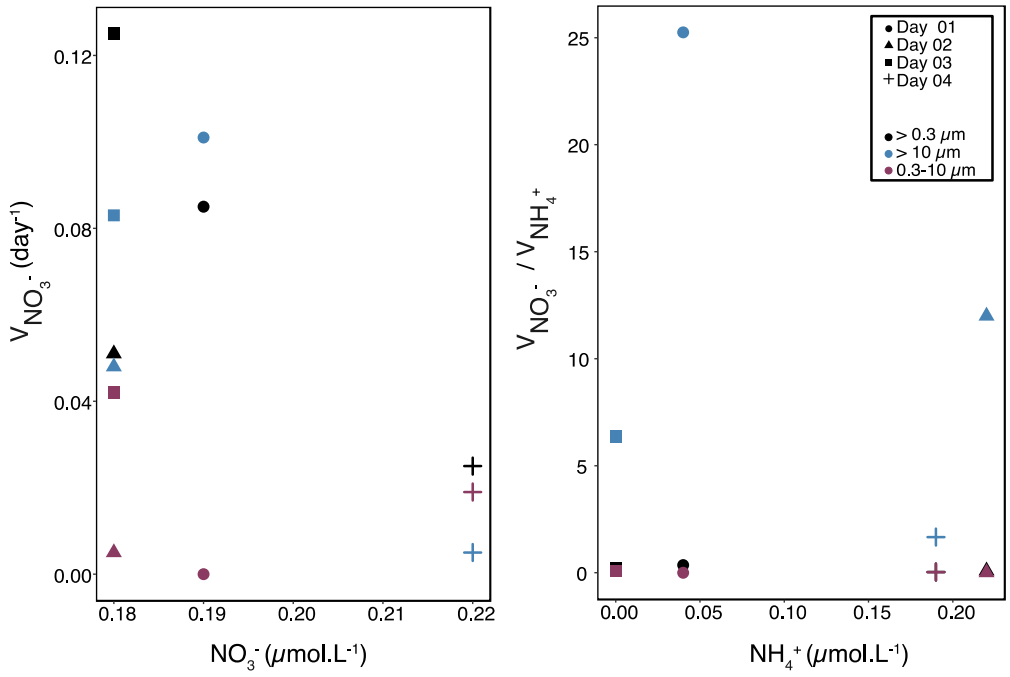

Figure S3.5. A) Specific rate of nitrate uptake (V_{NO3}) as a function of the measured nitrate concentrations and B) specific rate of nitrate uptake (V_{NO3}) normalised to V_{NH4} as a function of the measured ammonium concentrations for surface samples. The different sampling days are denoted by various symbols, with the total plankton in black, the >10 µm size fraction in blue and the nano-and picoplankton (0.3–10 µm) in pink.

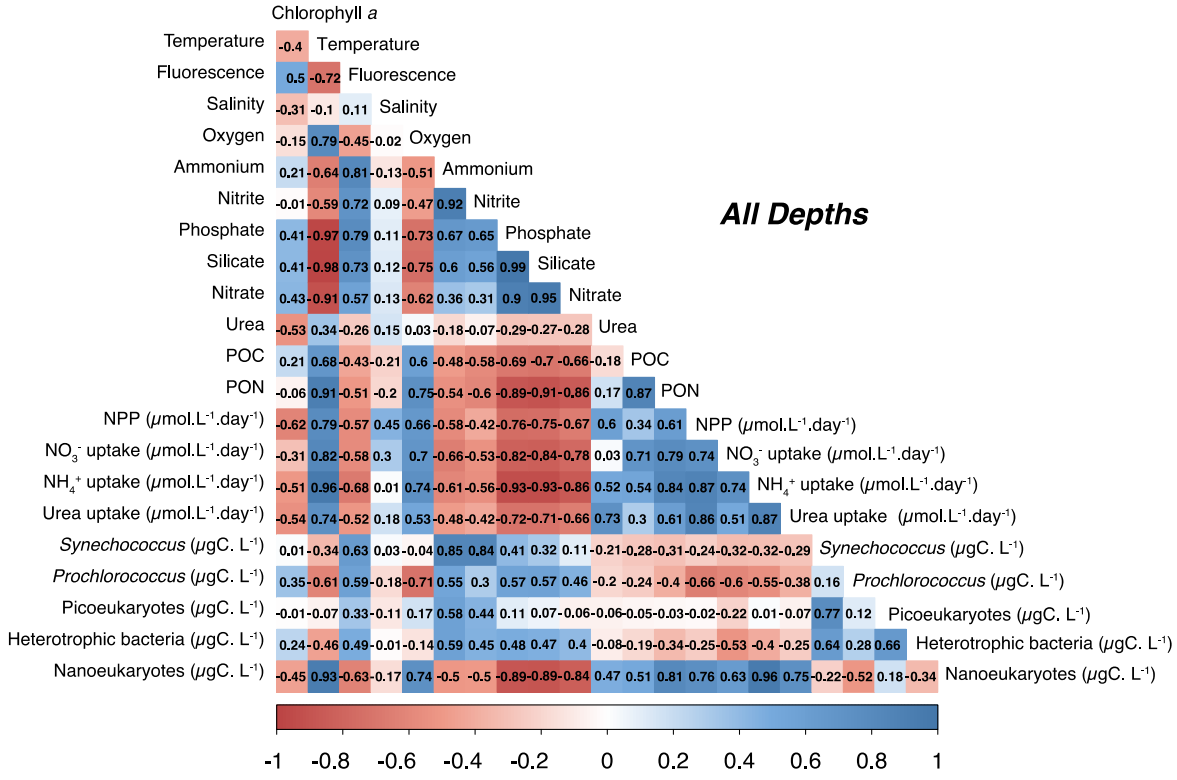

Figure S3.6. Correlation between measured environmental factors across all depths. Redundant variables were dropped from statistical analyses if the correlation was >0.9.

Table S3.2. Results of single factor ANOVAs comparing mean values of variables across three depths for 1) concentrations of inorganic and organic material, 2) uptake rates, 3) cell abundances, 4) carbon biomasses and 5) nitrogen biomasses. The degrees of freedom (DF) and sums of squares (SS) are shown for the influence of depth and the residuals, and the F statistics and resulting probabilities (p). Significant values ($p<0.05$) are shaded.

Variable	DF_{Depth}	$DF_{Residuals}$	SS_{Depth}	$SS_{Residuals}$	F	p
1) Concentrations						
Nitrate	2	36	2483.0	541.8	82.49	0.0001
Ammonium	2	36	3.5	19.9	3.15	0.06
Nitrite	2	36	1.5	2.2	11.94	0.0001
Urea	2	36	0.2	2.2	1.88	0.17
Silicate	2	36	13959.9	625.3	401.88	0.0001
Phosphate	2	36	39.8	3.4	209.60	0.0001
POC	2	22	462.4	1445.0	3.52	0.047
PON	2	22	9.8	5.5	19.38	0.0001
2) Uptake rates						
NPP_{total}	2	22	50.4	21.6	25.65	0.0001
$\rho NO_3^-{}_{total}$	2	22	0.4	0.2	23.38	0.0001
$\rho NH_4^+{}_{total}$	2	22	29.1	2.4	131.44	0.0001
$\rho Urea_{total}$	2	22	14.9	10.0	16.38	0.0001
$NPP_{>10\mu m}$	2	17	0.2	0.1	15.61	0.0001
$\rho NO_3^-{}_{>10\mu m}$	2	20	0.01	0.01	12.91	0.0003
$\rho NH_4^+{}_{>10\mu m}$	2	17	0.00005	0.00008	5.01	0.02
$\rho Urea_{>10\mu m}$	2	18	0.0001	0.0005	1.19	0.33
3) Cell abundances						
Nanoeukaryotes	2	34	4.9	0.5	158.43	0.001
Picoeukaryotes	2	34	0.1	1.2	1.78	0.19
Synechococcus	2	34	2.2	2.3	16.24	0.001
Het bacteria	2	32	2.5	3.1	13.04	0.001
Prochlorococcus	2	34	11.0	9.0	20.78	0.001
4) Carbon biomass						
Nanoeukaryotes	2	34	538.6	472.7	19.37	0.0001
Picoeukaryotes	2	34	13.7	52.7	4.41	0.02
Synechococcus	2	34	0.3	0.8	6.51	0.004
Het bacteria	2	32	13.8	46.4	4.77	0.02
Prochlorococcus	2	34	0.1	0.3	4.84	0.01
5) Nitrogen biomass						
Nanoeukaryotes	2	34	25.5	22.3	19.37	0.0001
Picoeukaryotes	2	34	0.5	2.0	4.41	0.02
Synechococcus	2	34	0.01	0.03	6.51	0.004
Het bacteria	2	32	1.0	3.4	4.77	0.02
Prochlorococcus	2	34	0.01	0.02	4.84	0.01

Table S3.3. Results of single factor ANOVAs comparing mean values of variables across sampling days, separated into the three depths, for 1) concentrations of inorganic and organic material, and 2) uptake rates. The degrees of freedom (DF) and sums of squares (SS) are shown for the influence of day and the residuals, and the F statistics and resulting probabilities (p). Significant values ($p<0.05$) are shaded.

Variable	Depth	DF_{Day}	$DF_{Residuals}$	SS_{Day}	$SS_{Residuals}$	F	p
1) Concentrations							
Nitrate:	1 m	3	8	0.004	0.05	0.25	0.86
	25 m	3	8	347.7	53.7	17.28	0.0007
	50 m	4	10	119.2	21.3	14.00	0.0004
Ammonium:	1 m	3	8	0.2	0.2	2.39	0.15
	25 m	3	8	5.0	9.6	1.37	0.32
	50 m	4	10	1.8	3.2	1.38	0.31
Nitrite:	1 m	3	8	0.01	0.01	2.14	0.17
	25 m	3	8	1.5	0.3	11.44	0.003
	50 m	4	10	0.3	0.04	24.15	0.0001
Urea:	1 m	3	8	0.7	0.7	3.02	0.09
	25 m	3	8	0.3	0.2	4.26	0.045
	50 m	4	10	0.4	0.1	15.96	0.0002
Silicate:	1 m	3	8	0.1	0.03	6.58	0.02
	25 m	3	8	186.1	195.5	2.54	0.13
	50 m	4	10	179.0	64.5	6.94	0.006
Phosphate:	1 m	3	8	0.1	0.3	0.78	0.54
	25 m	3	8	0.6	0.7	2.09	0.18
	50 m	4	10	1.4	0.4	7.72	0.004
POC	1 m	3	3	42.7	6.2	6.90	0.07
	25 m	3	4	156.2	5.5	38.08	0.002
	50 m	4	5	1067.9	166.6	8.01	0.02
PON	1 m	3	3	0.01	0.08	0.14	0.93
	25 m	3	4	2.4	0.04	93.21	0.0004
	50 m	4	5	2.2	0.8	3.73	0.09
2) Uptake rates							
NPP_{total}:	1 m	3	3	15.2	0.7	21.14	0.02
	25 m	3	4	5.2	0.4	16.60	0.01
	50 m	4	5	0.01	0.04	0.19	0.94
$\rho NO_3^-{}_{total}$:	1 m	3	3	0.2	0.02	11.88	0.04
	25 m	3	4	2.19×10^{-5}	6.56×10^{-7}	44.48	0.002
	50 m	4	5	9.16×10^{-7}	4.68×10^{-7}	2.45	0.18
$\rho NH_4^+{}_{total}$:	1 m	3	3	2.1	0.4	5.32	0.10
	25 m	3	4	0.003	0.002	2.33	0.22
	50 m	4	5	0.0001	0.0002	0.96	0.50
$\rho Urea_{total}$:	1 m	3	3	9.3	0.7	14.41	0.03
	25 m	3	4	0.008	0.002	6.71	0.05
	50 m	4	5	0.0004	0.0002	2.20	0.21
$NPP_{>10\mu m}$:	1 m	3	3	0.2	0.02	11.88	0.04
	25 m	2	2	0.1	0.01	12.84	0.07
	50 m	3	4	0.002	0.0002	14.27	0.01
$\rho NO_3^-{}_{>10\mu m}$:	1 m	3	4	0.005	0.0005	15.00	0.01
	25 m	2	3	1.6×10^{-7}	4.7×10^{-7}	5.04	0.11
	50 m	-	-	-	-	-	-
$\rho NH_4^+{}_{>10\mu m}$:	1 m	3	3	2.7×10^{-5}	1.4×10^{-5}	2.02	0.29
	25 m	2	2	3.0×10^{-5}	1.3×10^{-5}	2.26	0.31
	50 m	3	4	1.2×10^{-6}	6.3×10^{-8}	25.92	0.004
$\rho Urea_{>10\mu m}$:	1 m	2	2	8.0×10^{-6}	6.4×10^{-6}	1.26	0.44
	25 m	2	3	8.8×10^{-5}	4.6×10^{-5}	2.84	0.20
	50 m	4	5	3.0×10^{-4}	1.8×10^{-5}	20.44	0.00

Table S3.4. Results of single factor ANOVAs comparing mean values of variables across sampling days, separated into the three depths, for 1) cell abundances, 2) carbon biomasses and 3) nitrogen biomasses. The degrees of freedom (DF) and sums of squares (SS) are shown for the influence of day and the residuals, and the F statistics and resulting probabilities (p). Significant values ($p<0.05$) are shaded.

Variable	Depth	DF_{Day}	$DF_{Residuals}$	SS_{Day}	$SS_{Residuals}$	F	p
1) Cell abundances							
Nanoeuks:	1 m	3	7	0.3	0.008	88.12	0.0001
	25 m	3	8	0.1	0.05	4.75	0.03
	50 m	4	9	0.01	0.06	0.55	0.70
Picoeuks:	1 m	3	7	0.5	0.01	123.93	0.001
	25 m	3	8	0.2	0.1	3.98	0.05
	50 m	4	9	0.3	0.1	12.50	0.001
Synecho.:	1 m	3	7	0.9	0.01	158.13	0.0001
	25 m	3	8	0.9	0.2	15.26	0.001
	50 m	4	9	0.3	0.1	10.56	0.002
Het bact:	1 m	3	7	1.1	0.2	13.31	0.003
	25 m	3	8	0.2	0.3	1.24	0.37
	50 m	4	9	1.2	0.1	21.71	0.0002
Prochloro.:	1 m	3	7	3.9	0.2	39.88	0.0001
	25 m	3	8	4.6	0.1	219.26	0.0001
	50 m	4	9	0.09	0.1	1.99	0.18
2) Carbon biomass							
Nanoeuks:	1 m	3	7	411.7	3.0	320.33	0.0001
	25 m	3	8	2.3	1.9	3.19	0.08
	50 m	4	9	51.7	2.0	57.57	0.0001
Picoeuks:	1 m	3	7	8.8	2.8	7.30	0.02
	25 m	3	8	16.4	13.6	3.22	0.08
	50 m	4	9	10.3	0.8	30.89	0.0001
Synecho.:	1 m	3	7	0.02	0.01	9.66	0.007
	25 m	3	8	0.6	0.2	9.77	0.005
	50 m	4	9	0.03	0.0005	155.67	0.0001
Het bact:	1 m	3	7	9.2	3.8	5.64	0.03
	25 m	3	7	6.3	18.6	0.79	0.54
	50 m	4	8	7.5	1.1	14.10	0.001
Prochloro.:	1 m	3	7	0.06	0.003	54.61	0.0001
	25 m	3	8	0.04	0.0007	136.51	0.0001
	50 m	4	9	0.1	0.03	10.29	0.002
3) Nitrogen biomass							
Nanoeuks:	1 m	3	7	19.5	0.1	320.33	0.0001
	25 m	3	8	0.1	0.1	3.19	0.08
	50 m	4	9	2.4	0.1	57.57	0.0001
Picoeuks:	1 m	3	7	0.3	0.1	7.30	0.02
	25 m	3	8	0.6	0.5	3.22	0.08
	50 m	4	9	0.4	0.03	30.89	0.0001
Synecho.:	1 m	3	7	0.0007	0.0001	9.66	0.007
	25 m	3	8	0.02	0.01	9.77	0.005
	50 m	4	9	0.001	0.00002	155.67	0.0001
Het bact:	1 m	3	7	0.7	0.3	5.64	0.03
	25 m	3	7	0.5	1.4	0.79	0.54
	50 m	4	8	0.6	0.1	14.10	0.001
Prochloro.:	1 m	3	7	0.006	0.0002	54.61	0.0001
	25 m	3	8	0.003	0.00007	136.51	0.0001
	50 m	4	9	0.01	0.002	10.29	0.002

Table S3.5. Results of Tukey multiple comparison tests showing probability values for pairwise comparisons between different depths for mean values of variables showing 1) concentrations of inorganic and organic material, 2) uptake rates, 3) cell abundances, 4) carbon biomasses and 5) nitrogen biomasses. Significant values ($p<0.05$) are shaded.

Variable	1 m vs 25 m	1 m vs 50 m	25 m vs 50 m
1) Concentrations			
Nitrate	0.0001	0.0001	0.70
Ammonium	-	-	-
Nitrite	0.00007	0.01	0.11
Urea	-	-	-
Silicate	0.0001	0.0001	0.69
Phosphate	0.0001	0.0001	0.36
POC	0.04	0.43	0.28
PON	0.00002	0.0001	0.57
2) Uptake rates			
NPP_{total}	0.0001	0.000001	0.23
$\rho NO_3^-{}_{total}$	0.00002	0.0001	0.99
$\rho NH_4^+{}_{total}$	0.0001	0.0001	0.99
$\rho Urea_{total}$	0.002	0.00009	0.99
$NPP_{>10\mu m}$	0.008	0.10	0.0001
$\rho NO_3^-{}_{>10\mu m}$	0.002	0.0005	1.00
$\rho NH_4^+{}_{>10\mu m}$	0.54	0.12	0.02
$\rho Urea_{>10\mu m}$	-	-	-
3) Cell abundances			
Nanoeuks	0.0001	0.0001	0.57
Picoeuks	-	-	-
Synechococcus	0.0001	0.03	0.006
Het. bacteria	0.0001	0.006	0.16
Prochlorococcus	0.07	0.0001	0.008
4) Carbon biomass			
Nanoeuks	0.0001	0.00002	0.85
Picoeuks	0.94	0.07	0.03
Synechococcus	0.01	0.99	0.007
Het. bacteria	0.05	0.97	0.02
Prochlorococcus	0.97	0.05	0.02
5) Nitrogen biomass			
Nanoeuks	0.0001	0.00002	0.85
Picoeuks	0.94	0.07	0.03
Synechococcus	0.01	0.99	0.007
Het. bacteria	0.05	0.97	0.02
Prochlorococcus	0.97	0.05	0.02

Table S3.6. Results of Tukey multiple comparison tests showing probability values for pairwise comparisons between different days for mean values of variables at different depths, showing 1) concentrations of inorganic and organic material, and 2) uptake rates. Significant values ($p<0.05$) are shaded.

Variable		Day 1 vs 2	Day 1 vs 3	Day 1 vs 4	Day 1 vs 5	Day 2 vs 3	Day 2 vs 4	Day 2 vs 5	Day 3 vs 4	Day 3 vs 5	Day 4 vs 5
1) Concentrations											
Nitrate	25 m	0.002	1.00	0.039		0.001	0.11		0.034		
	50 m	0.019	0.087	0.11	0.91	0.0003	0.79	0.07	0.001	0.024	0.36
Nitrite	25 m	0.002	0.50	0.16		0.01	0.047		0.79		
	50 m	0.0004	0.04	0.00006	0.45	0.05	0.51	0.004	0.004	0.45	0.0004
Urea	25 m	0.86	0.04	0.26		0.12	0.63		0.57		
	50 m	0.001	0.005	0.0002	0.11	0.88	0.58	0.08	0.19	0.3	0.008
Silicate	1 m	0.21	0.99	0.19		0.13	0.01		0.29		
	50 m	0.55	0.01	0.68	0.98	0.12	0.99	0.30	0.09	0.005	0.40
Phosphate	50 m	0.02	0.008	0.10	0.94	0.97	0.84	0.06	0.49	0.02	0.29
POC	25 m	0.80	0.054	0.002		0.12	0.003		0.016		
	50 m	0.14	0.025	0.042	0.026	0.46	0.74	0.47	0.97	1.00	0.98
PON	25 m	0.020	0.006	0.0003		0.31	0.001		0.003		
2) Uptake rates											
NPP_{total}	1 m	0.37	0.02	0.06		0.03	0.15		0.15		
	25 m	0.56	0.009	0.38		0.02	0.97		0.03		
$\rho NO_3^-{}_{total}$	1 m	0.45	0.48	0.16		0.08	0.49		0.03		
	25 m	0.88	0.003	0.87		0.004	0.52		0.002		
$\rho Urea_{total}$	1 m	0.82	0.11	0.04		0.14	0.04		0.29		
$NPP_{>10\mu m}$	1 m	0.89	0.009	1.00		0.006	0.82		0.005		
	50 m					0.03	0.30	0.01	0.15	0.76	0.06
$\rho NO_3^-{}_{>10\mu m}$	1 m	0.06	0.30	0.01		0.37	0.20		0.04		
$\rho NH_4^+{}_{>10\mu m}$	50m					0.68	0.02	0.005	0.05	0.009	0.21
$\rho Urea_{>10\mu m}$	50m	0.004	0.005	0.005	0.004	1.00	1.00	1.00	1.00	0.99	1.0

Table S3.7. Results of Tukey multiple comparison tests showing probability values for pairwise comparisons between different days for mean values of variables at different depths, showing 1) cell abundances, 2) carbon biomasses, and 3) nitrogen biomasses. Significant values ($p<0.05$) are shaded.

Variable		Day 1 vs 2	Day 1 vs 3	Day 1 vs 4	Day 1 vs 5	Day 2 vs 3	Day 2 vs 4	Day 2 vs 5	Day 3 vs 4	Day 3 vs 5	Day 4 vs 5
1) Cell abundances											
Nanoeukaryotes	1 m	0.0001	0.0004	0.0001		0.007	0.12		0.02		
	25 m	0.21	0.99	0.44		0.30	0.02		0.32		
Picoeukaryotes	1 m	0.0001	0.0001	0.0001		0.0001	0.0008		0.57		
	50 m	1.00	0.002	0.07	0.74	0.002	0.05	0.62	0.35	0.01	0.31
Synechococcus	1 m	0.0001	0.0004	0.003		0.00001	0.00001		0.56		
	25 m	0.002	0.86	0.95		0.004	0.003		0.99		
	50 m	0.17	0.03	0.79	0.56	0.001	0.05	0.02	0.24	0.25	1.00
Het bacteria	1 m	0.19	0.12	0.06		0.007	0.66		0.003		
	50 m	0.98	0.0008	0.001	0.37	0.001	0.002	0.63	0.99	0.005	0.009
Prochlorococcus	1 m	0.0003	0.009	0.001		0.004	0.16		0.003		
	25 m	0.18	0.0001	0.0001		0.0001	0.0001		0.002		
2) Carbon biomass											
Nanoeukaryotes	1 m	0.0001	0.0001	0.0001		0.0001	0.006		0.003		
	50 m	0.0001	0.0001	0.0001	0.0001	0.99	1.00	1.00	0.98	1.00	0.99
Picoeukaryotes	1 m	0.17	0.29	0.58		0.01	0.04		0.97		
	50 m	0.0001	0.85	0.10	0.006	0.0001	0.003	0.13	0.33	0.002	0.08
Synechococcus	1 m	0.73	0.05	0.06		0.01	0.02		1.00		
	25 m	0.008	1.00	1.00		0.01	0.01		1.00		
	50 m	0.0001	0.001	0.0001	0.0001	0.0001	0.0001	0.0001	0.008	0.009	0.98
Het. bacteria	1 m	0.09	0.02	0.39		0.72	0.82		0.34		
	50 m	0.002	1.00	1.00	0.03	0.005	0.005	0.30	1.00	0.05	0.06
Prochlorococcus	1 m	0.0001	0.0001	0.0007		0.66	0.30		0.08		
	25 m	0.003	0.0001	0.0001		0.0001	0.0001		0.83		
	50 m	0.01	0.04	0.04	0.001	0.92	0.99	0.41	1.00	0.14	0.33
3) Nitrogen biomass											
Nanoeukaryotes	1 m	0.0001	0.0001	0.0001		0.0001	0.006		0.003		
	50 m	0.0001	0.0001	0.0001	0.0001	0.99	1.00	1.00	0.98	1.00	0.99
Picoeukaryotes	1 m	0.17	0.29	0.58		0.01	0.04		0.97		
	50 m	0.0001	0.85	0.10	0.006	0.0001	0.003	0.13	0.33	0.002	0.08
Synechococcus	1 m	0.73	0.05	0.06		0.01	0.02		1.00		
	25 m	0.008	1.00	1.00		0.01	0.01		1.00		
	50 m	0.0001	0.001	0.0001	0.0001	0.0001	0.0001	0.0001	0.008	0.009	0.98

Table S3.7. Continued.

Variable		Day 1 vs 2	Day 1 vs 3	Day 1 vs 4	Day 1 vs 5	Day 2 vs 3	Day 2 vs 4	Day 2 vs 5	Day 3 vs 4	Day 3 vs 5	Day 4 vs 5
Het bacteria	1 m	0.09	0.02	0.39		0.72	0.82		0.34		
	50 m	0.002	1.00	1.00	0.03	0.005	0.005	0.30	1.00	0.05	0.06
Prochlorococcus	1 m	0.0001	0.0001	0.0007		0.66	0.30		0.08		
	25 m	0.003	0.0001	0.0001		0.0001	0.0001		0.83		
	50 m	0.01	0.04	0.04	0.002	0.92	0.99	0.41	1.00	0.14	0.33

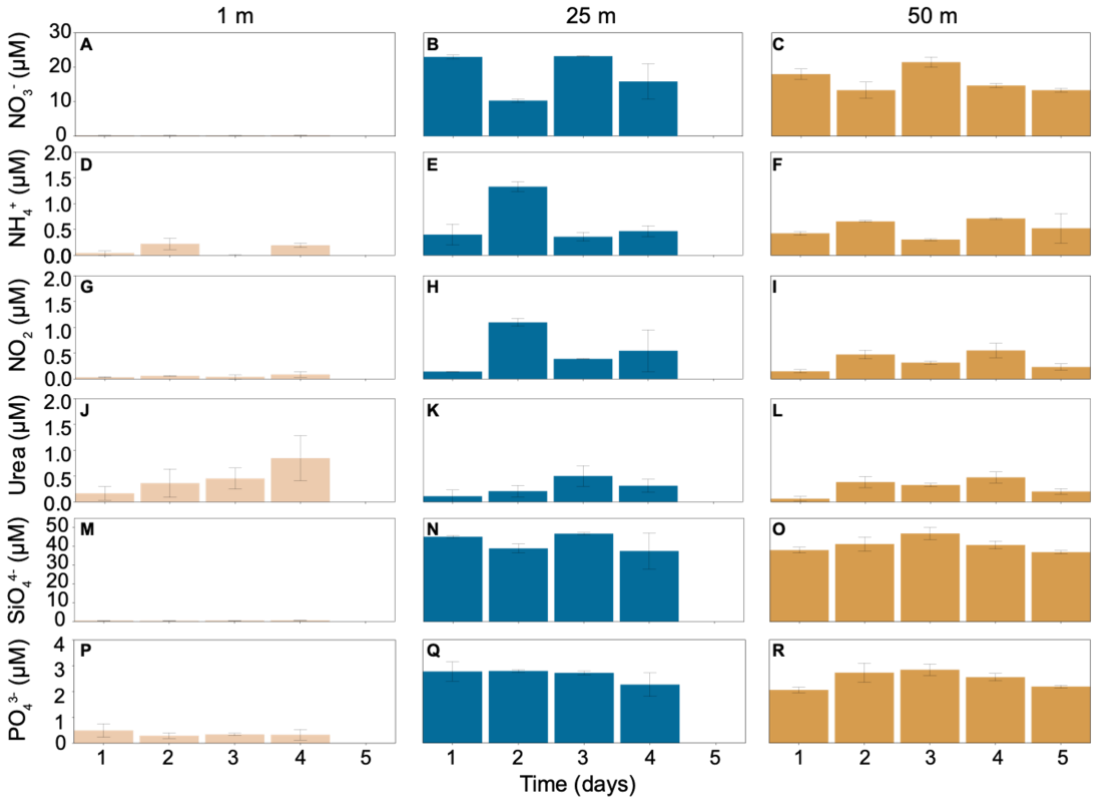

Figure S4.1. Nutrient concentrations at three depths from a station in St. Helena Bay in March 2018. The measured nutrients include (A–C) nitrate (NO_3^- (µM)), (D–F) ammonium (NH_4^+ (µM)), (G–I) nitrite (NO^2 (µM)), (J–L) urea (µM), (M–O) silicate (SiO_4^{4-} (µM)), and (P-R) phosphate (PO_4^{3-}). Error bars indicate the standard deviation. On day 5 there were no nutrients measured at 1 m and 25 m.

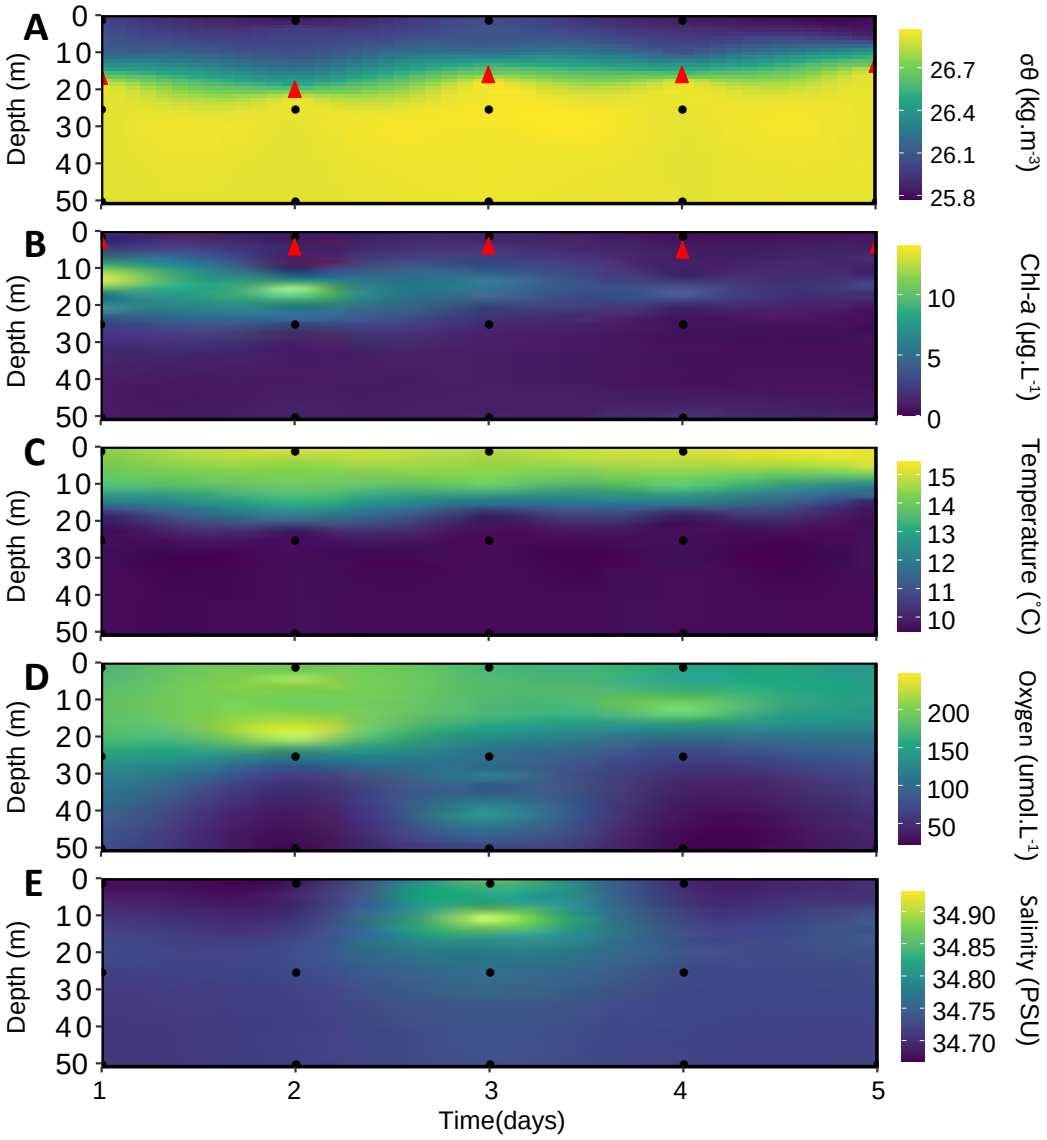

Figure S4.2. Profiles of the water column in St. Helena Bay in March 2018 showing potential density anomaly σθ (A; ($kg.m^{-3}$)), chlorophyll-a concentrations (B; $\mu g.L^{-1}$), temperature (C; ˚C), oxygen concentrations (D; $\mu mol.L^{-1}$) and salinity (E, PSU). Black dots indicate the depths at which discrete samples were taken. Red triangles in figure A show the mixed layer depth (MLD) and in figure B the euphotic zone depth (Z_{eu}) on each day of the experiment.

Table S4.1. The number of initial contigs, the number of contigs after quality control, GC content (% ± Stdev), number of contigs with predicted coding reads and InterPro matches in each of the 13 metagenomes.

Assembly name	Average contig length (basepairs± Stdev)	Initial contigs (number of contigs)	After QC and length filtering (number of contigs)	GC content (%± Stdev)	Contigs with predicted coding readings	Contigs with InterPro Matches
Day01_1m	240.72 ± 34.41	2 495 375	275 501	41.88 ± 8.89	273 919	165 451
Day01_25m	240.10 ± 36.30	3 017 935	281 870	39.56 ± 9.03	279 573	175 899
Day01_50m	242.47 ± 32.86	2 429 980	305 393	39.62 ± 9.94	304 747	231 074
Day02_1m	245.52 ± 32.22	1 300 849	251 917	41.94 ± 9.18	251 379	184 039
Day02_25m	246.68 ± 32.51	1 917 851	284 988	41.25 ± 10.47	284 212	204 393
Day02_50m	242.58 ± 33.44	1 954 262	271 093	39.44 ± 9.85	270 538	209 100
Day03_1m	246.68 ± 32.23	1 021 716	237 652	42.27 ± 9.43	237 264	184 835
Day03_25m	247.41 ± 31.99	1 768 208	298 145	40.08 ± 9.68	297 496	230 695
Day03_50m	243.56 ± 33.88	2 031 511	299 480	40.28 ± 9.96	298 863	232 572
Day04_1m	243.20 ± 34.33	1 102 731	245 621	41.35 ± 9.34	245 163	183 743
Day04_25m	244.39 ± 33.62	2 048 544	319 983	40.91 ± 10.03	319 331	247 411
Day04_50m	244.16 ± 34.22	1 675 750	283 679	42.75 ± 10.30	283 114	226 725
Day05_50m	244.39 ± 33.91	2 051 516	315 843	40.99 ± 10.33	315 126	241 874

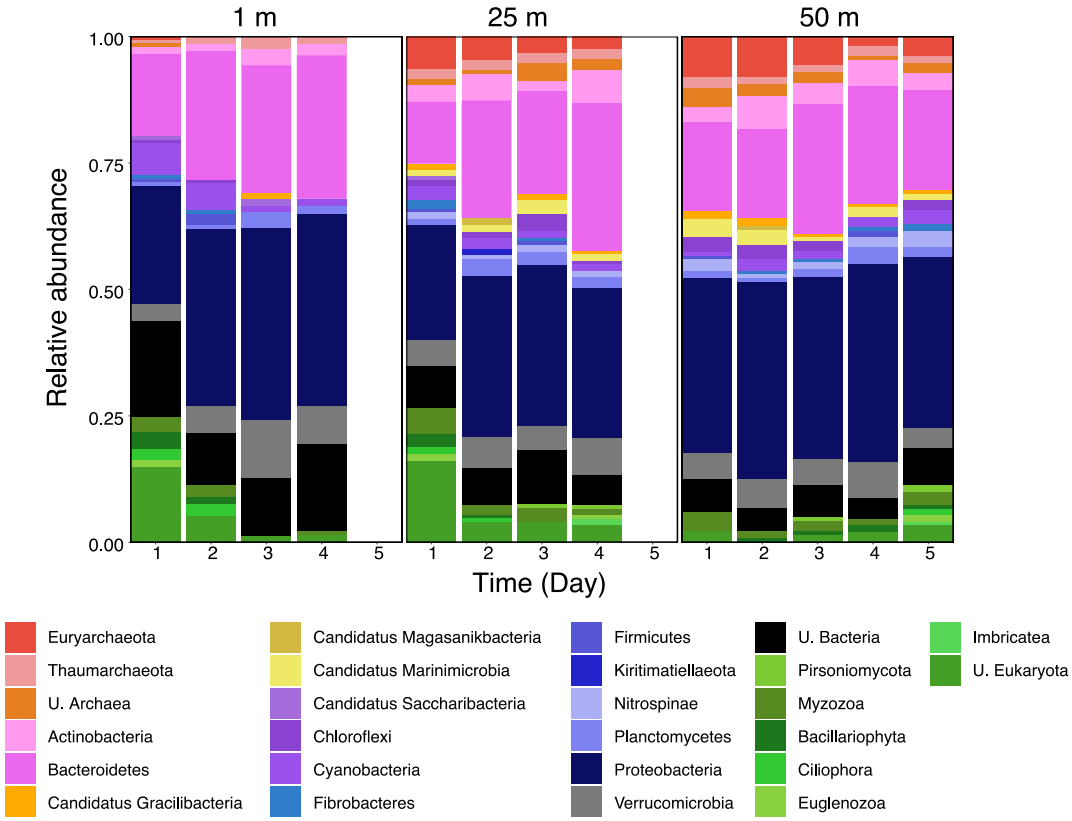

Figure S4.3. Relative abundances of archaea, bacteria, and eukaryote phyla on each sampling day at 1m, 25m and 50 m as determined from assembled metagenome reads. Only phyla with a relative abundance of >1% in one sample are presented here. Blank columns represent missing samples.

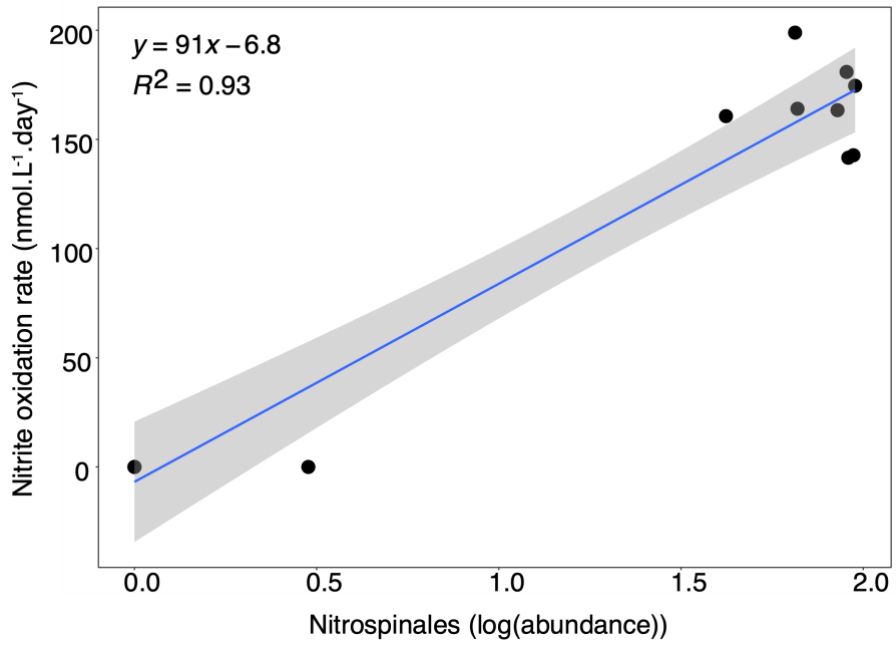

Figure S6.7. The positive relationship between log transformed Nitrospinales abundances and nitrite oxidation rates (nmol.L^{-1}.day^{-1}).

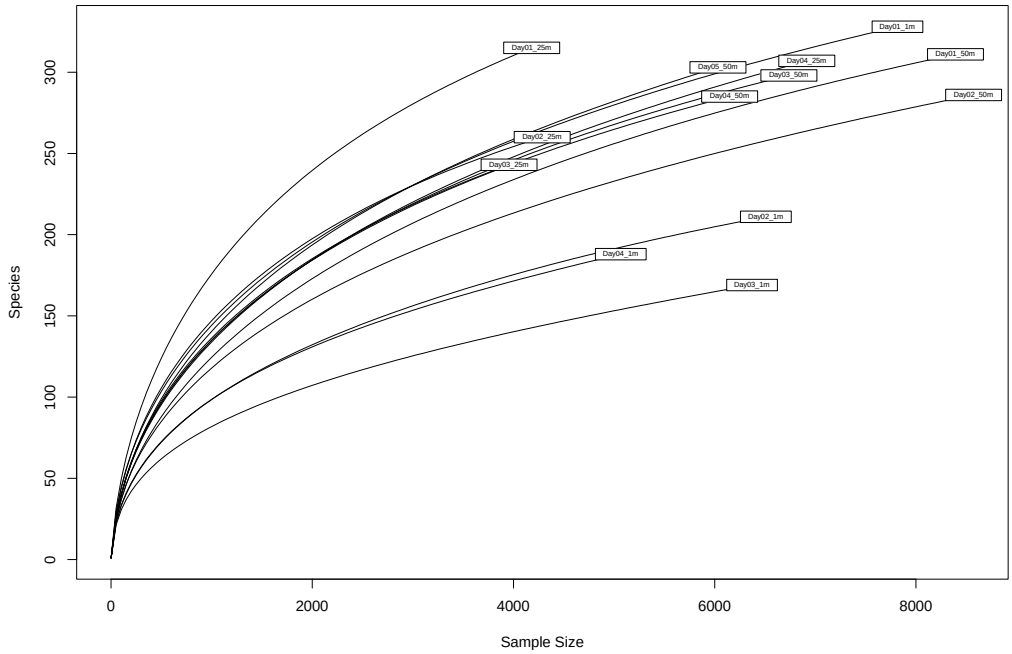

Figure S4.5. Rarefaction curves of raw reads (no assembly) metagenomes from the three sampling depths and 5 sampling depths.

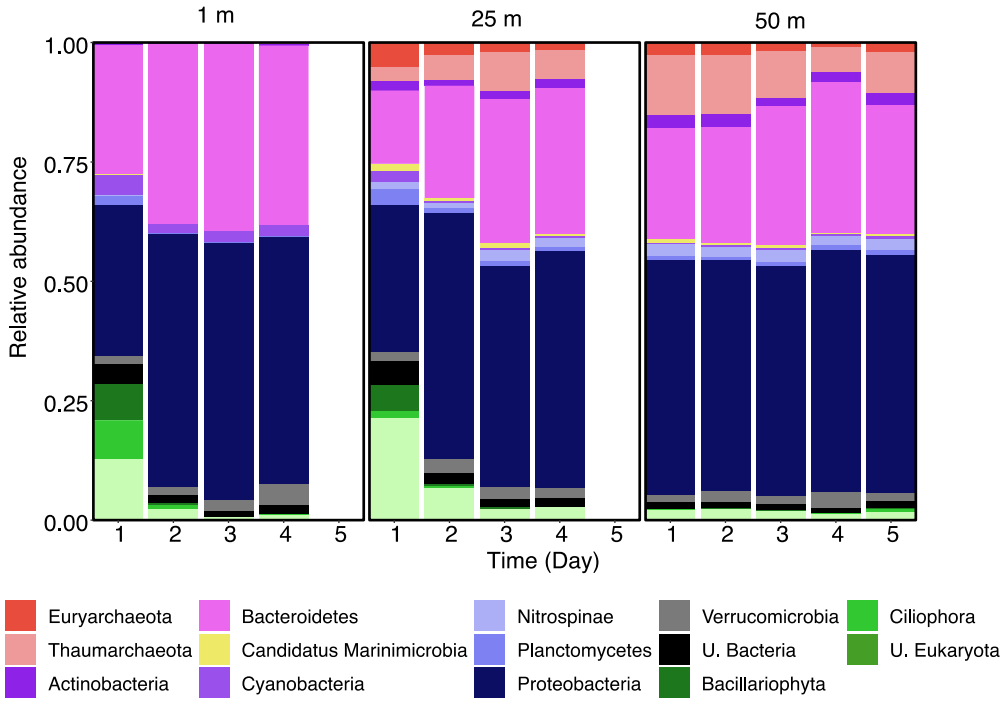

Figure S4.6. Relative abundances of archaea, bacteria, and eukaryote phyla on each sampling day at 1m, 25m and 50 m as determined from raw metagenome reads. Only phyla with a relative abundance of >1% in one sample are presented here. Blank columns represent missing samples.

Table S4.2. Mean percentage relative abundances (± standard deviation) of genes associated with pathways of interest in this study at each depth (1 m, 25 m, and 50 m).

Variable	1 m	25m	50 m
1) Pathway			
Photosystem I	0.026±0.014	0.014±0.011	0.004±0.003
Photosystem II	0.065±0.038	0.020±0.011	0.011±0.004
APP	0.011±0.003	0.005±0.002	0.007±0.001
Rhodopsin	0.026±0.002	0.019±0.003	0.020±0.001
Methanogenesis	0.013±0.003	0.022±0.001	0.024±0.002
Methane oxidation	0.001±0.001	0.005±0.002	0.006±0.001
BNF	0.011±0.002	0.003±0.002	0.003±0.001
Ammonia oxidation	0.001±0.001	0.006±0.002	0.006±0.001
Nitrite oxidation	0.015±0.002	0.039±0.009	0.037±0.005
Nitrate reduction	0.281±0.004	0.084±0.022	0.076±0.012
DNRA	0.046±0.005	0.095±0.027	0.089±0.015
ANRA	0.007±0.002	0.003±0.002	0.004±0.001
Remineralization	0.019±0.006	0.017±0.005	0.017±0.002
Denitrification	0.039±0.005	0.145±0.044	0.128±0.022
Anammox	0.004±0.001	0.025±0.003	0.024±0.003
Comammox	0.016±0.002	0.025±0.006	0.044±0.006
N_damo	0.001±0.001	0.005±0.003	0.004±0.002
Thiosulphate oxidation	0.064±0.004	0.088±0.032	0.091±0.013
DSRA	0.022±0.002	0.053±0.004	0.056±0.006
ASRA	0.156±0.017	0.124±0.011	0.125±0.013
Sulphur ABC transporter	-	0.001	0.001±0.000
Nitrate/nitrite ABC transporter	0.016±0.002	0.004±0.001	0.003±0.002
Nitrate/nitrite MFS transporter	0.017±0.004	0.036±0.010	0.035±0.005
Nitrite transporter	-	0.002±0.001	0.003±0.001
Phosphate transporter	0.143±0.005	0.077±0.018	0.080±0.012
Phosphonate transporter	0.038±0.004	0.092±0.007	0.105±0.010
Urea transporter	0.045±0.004	0.028±0.005	0.034±0.003
Ammonium transporter	0.171±0.003	0.153±0.004	0.159±0.004

Table S4.3. Mean relative abundances (no.of taxa) (± standard deviation) of selected taxa in at each depth (1 m, 25 m, and 50 m).

Variable	1 m	25 m	50 m
1) Phylum			
Euryarchaeota	3.8±3.5	173.8±91.6	127.2±45.6
Thaumarchaeota	9.5±5.7	350.3±136.4	602.4±184.8
Actinobacteria	15.8±3.2	96.5±23.3	144.0±25.7
Bacteroidetes	2222.0±371.2	1538.8±463.9	1674.6±212.0
Candidatus_Marinimicrobia	1.0±1.4	57.0±31.8	37.8±16.1
Cyanobacteria	164.0±71.9	50.0±56.1	22.4±9.9
Nitrospinae	1.0±1.4	107.5±36.5 1	143.8±21.1
Planctomycetes	46.0±49.4	89.8±74.6	49.6±7.4
Proteobacteria	2979.3±688.1	2744.3±591.4	3058.4±68.1
Verrucomicrobia	159.3±80.7	140.3±31.3	129.0±48.5
U. Bacteria	140.5±85.3	168.0±92.0	78.0±13.7
Bacillariophyta	122.3±225.5	98.0±160.2	11.0±6.4
Ciliophora	146.0±242.5	28.0±35.1	12,4±7.9
U. Eukaryota	253.0±352.7	499.3±543.6	110.6±23.0
2) Order			
Unclassified Thermoplasmata	2.0±4.0	160.0±75.9	120.8±44.9
Unclassified Thaumarchaeota	2.0±1.6	70.0±27.6	108.2±38.3
Nitrosopumilales	7.5±4.4	266.3±100.9	473.4±145.3
Unclassified Acidimicrobiia	7.5±2.9	43.3±14.5	59.8±12.7
Candidatus Actinomarinales	3.0±2.6	40.0±9.1	63.6±17.9
Unclassified Bacteroidia	2.0±2.2	61.3±19.8	68.6±5.7
Flavobacteriales	1908.5±341.8	1242.5±473.2	1437.2±175.9
Saprospirales	59.3±25.6	47.8±39.8	15.0±6.3
Sphingobacteriales	194.0±66.5	77.5±68.4	52.2±30.0
Unclassified Candidatus Marinimicrobia	1.0±1.4	57.0±31.8	37.8±16.1
Unclassified Cyanobacteria	39.0±20.1	14.3±18.1	6.2±3.9
Nostocales	20.3±33.9	23.5±36.4	1.2±1.3
Synechococcales	99.0±15.1	11.0±1.8	14.6±6.8
Nitrospinales	1.0±1.4	105.8±37.2	143.4±21.1
Gemmatales	26.8±50.2	39.0±63.6	1.6±1.7
Unclassified Proteobacteria	36.0±13.2	50.5±15.2	29.2±5.4
Unclassified Alphaproteobacteria	148.8±43.5	62.3±15.9	69.8±10.9
Pelagibacterales	94.5±29.3	397.5±120.4	613.6±150.9
Rhodobacterales	865.3±227.2	451.8±247.4	476.4±104.8
Rhodospirillales	22.3±9.9	44.0±2.8	65.2±15.9
Nitrosomonadales	171.8±72.9	77.0±34.9	89.0±18.9
Unclassified Deltaproteobacteria	11.3±8.3	109.8±39.7	106.6±20.8
Desulfovibrionales	4.0±6.2	22.0±38.1	1.0±1.7
Campylobacterales	0.5±0.6	53.0±72.7	18.2±8.4

Table S4.3. Continued.

Unclassified Gammaproteobacteria	866.3±330.2	764.5±204.4	864.6±62.0
Alteromonadales	97.8±33.6	101.5±30.7	112.0±49.5
Cellvibrionales	553.3±166.4	146.0±71.1	169.2±39.3
Oceanospirillales	31.3±9.4	251.8±86.8	244.0±43.4
Unclassified Verrucomicrobia	18.3±9.3	39.5±35.2	23.4±5.4
Verrucomicrobiales	107.8±60.9	44.3±13.9	54.4±39.6
Unclassified Bacteria	140.5±85.3	165.8±93.8	76.2±13.7
Unclassified Dinophyceae	61.3±100.8	115.0±148.9	10.6±5.2
Syndiniales	40.8±48.5	159.8±157.5	52.6±30.8
Unclassified Bacillariophyta	74.0±136.2	49.0±83.4	5.0±4.0
Unclassified Bacillariophyceae	18.3±35.2	16.3±29.9	2.2±2.2
Unclassified Spirotrichea	43.8±65.9	15.5±19.8	9.2±7.2
Tintinnida	93.0±164.7	2.5±3.9	0.0±0.0
Unclassified Eukaryota	82.0±113.6	161.3±182.1	27.0±4.4

7. Reference List

Allen, A. E., Howard-Jones, M. H., Booth, M. G., Frischer, M. E., Verity, P. G., Bronk, D. A., et al. (2002). Importance of heterotrophic bacterial assimilation of ammonium and nitrate in the Barents Sea during summer. *Journal of Marine Systsems* 38, 93-108. doi: 10.1016/S0924-7963(02)00171-9

Alvarez, L., Sanchez-Hevia, D., Sánchez, M., and Berenguer, J. (2019). A new family of nitrate/nitrite transporters involved in denitrification. *International Microbiology* 22, 19–28. doi:10.1007/s10123-018-0023-0.

Amend, A., Burgaud, G., Cunliffe, M., Edgcomb, V. P., Ettinger, C. L., Gutiérrez, M. H., et al. (2019). Fungi in the marine environment: Open questions and unsolved problems. *mBio* 10:e01189-18. doi:10.1128/mBio.01189-18.

Anderson, S. R., and Harvey, E. L. (2020). Temporal Variability and Ecological Interactions of Parasitic Marine Syndiniales in Coastal Protist Communities. *mSphere* 5, 1–16. doi:10.1128/msphere.00209-20.

Andrews, W. R. H., and Hutchings, L. (1980). Upwelling in the Southern Benguela Current. *Progress in Oceanography* 9, 1–81. doi:https://doi.org/10.1016/0079-6611(80)90015-4.

Apprill, A., Mcnally, S., Parsons, R., and Weber, L. (2015). Minor revision to V4 region SSU rRNA 806R gene primer greatly increases detection of SAR11 bacterioplankton. *Aquatic Microbial Ecology* 75, 129–137. doi:10.3354/ame01753.

Arístegui, J., Gasol, J. M., Duarte, C. M., and Herndld, G. J. (2009). Microbial oceanography of the dark ocean's pelagic realm. *Limnology and Oceanography* 54, 1501–1529. doi:10.4319/lo.2009.54.5.1501.

Auladell, A., Sánchez, P., Sánchez, O., Gasol, J. M., and Ferrera, I. (2019). Long-term seasonal and interannual variability of marine aerobic anoxygenic photoheterotrophic bacteria. *ISME Journal.* doi:10.1038/s41396-019-0401-4.

Aylward, F. O., Boeuf, D., Mende, D. R., Wood-Charlson, E. M., Vislova, A., Eppley, J. M., et al. (2017). Diel cycling and long-term persistence of viruses in the ocean's euphotic zone. *Proceedings of the National Academy of Sciences of the United States of America*, 201714821. doi:10.1073/pnas.1714821114.

Azam, F. (1998). Microbial Control of Oceanic Carbon Flux: The Plot Thickens. *Science* 280, 694–696. doi:10.1126/science.280.5364.694.

Azam, F., Fenchel, T., Field, J. G., Gray, J. S., Meyer-Reil, L. A., and Thingstad, F. (1983). The ecological role of water-column microbes in the sea. *Marine Ecology- Progress Series* 10, 257–263.

Baldani, J. I., Rouws, L., Cruz, L. M., Olivares, F. L., Schmid, M., and Hartmann, A. (2014). "The Family Oxalobacteraceae," in *The Prokaryotes: Alphaproteobacteria and Betaproteobacteria*, eds. E. Rosenberg, E. F. DeLong, S. Lory, E. Stackebrandt, and F. Thompson (Berlin, Heidelberg: Springer Berlin Heidelberg), 919–974. doi:10.1007/978-3-642-30197-1_291.

Bale, N. J., Villanueva, L., Fan, H., Stal, L. J., Hopmans, E. C., Schouten, S., et al. (2014). Occurrence and activity of anammox bacteria in surface sediments of the southern North Sea. *FEMS Microbiology Ecology* 89, 99–110. doi:10.1111/1574-6941.12338.

Balzano, S., Abs, E., and Leterme, S. C. (2015). Protist diversity along a salinity gradient in a coastal lagoon. *Aquatic Microbial Ecology* 74, 263–277. doi:10.3354/ame01740.

Barber, R. T., and Hiscock, M. R. (2006). A rising tide lifts all phytoplankton: Growth response of other phytoplankton taxa in diatom-dominated blooms. *Global Biogeochemical Cycles* 20. doi:10.1029/2006GB002726.

Barlow, R., Lamont, T., Mitchell-Innes, B., Lucas, M., and Thomalla, S. (2009). Primary production in the Benguela ecosystem, 1999-2002. *African Journal of Marine Science* 31, 97–101. doi:10.2989/AJMS.2009.31.1.9.780.

Beck, M. W. (2019). ggord: Ordination Plots with ggplot2.

Beja, O., Aravind, L., Koonin, E. V, Suzuki, M. T., Hadd, A., Nguyen, L. P., et al. (2000). Bacterial Rhodopsin: Evidence for a New Type of Phototrophy in the Sea. *Science* 289, 1902.

Beman, J. M., and Carolan, M. T. (2013). Deoxygenation alters bacterial diversity and community composition in the ocean's largest oxygen minimum zone. *Nature Communications* 4, 2705.

Beman, J. M., Leilei Shih, J., and Popp, B. N. (2013). Nitrite oxidation in the upper water column and oxygen minimum zone of the eastern tropical North Pacific Ocean. *ISME Journal* 7, 2192–2205. doi:10.1038/ismej.2013.96.

Bergen, B., Herlemann, D. P. R., and Jürgens, K. (2015). Zonation of bacterioplankton communities along aging upwelled water in the northern Benguela upwelling. *Frontiers In Microbiology* 6, 621. doi:10.3389/fmicb.2015.00621.

Bergh, Ø., BØrsheim, K. Y., Bratbak, G., and Heldal, M. (1989). High abundance of viruses found in aquatic environments. *Nature* 340, 467. http://dx.doi.org/10.1038/340467a0.

Bergo, N. M., Signori, C. N., Amado, A. M., Brandini, F. P., and Pellizari, V. H. (2017). The partitioning of carbon biomass among the pico-and nano-plankton community in the South Brazilian bight during a strong summer intrusion of south atlantic central water. *Frontiers in Marine Science* 4, 1–12. doi:10.3389/fmars.2017.00238.

Bernardet, J.-F., and Nakagawa, Y. (2006). "An Introduction to the Family Flavobacteriaceae," in *The Prokaryotes: Volume 7: Proteobacteria: Delta, Epsilon Subclass*, ed. S. and R. E. and S. K.-H. and S. E. Dworkin Martin and Falkow (New York, NY: Springer New York), 455–480. doi:10.1007/0-387-30747-8_16.

Berry, A. M., Barabote, R. D., and Normand, P. (2014). "The Family Acidothermaceae," in *The Prokaryotes: Actinobacteria*, ed. E. F. and L. S. and S. E. and T. F. Rosenberg Eugene and E. DeLong (Berlin, Heidelberg: Springer Berlin Heidelberg), 13–19. doi:10.1007/978-3-642-30138-4_199.

Biddanda, B. A., and Pomeroy, L. R. (1988). Microbial aggregation and degradation of phytoplankton-derived detritus in seawater. I. Microbial succession. *Marine Ecology Progress Series* 42, 79–88.

Bidle, K. D., and Azam, F. (2001). Bacterial control of silicon regeneration from diatom detritus: Significance of bacterial ectohydrolases and species identity. *Limnology and Oceanography* 46, 1606–1623. doi:https://doi.org/10.4319/lo.2001.46.7.1606.

Biers, E. J., Sun, S., and Howard, E. C. (2009). Prokaryotic genomes and diversity in surface ocean waters: interrogating the global ocean sampling metagenome. *Applied and environmental microbiology* 75, 2221–2229.

Billen, G. (1976). Evaluation of nitrifying activity in sediments by dark ^{14}C-bicarbonate incorporation. *Water Research* 10, 51–57. doi:https://doi.org/10.1016/0043-1354(76)90157-3.

Bjorbækmo, M. F. M., Evenstad, A., Røsæg, L. L., Krabberød, A. K., and Logares, R. (2020). The planktonic protist interactome: where do we stand after a century of research? *ISME Journal* 14, 544–559. doi:10.1038/s41396-019-0542-5.

Blamey, L. K., Shannon, L. J., Bolton, J. J., Crawford, R. J. M., Dufois, F., Evers-King, H., et al. (2015). Ecosystem change in the southern Benguela and the underlying processes. *Journal of Marine Systems* 144, 9–29. doi:10.1016/j.jmarsys.2014.11.006.

Blaxter, M., Mann, J., Chapman, T., Thomas, F., Whitton, C., Floyd, R., et al. (2005). Defining operational taxonomic units using DNA barcode data. *Philosophical Transactions of the Royal Society B: Biological Sciences* 360, 1935–1943. doi:10.1098/rstb.2005.1725.

Bombar, D., Paerl, R. W., and Riemann, L. (2016). Marine Non-Cyanobacterial Diazotrophs: Moving beyond Molecular Detection. *Trends in Microbiology* 24, 916–927. doi:10.1016/j.tim.2016.07.002.

Bowman, J. P. (2014). "The Family Cryomorphaceae," in *The Prokaryotes: Other Major Lineages of Bacteria and The Archaea*, eds. E. Rosenberg, E. F. DeLong, S. Lory, E. Stackebrandt, and F. Thompson (Berlin, Heidelberg: Springer Berlin Heidelberg), 539–550. doi:10.1007/978-3-642-38954-2_135.

Boyd, P.W., Sundby S., and Pörtner H.-O. (2014). "Cross-chapter box on net primary production in the ocean." in*: Climate Change 2014: Impacts, Adaptation, and Vulnerability. Part A: Global and Sectoral Aspects. Contribution of Working Group II to the Fifth Assessment Report of the Intergovernmental Panel on Climate Change*, eds. Field, C.B., V.R. Barros, D.J. Dokken, K.J. Mach, M.D. Mastrandrea, T.E. Bilir, M. Chatterjee, K.L. Ebi, Y.O. Estrada, R.C. Genova, B. Girma, E.S. Kissel, A.N. Levy, S. MacCracken, P.R. Mastrandrea, and L.L. White. (Cambridge University Press, Cambridge, United Kingdom and New York, NY, USA), 133-136.

Bradley, P. B., Sanderson, M. P., Frischer, M. E., Brofft, J., Booth, M. G., Kerkhof, L. J., et al. (2010). Inorganic and organic nitrogen uptake by phytoplankton and heterotrophic bacteria in the stratified Mid-Atlantic Bight. *Estuarine, Coastal and Shelf Science* 88, 429–441. doi:10.1016/j.ecss.2010.02.001.

Bratbak, G., Heldal, M., Thingstad, T. F., and Tuomi, P. (1996). Dynamics of virus abundance in coastal seawater. *FEMS Microbiology Ecology* 19, 263–269. doi:10.1016/0168-6496(96)00023-2.

Bratbak, G., Thingstad, F., and Heldal, M. (1994). Viruses and the microbial loop. *Microbial Ecology* 28, 209–221. doi:10.1007/BF00166811.

Brink, K. H., Abrantes, F. F. G., Bernal, P. A., Dugdale, R. C., Estrada, M., Hutchings, L., et al. (1995). Group Report: How do coastal upwelling systems operate as integrated physical, chemical, and biological systems and influence the geological record? The role of physical processes in defining the spatial structures of biological and chemical variables. *Environmental Sciences Research Report ES* 18, 103–124.

Bristow, L. A. (2018). Anoxia in the snow. *Nature Geoscience* 11, 226–227. doi:10.1038/s41561-018-0088-6.

Bristow, L. A., Callbeck, C. M., Larsen, M., Altabet, M. A., Dekaezemacker, J., Forth, M., et al. (2017). N_2 production rates limited by nitrite availability in the Bay of Bengal oxygen minimum zone. *Nature Geoscience* 10, 24–29. doi:10.1038/ngeo2847.

Bristow, L. A., Dalsgaard, T., Tiano, L., Mills, D. B., Bertagnolli, A. D., Wright, J. J., et al. (2016). Ammonium and nitrite oxidation at nanomolar oxygen concentrations in oxygen minimum zone waters. *Proceedings of the National Academy of Sciences of the United States of America* 113, 10601–10606. doi:10.1073/pnas.1600359113.

Bronk, D., Gilbert, P. M., Alone, T. C. T., Banahan, S., and Sahlsten, E. (1998). Inorganic and organic nitrogen cycling in Chesapeake Bay: autotrophic versus heterotrophic processes and relationships to carbon flux. *Aquatic Microbial Ecology* 15, 177-189.

Brown, P. C. (1984). Primary production at two contrasting nearshore sites in the Southern Benguela upwelling region, 1977—1979. *South African Journal of Marine Science* 2, 205–215. doi:10.2989/02577618409504369.

Brown, P. C., and Field, J. G. (1986). Factors limiting phytoplankton production in a nearshore upwelling area. *Journal of Plankton Research* 8, 55–68.

Brown, P. C., Painting, S. J., and Cochrane, K. L. (1991). Estimates of phytoplankton and bacterial biomass and production in the northern and southern Benguela ecosystems. *South African Journal of Marine Science* 11, 537–564. doi:10.2989/025776191784287673.

Burger, J. M., Moloney, C. L., Walker, D. R., Parrott, R. G., and Fawcett, S. E. (2020). Drivers of short-term variability in phytoplankton production in an embayment of the southern Benguela upwelling system. *Journal of Marine Systems* 208. doi:10.1016/j.jmarsys.2020.103341.

Bunse, C., and Pinhassi, J. (2017). Marine Bacterioplankton Seasonal Succession Dynamics. *Trends in Microbiology* 25, 494–505. doi:10.1016/j.tim.2016.12.013.

Cachon, M., and Caram, B. (1979). A symbiotic green alga, *Pedinomonas symbiotica* sp. nov. (Prasinophyceae), in the radiolarian *Thalassolampe margarodes*. *Phycologia* 18, 177–184. doi:10.2216/i0031-8884-18-3-177.1.

Callbeck, C. M., Lavik, G., Ferdelman, T. G., Fuchs, B., Gruber-Vodicka, H. R., Hach, P. F., et al. (2018). Oxygen minimum zone cryptic sulfur cycling sustained by

offshore transport of key sulfur oxidizing bacteria. *Nature Communications* 9. doi:10.1038/s41467-018-04041-x.

Campbell, L., and Carpenter, E. (1986). Estimating the grazing pressure of heterotrophic nanoplankton on *Synechococcus* spp. using the sea water dilution and selective inhibitor techniques. *Marine Ecology Progress Series* 33, 121–129. doi:10.3354/meps033121.

Canfield, D. E., Stewart, F. J., Thamdrup, B., de Brabandere, L., Dalsgaard, T., Delong, E. F., et al. (2010). A Cryptic Sulfur Cycle in Oxygen-Minimum-Zone Waters off the Chilean Coast. *Science* 330, 1375–1378. doi:10.1126/science.1196889.

Capone, D. G., Zehr, J. P., Paerl, H. W., Bergman, B., and Carpenter, E. J. (1997). *Trichodesmium*, a Globally Significant Marine Cyanobacterium. *Science* 276, 1221. doi:10.1126/science.276.5316.1221.

Caporaso, J. G., Kuczynski, J., Stombaugh, J., Bittinger, K., Bushman, F. D., Costello, E. K., et al. (2010). QIIME allows analysis of high-throughput community sequencing data. *Nature Methods* 7, 335–336. doi:10.1038/nmeth.f.303.

Caporaso, J. G., Lauber, C. L., Walters, W. A., Berg-Lyons, D., Lozupone, C. A., Turnbaugh, P. J., et al. (2011). Global patterns of 16S rRNA diversity at a depth of millions of sequences per sample. *Proceedings of the National Academy of Sciences of the United States of America* 108, 4516–4522. doi:10.1073/pnas.1000080107.

Carr, M. E., and Kearns, E. J. (2003). Production regimes in four Eastern Boundary Current systems. *Deep-Sea Research Part II: Topical Studies in Oceanography* 50, 3199–3221. doi:10.1016/j.dsr2.2003.07.015.

Chafee, M., Fernàndez-Guerra, A., Buttigieg, P. L., Gerdts, G., Eren, A. M., Teeling, H., et al. (2018). Recurrent patterns of microdiversity in a temperate coastal marine environment. *ISME Journal* 12, 237–252. doi:10.1038/ismej.2017.165.

Chaffron, S., Rehrauer, H., Pernthaler, J., and von Mering, C. (2010). A global network of coexisting microbes from environmental and whole-genome sequence data. *Genome Research* 20, 947–959. doi:10.1101/gr.104521.109.

Chang, Y.-H., and Stackebrandt, E. (2014). "The Family Sporolactobacillaceae," in *The Prokaryotes: Firmicutes and Tenericutes*, eds. E. Rosenberg, E. F. DeLong, S. Lory, E. Stackebrandt, and F. Thompson (Berlin, Heidelberg: Springer Berlin Heidelberg), 353–362. doi:10.1007/978-3-642-30120-9_348.

Chavez, F. P. (1991). Horizontal transport and the distribution of nutrients in the coastal transition zone off northern California: effects on primary production, phytoplankton biomass and species composition. *Journal of Geophysical Research* 96, 14833–14848. doi:10.1029/91jc01163.

Chavez, F. P., and Messié, M. (2009). A comparison of Eastern Boundary Upwelling Ecosystems. *Progress in Oceanography* 83, 80–96. doi:10.1016/j.pocean.2009.07.032.

Chen, Y., and Murrell, J. C. (2010). When metagenomics meets stable-isotope probing: Progress and perspectives. *Trends in Microbiology* 18, 157–163. doi:10.1016/j.tim.2010.02.002.

Cho, B. C., Park, M. G., Shim, J. H., and Azam, F. (1996). Significance of bacteria in urea dynamics in coastal surface waters. *Marine Ecology Progress Series* 142, 19–26.

Choi, D. H., An, S. M., Yang, E. C., Lee, H., Shim, J. S., Jeong, J. Y., et al. (2018). Daily variation in the prokaryotic community during a spring bloom in shelf waters of the East China Sea. *FEMS microbiology ecology* 94, 1–9. doi:10.1093/femsec/fiy134.

Coats, D. W., Coats, D. W., Park, M. G., and Park, M. G. (2002). Parasitism of photosynthetic dinoflagellates by three strains of. *Aquatic Microbial Ecology* 528, 520–528. doi:10.1046/j.1529-8817.2002.01200.x.

Codispoti, L. A., and Christensen, J. P. (1985). Nitrification, denitrification and nitrous oxide cycling in the eastern tropical South Pacific ocean. *Marine Chemistry* 16, 277–300. doi:https://doi.org/10.1016/0304-4203(85)90051-9.

Collado-Fabbri, S., Vaulot, D., and Ulloa, O. (2011). Structure and seasonal dynamics of the eukaryotic picophytoplankton community in a wind-driven coastal upwelling ecosystem. *Limnology and Oceanography* 56, 2334–2346. doi:10.4319/lo.2011.56.6.2334.

Cottrell, M. T., and Kirchman, D. L. (2009). Photoheterotrophic microbes in the Arctic Ocean in summer and winter. *Applied and Environmental Microbiology* 75, 4958–4966. doi:10.1128/AEM.00117-09.

Countway, P. D., Vigil, P. D., Schnetzer, A., Moorthi, S. D., and Caron, D. A. (2010). Seasonal analysis of protistan community structure and diversity at the USC Microbial Observatory (San Pedro Channel, North Pacific Ocean). *Limnology and Oceanography* 55, 2381–2396. doi:10.4319/lo.2010.55.6.2381.

Cram, J. A., Parada, A. E., and Fuhrman, J. A. (2016). Dilution reveals how viral lysis and grazing shape microbial communities. *Limnology and Oceanography* 61, 889–905. doi:10.1002/lno.10259.

Croll, D. A., Marinovic, B., Benson, S., Chavez, F. P., Black, N., Ternullo, R., et al. (2005). From wind to whales: trophic links in a coastal upwelling system. *Marine Ecology Progress Series* 289, 117–130.

Csardi, G., and Nepusz, T. (2006). The igraph software package for complex network research. *InterJournal* Complex Sy, 1695.

Cuadrat, R. R. C., Cury, J. C., and Dávila, A. M. R. (2015). Metagenomic analysis of upwelling-affected Brazilian coastal seawater reveals sequence domains of type I PKS and modular NRPS. *International Journal of Molecular Sciences* 16, 28285–28295. doi:10.3390/ijms161226101.

Cuevas, L. A., Daneri, G., Jacob, B., and Montero, P. (2004). Microbial abundance and activity in the seasonal upwelling area off Concepción (∼36°S), central Chile: A comparison of upwelling and non-upwelling conditions. *Deep-Sea Research Part II: Topical Studies in Oceanography* 51, 2427–2440. doi:10.1016/j.dsr2.2004.07.026.

Cullen, J. J. (2001). "Primary Production Methods," in *Encyclopedia of Ocean Sciences* (Elsevier), 2277–2284. doi:10.1006/rwos.2001.0203.

Cushing, D. H. (1989). A difference in structure between ecosystems in strongly stratified waters and in those that are only weakly stratified. *Journal of Plankton Research* 11, 1–13.

Daims, H., Lebedeva, E. v, Pjevac, P., Han, P., Herbold, C., Albertsen, M., et al. (2015). Complete nitrification by Nitrospira bacteria. *Nature* 528, 504–509. doi:10.1038/nature16461.

Daims, H., Lücker, S., and Wagner, M. (2016). A New Perspective on Microbes Formerly Known as Nitrite-Oxidizing Bacteria. *Trends in Microbiology* 24, 699–712. doi:10.1016/j.tim.2016.05.004.

Dalsgaard, T., Stewart, F. J., Thamdrup, B., de Brabandere, L., Revsbech, N. P., Ulloa, O., et al. (2014). Oxygen at nanomolar levels reversibly suppresses process rates and gene expression in anammox and denitrification in the oxygen minimum zone off Northern Chile. *mBio* 5. doi:10.1128/mBio.01966-14.

Dalsgaard, T., Thamdrup, B., and Canfield, D. E. (2005). Anaerobic ammonium oxidation (anammox) in the marine environment. *Research in Microbiology* 156, 457–464. doi:10.1016/j.resmic.2005.01.011.

Dalsgaard, T., Thamdrup, B., Farías, L., and Revsbech, N. P. (2012). Anammox and denitrification in the oxygen minimum zone of the eastern South Pacific. *Limnology and Oceanography* 57, 1331–1346. doi:10.4319/lo.2012.57.5.1331.

Daneri, G., Lizárraga, L., Montero, P., González, H. E., and Tapia, F. J. (2012). Wind forcing and short-term variability of phytoplankton and heterotrophic bacterioplankton in the coastal zone of the Concepción upwelling system (Central Chile). *Progress in Oceanography* 92–95. doi:10.1016/j.pocean.2011.07.013.

Dang, H., Li, T., Chen, M., and Huang, G. (2008). Cross-ocean distribution of Rhodobacterales bacteria as primary surface colonizers in temperate coastal marine waters. *Applied and Environmental Microbiology* 74, 52–60. doi:10.1128/AEM.01400-07.

Dastager, S. G., Krishnamurthi, S., Rameshkumar, N., and Dharne, M. (2014). "The Family Micrococcaceae," in *The Prokaryotes: Actinobacteria*, eds. E. Rosenberg, E. F. DeLong, S. Lory, E. Stackebrandt, and F. Thompson (Berlin, Heidelberg: Springer Berlin Heidelberg), 455–498. doi:10.1007/978-3-642-30138-4_168.

de Boyer Montégut, C., Madec, G., Fischer, A. S., Lazar, A., and Iudicone, D. (2004). Mixed layer depth over the global ocean: An examination of profile data and a profile-based climatology. *Journal of Geophysical Research C: Oceans* 109, 1–20. doi:10.1029/2004JC002378.

de la Haba, R. R., Arahal, D. R., Sánchez-Porro, C., and Ventosa, A. (2014). "The Family Halomonadaceae," in *The Prokaryotes: Gammaproteobacteria*, ed. E. F. and L. S. and S. E. and T. F. Rosenberg Eugene and DeLong (Berlin, Heidelberg: Springer Berlin Heidelberg), 325–360. doi:10.1007/978-3-642-38922-1_235.

Delmont, T. O., Quince, C., Shaiber, A., Esen, Ö. C., Lee, S. T., Rappé, M. S., et al. (2018). Nitrogen-fixing populations of Planctomycetes and Proteobacteria are abundant in surface ocean metagenomes. *Nature Microbiology* 3, 804–813. doi:10.1038/s41564-018-0176-9.

Delong, E. F. (1992). Archaea in coastal marine environments. *Proceedings of the National Academy of Sciences* 89, 5685–5689.

Delong, E. F. (1998). Everything in moderation: Archaea as “non-extremophiles.” *Current Opinion in Genetics and Development* 8, 649–654. doi:10.1016/S0959-437X(98)80032-4.

DeLong, E. F. (2021). Exploring Marine Planktonic Archaea: Then and Now. *Frontiers in Microbiology* 11. doi:10.3389/fmicb.2020.616086.

DeLong, E. F., Franks, D. G., and Alldredge, A. L. (1993). Phylogenetic diversity of aggregate-attached vs. free-living marine bacterial assemblages. *Limnology and Oceanography* 38, 924–934. doi:10.4319/lo.1993.38.5.0924.

Dicks, L., and Endo, A. (2014). “The Family Lactobacillaceae: Genera Other than Lactobacillus,” in *The Prokaryotes: Firmicutes and Tenericutes*, eds. E. Rosenberg, E. F. DeLong, S. Lory, E. Stackebrandt, and F. Thompson (Berlin, Heidelberg: Springer Berlin Heidelberg), 203–212. doi:10.1007/978-3-642-30120-9_207.

Dortch, Q. (1990). The interaction between ammonium and nitrate uptake in phytoplankton. *Marine Ecology Progress Series* 61, 183–201.

Ducklow, H. W. (2000). Bacterial production and biomass in the oceans, in *Microbial Ecology of the Oceans*, ed. D. L. Kirchman, 85. (Wiley-Liss). 85-120.

Dugdale, R. C., and Goering, J. J. (1967). Uptake of New and Regenerated Forms of Nitrogen in Primary Productivity. *Limnology and Oceanography* 12, 196–206. doi:10.4319/lo.1967.12.2.0196.

Dugdale, R. C., Goering, J. J., Barber, R. T., Smith, R. L., and Packard, T. T. (1977). Denitrification and hydrogen sulfide in the Peru upwelling region during 1976. *Deep Sea Research* 24, 601–608. doi:https://doi.org/10.1016/0146-6291(77)90530-6.

Dugdale, R. C., and Wilkerson, F. P. (1986). The use of ^{15}N to measure nitrogen uptake; experimental considerations. *Limnology and Oceanography* 31, 673–689.

Dugdale, R. C., Wilkerson, F. P., Hogue, V. E., and Marchi, A. (2006). Nutrient controls on new production in the Bodega Bay, California, coastal upwelling plume. *Deep-Sea Research Part II: Topical Studies in Oceanography* 53, 3049–3062. doi:10.1016/j.dsr2.2006.07.009.

Dumack, K., Bonkowski, M., Clauß, S., and Völcker, E. (2018). Phylogeny and redescription of the testate amoeba *Diaphoropodon archeri* (Chlamydophryidae, Thecofilosea, Cercozoa), De Saedeleer 1934, and annotations on the polyphyly of testate amoebae with agglutinated tests in the cercozoa. *Journal of Eukaryotic Microbiology* 65, 308–314. doi:10.1111/jeu.12474.

Duncombe Rae, C. M. (2005). A demonstration of the hydrographic partition of the Benguela upwelling ecosystem at 26°40'S. *African Journal of Marine Science* 27, 617–628. doi:10.2989/18142320509504122.

Dupont, C. L., Rusch, D. B., Yooseph, S., Lombardo, M.-J., Alexander Richter, R., Valas, R., et al. (2012). Genomic insights to SAR86, an abundant and uncultivated marine bacterial lineage. *The ISME Journal* 6, 1186–1199. doi:10.1038/ismej.2011.189.

Eilers, H., Pernthaler, J., Peplies, J., Glöckner, F. O., Gerdts, G., and Amann, R. (2001). Isolation of Novel Pelagic Bacteria from the German Bight and Their Seasonal Contributions to Surface Picoplankton. *Applied and Environmental Microbiology* 67, 5134–5142. doi:10.1128/aem.67.11.5134-5142.2001.

Elodie, G., Dadou, I., Vu, L., Cambon, G., Sudre, J., Garcon, V., et al. (2013). Coupled physical/biogeochemical modeling including O_2-dependent processes in the Eastern Boundary Upwelling Systems: Application in the Benguela. *Biogeosciences* 10. doi:10.5194/bg-10-3559-2013.

Eloe-Fadrosh, E. A., Ivanova, N. N., Woyke, T., and Kyrpides, N. C. (2016). Metagenomics uncovers gaps in amplicon-based detection of microbial diversity. *Nature Microbiology* 1, 15032. doi:10.1038/nmicrobiol.2015.32.

Eppley, R. W., and Peterson, B. J. (1979). Particulate organic matter flux and planktonic new production in the deep ocean. *Nature* 282, 677–680. doi:10.1038/282677a0.

Espinoza-González, O., Figueiras, F. G., Crespo, B. G., Teixeira, I. G., and Castro, C. G. (2012). Autotrophic and heterotrophic microbial plankton biomass in the NW Iberian upwelling: Seasonal assessment of metabolic balance. *Aquatic Microbial Ecology* 67, 77–89. doi:10.3354/ame01584.

Estep, K. W., Davis, P. G., Keller, M. D., and Sieburth, J. M. (1986). How important are oceanic algal nanoflagellates in bacterivory? *Limnology and oceanography* 31, 646–650.

Falkowski, P. G. (1997). Evolution of the nitrogen cycle and its influence on the biological sequestration of CO2 in the ocean. *Nature* 387, 272–275. doi:10.1038/387272a0.

Falkowski, P. G., Barber, R. T., and Smetacek, V. (1998). Biogeochemical Controls and Feedbacks on Ocean Primary Production. *Science* 281, 200–206. doi:10.1126/science.281.5374.200.

Falkowski, P. G., Fenchel, T., and Delong, E. F. (2008). The microbial engines that drive earth's biogeochemical cycles. *Science* 320, 1034–1039. doi:10.1126/science.1153213.

Falkowski, P. G., Laws, E. A., Barber, R. T., and Murray, J. W. (2003). "Phytoplankton and Their Role in Primary, New, and Export Production," in *Ocean Biogeochemistry* (Springer Berlin Heidelberg), 99–121. doi:10.1007/978-3-642-55844-3_5.

Falkowski, P., and Raven, J. (2013). "9. Photosynthesis and Primary Production in Nature," in *Aquatic Photosynthesis* (Princeton University Press), 319–363. doi:10.1515/9781400849727.319.

Faust, K., Bauchinger, F., Laroche, B., de Buyl, S., Lahti, L., Washburne, A. D., et al. (2018). Signatures of ecological processes in microbial community time series. *Microbiome* 6, 1–13. doi:10.1186/s40168-018-0496-2.

Faust, K., Lahti, L., Gonze, D., de Vos, W. M., and Raes, J. (2015). Metagenomics meets time series analysis: Unraveling microbial community dynamics. *Current Opinion in Microbiology* 25, 56–66. doi:10.1016/j.mib.2015.04.004.

Faust, K., and Raes, J. (2012). Microbial interactions: from networks to models. *Nature Reviews Microbiology* 10, 538–550. doi:10.1038/nrmicro2832.

Fawcett, S. E., and Ward, B. B. (2011). Phytoplankton succession and nitrogen utilization during the development of an upwelling bloom. *Marine Ecology Progress Series* 428, 13–31. doi:10.3354/meps09070.

Fell, J. (1976). Yeasts in oceanic regions, in *Recent advances in aquatic mycology*, ed. E. Jones (London, United Kingdom: Elek Science), 93–124.

Fenchel, T. (1968). The ecology of marine microbenthos III. The reproductive potential of ciliates. *Ophelia* 5, 123–136. doi:10.1080/00785326.1968.10409627.

Fenchel, T. (1988). Marine plankton food chains. *Annual Review of Ecology and Systematics* 19, 19–38.

Fenchel, T. (2008). The microbial loop - 25 years later. *Journal of Experimental Marine Biology and Ecology* 366, 99–103. doi:10.1016/j.jembe.2008.07.013.

Fenchel, T., and Finlay, B. (2008). Oxygen and the spatial structure of microbial communities. *Biological Reviews* 83, 553–569. doi:10.1111/j.1469-185X.2008.00054.x.

Fenchel, T., Kristensen, L. D., and Rasmussen, L. (1990). Water column anoxia: vertical zonation of planktonic protozoa. *Marine Ecology Progress Series* 62, 1–10.

Finkel, O. M., Béjà, O., and Belkin, S. (2013). Global abundance of microbial rhodopsins. *ISME Journal* 7, 448–451. doi:10.1038/ismej.2012.112.

Finkel, Z. V. (2014). "Marine net primary production," in *Global Environmental Change* (Springer Netherlands), 117–124. doi:10.1007/978-94-007-5784-4_42.

Finkel, Z. V, Beardall, J., Flynn, K. J., Quigg, A., Rees, T. A. V, and Raven, J. A. (2010). Phytoplankton in a changing world: cell size and elemental stoichiometry. *Journal of Plankton Research* 32, 119–137. doi:10.1093/plankt/fbp098.

Finkel, Z. V., Platt, T., Sathyendranath, S., Kepkay, P., Jellett, J., Irwin, B., et al. (2001). Light absorption and size scaling of light-limited metabolism in marine diatoms. *Limnology and oceanography* 46, 86–94.

Flynn, R. F., Burger, J. M., Pillay, K., and Fawcett, S. E. (2018). Wintertime rates of net primary production and nitrate and ammonium uptake in the southern Benguela upwelling system. *African Journal of Marine Science* 40, 253–266. doi:10.2989/1814232X.2018.1502095.

Flynn, R. F., Granger, J., Veitch, J. A., Siedlecki, S., Burger, J. M., Pillay, K., et al. (2020). On-Shelf Nutrient Trapping Enhances the Fertility of the Southern Benguela Upwelling System. *Journal of Geophysical Research: Oceans* 125. doi:10.1029/2019JC015948.

Fogg, G. E. (1995). Some comments on picoplankton and its importance in the pelagic ecosystem. *Aquatic Microbial Ecology* 9, 33–39.

Fox, J., and Weisberg, S. (2019). *An R Companion to Applied Regression*. Third Edition. Thousand Oaks, CA: Sage Available at: https://r-forge.r-project.org/projects/car/,.

Francis, C. A., Roberts, K. J., Beman, J. M., Santoro, A. E., and Oakley, B. B. (2005). Ubiquity and diversity of ammonia-oxidizing archaea in water columns and sediments of the ocean. *Proceedings of the National Academy of Sciences of the United States of America* 102, 14683–14688.

French, D. P., Furnas, M. J., and Smayda, T. J. (1983). Diel changes in nitrite concentration in the chlorophyll maximum in the Gulf of Mexico. *Deep Sea Research Part A. Oceanographic Research Papers* 30, 707–722. doi:https://doi.org/10.1016/0198-0149(83)90018-3.

Frings, P. J., Clymans, W., Fontorbe, G., de La Rocha, C. L., and Conley, D. J. (2016). The continental Si cycle and its impact on the ocean Si isotope budget. *Chemical Geology* 425, 12–36. doi:10.1016/j.chemgeo.2016.01.020.

Fuhrman, J. A., Cram, J. A., and Needham, D. M. (2015). Marine microbial community dynamics and their ecological interpretation. *Nature Reviews Microbiology* 13, 133–146. doi:10.1038/nrmicro3417.

Fuhrman, J. A., Eppley, R. W., Hagström, Å., and Azam, F. (1985). Diel variations in bacterioplankton, phytoplankton, and related parameters in the Southern California Bight. *Marine Ecology Progress Series* 27, 9–20.

Fuhrman, J. A., Hewson, I., Schwalbach, M. S., Steele, J. A., Brown, M. V., and Naeem, S. (2006). Annually reoccurring bacterial communities are predictable from ocean conditions. *Proceedings of the National Academy of Sciences of the United States of America* 103, 13104–13109. doi:10.1073/pnas.0602399103.

Fuhrman, J. A., McCallum, K., and Davis, A. A. (1992). Novel major archaebacterial group from marine plankton. *Nature* 356, 148–149. doi:10.1038/356148a0.

Fuhrman, J., and Suttle, C. (1993). Viruses in Marine Planktonic Systems. *Oceanography* 6, 51–63. doi:10.5670/oceanog.1993.14.

Füssel, J., Lam, P., Lavik, G., Jensen, M. M., Holtappels, M., Günter, M., et al. (2012). Nitrite oxidation in the Namibian oxygen minimum zone. *ISME Journal* 6, 1200–1209. doi:10.1038/ismej.2011.178.

Geider, R. J. (1987). Light and temperature dependence of the carbon to chlorophyll *a* ratio in microalgae and Cyanobacteria: implications for physiology and growth of phytoplankton. *New Phytologist* 106, 1–34. doi:https://doi.org/10.1111/j.1469-8137.1987.tb04788.x.

Ganesh, S., Bristow, L. A., Larsen, M., Sarode, N., Thamdrup, B., and Stewart, F. J. (2015). Size-fraction partitioning of community gene transcription and nitrogen metabolism in a marine oxygen minimum zone. *ISME Journal* 9, 2682–2696. doi:10.1038/ismej.2015.44.

Ganesh, S., Parris, D. J., Delong, E. F., and Stewart, F. J. (2014). Metagenomic analysis of size-fractionated picoplankton in a marine oxygen minimum zone. *ISME Journal* 8, 187–211. doi:10.1038/ismej.2013.144.

Geider, R. J., MacIntyre, H. L., and Kana, T. M. (1997). Dynamic model of phytoplankton growth and acclimation: responses of the balanced growth rate and the chlorophyll *a*:carbon ratio to light, nutrient-limitation and temperature. *Marine Ecology Progress Series* 148, 187–200.

Gilbert, J. A., Field, D., Swift, P., Thomas, S., Cummings, D., Temperton, B., et al. (2010). The taxonomic and functional diversity of microbes at a temperate coastal site: A "multi-omic" study of seasonal and diel temporal variation. *PLoS ONE* 5, e15545. doi:10.1371/journal.pone.0015545.

Gilbert, J. A., Steele, J. A., Caporaso, J. G., Steinbrück, L., Reeder, J., Temperton, B., et al. (2012). Defining seasonal marine microbial community dynamics. *ISME Journal* 6, 298–308. doi:10.1038/ismej.2011.107.

Giovannoni, S. J., Bibbs, L., Cho, J. C., Stapels, M. D., Desiderio, R., Vergin, K. L., et al. (2005). Proteorhodopsin in the ubiquitous marine bacterium SAR11. *Nature* 438, 82–85. doi:10.1038/nature04032.

Giovannoni, S. J., and Stingl, U. (2005). Molecular diversity and ecology of microbial plankton. *Nature* 437, 343–348. doi:10.1038/nature04158.

Glaubitz, S., Kießlich, K., Meeske, C., Labrenz, M., and Jürgens, K. (2013). SUP05 Dominates the gammaproteobacterial sulfur oxidizer assemblages in pelagic redoxclines of the central baltic and black seas. *Applied and Environmental Microbiology* 79, 2767–2776. doi:10.1128/AEM.03777-12.

Glöckner, F. O., Yilmaz, P., Quast, C., Gerken, J., Beccati, A., Ciuprina, A., et al. (2017). 25 years of serving the community with ribosomal RNA gene reference databases and tools. *Journal of Biotechnology* 261, 169–176. doi:10.1016/j.jbiotec.2017.06.1198.

Gobler, C. J., Davis, T. W., Deonarine, S. N., Saxton, M. A., Lavrentyev, P. J., Jochem, F. J., et al. (2008). Grazing and virus-induced mortality of microbial populations before and during the onset of annual hypoxia in Lake Erie. *Aquatic Microbial Ecology* 51, 117–128. doi:10.3354/ame01180.

Golterman, H. L. (1983). The Winkler Determination, in *Polarographic Oxygen Sensors: Aquatic and Physiological Applications*, eds. E. Gnaiger and H. Forstner (Berlin, Heidelberg: Springer Berlin Heidelberg), 346–351. doi:10.1007/978-3-642-81863-9_31.

Gong, W., and Marchetti, A. (2019). Estimation of 18S Gene Copy Number in Marine Eukaryotic Plankton Using a Next-Generation Sequencing Approach. *Frontiers in Marine Science* 6. Available at: https://www.frontiersin.org/article/10.3389/fmars.2019.00219.

Granger, J., and Sigman, D. M. (2009). Removal of nitrite with sulfamic acid for nitrate N and O isotope analysis with the denitrifier method. *Rapid Communications in Mass Spectrometry* 23, 3753–3762. doi:https://doi.org/10.1002/rcm.4307.

Grasshoff, K., Kremling, K., and Ehrhardt, M. (1983). *Methods of Seawater Analysis*. Wiley, Weinjeim, Germany.

Gregoracci, G. B., dos Santos Soares, A. C., Miranda, M. D., Coutinho, R., and Thompson, F. L. (2015). Insights into the microbial and viral dynamics of a coastal downwelling-upwelling transition. *PLoS ONE* 10, 1–14. doi:10.1371/journal.pone.0137090.

Grossart, H. P., Levold, F., Allgaier, M., Simon, M., and Brinkhoff, T. (2005). Marine diatom species harbour distinct bacterial communities. *Environmental Microbiology* 7, 860–873. doi:10.1111/j.1462-2920.2005.00759.x.

Gruber, N., and Galloway, J. N. (2008). An Earth-system perspective of the global nitrogen cycle. *Nature* 451, 293–296. doi:10.1038/nature06592.

Guidi, L., Chaffron, S., Bittner, L., Eveillard, D., Larhlimi, A., Roux, S., et al. (2016). Plankton networks driving carbon export in the oligotrophic ocean. *Nature* 532, 465–470. doi:10.1038/nature16942.

Guieu, C., Aumont, O., Paytan, A., Bopp, L., Law, C. S., Mahowald, N., et al. (2014). The significance of the episodic nature of atmospheric deposition to Low Nutrient Low Chlorophyll regions. *Global Biogeochemical Cycles* 28, 1179–1198. doi:10.1002/2014GB004852.

Guillou, L., Alves-de-Souza, C., Siano Dr, R., and González, H. (2010). The ecological significance of small, eukaryotic parasites in marine ecosystems. *Microbiology Today* 37, 92–95.

Guillou, L., Bachar, D., Audic, S., Bass, D., Berney, C., Bittner, L., et al. (2012). The Protist ribosomal reference database (PR2): A catalog of unicellular eukaryote small sub-unit rRNA sequences with curated taxonomy. *Nucleic Acids Research* 41. 1–8. doi:10.1093/nar/gks1160.

Guillou, L., Viprey, M., Chambouvet, A., Welsh, R. M., Kirkham, A. R., Massana, R., et al. (2008). Widespread occurrence and genetic diversity of marine parasitoids belonging to Syndiniales (Alveolata). *Environmental Microbiology* 10, 3349–3365. doi:10.1111/j.1462-2920.2008.01731.x.

Gutiérrez, M. H., Jara, A. M., and Pantoja, S. (2016). Fungal parasites infect marine diatoms in the upwelling ecosystem of the Humboldt current system off central Chile. *Environmental Microbiology* 18, 1646–1653. doi:10.1111/1462-2920.13257.

Hackett, J. D., Anderson, D. M., Erdner, D. L., and Bhattacharya, D. (2004). Dinoflagellates: A remarkable evolutionary experiment. *American Journal of Botany* 91, 1523–1534. doi:10.3732/ajb.91.10.1523.

Hahn, M. W., and Höfle, M. G. (2006). Grazing of protozoa and its effect on populations of aquatic bacteria. *FEMS Microbiology Ecology* 35, 113–121. doi:10.1111/j.1574-6941.2001.tb00794.x.

Hall-Stoodley, L., Costerton, J. W., and Stoodley, P. (2004). Bacterial biofilms: From the natural environment to infectious diseases. *Nature Reviews Microbiology* 2, 95–108. doi:10.1038/nrmicro821.

Hallam, S. J., Mincer, T. J., Schleper, C., Preston, C. M., Roberts, K., Richardson, P. M., et al. (2006). Pathways of carbon assimilation and ammonia oxidation suggested by environmental genomic analyses of marine Crenarchaeota. *PLoS Biology* 4, 520–536. doi:10.1371/journal.pbio.0040095.

Han, H., Hemp, J., Pace, L. A., Ouyang, H., Ganesan, K., Roh, J. H., et al. (2011). Adaptation of aerobic respiration to low O2 environments. *Proceedings of the National Academy of Sciences of the United State sof America* 108, 14109–14114. doi:10.1073/pnas.1018958108/-/DCSupplemental.

Haro-Moreno, J. M., Rodriguez-Valera, F., Rosselli, R., Martinez-Hernandez, F., Roda-Garcia, J. J., Gomez, M. L., et al. (2020). Ecogenomics of the SAR11 clade. *Environmental Microbiology* 22, 1748–1763. doi:10.1111/1462-2920.14896.

Harrell, F. E., and Dupont, C. (2020). Package ‘ Hmisc .’

Hatosy, S. M., Martiny, J. B. H., Sachdeva, R., Steele, J., Fuhrman, J. A., and Martiny, A. C. (2013). Beta diversity of marine bacteria depends on temporal scale. *Ecology* 94, 1898–1904. doi:10.1890/12-2125.1.

Heidelberg, K. B., Gilbert, J. A., and Joint, I. (2010). Marine genomics: At the interface of marine microbial ecology and biodiscovery: Minireview. *Microbial Biotechnology* 3, 531–543. doi:10.1111/j.1751-7915.2010.00193.x.

Hernández-Hernández, N., Arístegui, J., Montero, M. F., Velasco-Senovilla, E., Baltar, F., Marrero-Díaz, Á., et al. (2020). Drivers of Plankton Distribution Across Mesoscale

Eddies at Submesoscale Range. *Frontiers in Marine Science* 7. doi:10.3389/fmars.2020.00667.

Hernando-Morales, V., Varela, M. M., Needham, D. M., Cram, J., Fuhrman, J. A., and Teira, E. (2018). Vertical and seasonal patterns control bacterioplankton communities at two horizontally coherent coastal upwelling sites off Galicia (NW Spain). *Microbial Ecology* 76, 866–884. doi:10.1007/s00248-018-1179-z.

Holmes, R. M., Aminot, A., Kérouel, R., Hooker, B. A., and Peterson, B. J. (1999). A simple and precise method for measuring ammonium in marine and freshwater ecosystems. *Canadian Journal of Fisheries and Aquatic Sciences* 56, 1801–1808.

Hu, S. (2017). RNA (and optional DNA) extraction from environmental samples (filters). *protocols.io*.

Hu, S. K., Connell, P. E., Mesrop, L. Y., and Caron, D. A. (2018). A Hard Day's night: Diel shifts in microbial eukaryotic activity in the North Pacific Subtropical Gyre. *Frontiers in Marine Science* 5. doi:10.3389/fmars.2018.00351.

Hutchings, L., van der Lingen, C. D., Shannon, L. J., Crawford, R. J. M., Verheye, H. M. S., Bartholomae, C. H., et al. (2009). The Benguela Current: An ecosystem of four components. *Progress in Oceanography* 83, 15–32. doi:10.1016/j.pocean.2009.07.046.

Hutchinson, G. E. (1961). The Paradox of the Plankton. *The American Naturalist* 95, 137–145.

Ivanova, E. P., Ng, H. J., and Webb, H. K. (2014). "The Family Pseudoalteromonadaceae," in *The Prokaryotes: Gammaproteobacteria*, eds. E. Rosenberg, E. F. DeLong, S. Lory, E. Stackebrandt, and F. Thompson (Berlin, Heidelberg: Springer Berlin Heidelberg), 575–582. doi:10.1007/978-3-642-38922-1_229.

Iverson, V., Morris, R. M., Frazar, C. D., Berthiaume, C. T., Morales, R. L., and Armbrust, E. V. (2012). Untangling genomes from metagenomes: Revealing an uncultured class of marine euryarchaeota. *Science* 335, 587–590. doi:10.1126/science.1212665.

Jardillier, L., Zubkov, M. V, Pearman, J., and Scanlan, D. J. (2010). Significant CO2 fixation by small prymnesiophytes in the subtropical and tropical northeast Atlantic Ocean. *The ISME Journal* 4, 1180–1192. doi:10.1038/ismej.2010.36.

Jarre, A., Hutchings, L., Crichton, M., Wieland, K., Lamont, T., Blamey, L. K., et al. (2015). Oxygen-depleted bottom waters along the west coast of South Africa, 1950-2011. *Fisheries Oceanography* 24, 56–73. doi:10.1111/fog.12076.

Jochem, F. J. (2003). Photo- and heterotrophic pico- and nanoplankton in the Mississippi River plume: Distribution and grazing activity. *Journal of Plankton Research* 25, 1201–1214. doi:10.1093/plankt/fbg087.

Johnson, Z. I. (2006). Niche Partitioning Among *Prochlorococcus* Ecotypes Along Ocean-Scale Environmental Gradients. *Science* 311, 1737–1740. doi:10.1126/science.1118052.

Jürgens, K., and Massana, R. (2008). Protist grazing on marine bacterioplankton. *Microbial Ecology of the Oceans*, 383–441. doi:10.1002/9780470281840.ch11.

Kamp, A., de Beer, D., Nitsch, J. L., Lavik, G., and Stief, P. (2011). Diatoms respire nitrate to survive dark and anoxic conditions. *Proceedings of the National Academy of Sciences of the United States of America* 108, 5649–5654. doi:10.1073/pnas.1015744108.

Kämpfer, P. (2015). "Sphingobacteriales ord. nov," in *Bergeys Manual of Systematics of Archaea and Bacteria*, eds. M.E. Trujillo, S. Dedysh, P. DeVos, B. Hedlund, P. Kämpfer, F.A. Rainey and W.B. Whitman (American Cancer Society). doi:10.1002/9781118960608.obm00034.

Karl, D. M. (2007). Microbial oceanography: paradigms, processes and promise. *Nature Reviews Microbiology* 5, 759–769. doi:10.1038/nrmicro1749.

Kartal, B., van Niftrik, L., Keltjens, J. T., Op den Camp, H. J. M., and Jetten, M. S. M. (2012). "Anammox—Growth Physiology, Cell Biology, and Metabolism," in *Advances in Microbial Physiology*, ed. R. K. Poole (Academic Press), 211–262. doi:https://doi.org/10.1016/B978-0-12-398264-3.00003-6.

Kassambara, A., and Mundt, F. (2020). factoextra: Extract and Visualize the Results of Multivariate Data Analyses. Available at: https://CRAN.R-project.org/package=factoextra [Accessed August 30, 2020].

Kelley, D. (2013). The OCE package.

Kerkhof, L., Voytek, M., Sherrell, R., Millie, D., and Schofield, O. (1999). Variability in bacterial community structure during upwelling in the coastal ocean. *Hydrobiologia* 401, 139–148. doi:10.1023/A:1003734310515.

Kirchman, D. L. (1994). The uptake of inorganic nutrients by heterotrophic bacteria. *Microbial Ecology* 28, 255–271. doi:10.1007/BF00166816.

Kirchman, D. L. (2000). "Uptake and regeneration of inorganic nutrients by marine heterotrophic bacteria." in *Microbial Ecology of the Oceans*,ed. D.L Kirchman (Wiley and Sons) 261–288.

Kirchman, D. L. (2006). The ecology of Cytophaga-Flavobacteria in aquatic environments. *FEMS Microbiology Ecology* 39, 91–100. doi:10.1016/S0168-6496(01)00206-9.

Kirchman, D. L., Ducklow, H. W., McCarthy, J. J., and Garside, C. (1994). Biomass and nitrogen uptake by heterotrophic bacteria during the spring phytoplankton bloom in the North Atlantic Ocean. *Deep Sea Research Part I: Oceanographic Research Papers* 41, 879–895. doi:https://doi.org/10.1016/0967-0637(94)90081-7.

Klindworth, A., Mann, A. J., Huang, S., Wichels, A., Quast, C., Waldmann, J., et al. (2014). Diversity and activity of marine bacterioplankton during a diatom bloom in the North Sea assessed by total RNA and pyrotag sequencing. *Marine Genomics* 18, 185–192. doi:https://doi.org/10.1016/j.margen.2014.08.007.

Kneip, C., Lockhart, P., Voß, C., and Maier, U. G. (2007). Nitrogen fixation in eukaryotes - New models for symbiosis. *BMC Evolutionary Biology* 7–55. doi:10.1186/1471-2148-7-55.

Koblížek, M. (2015). Ecology of aerobic anoxygenic phototrophs in aquatic environments. *FEMS Microbiology Reviews* 39, 854–870. doi:10.1093/femsre/fuv032.

Kolber, Z. S., van Dover, C. L., Niederman, R. A., and Falkowski, P. G. (2000). Bacterial photosynthesis in surface waters of the open ocean. *Nature* 407, 177–179. doi:10.1038/35025044.

Könneke, M., Bernhard, A. E., de La Torre, J. R., Walker, C. B., Waterbury, J. B., and Stahl, D. A. (2005). Isolation of an autotrophic ammonia-oxidizing marine archaeon. *Nature* 437, 543–546. doi:10.1038/nature03911.

Kovalev, K., Volkov, D., Astashkin, R., Alekseev, A., Gushchin, I., Haro-Moreno, J. M., et al. (2020). High-resolution structural insights into the heliorhodopsin family. *Proceedings of the National Academy of Sciences of the United States of America* 117, 4131–4141. doi:10.1073/pnas.1915888117.

Kozich, J. J., Westcott, S. L., Baxter, N. T., Highlander, S. K., and Schloss, P. D. (2013). Development of a dual-index sequencing strategy and curation pipeline for analyzing

amplicon sequence data on the miseq illumina sequencing platform. *Applied and Environmental Microbiology* 79, 5112–5120. doi:10.1128/AEM.01043-13.

Krause, S., le Roux, X., Niklaus, P. A., van Bodegom, P. M., Lennon T., J. T., Bertilsson, S., et al. (2014). Trait-based approaches for understanding microbial biodiversity and ecosystem functioning. *Frontiers in Microbiology* 5, 1–10. doi:10.3389/fmicb.2014.00251.

Kubiszyn, A. M., and Wiktor, J. M. (2016). The *Gymnodinium* and *Gyrodinium* (Dinoflagellata: Gymnodiniaceae) of the West Spitsbergen waters (1999–2010): biodiversity and morphological description of unidentified species. *Polar Biology* 39, 1739–1747. doi:10.1007/s00300-015-1764-2.

Kuipers, B., van Noort, G., Vosjan, J., and Herndl, G. (2000). Diel periodicity of bacterioplankton in the euphotic zone of the subtropical Atlantic Ocean. *Marine Ecology Progress Series* 201, 13–25.

Kuypers, M. M. M., Marchant, H. K., and Kartal, B. (2018). The microbial nitrogen-cycling network. *Nature Reviews Microbiology* 16, 263–276. https://doi.org/10.1038/nrmicro.2018.9

Ladau, J., and Eloe-Fadrosh, E. A. (2019). Spatial, Temporal, and Phylogenetic Scales of Microbial Ecology. *Trends in Microbiology* 27, 662–669. doi:10.1016/j.tim.2019.03.003.

Lagkouvardos, I., Lesker, T. R., Hitch, T. C. A., Gálvez, E. J. C., Smit, N., Neuhaus, K., et al. (2019). Sequence and cultivation study of *Muribaculaceae* reveals novel species, host preference, and functional potential of this yet undescribed family. *Microbiome* 7, 1–15. doi:10.1186/s40168-019-0637-2.

Lahti, L., and Shetty, S. (2019). Microbiome R package.

Lam, P., and Kuypers, M. M. M. (2011). Microbial nitrogen cycling processes in oxygen minimum zones. *Annual Review of Marine Science* 3, 317–345. doi:10.1146/annurev-marine-120709-142814.

Lamont, T., Barlow, R. G., and Kyewalyanga, M. S. (2014). Physical drivers of phytoplankton production in the southern Benguela upwelling system. *Deep Sea Research Part I: Oceanographic Research Papers* 90, 1–16. doi:10.1016/j.dsr.2014.03.003.

Lamont, T., Hutchings, L., van den Berg, M. A., Goschen, W. S., and Barlow, R. G. (2015). Hydrographic variability in the St. Helena Bay region of the southern Benguela

ecosystem. *Journal of Geophysical Research: Oceans* 120, 2920–2944. doi:10.1002/2014JC010619.

Largier, J. L. (2020). Upwelling Bays: How Coastal Upwelling Controls Circulation, Habitat, and Productivity in Bays. *Annual Reviews* 12, 415–447. doi:10.1146/annurev-marine-010419.

Lê, S., Josse, J., and Husson, F. (2008). FactoMineR : An R Package for Multivariate Analysis. *Journal of Statistical Software* 25, 1–18. doi:10.18637/jss.v025.i01.

Leblanc, K., Quéguiner, B., Diaz, F., Cornet, V., Michel-Rodriguez, M., Durrieu De Madron, X., et al. (2018). Nanoplanktonic diatoms are globally overlooked but play a role in spring blooms and carbon export. *Nature Communications* 9, 1–12. doi:10.1038/s41467-018-03376-9.

Lee, S., and Fuhrman, J. A. (1987). Relationships between Biovolume and Biomass of Naturally Derived Marine Bacterioplankton. *Applied and Environmental Microbiology* 53, 1298.

Letscher, R. T., Knapp, A. N., James, A. K., Carlson, C. A., Santoro, A. E., and Hansell, D. A. (2015). Microbial community composition and nitrogen availability influence DOC remineralization in the South Pacific Gyre. *Marine Chemistry* 177, 325–334. doi:10.1016/j.marchem.2015.06.024.

L'Helguen, S., Slawyk, G., and le Corre, P. (2005). Seasonal patterns of urea regeneration by size-fractionated microheterotrophs in well-mixed temperate coastal waters. *Journal of Plankton Research* 27, 263–270. doi:10.1093/plankt/fbh174.

Lindh, M. V., Sjöstedt, J., Andersson, A. F., Baltar, F., Hugerth, L. W., Lundin, D., et al. (2015). Disentangling seasonal bacterioplankton population dynamics by high-frequency sampling. *Environmental Microbiology* 17, 2459–2476. doi:10.1111/1462-2920.12720.

Litchman, E. (2007). "Resource Competition and the Ecological Success of Phytoplankton," in *Evolution of Primary Producers in the Sea*, eds. P. G. Falkowski and A. H. Knoll (Burlington: Academic Press), 351–375. doi:https://doi.org/10.1016/B978-012370518-1/50017-5.

Logares, R., Sunagawa, S., Salazar, G., Cornejo-Castillo, F. M., Ferrera, I., Sarmento, H., et al. (2014). Metagenomic 16S rDNA Illumina tags are a powerful alternative to amplicon sequencing to explore diversity and structure of microbial communities. *Environmental Microbiology* 16, 2659–2671. doi:10.1111/1462-2920.12250.

Lomstein, B. A., Blackburn, T. H., and Henriksen, K. (1989). Aspects of nitrogen and carbon cycling in the northern Bering Shelf sediment. I. The significance of urea turnover in the mineralization of NH4+. *Marine Ecology Progress Series* 57, 237–247.

Lory, S. (2014). "The Family Staphylococcaceae," in *The Prokaryotes: Firmicutes and Tenericutes*, eds. E. Rosenberg, E. F. DeLong, S. Lory, E. Stackebrandt, and F. Thompson (Berlin, Heidelberg: Springer Berlin Heidelberg), 363–366. doi:10.1007/978-3-642-30120-9_350.

Losada, M., and Guerrero, M. (1979). "The photosynthetic reduction of nitrate and its regulation." in *Photosynthesis in Relation to Model Systems,* ed., J. Barber (Elsevier), 365–408.

Lundholm, N., Ribeiro, S., Andersen, T. J., Koch, T., Godhe, A., Ekelund, F., et al. (2011). Buried alive – germination of up to a century-old marine protist resting stages. *Phycologia* 50, 629–640. doi:10.2216/11-16.1.

Malone, T. C. (1980). "Size-Fractionated Primary Productivity of Marine Phytoplankton," in *Primary Productivity in the Sea,* ed. P. G. Falkowski (Boston, MA: Springer US), 301–319. doi:10.1007/978-1-4684-3890-1_17.

Marañón, E. (2009). "Phytoplankton size structure," in *Elements of Physical Oceonography: A Derivative of the Encylopedia of Ocean Sciences* (Elsevier), 85–92. doi:10.1016/B978-0-12-409548-9.11405-8.

Marañón, E., Cermeño, P., López-Sandoval, D. C., Rodríguez-Ramos, T., Sobrino, C., Huete-Ortega, M., et al. (2013). Unimodal size scaling of phytoplankton growth and the size dependence of nutrient uptake and use. *Ecology Letters* 16, 371–379. doi:10.1111/ele.12052.

Marie, D., Partensky, F., Jacquet, S., and Vaulot, D. (1997). Enumeration and cell cycle analysis of natural populations of marine picoplankton by flow cytometry using the nucleic acid stain SYBR Green I. *Applied and Environmental Microbiology* 63, 186–193.

Martin-Platero, A. M., Cleary, B., Kauffman, K., Preheim, S. P., McGillicuddy, D. J., Alm, E. J., et al. (2018). High resolution time series reveals cohesive but short-lived communities in coastal plankton. *Nature Communications* 9, 1–11. doi:10.1038/s41467-017-02571-4.

Martinez, A., Tyson, G. W., and Delong, E. F. (2010). Widespread known and novel phosphonate utilization pathways in marine bacteria revealed by functional screening

and metagenomic analyses. *Environmental Microbiology* 12, 222–238. doi:10.1111/j.1462-2920.2009.02062.x.

Massana, R. (2011). Eukaryotic picoplankton in surface oceans. *Annual Review of Microbiology* 65, 91–110. doi:10.1146/annurev-micro-090110-102903.

Massana, R., Balagué, V., Guillou, L., and Pedrós-Alió, C. (2004). Picoeukaryotic diversity in an oligotrophic coastal site studied by molecular and culturing approaches. *FEMS Microbiology Ecology* 50, 231–243. doi:10.1016/j.femsec.2004.07.001.

Massana, R., and Logares, R. (2013). Eukaryotic versus prokaryotic marine picoplankton ecology. *Environmental Microbiology* 15, 1254–1261. doi:10.1111/1462-2920.12043.

Massana, R., Terrado, R., Forn, I., Lovejoy, C., and Pedrós-Alió, C. (2006). Distribution and abundance of uncultured heterotrophic flagellates in the world oceans. *Environmental Microbiology* 8, 1515–1522. doi:10.1111/j.1462-2920.2006.01042.x.

Matias Rodrigues, J. F., Schmidt, T. S. B., Tackmann, J., and von Mering, C. (2017). MAPseq: Highly efficient k-mer search with confidence estimates, for rRNA sequence analysis. *Bioinformatics* 33, 3808–3810. doi:10.1093/bioinformatics/btx517.

McCarthy, M. J., Newell, S. E., Carini, S. A., and Gardner, W. S. (2015). Denitrification dominates sediment nitrogen removal and is enhanced by bottom-water hypoxia in the Northern Gulf of Mexico. *Estuaries and Coasts* 38, 2279–2294. doi:10.1007/s12237-015-9964-0.

McIlroy, S., Jonand, N., and Per, H. (2014). "The Family Saprospiraceae," in *The Prokaryotes: Other Major Lineages of Bacteria and The Archaea*, ed. E. F. and L. S. and S. E. and T. F. Rosenberg Eugene and DeLong (Berlin, Heidelberg: Springer Berlin Heidelberg), 863–889. doi:10.1007/978-3-642-38954-2_138.

McIlvin, M. R., and Casciotti, K. L. (2011). Technical updates to the bacterial method for nitrate isotopic analyses. *Analytical Chemistry* 83, 1850–1856. doi:10.1021/ac1028984.

McManus, G. B., Costas, B. A., Dam, H. G., Lopes, R. M., Gaeta, S. A., Susini, S. M., et al. (2007). Microzooplankton grazing of phytoplankton in a tropical upwelling region. *Hydrobiologia* 575, 69–81. doi:10.1007/s10750-006-0279-9.

McMinn, A., and Martin, A. (2013). Dark survival in a warming world. *Proceedings of the Royal Society B: Biological Sciences* 280, 20122909. doi:10.1098/rspb.2012.2909.

McMurdie, P. J., and Holmes, S. (2013). Phyloseq: An R Package for Reproducible Interactive Analysis and Graphics of Microbiome Census Data. *PLoS ONE* 8. doi:10.1371/journal.pone.0061217.

Medinger, R., Nolte, V., Pandey, R. V., Jost, S., Ottenwälder, B., Schlötterer, C., et al. (2010). Diversity in a hidden world: Potential and limitation of next-generation sequencing for surveys of molecular diversity of eukaryotic microorganisms. *Molecular Ecology* 19, 32–40. doi:10.1111/j.1365-294X.2009.04478.x.

Middelboe, M., and Brussaard, C. (2017). Marine Viruses: Key Players in Marine Ecosystems. *Viruses* 9, 302. doi:10.3390/v9100302.

Miller, C. A., and Glibert, P. M. (1998). Nitrogen excretion by the calanoid copepod *Acartia tonsa*: results of mesocosm experiments. *Journal of Plankton Research* 20, 1767–1780. doi:10.1093/plankt/20.9.1767.

Mitchell, A. L., Almeida, A., Beracochea, M., Boland, M., Burgin, J., Cochrane, G., et al. (2019). MGnify: the microbiome analysis resource in 2020. *Nucleic acids research* 48, D570–D578. doi:10.1093/nar/gkz1035.

Mitra, A., Flynn, K. J., Burkholder, J. M., Berge, T., Calbet, A., Raven, J. A., et al. (2014). The role of mixotrophic protists in the biological carbon pump. *Biogeosciences* 11, 995–1005. doi:10.5194/bg-11-995-2014.

Mitra, A., Flynn, K. J., Tillmann, U., Raven, J. A., Caron, D., Stoecker, D. K., et al. (2016). Defining Planktonic Protist Functional Groups on Mechanisms for Energy and Nutrient Acquisition: Incorporation of Diverse Mixotrophic Strategies. *Protist* 167, 106–120. doi:10.1016/j.protis.2016.01.003.

Moir, J. W. B., and Wood, N. J. (2001). Nitrate and nitrite transport in bacteria. *Cellular and Molecular Life Sciences CMLS* 58, 215–224. doi:10.1007/PL00000849.

Moncoiffé, G., Alvarez-Salgado, X. A., Figueiras, F. G., and Savidge, G. (2000). Seasonal and short-time-scale dynamics of microplankton community production and respiration in an inshore upwelling system. *Marine Ecology Progress Series* 196, 111–126. doi:10.3354/meps196111.

Montecino, V., Astoreca, R., Alarcón, G., Retamal, L., and Pizarro, G. (2004). Bio-optical characteristics and primary productivity during upwelling and non-upwelling conditions in a highly productive coastal ecosystem off central Chile (~36°S). *Deep-Sea Research Part II: Topical Studies in Oceanography* 51, 2413–2426.

Monteiro, P. M. S., van der Plas, A. K., Bailey, G. W., Malanotte-Rizzoli, P., Duncombe Rae, C. M., Byrnes, D., et al. (2006). "Low Oxygen Water (LOW) forcing scales amenable to forecasting in the Benguela ecosystem," in *Large Marine Ecosystems*, eds. V. Shannon, G. Hempel, P. Malanotte-Rizzoli, C. Moloney, and J. Woods (Elsevier), 295–308. doi:https://doi.org/10.1016/S1570-0461(06)80018-2.

Moore, L. R., Post, A. F., Rocap, G., and Chisholm, S. W. (2002). Utilization of different nitrogen sources by the marine cyanobacteria *Prochlorococcus* and *Synechococcus*. *Limnology and Oceanography* 47, 989–996.

Moore, L. R., Rocap, G., and Chisholm, S. W. (1998). Physiology and molecular phylogeny of coexisting *Prochlorococcus* ecotypes. *Nature* 393, 464–467. doi:10.1038/30965.

Morris, R. M., Rappé, M. S., Connon, S. A., Vergin, K. L., Siebold, W. A., Carlson, C. A., et al. (2002). SAR11 clade dominates ocean surface bacterioplankton communities. *Nature* 420, 806–810. doi:10.1038/nature01240.

Morris, R. M., Vergin, K. L., Cho, J.-C., Rappé, M. S., Carlson, C. A., and Giovannoni, S. J. (2005). Temporal and spatial response of bacterioplankton lineages to annual convective overturn at the Bermuda Atlantic Time-series Study site. *Limnology and Oceanography* 50, 1687–1696. doi:10.4319/lo.2005.50.5.1687.

Mullins, T. D., Britschgi, T. B., Krest, R. L., and Giovannoni, S. J. (1995). Genetic comparisons reveal the same unknown bacterial lineages in Atlantic and Pacific bacterioplankton communities. *Limnology and Oceanography* 40, 148–158.

Murphy, J., and Riley, J. (1962). A modified single solution method for the determination of phosphate in natural waters. *Analytica Chimica Acta* 27, 36–39.

Muyzer, G., de Waal, E. C., and Uitterlinden, A. G. (1993). Profiling of complex microbial populations by denaturing gradient gel electrophoresis analysis of polymerase chain reaction-amplified genes coding for 16S rRNA. *Applied and Environmental Microbiology* 59, 695–700. doi:10.1128/aem.59.3.695-700.1993.

Nagahama, T. (2006). Yeast Biodiversity in Freshwater, Marine and Deep-Sea Environments, in *Biodiversity and Ecophysiology of Yeasts* The Yeast Handbook., eds. G. Péter and C. Rosa (Springer Berlin Heidelberg), 241–262. doi:10.1007/3-540-30985-3_12.

Nagahama, T., Hamamoto, M., Nakase, T., and Horikoshi, K. (2003a). *Rhodotorula benthica* sp. nov. and *Rhodotorula calyptogenae* sp. nov., novel yeast species from animals collected from the deep-sea floor, and *Rhodotorula lysiniphila* sp. nov., which

is related phylogenetically. *International Journal of Systematic and Evolutionary Microbiology* 53, 897–903. doi:10.1099/ijs.0.02395-0.

Nagahama, T., Hamamoto, M., Nakase, T., Takaki, Y., and Horikoshi, K. (2003b). *Cryptococcus surugaensis* sp. nov., a novel yeast species from sediment collected on the deep-sea floor of Suruga Bay. *International Journal of Systematic and Evolutionary Microbiology* 53, 2095–2098. doi:10.1099/ijs.0.02712-0.

Needham, D. M., Fichot, E. B., Wang, E., Berdjeb, L., Cram, J. A., Fichot, C. G., et al. (2018). Dynamics and interactions of highly resolved marine plankton via automated high-frequency sampling. *ISME Journal* 12, 2417–2432. doi:10.1038/s41396-018-0169-y.

Needham, D. M., and Fuhrman, J. A. (2016). Pronounced daily succession of phytoplankton, archaea and bacteria following a spring bloom. *Nature Microbiology* 1, 16005. doi: https://doi.org/10.1038/nmicrobiol.2016.5

Nelson, G., and Hutchings, L. (1983). The Benguela upwelling area. *Progress in Oceanography* 12, 333–356. doi:https://doi.org/10.1016/0079-6611(83)90013-7.

Newell, G. E., and Newell, R. C. (1966). Marine Plankton, A practical guide, Hutchinson Educational Ltd.

Not, F., del Campo, J., Balagué, V., de Vargas, C., and Massana, R. (2009). New insights into the diversity of marine picoeukaryotes. *PLoS ONE* 4. doi:10.1371/journal.pone.0007143.

Nygaard, K., and Tobiesen, A. (1993). Bacterivory in algae: A survival strategy during nutrient limitation. *Limnology and Oceanography* 38, 273–279. doi: 10.4319/lo.1993.38.2.0273

Octavia, S., and Lan, R. (2014). "The Family Enterobacteriaceae," in *The Prokaryotes: Gammaproteobacteria*, eds. E. Rosenberg, E. F. DeLong, S. Lory, E. Stackebrandt, and F. Thompson (Berlin, Heidelberg: Springer Berlin Heidelberg), 225–286. doi:10.1007/978-3-642-38922-1_167.

Oksanen, J. (2016). Vegan : ecological diversity.

Olson, R. J. (1981). Differential photoinhibition of marine nitrifying bacteria: a possible mechanism for the formation of the primary nitrite maximum. *Journal of Marine Research* 39, 227–238.

Pachiadaki, M. G., Sintes, E., Bergauer, K., Brown, J. M., Record, N. R., Swan, B. K., et al. (2017). Major role of nitrite-oxidizing bacteria in dark ocean carbon fixation. *Science* 358, 1046–1051. doi: 10.1126/science.aan8260

Painter, S. C., Patey, M. D., Tarran, G. A., and Torres-Valdés, S. (2014). Picoeukaryote distribution in relation to nitrate uptake in the oceanic nitracline. *Aquatic Microbial Ecology* 72, 195–213. doi:10.3354/ame01695.

Painting, S. J., Lucas, M. I., and Muir, D. G. (1989). Fluctuations in heterotrophic bacterial community structure, activity and production in response to development and decay of phytoplankton in a microcosm. *Marine Ecology-Progress Series* 53, 129–141.

Painting, S. J., Lucas, M. I., Peterson, W. T., Brown, P. C., Hutchings, L., and Mitchell-Innes, B. A. (1993). Dynamics of bacterioplankton, phytoplankton and mesozooplankton communities during the development of an upwelling plume in the southern Benguela. *Marine Ecology-Progress Series* 100, 35–53.

Painting, S. J., Moloney, C. L., and Lucas, M. I. (1993). Simulation and field measurements of phytoplankton-bacteria-zooplankton interactions in the southern Benguela Upwelling region. *Mar Ecol Prog Ser* 100, 55–69.

Painting, S. J., Moloney, C. L., Probyn, T. A., and Tibbles, B. (1992). Microheterotrophic pathways in the southern Benguela upwelling system. *South African Journal of Marine Science* 12, 527–543. doi:10.2989/02577619209504723.

Pajares, S., and Ramos, R. (2019). Processes and Microorganisms Involved in the Marine Nitrogen Cycle: Knowledge and Gaps. *Frontiers in Marine Science* 6. doi:10.3389/fmars.2019.00739.

Palleroni, N. J. (1981). "Introduction to the Family Pseudomonadaceae," in *The Prokaryotes: A Handbook on Habitats, Isolation, and Identification of Bacteria*, eds. M. P. Starr, H. Stolp, H. G. Trüper, A. Balows, and H. G. Schlegel (Berlin, Heidelberg: Springer Berlin Heidelberg), 655–665. doi:10.1007/978-3-662-13187-9_58.

Parks, D. H., Chuvochina, M., Chaumeil, P.-A., Rinke, C., Mussig, A. J., and Hugenholtz, P. (2020). A complete domain-to-species taxonomy for Bacteria and Archaea. *Nature Biotechnology* 38, 1079–1086. doi:10.1038/s41587-020-0501-8.

Parris, D. J., Ganesh, S., Virginia, P., Delong, E. F., Stewart, F. J., Hole, W., et al. (2014). Microbial eukaryote diversity in the marine oxygen minimum zone off northern Chile. 5, 1–11. doi:10.3389/fmicb.2014.00543.

Partensky, F., Blanchot, J., and Vaulot, D. (1999a). Differential distribution and ecology of *Prochlorococcus* and *Synechococcus* in oceanic waters: a review. *Bulletin de l'Institut océanographique* 19, 457–475.

Partensky, F., Hess, W. R., and Vaulot, D. (1999b). *Prochlorococcus*, a marine photosynthetic prokaryote of global significance. *Microbiol.Mol Biol.Rev.* 63, 106–127. doi:doi:1092-2172/99/$04.00.

Peng, L., Ni, B. J., Ye, L., and Yuan, Z. (2015). The combined effect of dissolved oxygen and nitrite on N_2O production by ammonia oxidizing bacteria in an enriched nitrifying sludge. *Water Research* 73, 29–36. doi:10.1016/j.watres.2015.01.021.

Pester, M., Rattei, T., Flechl, S., Gröngröft, A., Richter, A., Overmann, J., et al. (2012). AmoA-based consensus phylogeny of ammonia-oxidizing archaea and deep sequencing of *amo*A genes from soils of four different geographic regions. *Environmental Microbiology* 14, 525–539. doi:10.1111/j.1462-2920.2011.02666.x.

Pester, M., Schleper, C., and Wagner, M. (2011). The Thaumarchaeota: An emerging view of their phylogeny and ecophysiology. *Current Opinion in Microbiology* 14, 300–306. doi:10.1016/j.mib.2011.04.007.

Pitcher, A., Villanueva, L., Hopmans, E. C., Schouten, S., Reichart, G. J., and Sinninghe Damsté, J. S. (2011). Niche segregation of ammonia-oxidizing archaea and anammox bacteria in the Arabian Sea oxygen minimum zone. *ISME Journal* 5, 1896–1904. doi:10.1038/ismej.2011.60.

Pitcher, G. C., Brown, P. C., and Mitchell-Innes, B. A. (1992). Spatio-temporal variability of phytoplankton in the southern Benguela upwelling system. *South African Journal of Marine Science* 12, 439–456. doi:10.2989/02577619209504717.

Pitcher, G. C., and Probyn, T. A. (2011). Anoxia in southern Benguela during the autumn of 2009 and its linkage to a bloom of the dinoflagellate *Ceratium balechii*. *Harmful Algae* 11, 23–32. doi:10.1016/j.hal.2011.07.001.

Pitcher, G. C., and Probyn, T. A. (2016). Suffocating Phytoplankton, Suffocating Waters—Red Tides and Anoxia. *Frontiers in Marine Science* 3, 1–10. doi:10.3389/fmars.2016.00186.

Pitcher, G. C., and Probyn, T. A. (2017). Seasonal and sub-seasonal oxygen and nutrient fluctuations in an embayment of an eastern boundary upwelling system: St. Helena Bay. *African Journal of Marine Science* 39, 95–110. doi:10.2989/1814232X.2017.1305989.

Pitcher, G. C., Probyn, T. A., du Randt, A., Lucas, A. J., Bernard, S., Evers-King, H., et al. (2014). Dynamics of oxygen depletion in the nearshore of a coastal embayment of the southern Benguela upwelling system. *Journal of Geophysical Research: Oceans* 119, 2183–2200. doi:10.1002/2013JC009443.

Pitcher, G. C., Walker, D. R., Mitchell-Innes, B. A., and Moloney, C. L. (1991). Short-term variability during an anchor station study in the southern Benguela upwelling system: Phytoplankton dynamics. *Progress in Oceanography*. 28, 39–64.

Probyn, T. (1985). Nitrogen uptake by size-fractionated phytoplankton populations in the southern Benguela upwelling system. *Marine Ecology Progress Series* 22, 249–258. doi:10.3354/meps022249.

Probyn, T. A. (1990). Size-fractionated measurements of nitrogen uptake in aged upwelled waters: Implications for pelagic food webs. *Limnology and Oceanography* 35, 202–210. doi:https://doi.org/10.4319/lo.1990.35.1.0202.

Probyn, T. A. (1992). The inorganic nitrogen nutrition of phytoplankton in the southern Benguela: New production, phytoplankton size and implications for pelagic foodwebs. *South African Journal of Marine Science* 12, 411–420. doi:10.2989/02577619209504715.

Pujalte, M. J., Lucena, T., Ruvira, M. A., Arahal, D. R., and Macián, M. C. (2014). "The Family Rhodobacteraceae," in *The Prokaryotes: Alphaproteobacteria and Betaproteobacteria*, eds. E. Rosenberg, E. F. DeLong, S. Lory, E. Stackebrandt, and F. Thompson (Berlin, Heidelberg: Springer Berlin Heidelberg), 439–512. doi:10.1007/978-3-642-30197-1_377.

Purkhold, U., Pommerening-Röser, A., Juretschko, S., Schmid, M. C., Koops, H.-P., and Wagner, M. (2000). Phylogeny of All Recognized Species of Ammonia Oxidizers Based on Comparative 16S rRNA and amoA Sequence Analysis: Implications for Molecular Diversity Surveys. *Applied and Environmental Microbiology* 66, 5368–5382.

Qin, W., Amin, S. A., Martens-Habbena, W., Walker, C. B., Urakawa, H., Devol, A. H., et al. (2014). Marine ammonia-oxidizing archaeal isolates display obligate mixotrophy and wide ecotypic variation. *Proceedings of the National Academy of Sciences of the United States of America* 111, 12504–12509. doi:10.1073/pnas.1324115111.

Qin, W., Martens-Habbena, W., Kobelt, J. N., and Stahl, D. A. (2016). " Candidatus Nitrosopumilaceae ," in *Bergey's Manual of Systematics of Archaea and Bacteria* (Wiley), 1–2. doi:10.1002/9781118960608.fbm00262.

Quast, C., Pruesse, E., Yilmaz, P., Gerken, J., Schweer, T., Yarza, P., et al. (2013). The SILVA ribosomal RNA gene database project: Improved data processing and web-based tools. *Nucleic Acids Research* 41, 590–596. doi:10.1093/nar/gks1219.

R Core Team (2013). R: A language and environment for statistical computing. Available at: http://www.r-project.org/.

Ramond, P., Siano, R., and Sourisseau, M. (2018). Functional traits of marine protists. *SEANOE*. https://doi.org/10.17882/51662

Ramond, P., Sourisseau, M., Simon, N., Romac, S., Schmitt, S., Rigaut-Jalabert, F., et al. (2019). Coupling between taxonomic and functional diversity in protistan coastal communities. *Environmental Microbiology* 21, 730–749. doi:10.1111/1462-2920.14537.

Rappé, M. S., Connon, S. A., Vergin, K. L., and Giovannoni, S. J. (2002). Cultivation of the ubiquitous SAR11 marine bacterioplankton clade. *Nature* 418, 630–633.

Raven, J. A. (1984). A cost-benefit analysis of photon absorption by photosynthetic unicells. *New Phytologist* 98, 593–625. doi:https://doi.org/10.1111/j.1469-8137.1984.tb04152.x.

Raven, J. A. (1998). The twelfth Tansley Lecture. Small is beautiful: the picophytoplankton. *Functional Ecology* 12, 503–513. doi:https://doi.org/10.1046/j.1365-2435.1998.00233.x.

Reji, L., Tolar, B. B., Chavez, F. P., and Francis, C. A. (2020). Depth-Differentiation and Seasonality of Planktonic Microbial Assemblages in the Monterey Bay Upwelling System. *Frontiers in Microbiology* 11. doi:10.3389/fmicb.2020.01075.

Rho, M., Tang, H., and Ye, Y. (2010). FragGeneScan: Predicting genes in short and error-prone reads. *Nucleic Acids Research* 38. doi:10.1093/nar/gkq747.

Rinke, C., Chuvochina, M., Mussig, A. J., Chaumeil, P.-A., Davín, A. A., Waite, D. W., et al. (2021). A standardized archaeal taxonomy for the Genome Taxonomy Database. *Nature Microbiology* 6, 946–959. doi:10.1038/s41564-021-00918-8.

Robinson, C. (2019). Microbial respiration, the engine of ocean deoxygenation. *Frontiers in Marine Science* 5, 1–13. doi:10.3389/fmars.2018.00533.

Rocke, E., Cheung, S. Y., Gebe, Z., Dames, N. R., Liu, H. B., and Moloney, C. L. (2020). Marine Microbial Community Composition During the Upwelling Season in the Southern Benguela. *Frontiers in Marine Science* 7, 255. doi:10.3389/fmars.2020.00255.

Rocke, E., Jing, H., and Liu, H. (2013). Phylogenetic composition and distribution of picoeukaryotes in the hypoxic northwestern coast of the Gulf of Mexico. *Microbiology Open* 2, 130–143. doi:10.1002/mbo3.57.

Rocke, E., Jing, H., Xia, X., and Liu, H. (2016). Effects of hypoxia on the phylogenetic composition and species distribution of protists in a subtropical harbor. *Microbial Ecology* 72, 96–105. doi:10.1007/s00248-016-0751-7.

Rocke, E., Pachiadaki, M. G., Cobban, A., and Kujawinski, E. B. (2015). Protist Community Grazing on Prokaryotic Prey in Deep Ocean Water Masses. 1–14. doi:10.1371/journal.pone.0124505.

Roux, S., Chan, L. K., Egan, R., Malmstrom, R. R., McMahon, K. D., and Sullivan, M. B. (2017). Ecogenomics of virophages and their giant virus hosts assessed through time series metagenomics. *Nature Communications* 8, 858 doi:10.1038/s41467-017-01086-2.

Santoro, A. E., Casciotti, K. L., and Francis, C. A. (2010). Activity, abundance and diversity of nitrifying archaea and bacteria in the central California Current. *Environmental Microbiology* 12, 1989–2006. doi:https://doi.org/10.1111/j.1462-2920.2010.02205.x.

Santoro, A. E., Dupont, C. L., Richter, R. A., Craig, M. T., Carini, P., McIlvin, M. R., et al. (2015). Genomic and proteomic characterization of "*Candidatus Nitrosopelagicus brevis*": An ammonia-oxidizing archaeon from the open ocean. *Proceedings of the National Academy of Sciences of the United States of America* 112, 1173–1178. doi:10.1073/pnas.1416223112.

Sassenhagen, I., Irion, S., Jardillier, L., Moreira, D., and Christaki, U. (2020). Protist Interactions and Community Structure During Early Autumn in the Kerguelen Region (Southern Ocean). *Protist* 171. doi:10.1016/j.protis.2019.125709.

Satomi, M. (2014). "The Family Shewanellaceae," in *The Prokaryotes: Gammaproteobacteria*, ed. E. F. and L. S. and S. E. and T. F. Rosenberg Eugene and DeLong (Berlin, Heidelberg: Springer Berlin Heidelberg), 597–625. doi:10.1007/978-3-642-38922-1_226.

Seitzinger, S. P. (1988). Denitrification in freshwater and coastal marine ecosystems: Ecological and geochemical significance. *Limnology and Oceanography* 33, 702–724. doi:10.4319/lo.1988.33.4part2.0702.

Schloss, P. D., Westcott, S. L., Ryabin, T., Hall, J. R., Hartmann, M., Hollister, E. B., et al. (2009). Introducing mothur: Open-source, platform-independent, community-supported software for describing and comparing microbial communities. *Applied and Environmental Microbiology* 75, 7537–7541. doi:10.1128/AEM.01541-09.

Severin, T., Sauret, C., Boutrif, M., Duhaut, T., Kessouri, F., Oriol, L., et al. (2016). Impact of an intense water column mixing (0–1500 m) on prokaryotic diversity and activities during an open-ocean convection event in the NW Mediterranean Sea. *Environmental Microbiology* 18, 4378–4390. doi:10.1111/1462-2920.13324.

Shannon, L. V, and Nelson, G. (1996). "The Benguela: Large Scale Features and Processes and System Variability," in *The South Atlantic: Present and Past Circulation*, eds. G. Wefer, W. H. Berger, G. Siedler, and D. J. Webb (Berlin, Heidelberg: Springer Berlin Heidelberg), 163–210. doi:10.1007/978-3-642-80353-6_9.

Sheng, Y. P., and Lick, W. (1979). Transport and resuspension of sediments in a shallow lake. *Journal of Geophysical Research* 84, 1809–1826. doi:10.1029/jc084ic04p01809.

Shiozaki, T., Ijichi, M., Isobe, K., Hashihama, F., Nakamura, K. I., Ehama, M., et al. (2016). Nitrification and its influence on biogeochemical cycles from the equatorial Pacific to the Arctic Ocean. *ISME Journal* 10, 2184–2197. doi:10.1038/ismej.2016.18.

Sigman, D. M., Casciotti, K. L., Andreani, M., Barford, C., Galanter, M., and Böhlke, J. K. (2001). A bacterial method for the nitrogen isotopic analysis of nitrate in seawater and freshwater. *Analytical Chemistry* 73, 4145–4153. doi:10.1021/ac010088e.

Snider, D., Thompson, K., Wagner-Riddle, C., Spoelstra, J., and Dunfield, K. (2015). Molecular techniques and stable isotope ratios at natural abundance give complementary inferences about N_2O production pathways in an agricultural soil following a rainfall event. *Soil Biology and Biochemistry* 88, 197–213. doi:https://doi.org/10.1016/j.soilbio.2015.05.021.

Sommer, U., Charalampous, E., Genitsaris, S., and Moustaka-Gouni, M. (2017). Benefits, costs and taxonomic distribution of marine phytoplankton body size. *Journal of Plankton Research* 39, 494–508. doi:10.1093/plankt/fbw071.

Sowell, S. M., Wilhelm, L. J., Norbeck, A. D., Lipton, M. S., Nicora, C. D., Barofsky, D. F., et al. (2009). Transport functions dominate the SAR11 metaproteome at low-

nutrient extremes in the Sargasso Sea. *ISME Journal* 3, 93–105. doi:10.1038/ismej.2008.83.

Spring, S., Scheuner, C., Göker, M., and Klenk, H. P. (2015). A taxonomic framework for emerging groups of ecologically important marine gammaproteobacteria based on the reconstruction of evolutionary relationships using genome-scale data. *Frontiers in Microbiology* 6. doi:10.3389/fmicb.2015.00281.

Ssekagiri, A. T., Sloan, W., and Ijaz, U. Z.(2017). microbiomeSeq: an R package for analysis of microbial communities in an environmental context. In ISCB Africa ASBCB Conference, Kumasi, Ghana. https://github.com/umerijaz/microbiomeSeq. doi:10.13140/RG.2.2.17108.71047

Staal, M., te Lintel Hekkert, S., Jan Brummer, G., Veldhuis, M., Sikkens, C., Persijn, S., et al. (2007). Nitrogen fixation along a north-south transect in the eastern Atlantic Ocean. *Limnology and Oceanography* 52, 1305–1316. doi:https://doi.org/10.4319/lo.2007.52.4.1305.

Stackebrandt, E. (2014). "The family Lachnospiraceae," in *The Prokaryotes: Firmicutes and Tenericutes* (Springer-Verlag Berlin Heidelberg), 197–201. doi:10.1007/978-3-642-30120-9_363.

Stevens, H., and Ulloa, O. (2008). Bacterial diversity in the oxygen minimum zone of the eastern tropical South Pacific. *Environmental Microbiology* 10, 1244–1259. doi:10.1111/j.1462-2920.2007.01539.x.

Stockner, J. G. (1988). Phototrophic picoplankton : freshwater ecosystems An overview from marine and. *Limnology and oceanography* 33, 765–775. doi:10.4319/lo.1988.33.4_part_2.0765.

Stoeck, T., Bass, D., Nebel, M., Christen, R., Jones, M. D. M., Breiner, H. W., et al. (2010). Multiple marker parallel tag environmental DNA sequencing reveals a highly complex eukaryotic community in marine anoxic water. *Molecular Ecology* 19, 21–31. doi:10.1111/j.1365-294X.2009.04480.x.

Suh, S.-S., Park, M., Hwang, J., Kil, E.-J., Jung, S. W., Lee, S., et al. (2015). Seasonal Dynamics of Marine Microbial Community in the South Sea of Korea. *Plos One* 10, e0131633. doi:10.1371/journal.pone.0131633.

Sun, X., Ji, Q., Jayakumar, A., and Ward, B. B. (2017). Dependence of nitrite oxidation on nitrite and oxygen in low-oxygen seawater. *Geophysical Research Letters* 44, 7883–7891. doi:10.1002/2017GL074355.

Sun, J., Steindler, L., Thrash, J. C., Halsey, K. H., Smith, D. P., Carter, A. E., et al. (2011). One carbon metabolism in SAR11 pelagic marine bacteria. *PLoS ONE* 6. doi:10.1371/journal.pone.0023973.

Sverdrup, H. U. (1953). On conditions for the vernal blooming of phytoplankton. *ICES Journal of Marine Science* 18, 287–295. doi:10.1093/icesjms/18.3.287.

Suttle, C. A. (1994). The Significance of Viruses to Mortality in Aquatic Micorbial Communities. *Microbial Ecology* 28, 237–243.

Suttle, C. A. (2007). Marine viruses — major players in the global ecosystem. *Nature Reviews Microbiology* 5, 801–812. doi:10.1038/nrmicro1750.

Takaya, N. (2002). Dissimilatory nitrate reduction metabolisms and their control in fungi. *Journal of Bioscience and Bioengineering* 94, 506–510. doi:https://doi.org/10.1016/S1389-1723(02)80187-6.

Tang, T., Kisslinger, K., and Lee, C. (2014). Silicate deposition during decomposition of cyanobacteria may promote export of picophytoplankton to the deep ocean. *Nature Communications* 5. doi:10.1038/ncomms5143.

Teeling, H., Fuchs, B. M., Becher, D., Klockow, C., Gardebrecht, A., Bennke, C. M., et al. (2012). Substrate-controlled succession of marine bacterioplankton populations induced by a phytoplankton bloom. *Science* 336, 608–611. doi:10.1126/science.1218344.

Teeling, H., Fuchs, B. M., Bennke, C. M., Krü ger, K., Chafee, M., Kappelmann, L., et al. (2016). Recurring patterns in bacterioplankton dynamics during coastal spring algae blooms. doi:10.7554/eLife.11888.001.

Teixeira, I. G., Figueiras, F. G., Crespo, B. G., and Piedracoba, S. (2011). Microzooplankton feeding impact in a coastal upwelling system on the NW Iberian margin: The Ría de Vigo. *Estuarine, Coastal and Shelf Science* 91, 110–120. doi:10.1016/j.ecss.2010.10.012.

Teixeira, L. M., and Merquior, V. L. C. (2014). “The Family Moraxellaceae,” in *The Prokaryotes: Gammaproteobacteria*, eds. E. Rosenberg, E. F. DeLong, S. Lory, E. Stackebrandt, and F. Thompson (Berlin, Heidelberg: Springer Berlin Heidelberg), 443–476. doi:10.1007/978-3-642-38922-1_245.

Therkildsen, Isaksen, M. F., and Lomstein, B. (1997). Urea production by the marine bacteria Delaya venusta and Pseudomonas stutzeri grown in a minimal medium. *Aquatic Microbial Ecology* 13, 213–217. doi:10.3354/ame013213.

Thompson, A. W., Foster, R. A., Krupke, A., Carter, B. J., Musat, N., Vaulot, D., et al. (2012). Unicellular Cyanobacterium Symbiotic with a Single-Celled Eukaryotic Alga. *Science* 337, 1546. doi:10.1126/science.1222700.

Tiedje, J. (1988). "Ecology of denitrification and dissimilatory nitrate reduction to ammonium," in *Environmental Microbiology of Anaerobes*, ed. A.J.B. Zehnder (Wiley and Sons, New York), 179–244.

Tittel, J., Bissinger, V., Zippel, B., Gaedke, U., Bell, E., Lorke, A., et al. (2003). Mixotrophs combine resource use to outcompete specialists: Implications for aquatic food webs. *Proceedings of the National Academy of Sciences of the United States of America* 100, 12776–12781.

Torondel, B., Ensink, J. H. J., Gundogdu, O., Ijaz, U. Z., Parkhill, J., Abdelahi, F., et al. (2016). Assessment of the influence of intrinsic environmental and geographical factors on the bacterial ecology of pit latrines. *Microbial Biotechnology* 9, 209–223. doi:https://doi.org/10.1111/1751-7915.12334.

Treusch, A. H., Vergin, K. L., Finlay, L. A., Donatz, M. G., Burton, R. M., Carlson, C. A., et al. (2009). Seasonality and vertical structure of microbial communities in an ocean gyre. *The ISME journal* 3, 1148–1163.

Troncoso, V. A., Daneri, G., Cuevas, L. A., Jacob, B., and Montero, P. (2003). Bacterial carbon flow in the Humboldt Current System off Chile. *Marine Ecology-Progress Series* 250, 1–12.

Tyrrell, T., and Lucas, M. I. (2002). Geochemical evidence of denitrification in the Benguela upwelling system. *Continental Shelf Research* 22, 2497-2511. doi: https://doi.org/10.1016/S0278-4343(02)00077-8.

Ulloa, O., Canfield, D. E., DeLong, E. F., Letelier, R. M., and Stewart, F. J. (2012). Microbial oceanography of anoxic oxygen minimum zones. *Proceedings of the National Academy of Sciences of the United States of America* 109, 15996–16003. doi:10.1073/pnas.1205009109.

Våge, S., Pree, B., and Thingstad, T. F. (2016). Linking internal and external bacterial community control gives mechanistic framework for pelagic virus-to-bacteria ratios. *Environmental Microbiology* 18, 3932–3948. doi:10.1111/1462-2920.13391.

Vallina, S. M., Follows, M. J., Dutkiewicz, S., Montoya, J. M., Cermeno, P., and Loreau, M. (2014). Global relationship between phytoplankton diversity and productivity in the ocean. *Nature Communications* 5. doi:10.1038/ncomms5299.

van Dongen-Vogels, V., Seymour, J. R., Middleton, J. F., Mitchell, J. G., and Seuront, L. (2011). Influence of local physical events on picophytoplankton spatial and temporal dynamics in South Australian continental shelf waters. *Journal of Plankton Research* 33, 1825–1841. doi:10.1093/plankt/fbr077.

van de Vossenberg, J., Rattray, J. E., Geerts, W., Kartal, B., van Niftrik, L., van Donselaar, E. G., et al. (2008). Enrichment and characterization of marine anammox bacteria associated with global nitrogen gas production. *Environmental Microbiology* 10, 3120–3129. doi:https://doi.org/10.1111/j.1462-2920.2008.01643.x.

van der Lingen, C. D., Fréon, P., Hutchings, L., Roy, C., Bailey, G. W., Bartholomae, C., et al. (2006). "Forecasting shelf processes of relevance to living marine resources in the BCLME," in *Large Marine Ecosystems*, eds. V. Shannon, G. Hempel, P. Malanotte-Rizzoli, C. Moloney, and J. Woods (Elsevier), 309–347. doi:https://doi.org/10.1016/S1570-0461(06)80019-4.

van Oostende, N., Dunne, J. P., Fawcett, S. E., and Ward, B. B. (2015). Phytoplankton succession explains size-partitioning of new production following upwelling-induced blooms. *Journal of Marine Systems* 148, 14–25. doi:10.1016/j.jmarsys.2015.01.009.

Vaulot, D., Eikrem, W., Viprey, M., and Moreau, H. (2008). The diversity of small eukaryotic phytoplankton (≤3 μm) in marine ecosystems. *FEMS Microbiology Reviews* 32, 795–820. doi:10.1111/j.1574-6976.2008.00121.x.

Verheye-Dua, F., and Lucas, M. I. (1988). Southern Benguela frontal region. 1. Hydrology, phytoplankton and bacterioplankton. *Marine Ecologyl Progress Series* 47, 271–280. doi:10.3354/meps047271.

Villareal, T. A. (1992). "Marine Nitrogen-Fixing Diatom-Cyanobacteria Symbioses," in *Marine Pelagic Cyanobacteria: Trichodesmium and other Diazotrophs*, eds. E. J. Carpenter, D. G. Capone, and J. G. Rueter (Dordrecht: Springer Netherlands), 163–175. doi:10.1007/978-94-015-7977-3_10.

Villarreal-Chiu, J. F., Quinn, J. P., and McGrath, J. W. (2012). The genes and enzymes of phosphonate metabolism by bacteria, and their distribution in the marine environment. *Frontiers in Microbiology* 3. doi:10.3389/fmicb.2012.00019.

Vitousek, P. M., and Howarth, R. W. (1991). Nitrogen limitation on land and in the sea: How can it occur? *Biogeochemistry* 13, 87–115. doi:10.1007/BF00002772.

Volk, T., and Hoffert, M. I. (1985). "Ocean Carbon Pumps: Analysis of Relative Strengths and Efficiencies in Ocean-Driven Atmospheric CO_2 Changes," in *In The Carbon Cycle*

and Atmospheric CO_2: Natural Variations Archean to Present, eds. E.T Sundquist and W.S. Broecker. doi:10.1029/GM032p0099.

Walker, C. B., de la Torre, J. R., Klotz, M. G., Urakawa, H., Pinel, N., Arp, D. J., et al. (2010). *Nitrosopumilus maritimus* genome reveals unique mechanisms for nitrification and autotrophy in globally distributed marine crenarchaea. *Proceedings of the National Academy of Sciences* 107, 8818–8823. doi:10.1073/pnas.0913533107.

Walker, D. R., and Peterson, W. T. (1991). Relationships between hydrography, phytoplankton production, biomass, cell size and species composition, and copepod production in the southern benguela upwelling system in april 1988. *South African Journal of Marine Science* 11, 289–305. doi:10.2989/025776191784287529.

Walker, D. R., and Pitcher, G. C. (1991). The dynamics of phytoplankton populations, including a red-tide bloom, during a quiescent period in St. Helena Bay, South Africa. *South African Journal of Marine Science* 10, 61–70. doi:10.2989/02577619109504620.

Walsh, E. A., Kirkpatrick, J. B., Rutherford, S. D., Smith, D. C., Sogin, M., and D'Hondt, S. (2016). Bacterial diversity and community composition from seasurface to subseafloor. *ISME Journal* 10, 979–989. doi:10.1038/ismej.2015.175.

Ward, B. A. (2019). Mixotroph ecology: More than the sum of its parts. *Proceedings of the National Academy of Sciences of the United States of America* 116, 5846–5848. doi:10.1073/pnas.1902106116.

Ward, B. B. (2008). "Nitrification in Marine Systems" in *Nitrogen in the Marine Environment*, eds. D.G. Capone, D.A. Bronk, M.R. Mulholland and E.J. Carpenter (Academic Press) 199–261. doi:10.1016/B978-0-12-372522-6.00005-0.

Ward, B. B., Capone, D. G., and Zehr, J. P. (2007). What's new in the nitrogen cycle? *Oceanography* 20, 101–109.

Ward, C. S., Yung, C.-M., Davis, K. M., Blinebry, S. K., Williams, T. C., Johnson, Z. I., et al. (2017). Annual community patterns are driven by seasonal switching between closely related marine bacteria. *The ISME Journal* 11, 1412–1422. doi:10.1038/ismej.2017.4.

Wassmann, P., Vernet, M., Mitchell, B. G., and Rey, F. (1990). Mass sedimentation of Phaeocystis pouchetii in the Barents Sea. *Marine Ecology Progress Series* 66, 183–195. Available at: http://www.jstor.org/stable/24844656.

Webster, N. S., and Taylor, M. W. (2012). Marine sponges and their microbial symbionts: Love and other relationships. *Environmental Microbiology* 14, 335–346. doi:10.1111/j.1462-2920.2011.02460.x.

Weeks, S. J., Barlow, R., Roy, C., and Shillington, F. A. (2006). Remotely sensed variability of temperature and chlorophyll in the southern Benguela: upwelling frequency and phytoplankton response. *African Journal of Marine Science* 28, 493–509. doi:10.2989/18142320609504201.

Weithoff, G., Lorke, A., and Walz, N. (2000). Effects of water-column mixing on bacteria, phytoplankton, and rotifers under different levels of herbivory in a shallow eutrophic lake. *Oecologia* 125, 91–100.

Welschmeyer, N. A. (1994). Fluorometric analysis of chlorophyll a in the presence of chlorophyll b and pheopigments. *Limnology and Oceanography* 39, 1985–1992. doi:10.4319/lo.1994.39.8.1985.

Welsh, A., Chee-Sanford, J. C., Connor, L. M., Löffler, F. E., and Sanford, R. A. (2014). Refined NrfA Phylogeny Improves PCR-Based nrfA Gene Detection. *Applied and Environmental Microbiology* 80, 2110. doi:10.1128/AEM.03443-13.

Wickham, H. (2016). *ggplot2: Elegant Graphics for Data Analysis*. Springer-Verlag New York.

Wilcox, H., and Worden Lab (2009). DNA Extraction - Sucrose Lysis Method.

Willey, J., Sherwood, L., and Woolverton, C. (2011). *Prescott's Microbiology*. McGraw-Hill.

Worden, A. Z., Lee, J.-H., Mock, T., Rouze, P., Simmons, M. P., Aerts, A. L., et al. (2009). Green Evolution and Dynamic Adaptations Revealed by Genomes of the Marine Picoeukaryotes Micromonas. *Science* 324, 268–272. doi:10.1126/science.1167222.

Worden, A. Z., and Not, F. (2008). Ecology and Diversity of Picoeukaryotes. *Microbial Ecology of the Oceans: Second Edition*, 159–205. doi:10.1002/9780470281840.ch6.

Wright, J. J., Konwar, K. M., and Hallam, S. J. (2012). Microbial ecology of expanding oxygen minimum zones. *Nature Reviews Microbiology* 10, 381–394.

Wuchter, C., Abbas, B., Coolen, M. J. L., Herfort, L., van Bleijswijk, J., Timmers, P., et al. (2006). Archaeal nitrification in the ocean. *Proceedings of the National Academy of Sciences* 103, 12317. doi:10.1073/pnas.0600756103.

Xu, L., Wu, Y. H., Jian, S. L., Wang, C. S., Wu, M., Cheng, L., et al. (2016). *Pseudohongiella nitratireducens* sp. Nov., isolated from seawater, and emended

description of the genus *Pseudohongiella*. *International Journal of Systematic and Evolutionary Microbiology* 66, 5155–5160. doi:10.1099/ijsem.0.001489.

Yilmaz, P., Iversen, M. H., Hankeln, W., Kottmann, R., Quast, C., and Glockner, F. O. (2012). Ecological structuring of bacterial and archaeal taxa in surface ocean waters. *FEMS Microbiology Ecology* 81, 373–385. doi:10.1111/j.1574-6941.2012.01357.x.

Yilmaz, P., Parfrey, L. W., Yarza, P., Gerken, J., Pruesse, E., Quast, C., et al. (2014). The SILVA and "all-species Living Tree Project (LTP)" taxonomic frameworks. *Nucleic Acids Research* 42, 643–648. doi:10.1093/nar/gkt1209.

Yilmaz, P., Yarza, P., Rapp, J. Z., and Glöckner, F. O. (2016). Expanding the world of marine bacterial and archaeal clades. *Frontiers in Microbiology* 6, 1–29. doi:10.3389/fmicb.2015.01524.

Yool, A., and Tyrrell, T. (2003). Role of diatoms in regulating the ocean's silicon cycle. *Global Biogeochemical Cycles* 17. doi:10.1029/2002gb002018.

Yoon, J., Matsuo, Y., Adachi, K., Nozawa, M., Matsuda, S., Kasai, H., et al. (2008). Description of *Persicirhabdus sediminis* gen. nov., sp. nov., *Roseibacillus ishigakijimensis* gen. nov., sp. nov., *Roseibacillus ponti* sp. nov., *Roseibacillus persicicus* sp. nov., *Luteolibacter pohnpeiensis* gen. nov., sp. nov. and *Luteolibacter algae* sp. no. *International Journal of Systematic and Evolutionary Microbiology* 58, 998–1007. doi:10.1099/ijs.0.65520-0.

Zakem, E. J., Al-Haj, A., Church, M. J., van Dijken, G. L., Dutkiewicz, S., Foster, S. Q., et al. (2018). Ecological control of nitrite in the upper ocean. *Nature Communications* 9. doi:10.1038/s41467-018-03553-w.

Zehr, J. P., Jenkins, B. D., Short, S. M., and Steward, G. F. (2003). Nitrogenase gene diversity and microbial community structure: a cross-system comparison. *Environmental Microbiology* 5, 539–554. doi:https://doi.org/10.1046/j.1462-2920.2003.00451.x.

Zehr, J. P., and Kudela, R. M. (2011). Nitrogen Cycle of the Open Ocean : From Genes to Ecosystems. *Annual Review of Marine Science*, 197–225. doi:10.1146/annurev-marine-120709-142819.

Zehr, J. P., Shilova, I. N., Farnelid, H. M., Muñoz-Marín, M. del C., and Turk-Kubo, K. A. (2016). Unusual marine unicellular symbiosis with the nitrogen-fixing cyanobacterium UCYN-A. *Nature Microbiology* 2, 16214. doi:10.1038/nmicrobiol.2016.214.

Zehr, J. P., and Ward, B. B. (2002). Nitrogen Cycling in the Ocean: New Perspectives on Processes and Paradigms. *Applied and Environmental Microbiology* 68.3, 1015–1024. doi:10.1128/AEM.68.3.1015.

Zehr, J. P., Waterbury, J. B., Turner, P. J., Montoya, J. P., Omoregie, E., Steward, G. F., et al. (2001). Unicellular cyanobacteria fix N_2 in the subtropical North Pacific Ocean. *Nature* 412, 635–638. doi:10.1038/35088063.

Zubkov, M. V, Sleigh, M. A., Tarran, G. A., Burkill, P. H., and Leakey, R. J. G. (1998). Picoplanktonic community structure on an Atlantic transect from 50°N to 50°S. *Deep Sea Research Part I: Oceanographic Research Papers* 45, 1339–1355. doi:https://doi.org/10.1016/S0967-0637(98)00015-6.